Alternative splicing-derived isoforms of the NaCl cotransporter and their role in hypertension

Omar A.Z. Tutakhel

The research presented in this thesis was performed at the department of Physiology, Radboud Institute for Molecular Life Sciences, Radboud university medical center, Radboud University, The Netherlands and financially supported by the Dutch Kidney Foundation, grant PHD12.14, Eurocept Homecare and Sysmex Malvern.

ISBN: 978-94-92896-08-7

Cover design: Promotie in Zicht, Arnhem, The Netherlands

Lay-out: Omar A.Z. Tutakhel, Nijmegen, The Netherlands

Print: Ipskamp Drukkers, Nijmegen, The Netherlands

Thesis number: RIMLS 2018-06

Alternative splicing-derived isoforms of the NaCl cotransporter and their role in hypertension

Proefschrift

ter verkrijging van de graad van doctor
aan de Radboud Universiteit Nijmegen
op het gezag van de Rector Magnificus prof. dr. J.H.J.M. Krieken,
volgens besluit van het College van decanen
in het openbaar te verdedigen op donderdag 15 februari 2018
om 16:30 uur precies

door

Omar A.Z. Tutakhel
geboren op 20 februari 1988
te Kaboel, Afghanistan

Promotoren

Prof. dr. R.J.M. Bindels

Prof. dr. J.G.J. Hoenderop

Prof. dr. E.J. Hoorn, Erasmus MC

Copromotor

Dr. J. van der Wijst

Manuscriptcommissie

Prof. dr. F.G.M. Russel, voorzitter

Prof. dr. R. Roepman

Dr. J.A. Joles, UMC Utrecht

Table of contents

1

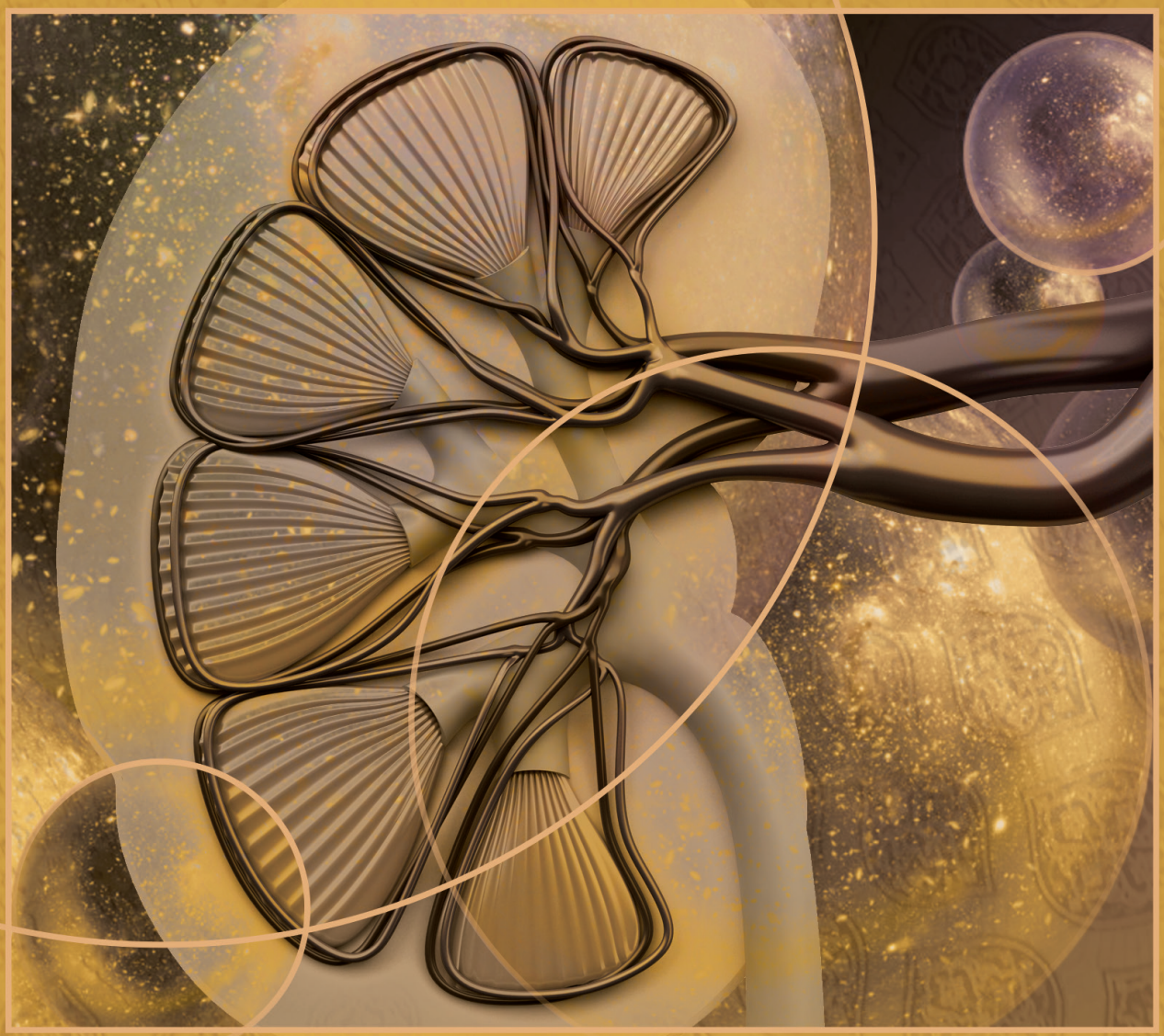

Introduction to the role of NaCl cotransporter in hypertension

Hypertension

Prevalence of hypertension

High blood pressure (hypertension) is the major risk factor for cardiovascular disease, chronic kidney disease and overall increased risk of mortality (36, 81, 87, 90). With a prevalence of 1.4 billion people worldwide, representing 1 in every 4 adults, it has become the most critical and expensive public health problem (81). Global prevalence is predicted to increase to 1.6 billion by 2025 (21, 30, 53, 81, 87). Strikingly, ~50% of hypertensive patients are unaware of their condition (21) and hypertension is therefore often referred to as "the silent killer". Around 90% of hypertensive patients have primary or essential hypertension, which means that the origin of their disorder is unknown (16, 80). Hypertension is a complex disease, likely resulting from the combination of an inherited susceptibility and the exposure to environmental factors, such as a typical diet that is high in sodium (Na^+) and low in potassium (K^+) (40, 130).

Essential hypertension

Adults are usually diagnosed with hypertension when the systolic blood pressure is above 140 mmHg and/or diastolic blood pressure is greater than 90 mmHg (56, 58). Essential hypertension is defined as high blood pressure in which the secondary causes such as monogenic diseases, renal failure, aldosteronism and renovascular disease are not present. To date, the primary cause of hypertension is determined in less than 10% of hypertensive patients, leaving the vast majority of patients with an undefined cause of their hypertension. Usually a cluster of factors are involved, including high Na^+ intake in salt-sensitive patients (72, 131, 132), low K^+ intake (129-131), obesity (42, 54, 84, 131, 132), diabetes (24), adaptive immunity (68), high alcohol intake (20, 131, 145), sedentary lifestyle (20, 59, 64, 96), stress (95), hyperlipidaemia (80), and probably low calcium (Ca^{2+}) (3), magnesium (Mg^{2+}) and fiber intake (7, 118).

Salt-sensitive essential hypertension

Salt sensitivity is characterized by an increase or decrease in blood pressure in response to high or low dietary Na^+ intake, respectively. This is observed in ~30% of normotensives and ~65% hypertensives (1, 63). The interplay of genetic and environmental factors contributes to the development of salt sensitivity (63, 76). Declining glomerular filtration rate, aging, African descent, and obesity are associated with salt sensitivity (1). Salt-sensitive individuals consuming a high Na^+ diet retain more Na^+ than salt-resistant subjects (13). Additionally, in salt-sensitive patients the blood pressure response to Na^+ is modified by other components in their diet such as K^+, Ca^{2+} and Mg^{2+} (3, 63). Low dietary intake of K^+, Ca^{2+} and Mg^{2+}

potentiates the salt sensitivity of blood pressure regulation (3, 7, 63, 118, 129-131). Conversely, high dietary intake of these minerals can attenuate the development of Na^+-induced hypertension (7, 118, 129-131). Dietary K^+ exerts a powerful, dose-dependent inhibitory effect, as increased dietary K^+ can even abolish salt sensitivity in both normotensives and hypertensives (1, 85). The proper knowledge on the dietary intervention provides an important opportunity for further improvement of the blood pressure control in our society. Adequate intake of K^+, Ca^{2+} and Mg^{2+}, besides limiting the Na^+ consumption, is a viable health recommendation to reduce the risk of Na^+-induced hypertension (78). Therefore, adherence to dietary patterns similar to the DASH (Dietary Approaches to Stop Hypertension) diet can be beneficial to salt-sensitive individuals (109). However, the majority of hypertensive patients will need treatment with antihypertensive drugs to normalize their blood pressure (20). Despite the availability of effective and safe antihypertensive drugs, hypertension and its concomitant risk factors remain uncontrolled in most patients. Hence, there is a need to decode and understand the molecular mechanisms underlying the pathogenesis of hypertension, in order to develop effective diagnostic tools, advance prevention, and improve treatment strategies.

The kidneys are key to the regulation of blood pressure

Na^+ balance

Blood pressure is intimately associated with extracellular fluid volume homeostasis, which itself is determined by Na^+ content (86). Na^+ homeostasis is achieved by balancing the intake and excretion of Na^+. The kidneys are the principal route for Na^+ excretion and are therefore central to long-term stability of blood pressure (9, 22, 25, 86). Studies of Guyton and other investigators were particularly instrumental to linking Na^+ intake and kidney function to the pathogenesis of salt-sensitive hypertension (11, 38, 39, 68). Several physiological, genetic, and clinical studies have shown that an increased blood pressure is driven by a failure of the kidneys to excrete excess Na^+ in a typical high Na^+-low K^+ diet. Na^+ balance is, therefore, key to the homeostatic control of blood pressure. Na^+ is freely filtered at the glomerulus, with ~99% of the filtered load being reabsorbed by Na^+ transporters along the nephron, the smallest functional unit of the kidney (Fig 1) (86). The tubular system starts with the proximal tubule (PT), where ~65% of Na^+ is both passively (~15%) and actively (~50%) reabsorbed (8). In the PT, active Na^+ transport is mainly facilitated by the Na^+/H^+ exchanger type 3 (NHE3) and a variety of solute-specific symporters that reabsorb Na^+ together with phosphate (NaPi's) or organic solutes such as amino acids (*SLC6A19*), glucose (*SLC5A2*) and citrate (*SLC13A1*) (117). In the thick ascending limb of Henle's loop (TAL), ~25% of the filtered Na^+ load is reabsorbed by the furosemide-sensitive NaKCl

cotransporter (NKCC2). Fine-tuning (~7%) of Na^+ reabsorption primarily takes place in the distal convoluted tubule (DCT) by the thiazide-sensitive NaCl cotransporter (NCC) (29). This fine regulation of Na^+ is possible here because it is not affected by tubuloglomerular feedback (33). NCC is apically localized in epithelial cells lining DCT, with a robust expression in the early part of the DCT (DCT1) that decreases into the later part of the DCT (DCT2) (29, 69, 70, 91). Finally, residual Na^+ (~2%) is reabsorbed in the connecting tubule (CNT) and collecting duct (CD) by amiloride-sensitive epithelial Na^+ channel (ENaC) (86). The ENaC abundance increases gradually along the DCT2 and is highly expressed in the CNT and CD (10, 69, 115). The Na^+ reabsorption is an energy consuming process, which is mainly driven by the Na^+/K^+ pump (Na/K-ATPase) localized in the basolateral membrane of all epithelial cells along the nephron (Fig. 1) (116). The Na/K-ATPase transports Na^+ out of the cell and K^+ into the cell by consuming adenosine triphosphate (ATP) (116). Na^+ extrusion from the cell provides the chemical gradient, necessary as driving force for the Na^+ transporters in the apical plasma membrane.

NCC in health and disease

NCC isoforms

Although only ~7% of filtered Na^+ is reabsorbed by NCC, this transport is essential for blood pressure control. The influence of the NCC on blood pressure has been elucidated through observations of diseases that increase or decrease the abundance and/or activity of NCC (12, 35, 122, 143). The presence of NCC was first suggested in urinary bladder of the winter flounder (*Pseudopreuronectes americanus*) (100, 101). Later studies in this tissue demonstrated that the cotransporter was inhibited by thiazide diuretics (124) and the cDNA encoding NCC was cloned and characterized (32). NCC is encoded by the *SLC12A3* gene, which consists of 26 exons (55 kb). In humans, alternate splicing of *SLC12A3* gives rise to three separate isoforms (133), namely NCC_1 (121), NCC_2 (37), and NCC_3 (75). NCC_3 (NP_001119580.1) consists of 1021 amino acids and is the shortest and most extensively studied isoform, as the other two isoforms are not present in rodents (37). NCC_1 (NP_000330.2) is the longest isoform in which splicing of exon 20 results in nine extra amino acids compared to NCC_3 (Fig. 2) (121). NCC_2 (NP_001119579.1) is only one amino acid shorter than NCC_1 by missing glutamine (Q)95 (Fig. 2) (133). Subsequent studies confirmed the presence of both long and short forms of the exon 20 (20a and 20b respectively) as a result of splicing (74). Both NCC_1 and NCC_2 are similar in structure and were shown indistinguishable in experimental assays. Therefore, in this thesis, they will be referred to as NCC_{SV}. Interestingly, NCC_{SV} are only present in humans and higher primates. The importance of NCC_{SV} in (patho)physiological conditions remains unknown. Therefore, the

present thesis aims to investigate the role of NCC_{SV} as well as NCC_3 in several (patho)physiological conditions.

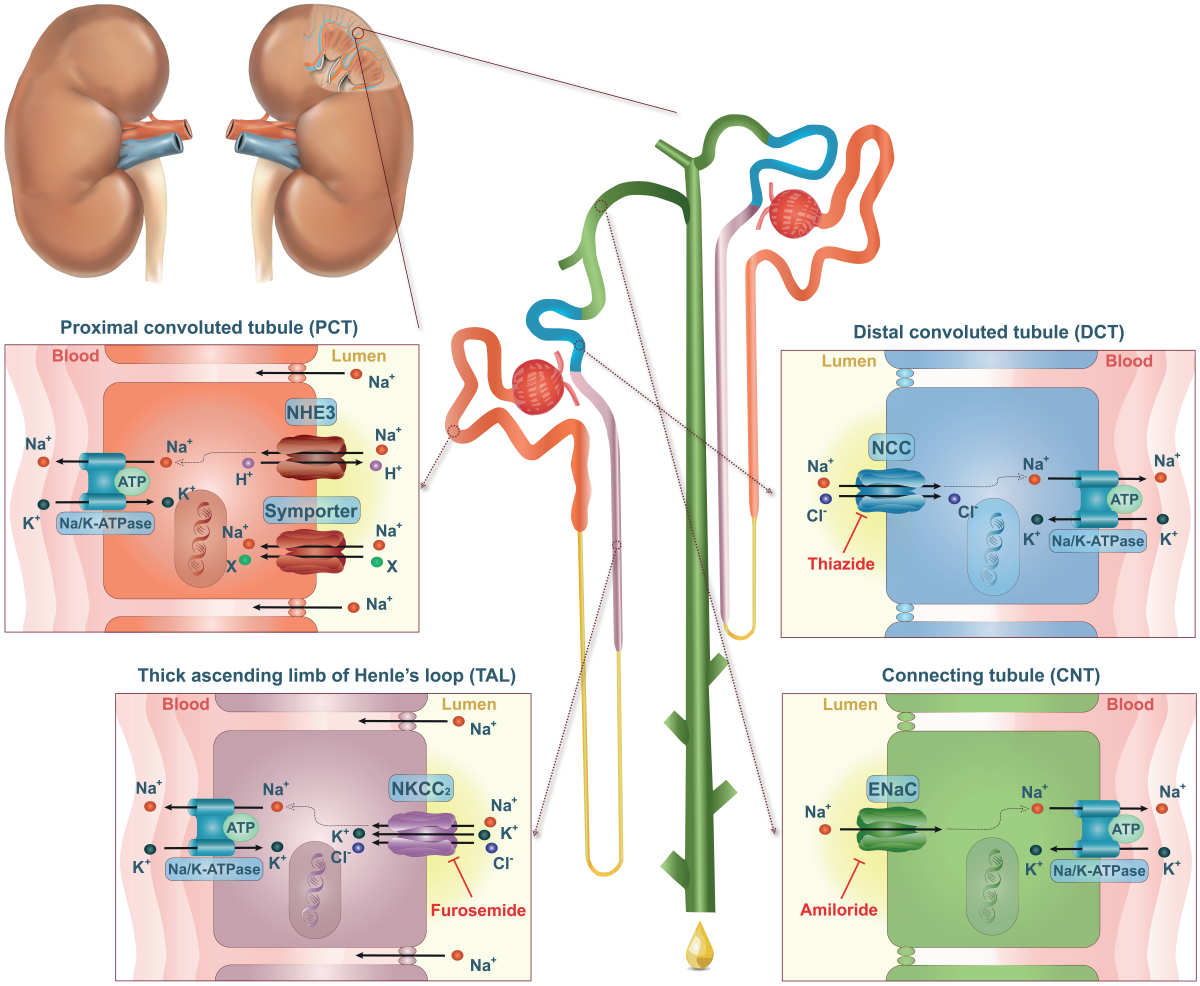

Figure 1 | Na^+ reabsorption in the kidney.

Na^+ transporters along the nephron are responsible for ~99% Na^+ reabsorption. Principal mechanisms of Na^+ reabsorption are shown in the different nephron segments. Basolateral extrusion of Na^+ to the blood occurs by the Na^+/K^+ pump (Na/K-ATPase). This provides the Na^+ gradient, which is the driving force for secondary Na^+ transporters, such as Na^+/H^+ exchanger type 3 (NHE3) and solute-specific symporters in proximal tubule (PT), furosemide-sensitive NaKCl cotransporter (NKCC2) in thick ascending limb of Henle's loop (TAL), thiazide-sensitive NaCl cotransporter (NCC) in distal convolute tubule (DCT) and amiloride-sensitive epithelial Na^+ channel (ENaC) that is localized in the apical membrane of connecting tubule (CNT) and collecting duct (CD).

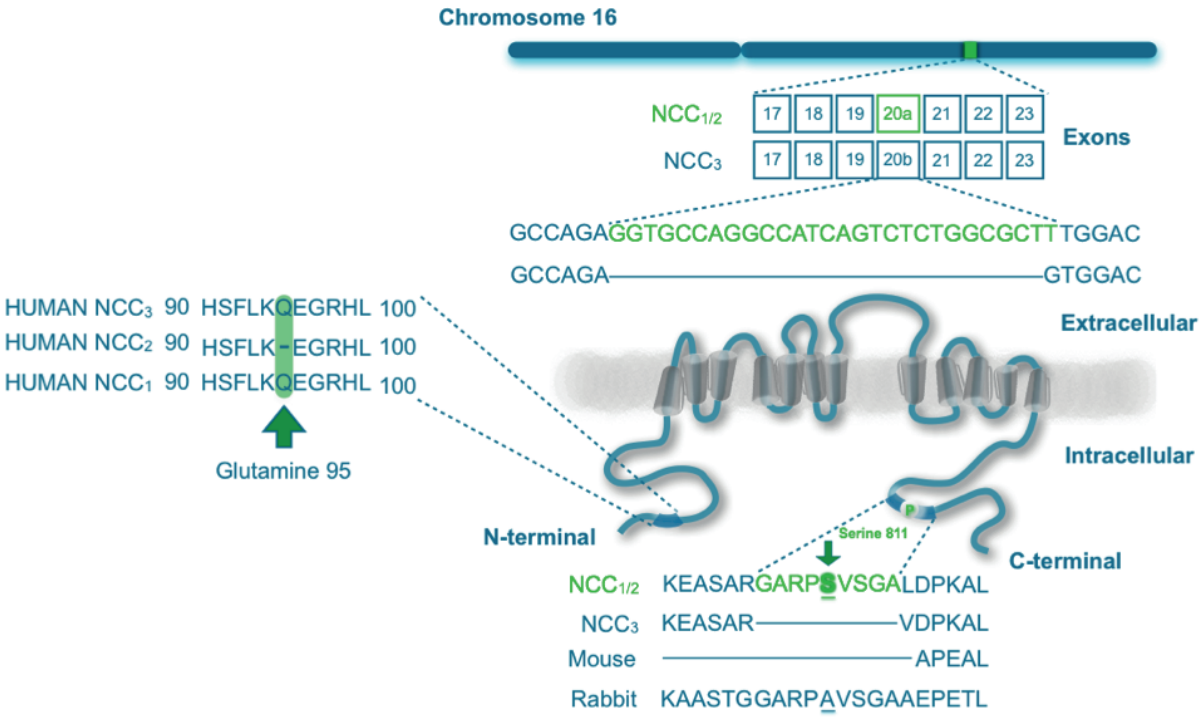

Figure 2 | Splicing of NCC gene.

Schematic representation of the *SLC12A3* gene including exon 20a that encodes for the NCC splice variant (NCC_{SV}, NCC isoform 1 and 2). Topological representation of NCC_{SV} with 12 transmembrane domains and large amino- and carboxy-terminal domains. Serine (S811) is highlighted as putative phosphorylation site in the carboxyl-terminal domain. Left panel shows a multiple alignment of the human NCC_1, NCC_2, and NCC_3 protein sequence. Lower panel shows a multiple sequence alignment of human, mouse, and rabbit NCC to demonstrate the additional nine amino acids in NCC_{SV}.

Genetic factors determining blood pressure

Gitelman syndrome

All hereditary diseases associated with increased or decreased arterial blood pressure are due to mutations in genes encoding renal ion transporters or their regulators (23, 44, 121, 143). Gitelman syndrome (OMIM 263800) is an autosomal recessive disease that results from loss of function mutations in the *NCC* gene. To date, more than 180 mutations throughout the whole NCC protein have been identified (134, 135, 139). Mutations identified in Gitelman syndrome can affect the function of NCC at different levels, including protein synthesis, trafficking, and activity (26). Gitelman syndrome is the most frequent hereditary tubular disorder (1:40,000), characterized by Na^+ wasting, hypokalemic metabolic alkalosis, hypomagnesemia, hypocalciuria and patients have lower blood pressure compared to their age-matched unaffected relatives (35, 122). However, the disease is usually asymptomatic or presents with mild symptoms, of which the most frequent are muscle weakness, desire for Na^+ intake, thirst, urge to urinate during the night and abdominal pain (62). A closely related

tubular salt wasting disorder is Bartter syndrome that results from mutations in the genes *SLC12A1* and *KCNJ1* encoding for NKCC2 and the renal outer medullary K^+ channel (ROMK), respectively (120, 122). Both syndromes are characterized by impaired Na^+ reabsorption that causes mild volume depletion, leading to prominent stimulation of the renin-angiotensin-aldosterone system (RAAS). In Bartter syndrome, this results from a defect in the TAL, while Na^+ transport in the DCT is disturbed in Gitelman syndrome. In both disorders, patients have a normal to low blood pressure despite high RAAS activation. This might conceivably blunt the hypertensive phenotype in patients with essential hypertension, secondary forms of hypertension or environmental factors leading to hypertension.

Familial hyperkalemic hypertension

Familial Hyperkalemic Hypertension (FHHt), also known as pseudohypoaldosteronism type II or Gordon syndrome (OMIM 145260), is a form of hypertension that results from gain of function of NCC. This is a consequence of mutations in *WNK1*, *WNK4* (encoding the with no lysine [WNK] kinases) (143), *KLHL3*, or *CUL3* (respectively coding for the Kelch-like 3 and Cullin 3 components of cullin–RING E3 ligase complexes that ubiquitinate substrates) (12). FHHt is an autosomal dominant or recessive disease, which is characterized by increased renal Na^+ reabsorption, arterial hypertension, hyperkalemia, metabolic acidosis, and hypercalciuria, low plasma renin levels, with normal or low serum aldosterone levels (65, 110, 143, 146). High blood pressure, hyperkalemia and metabolic acidosis in the absence of chronic renal failure are clinical clues to the diagnosis of FHHt that commonly presents at early age, during childhood or adolescence. Patients with these symptoms and clinical abnormalities can be tested for the known FHHt-causing mutations. Genetic screening can be useful to support the administration of thiazides, which act by blocking NCC (53, 77, 99). Strikingly, the hypertension as well as the hyperkalemia and metabolic disorders can be corrected by a low dose of thiazide-type diuretics (53, 77, 99). Therefore, several guidelines for management of hypertension in FFHt patients consider thiazide-type diuretics as first-line therapeutic tool to correct clinical manifestations and laboratory abnormalities caused by this syndrome (51, 53, 99). Hence, genetic testing is key for targeted treatment and can enable personalized control of blood pressure, thereby diminishing target organ damage and ultimately preventing cardiovascular events (108). Both Gitelman syndrome and FHHt demonstrate the relevance of NCC in the (patho)physiology of blood pressure.

Renin-angiotensin-aldosterone system

Aldosterone has been reported as the major regulatory hormone in the transport of Na^+ in the DCT segment of the kidney. The DCT together with CNT and CD are collectively termed the aldosterone-sensitive distal nephron (6, 19, 137). Remarkably, the effects of either Na^+

or K^+ abnormality on the RAAS components can be divergent. Aldosterone is produced by the adrenal gland in two physiological conditions namely hypovolemia and hyperkalemia. During hypovolemia aldosterone stimulates Na^+ reabsorption; during hyperkalemia, aldosterone enhances secretion of K^+ (6). The observation that a single hormone, i.e. aldosterone, has different effects on the Na^+ and K^+ transport has been termed the "aldosterone paradox". Remarkably, aldosterone is elevated in both hypovolemic and hyperkalemic states but leads to distinct physiological responses in the kidney (6). Since RAAS activation is the hallmark of volume depletion but angiotensin II is not affected by changes in the plasma K^+ concentration, it is suggested that angiotensin II plays an important role in discriminating between hypovolemic and hyperkalemic states.

Angiotensin II is known to regulate ENaC and ROMK directly via a complex interactive kinase network involving the WNK kinases (6). Angiotensin II stimulated K^+ deficiency driven by ENaC and ROMK results in increased activity of NCC (141). Recently, it has been shown that plasma K^+ levels directly modulates the WNK kinases in the DCT (130). There are four abundant WNK kinases along the aldosterone-sensitive distal nephron, namely WNK1, kidney-specific WNK1 (KS-WNK1), WNK3, and WNK4 (88). They can affect the Na^+ and K^+ transporters by modulating their trafficking to or from the plasma membrane and by modulating transport activity via phosphorylation. The latter involves the intermediary kinases SPAK (STE20/SPS1-related, proline alanine-rich kinase) and OSR1 (oxidative stress responsive protein type 1) that are phosphorylated and activated by WNK kinases. Subsequently, SPAK and OSR1 can phosphorylate NCC resulting in increased transport activity (28, 126, 151). While the exact mode of action of the different WNK kinases is still under debate, it is generally believed that WNK4 inhibits NCC activity by reducing its plasma membrane abundance. Angiotensin II can directly activate NCC and ENaC (138), but it is also shown to block the inhibitory effect of WNK4 that allows trafficking of NCC to the plasma membrane (150), ultimately increasing Na^+ reabsorption in DCT (113, 114). Furthermore, the WNK kinases can interact with the serum and glucocorticoid-inducible kinase 1 (SGK1) (89), which is known as an important kinase in the regulation of NCC and ENaC (5, 18, 50). Clinically, RAAS is activated in various disease states, including some forms of hypertension (142). Angiotensin receptor blockers are well-known anti-hypertensive drugs that reduce blood pressure by antagonizing angiotensin II type I receptors (43). This shows the clinical relevance of angiotensin II in regulation of the blood pressure (127). The presence of angiotensin II receptors in the basolateral and luminal membranes of DCT epithelial cells offers a potential role for angiotensin II to indirectly regulate Na^+ transport (41, 82).

Posttranslational modifications

Posttranslational modifications including glycosylation, ubiquitylation, and phosphorylation have been extensively investigated and play a crucial role in the regulation of NCC activity (34, 49). These cascades of processing can control the trafficking of the transporter to the plasma membrane and affect its stability at the plasma membrane (34, 49, 60).

Glycosylation

NCC is a membrane glycoprotein and contains 12 transmembrane segments (S) with large intracellular amino- and carboxy-terminal regions, and a large hydrophilic extracellular loop between S7 and S8 (Fig. 2) (32). This loop between S7 and S8, contains glycosylation sites that are essential for the cell surface expression of NCC, thiazide sensitivity and NCC activity (49). It has been suggested that NCC forms functional dimers (27, 33).

Ubiquitylation

Adding the ligands of ubiquitin to lysine residues of a target protein, marks the protein for degradation (34, 140). Ubiquitylation is a powerful way to modulate the activity of NCC protein and was suggested to be involved in endocytosis of the protein at the plasma membrane (Fig. 3) (2, 61). A well-known example of ubiquitin-mediated protein degradation occurs with ENaC, which is ubiquitylated by Nedd4-2 ubiquitin ligase (34). Liddle syndrome, a monogenic hypertensive disease, is caused by mutations in different subunits of ENaC that prevent binding to the Nedd4-2 ubiquitin ligase (34) or affecting the extracellular domain of ENaC (111). As a consequence the ENaC expression in the apical membrane or intrinsic channel activity is increased, resulting in enhanced Na^+ reabsorption that leads to hypertension (31, 123). Interestingly, it has also been shown that Nedd4-2 can interact with NCC, postulating a role for Nedd4-2-mediated ubiquitylation in NCC regulation (61). The SGK1-Nedd4-2 pathway that modulates ENaC activity might also be linked to NCC (5). Generally, aldosterone increases SGK1 expression, which in turn phosphorylates Nedd4-2, thereby promoting interaction with 14-3-3 proteins. Subsequently, this interaction reduces the ligase activity of Nedd4-2 towards ENaC (18, 50). There is increasing evidence that aldosterone and SGK1 also modulate NCC by the ubiquitin ligase Nedd4-2 (5). *In vitro*, Nedd4-2 activity induced a reduction in NCC surface expression and it was observed that activation of SGK1 disrupted the Nedd4-2-NCC interaction (5). In an inducible knockout model of Nedd4-2, knockdown of the ubiquitin ligase Nedd4-2 provoked a dramatic increase in NCC expression (5, 18). In addition, there are several studies indicating that phosphorylation of NCC could interfere with its ubiquitylation, thereby playing a dual role in modulating NCC function (107, 148).

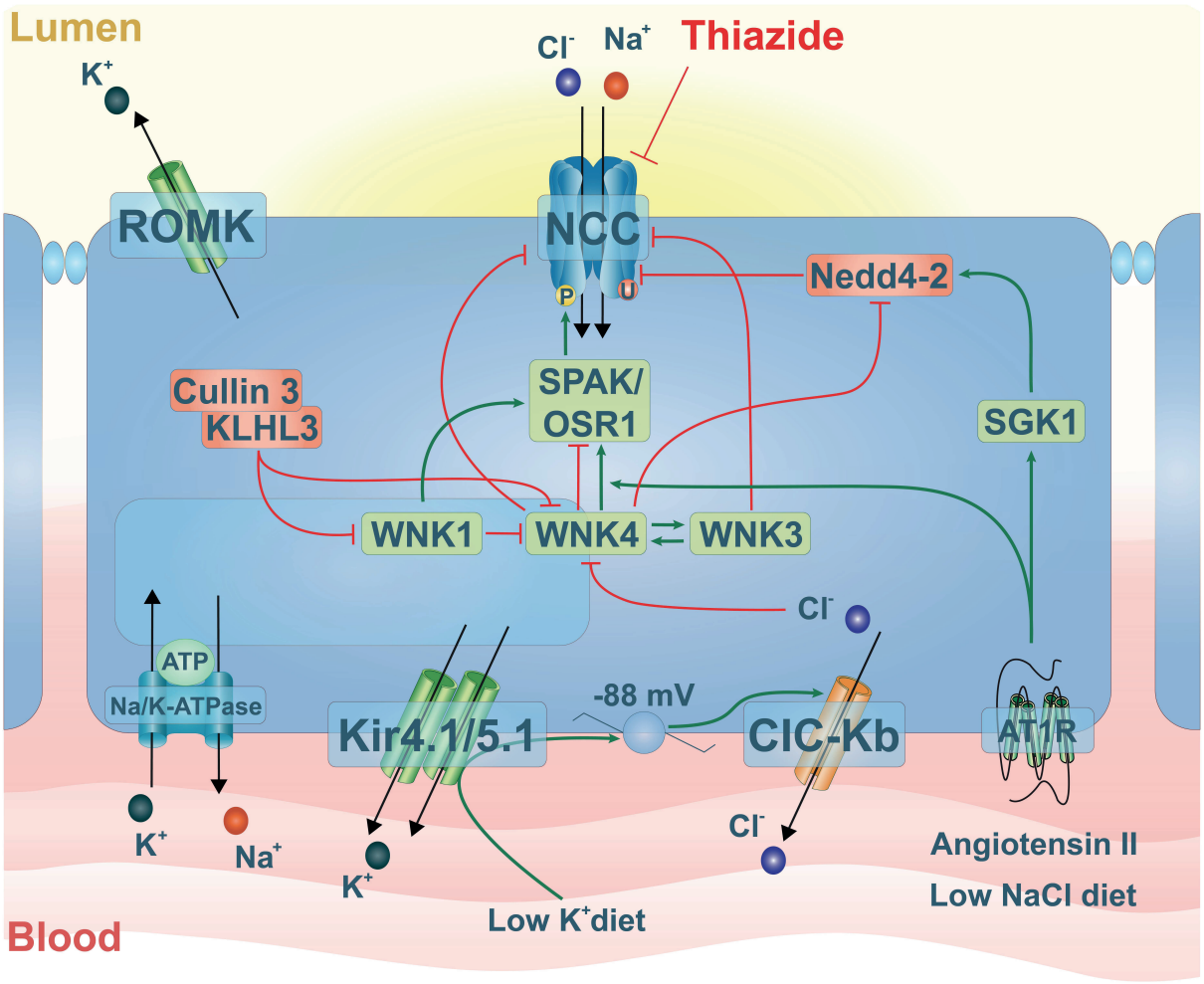

Figure 3 | NCC regulation by kinases.

Regulation of NCC by with no lysine (WNKs) kinases. The various interactions of the NCC regulatory pathway are shown as *green arrows* (stimulatory) or *red lines* (inhibitory). Phosphorylation is indicated with the symbol *P*. WNK4 is capable of activating SPAK (STE20/SPS1-related, proline alanine-rich kinase) and OSR1 (oxidative stress responsive protein type 1). WNK4 regulates Nedd4-2-mediated ubiquitylation of NCC. Kelch-like 3 (*KLHL3*) and Cullin 3 (*CUL3*), components of cullin–RING E3 ligase complexes, ubiquitinate WNK1 and WNK4 resulting in degradation of WNK1 and WNK4. The K^+ channel, comprising Kir4.1, likely with Kir5.1, appears to be the predominant conductive pathway for K^+ exit along the basolateral membrane. Cl^- channel (CLC-Kb) is responsible for efflux of Cl^-. Plasma K^+ levels regulate intracellular Cl^- concentration via modulating the basolateral membrane voltage. Low intracellular Cl^- stimulates WNK-SPAK/OSR1. Downstream, NCC is phosphorylated, activated, by SPAK/OSR1.

Phosphorylation of NCC

Phosphorylation is considered one of the most important posttranslational modification processes in the regulation of NCC activity. Therefore, protein phosphorylation mechanisms have been comprehensively investigated (102, 103, 147). The amino-terminal domain of NCC contains several key phosphorylation sites including threonines 48, 55 and 60 and serines 73 and 91 (T48, T55, T60, S73, S91 in humans, and T46, T53, T58, S71, S91 in rodents, respectively) (34). These residues are targets of the serine-threonine kinases SPAK

and OSR1, which are activated by WNK kinases (92, 110). Several studies have shown an increase in NCC activity by augmented phosphorylation at these sites (28, 92, 126, 151). To investigate the role of these residues, the sites of phosphorylation were eliminated by site-directed mutations, by changing T48; T55; T60; S73 and S91 to alanine (T48; T55A; T60A; S73A; S91A), representing the inactive form of the NCC protein as a non-phosphorylable amino acid. Eliminating T48, T55, T60, as well as S73 and S91, decreased basal activity of NCC and prevented activation of NCC (34, 102, 148). Interestingly, several studies have shown that changing T60 to a non-phosphorylated amino acid (T60A) prevented or reduced the phosphorylation at the other sites (T48, T55, S73 or S91), suggesting that T60 is a key modulator in the regulation of NCC activity (34, 102, 148). Table 1 shows a compilation of studies where different NCC phosphorylation sites have been analyzed under different conditions and stimuli. All three human NCC isoforms contain the T55 and T60 residues that are essential mediators of NCC activity. Recently, a new phosphorylation site located at S811 in NCC_{SV} was identified (37). For decades, NCC_3 has been extensively investigated in patho(physiological) conditions, leaving NCC_{SV} unexplored. To date, most studies measuring NCC activity used conventional models such as rodents, *Xenopus laevis* and renal cell lines. The lack of NCC_{SV} in these models and non-invasive method to investigate human NCC hampered studying the role of NCC_{SV} in renal Na^+ handling and blood pressure.

Calcineurin inhibitor-induced NCC activity

The calcineurin inhibitors (CNIs) cyclosporine A (CsA) and tacrolimus (Tac) are widely used to prevent rejection of transplanted organs (48). Although both CsA and Tac exert their principal immunosuppressive effects through inhibition of the same target protein, calcineurin, they differ in cytoplasmic-binding proteins, namely cyclophilins and FKBP12 for CsA and Tac, respectively (48). A common side effect of CNIs is hypertension, although CsA appears more hypertensinogenic than Tac (14, 15, 73). The clinical characteristics of CNI-treated patients sometimes resemble that of FHHt (4, 93). Several studies have shown that CNIs increase NCC activity possibly contributing to hypertension (47, 66). Some reports suggest that CNIs do not activate NCC directly, but it activates NCC via the WNKs, and that inhibition of calcineurin is required for this effect (66, 79). Recently, it was demonstrated in mice that acute Tac treatment increases the NCC activity, and this acute regulatory system mediated by calcineurin is shown to be independent of the WNK-SPAK signaling cascade (119).

Table 1 | Phosphorylation of NCC at specific phosphorylation sites under various experimental conditions.

Experimental model	Stimulus	Effect	Phosphorylation site*	Kinase involved	Ref
COS7 cells	$T^{55}D$ $T^{60}D$ and $S^{73}D$ NCC mutants	↑	T^{55}, T^{60}, S^{73}	?	(60)
Xenopus laevis oocytes	Angiotensin II	↑↑	T^{55}	WNK4-SPAK	(113)
Rat	ACEI	↓	T^{55}, T^{60}	SPAK	(67)
Rat	Angiotensin II	↑↑	T^{55}, T^{60}	SPAK	(67)
Xenopus laevis oocytes	Low concentration of Cl^-	↑↑	T^{55}, T^{60}, S^{73}	?	(92)
Rat	Vasopressin	↑	T^{55}, T^{60}	WNK4-SPAK/OSR1	(94)
HEK 293 cells	Hypotonic with low concentration of Cl^-	↑↑	T^{48}, T^{55}, T^{60}, S^{91}	WNK1-SPAK/OSR1	(102)
Mouse	Low NaCl diet	↑↑	S^{73}	WNK4-SPAK/OSR1	(19)
Mouse	Low NaCl and K^+ diet	↑↑	T^{55}, S^{73}	SGK1	(136)
Mouse	$Wnk4^{D561A/+}$ Knockin	↓↓	T^{60}	WNK4	(149)
Mouse	Angiotensin II / Aldosterone	↑↑	T^{55}, T^{60},	SPAK	(137)
Rat	Aldosterone / low Na^+ diet	↑	T^{55}, T^{60}, S^{124}	?	(106)
Mouse	$T^{60}M$ NCC Knockin	↓	T^{55}, T^{60}, S^{73}	independent of WNK4-SPAK	(148)
MDCK Cells	$T^{60}A$ and $T^{60}M$ NCC mutants	↓	T^{55}, T^{60}, S^{73}	independent of WNK4-SPAK	(148)
COS7 / HEK 293 cells	Angiotensin II / Forskolin	↑	?	PKC- and PKA-WNK4-SPAK	(17)
Mouse	Angiotensin II / vasopressin	↑	T^{60}	PKC- and PKA-WNK4	(17)

*Number corresponds to the human NCC sequence. $T^{55}D$, $T^{60}D$ and $S^{73}D$, constitutively phosphorylated NCC mutants; $T^{55}A$, $T^{60}A$, and $T^{60}M$, non-phosphorylated NCC mutants; HEK293 cells, Human embryonic kidney 293 cells; DCT, distal convoluted tubule; WNK, with no lysine; SPAK, Ste20-related proline-alanine-rich kinase; OSR1, oxidative stress response 1; ACEI, angiotensin-converting enzyme inhibitor; SGK1, glucocorticoid inducible kinase 1; MDCK, Madin-Darby canine kidney cells.

The current comprehensive model of NCC regulation

NCC is processed in the endoplasmic reticulum and Golgi apparatus, and trafficked to the plasma membrane, where it is activated by phosphorylation. For thiazide-sensitive Na^+ reabsorption to occur in the DCT, two processes must take place (125). First, a sufficient number of NCC must be present at the DCT apical membrane, which is regulated by many kinases that regulate the forward-trafficking and degradation process of the NCC protein. Second, NCC present at the DCT lumen must be switched on by phosphorylation (125). Two related serine-threonine kinases, SPAK (55) and OSR1 (128), phosphorylate NCC directly,

by transferring phosphate groups from ATP to serine and threonine residues present in the intracellular amino-terminal domain of NCC (102). Phosphorylation at these residues enhances the ability of the cotransporter to transport Na^+, presumably by altering its protein conformation. SPAK and OSR1 are the two downstream substrates of WNK1, WNK3 and WNK4 (40, 83, 88, 102). WNKs appear to modulate both the trafficking and phosphorylation of NCC by separate mechanisms (45). These intracellular signaling cascade that controls NCC abundance and activity has been extensively investigated in the past decade (Fig. 3). Proteins involved in ubiquitylation including Nedd4-2 (5, 105), KLHL3 (12, 71) and CUL3 (12) were also found to regulate NCC. Although, WNK1 and WNK4 mutations were the first to be implicated in the pathogenesis of FHHt, most FHHt-affected individuals harbor mutations in two other genes: the CUL3 and its adaptor, KLHL3 (12, 71). Together Cullin3 and KLHL3 form a Cullin-RING type E3 ubiquitin ligase complex that targets WNK kinases for ubiquitination to promote their proteasomal degradation (88). Additionally, SGK1 was also found to regulate NCC. However it is suggested that SGK1 does not interact directly with NCC, but rather through WNK4 and Nedd4-2 (5, 104, 110, 136). This pathway seems to be translated, at least in part, by SGK1-induced WNK4 phosphorylation that results in reduced inhibition of WNK4 on NCC (104, 110). Cell shrinkage or a decrease in intracellular Cl^- concentration, or both, triggers the phosphorylation of NCC. WNK1 crystal structure showed that WNK1 binds Cl^- near the catalytic lysine in subdomain 1, inhibiting its autophosphorylation and, in turn, activity (97). In low Cl^- conditions, this WNK1 auto-phosphorylation results in OSR1/SPAK-NCC phosphorylation cascade (88, 97). Recently, it has been shown that plasma K^+ levels regulate NCC through changes in intracellular Cl^- thereby modulating WNK kinases (130). Lower plasma K^+ concentration can enhance Cl^- efflux from DCT cells through both electrogenic and electroneutral mechanisms (129, 130). The extracellular K^+ levels, independent of hormonal effects, directly modulates the WNK-SPAK-OSR1-NCC cascade. This may explain, in part, the hypertension and cardiovascular mortality observed in individuals who consume a low K^+ diet and suggests that dietary K^+ deficiency activates NCC leading to hypertension.

Urinary extracellular vesicles

Almost all cells in our body release vesicles as way of intercellular communication. They are formed when multivesicular bodies within the cell merge with the plasma membrane and release internal vesicles into the extracellular space (Fig. 4) (46). In the kidney, these vesicles can be shed into the urine and are termed urinary extracellular vesicles (uEVs). uEVs, which also includes urinary exosomes, are nanosized vesicles (30-120 nm) that contain membrane and cytosolic protein, DNA and RNA that are conserved and protected

from degradation (98, 112). These uEVs contain membrane and cytosolic protein, DNA and RNA that are conserved and protected from degradation (112). The cargo of uEVs reflects changes in the expression of different proteins present in the epithelial cells of the DCT, including total NCC and phosphorylated form of NCC (Fig. 4) (52, 133, 137). Hence, urine provides a non-invasive source to study the regulation of NCC in the kidney (37, 137, 144). Indeed, it has been shown that patients with Gitelman syndrome display a decreased NCC abundance in uEVs (23, 57). Inversely, patients with FHHt demonstrate higher NCC levels in the kidney and this increased abundance was also observed in uEVs of patients with FHHt (137). Furthermore, administration of a mineralocorticoid like aldosterone rapidly increased the abundance of total and phosphorylated NCC in uEVs (144). This suggests that NCC abundance in uEVs reflects the actual state of NCC expression in the kidney. Together, the uEVs provide a unique novel tool to study the regulation of the three NCC isoforms in the human kidney, and may have clinical utility for biomarker investigation of a variety of physiological and pathological conditions.

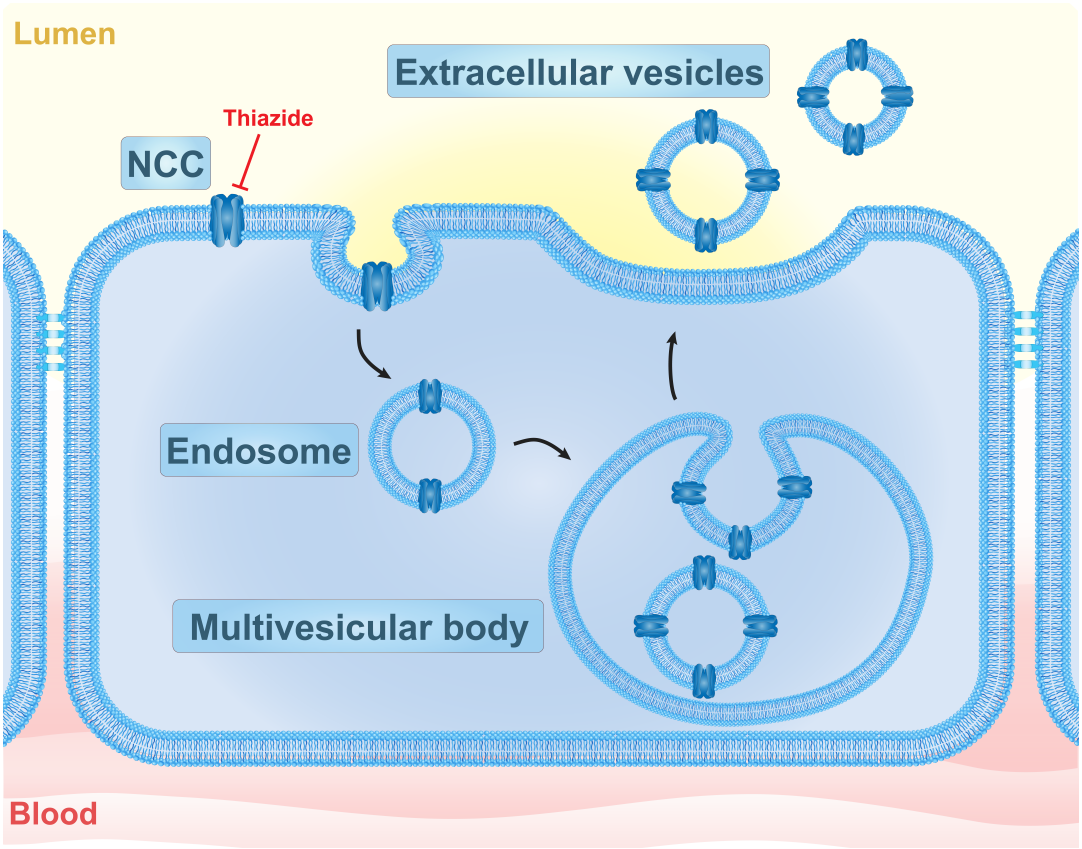

Figure 4 | Release of urinary extracellular vesicles in distal convoluted tubule (DCT).

The plasma membrane buds inward, forming a membrane-bound vacuole, an endosome. This endosome goes through several changes as it matures from an early endosome to a late endosome. Most notably, the endosomal membrane buds inward and pinches off to make membrane-bound vesicles inside the endosome and the endosome is now titled a multivesicular body. The multivesicular body travel to and fuse with the plasma membrane, releasing its contents, which, once existing outside the cell, are called exosomes (size 30–120 nm).

Aims of the thesis

The paragraphs above have illustrated the importance of NCC function in the (patho)physiology of hypertension. While the third isoform, NCC_3 has been the focus of intense research over the last decades, the regulation and function of NCC_{SV} in blood pressure control remained largely unexplored. To date, the detailed localization of NCC_{SV} in human kidney, the regulatory network, the relationship with NCC_3 and its relevance in renal Na^+ handling remains to be elucidated. A better understanding of these isoforms is critical to unravel the molecular events underlying the pathogenesis of essential hypertension, and to develop effective therapeutic strategies to combat the dysregulation of blood pressure. Therefore, this thesis aims to study the role of all three NCC isoforms in various (patho)physiological conditions. The goal of **Chapter 2** is to determine the abundance and localization of previously underrepresented NCC isoforms compared to NCC_3 in the human kidney. Additionally, the functional properties of the NCC_{SV} as well as its regulation in physiological conditions is studied. In **Chapter 3** the aim is to study the effect of various anti-hypertensive treatments on the abundance and phosphorylation of all three NCC isoforms in uEVs of essential hypertensive patients, and to explore the relationship between NCC abundance in uEVs and changes in blood pressure. The aim of **Chapter 4** is to investigate the role of the new S811 phosphorylation site in NCC_{SV} function, determine the interaction of NCC_{SV} with NCC_3 and to study the effect of NCC_{SV} S811 phosphorylation on the function of NCC_3. In **Chapter 5** of this thesis a large-scale study is performed to investigate the effect of CNIs, including cyclosporine A and tacrolimus on the abundance of both total and phosphorylated NCC in uEVs, and assessed whether NCC abundance in uEVs predicts the blood pressure response to thiazide diuretics. In order to confirm the effect of CNIs on NCC in the kidney, an *ex vivo* study is conducted in mice cortical tubules exposed to cyclosporine. In **Chapter 6**, in mice, the effect of high Na^+-low K^+ diet was not only investigated on NCC regulation, but its affect was also studied on Mg^{2+}, Ca^{2+} and phosphate (Pi) homeostasis. Finally, the results of this thesis are summarized and discussed in **Chapter 7**.

References

1. Adrogué HJ, Madias NE. Sodium surfeit and potassium deficit: keys to the pathogenesis of hypertension. *J Am Soc Hypertens* 8: 203–213, 2014.
2. Amit S, Ben-Neriah Y. NF-κB activation in cancer: a challenge for ubiquitination- and proteasome-based therapeutic approach. *Seminars in Cancer Biology* 13: 15–28, 2003.
3. Appel LJ, Moore TJ, Obarzanek E, Vollmer WM, Svetkey LP, Sacks FM, Bray GA, Vogt TM, Cutler JA, Windhauser MM, Lin PH, Karanja N. A clinical trial of the effects of dietary patterns on blood pressure. DASH Collaborative Research Group. *N Engl J Med* 336: 1117–1124, 1997.
4. Arnold JE, Healy JK. Hyperkalemia, hypertension and systemic acidosis without renal failure associated with a tubular defect in potassium excretion. *Am J Med* 47: 461–472, 1969.
5. Arroyo JP, Lagnaz D, Ronzaud C, Vazquez N, Ko BS, Moddes L, Ruffieux-Daidié D, Hausel P, Koesters R, Yang B, Stokes JB, Hoover RS, Gamba G, Staub O. Nedd4-2 modulates renal Na+-Cl- cotransporter via the aldosterone-SGK1-Nedd4-2 pathway. *J Am Soc Nephrol* 22: 1707–1719, 2011.
6. Arroyo JP, Ronzaud C, Lagnaz D, Staub O, Gamba G. Aldosterone paradox: differential regulation of ion transport in distal nephron. *Physiology (Bethesda)* 26: 115–123, 2011.
7. Ascherio A, Rimm EB, Giovannucci EL, Colditz GA, Rosner B, Willett WC, Sacks F, Stampfer MJ. A prospective study of nutritional factors and hypertension among US men. *Circulation* 86: 1475–1484, 1992.
8. Berry CA, Rector FC. Mechanism of proximal NaCl reabsorption in the proximal tubule of the mammalian kidney. *Semin Nephrol* 11: 86–97, 1991.
9. Bianchi G, Fox U, Di Francesco GF, Bardi U, Radice M. The hypertensive role of the kidney in spontaneously hypertensive rats. *Clin Sci Mol Med Suppl* 45 Suppl 1: 135s–9, 1973.
10. Biner HL, Arpin-Bott M-P, Loffing J, Wang X, Knepper M, Hebert SC, Kaissling B. Human cortical distal nephron: distribution of electrolyte and water transport pathways. *J Am Soc Nephrol* 13: 836–847, 2002.
11. Borst JG, Borst-de Geus A. Hypertension explained by Starling's theory of circulatory homoeostasis. *Lancet* 1: 677–682, 1963.
12. Boyden LM, Choi M, Choate KA, Nelson-Williams CJ, Farhi A, Toka HR, Tikhonova IR, Bjornson R, Mane SM, Colussi G, Lebel M, Gordon RD, Semmekrot BA, Poujol A, Välimäki MJ, De Ferrari ME, Sanjad SA, Gutkin M, Karet FE, Tucci JR, Stockigt JR, Keppler-Noreuil KM, Porter CC, Anand SK, Whiteford ML, Davis ID, Dewar SB, Bettinelli A, Fadrowski JJ, Belsha CW, Hunley TE, Nelson RD, Trachtman H, Cole TRP, Pinsk M, Bockenhauer D, Shenoy M, Vaidyanathan P, Foreman JW, Rasoulpour M, Thameem F, Al-Shahrouri HZ, Radhakrishnan J, Gharavi AG, Goilav B, Lifton RP. Mutations in kelch-like 3 and cullin 3 cause hypertension and electrolyte abnormalities. *Nature* 482: 98–102, 2012.
13. Campese VM, Parise M, Karubian F, Bigazzi R. Abnormal renal hemodynamics in black salt-sensitive patients with hypertension. *Hypertension* 18: 805–812, 1991.
14. Canzanello V. Evolution of cardiovascular risk after liver transplantation: A comparison of cyclosporine A and tacrolimus (FK506). *Liver Transplantation* 3: 1–9, 1997.
15. Canzanello VJ, Textor SC, Taler SJ, Schwartz LL, Porayko MK, Wiesner RH, Krom RAF. Late hypertension after liver transplantation: A comparison of cyclosporine and tacrolimus (FK 506). *Liver Transplantation and Surgery* 4: 328–334, 1998.
16. Carretero OA, Oparil S. Essential hypertension. Part I: definition and etiology. *Circulation* 101: 329–335, 2000.
17. Castañeda-Bueno M, Arroyo JP, Zhang J, Puthumana J, Yarborough O III, Shibata S, Rojas-Vega L, Gamba G, Rinehart J, Lifton RP. Phosphorylation by PKC and PKA regulate the kinase activity and downstream signaling of WNK4. *Proc Natl Acad Sci* 114: E879–E886, 2017.
18. Castañeda-Bueno M, Gamba G. Mechanisms of sodium-chloride cotransporter modulation by angiotensin II. *Curr Opin Nephrol Hypertens* 21: 516–522, 2012.
19. Chiga M, Rai T, Yang S-S, Ohta A, Takizawa T, Sasaki S, Uchida S. Dietary salt regulates the phosphorylation of OSR1/SPAK kinases and the sodium chloride cotransporter through aldosterone. *Kidney Int* 74: 1403–1409, 2008.
20. Chobanian AV. The Seventh Report of the Joint National Committee on Prevention, Detection,

Evaluation, and Treatment of High Blood Pressure: the JNC 7 report. *JAMA* 289: 2560–2572, 2003.

21. Chockalingam A. Impact of World Hypertension Day. *Can J Cardiol* 23: 517–519, 2007.
22. Coffman TM, Crowley SD. Kidney in hypertension: guyton redux. *Hypertension* 51: 811–816, 2008.
23. Corbetta S, Raimondo F, Tedeschi S, Syren M-L, Rebora P, Savoia A, Baldi L, Bettinelli A, Pitto M. Urinary exosomes in the diagnosis of Gitelman and Bartter syndromes. *Nephrology Dialysis Transplantation* 30: 621–630, 2015.
24. Cutler JA. High blood pressure and end-organ damage. *J Hypertens Suppl* 14: S3–6, 1996.
25. Dahl LK, Heine M. Primary role of renal homografts in setting chronic blood pressure levels in rats. *Circ Res* 36: 692–696, 1975.
26. de Jong JC, Van Der Vliet WA, van den Heuvel LPWJ, Willems PHGM, Knoers NVAM, Bindels RJM. Functional expression of mutations in the human NaCl cotransporter: evidence for impaired routing mechanisms in Gitelman's syndrome. *J Am Soc Nephrol* 13: 1442–1448, 2002.
27. de Jong JC, Willems PHGM, Mooren FJM, van den Heuvel LPWJ, Knoers NVAM, Bindels RJM. The structural unit of the thiazide-sensitive NaCl cotransporter is a homodimer. *J Biol Chem* 278: 24302–24307, 2003.
28. Dimke H, San-Cristobal P, de Graaf M, Lenders JW, Deinum J, Hoenderop JGJ, Bindels RJM. γ-Adducin stimulates the thiazide-sensitive NaCl cotransporter. *J Am Soc Nephrol* 22: 508–517, 2011.
29. Ellison DH, Velazquez H, Wright FS. Thiazide-sensitive sodium chloride cotransport in early distal tubule. *Am J Physiol* 253: F546–54, 1987.
30. ESH ESC Task Force for the Management of Arterial Hypertension. 2013 Practice guidelines for the management of arterial hypertension of the European Society of Hypertension (ESH) and the European Society of Cardiology (ESC). *J Hypertens* 31: 1925, 2013.
31. Fakitsas P, Adam G, Daidié D, van Bemmelen MX, Fouladkou F, Patrignani A, Wagner U, Warth R, Camargo SMR, Staub O, Verrey F. Early aldosterone-induced gene product regulates the epithelial sodium channel by deubiquitylation. *J Am Soc Nephrol* 18: 1084–1092, 2007.
32. Gamba G, Saltzberg SN, Lombardi M, Miyanoshita A, Lytton J, Hediger MA, Brenner BM, Hebert SC. Primary structure and functional expression of a cDNA encoding the thiazide-sensitive, electroneutral sodium-chloride cotransporter. *Proc Natl Acad Sci* 90: 2749–2753, 1993.
33. Gamba G. The thiazide-sensitive Na+-Cl- cotransporter: molecular biology, functional properties, and regulation by WNKs. *Am J Physiol Renal Physiol* 297: F838–48, 2009.
34. Gamba G. Regulation of the renal Na+-Cl− cotransporter by phosphorylation and ubiquitylation. *Am J Physiol Renal Physiol* 303: F1573–F1583, 2012.
35. Gitelman HJ, Graham JB, Welt LG. A new familial disorder characterized by hypokalemia and hypomagnesemia. *Trans Assoc Am Physicians* 79: 221–235, 1966.
36. Go AS, Mozaffarian D, Roger VL, Benjamin EJ, Berry JD, Blaha MJ, Dai S, Ford ES, Fox CS, Franco S, Fullerton HJ, Gillespie C, Hailpern SM, Heit JA, Howard VJ, Huffman MD, Judd SE, Kissela BM, Kittner SJ, Lackland DT, Lichtman JH, Lisabeth LD, Mackey RH, Magid DJ, Marcus GM, Marelli A, Matchar DB, McGuire DK, Mohler ER, Moy CS, Mussolino ME, Neumar RW, Nichol G, Pandey DK, Paynter NP, Reeves MJ, Sorlie PD, Stein J, Towfighi A, Turan TN, Virani SS, Wong ND, Woo D, Turner MB, American Heart Association Statistics Committee and Stroke Statistics Subcommittee. Heart disease and stroke statistics-2014 update: a report from the American Heart Association. *Circulation* 129: e28–e292, 2014.
37. Gonzales PA, Pisitkun T, Hoffert JD, Tchapyjnikov D, Star RA, Kleta R, Wang NS, Knepper MA. Large-scale proteomics and phosphoproteomics of urinary exosomes. *J Am Soc Nephrol* 20: 363–379, 2009.
38. Guyton AC, Coleman TG, Cowley AV, Scheel KW, Manning RD, Norman RA. Arterial pressure regulation. Overriding dominance of the kidneys in long-term regulation and in hypertension. *Am J Med* 52: 584–594, 1972.
39. Guyton AC. Blood pressure control-special role of the kidneys and body fluids. *Science* 252: 1813–1816, 1991.
40. Hadchouel J, Ellison DH, Gamba G. Regulation of Renal Electrolyte Transport by WNK and

SPAK-OSR1 Kinases. *Annu Rev Physiol* 78: 367–389, 2016.

41. Harrison-Bernard LM, Navar LG, Ho MM, Vinson GP, el-Dahr SS. Immunohistochemical localization of ANG II AT1 receptor in adult rat kidney using a monoclonal antibody. *Am J Physiol* 273: F170–7, 1997.
42. He J, Whelton PK, Appel LJ, Charleston J, Klag MJ. Long-term effects of weight loss and dietary sodium reduction on incidence of hypertension. *Hypertension* 35: 544–549, 2000.
43. Hegner G, Faust G, Freytag F, Meilenbrock S, Sullivan J, Bodin F. Valsartan, a new angiotensin II antagonist for the treatment of essential hypertension: efficacy and safety compared to hydrochlorothiazide. *Eur J Clin Pharmacol* 52: 173–177, 1997.
44. HJ G, JB G, LG W. A new familial disorder characterized by hypokalemia and hypomagnesemia. *Trans Assoc Am Physicians* 79: 221–235, 1965.
45. Hoorn EJ, Ellison DH. WNK kinases and the kidney. *Experimental Cell Research* 318: 1020–1026, 2012.
46. Hoorn EJ, Pisitkun T, Zietse R, GROSS P, FROKIAER J, WANG NS, Gonzales PA, Star RA, Knepper MA. Prospects for urinary proteomics: exosomes as a source of urinary biomarkers. *Nephrology (Carlton)* 10: 283–290, 2005.
47. Hoorn EJ, Walsh SB, McCormick JA, Fürstenberg A, Yang C-L, Roeschel T, Paliege A, Howie AJ, Conley J, Bachmann S, Unwin RJ, Ellison DH. The calcineurin inhibitor tacrolimus activates the renal sodium chloride cotransporter to cause hypertension. *Nat Med* 17: 1304–1309, 2011.
48. Hoorn EJ, Walsh SB, McCormick JA, Zietse R, Unwin RJ, Ellison DH. Pathogenesis of calcineurin inhibitor–induced hypertension. *J Nephrol* 25: 269–275, 2012.
49. Hoover RS, Poch E, Monroy A, Vazquez N, Nishio T, Gamba G, Hebert SC. N-Glycosylation at two sites critically alters thiazide binding and activity of the rat thiazide-sensitive Na(+):Cl(-) cotransporter. *J Am Soc Nephrol* 14: 271–282, 2003.
50. Ichimura T, Yamamura H, Sasamoto K, Tominaga Y, Taoka M, Kakiuchi K, Shinkawa T, Takahashi N, Shimada S, Isobe T. 14-3-3 Proteins Modulate the Expression of Epithelial Na+ Channels by Phosphorylation-dependent Interaction with Nedd4-2 Ubiquitin Ligase. *J Biol Chem* 280: 13187–13194, 2005.
51. Institute for Quality and Efficiency in Health Care. Different antihypertensive drugs as first line therapy in patients with essential hypertension: Executive summary of final report A05-09, Version 1.0.
52. Isobe K, Mori T, Asano T, Kawaguchi H, Nonoyama S, Kumagai N, Kamada F, Morimoto T, Hayashi M, Sohara E, Rai T, Sasaki S, Uchida S. Development of enzyme-linked immunosorbent assays for urinary thiazide-sensitive Na-Cl cotransporter measurement. *Am J Physiol Renal Physiol* 305: F1374–81, 2013.
53. James PA, Oparil S, Carter BL, Cushman WC, Dennison-Himmelfarb C, Handler J, Lackland DT, LeFevre ML, MacKenzie TD, Ogedegbe O, Smith SC, Svetkey LP, Taler SJ, Townsend RR, Wright JT, Narva AS, Ortiz E. 2014 evidence-based guideline for the management of high blood pressure in adults: report from the panel members appointed to the Eighth Joint National Committee (JNC 8). *JAMA* 311: 507–520, 2014.
54. Janghorbani M, Aminorroaya A, Amini M. Comparison of Different Obesity Indices for Predicting Incident Hypertension. *High Blood Press Cardiovasc Prev* 12: 114–10, 2017.
55. Johnston AM, Naselli G, Gonez LJ, Martin RM, Harrison LC, DeAizpurua HJ. SPAK, a STE20/SPS1-related kinase that activates the p38 pathway. *Oncogene* 19: 4290–4297, 2000.
56. Joint National Committee on Prevention DEATOHBP. The sixth report of the Joint National Committee on Prevention, Detection, Evaluation, and Treatment of High Blood Pressure (JNC VI). *Arch Intern Med* 157: 2413–2446, 1997.
57. Joo KW, Lee JW, Jang HR, Heo NJ, Jeon US, Oh YK, Lim CS, Na KY, Kim J, Cheong HII, Han JS. Reduced urinary excretion of thiazide-sensitive Na-Cl cotransporter in Gitelman syndrome: Preliminary data. *American Journal of Kidney Diseases* 50: 765–773, 2007.
58. Kearney PM, Whelton M, Reynolds K, Muntner P, Whelton PK, He J. Global burden of hypertension: analysis of worldwide data. *Lancet* 365: 217–223, 2005.
59. Kelley GA, Kelley KS. Progressive resistance exercise and resting blood pressure : A meta-analysis of randomized controlled trials. *Hypertension* 35: 838–843, 2000.
60. Khan MZH, Sohara E, Ohta A, Chiga M, Inoue Y, Isobe K, Wakabayashi M, Oi K, Rai T, Sasaki S, Uchida S. Phosphorylation of Na-Cl cotransporter by OSR1 and SPAK kinases

regulates its ubiquitination. *Biochem Biophys Res Commun* 425: 456–461, 2012.

61. Ko B, Kamsteeg E-J, Cooke LL, Moddes LN, Deen PMT, Hoover RS. RasGRP1 stimulation enhances ubiquitination and endocytosis of the sodium-chloride cotransporter. *Am J Physiol Renal Physiol* 299: F300–F309, 2010.
62. Koçkara AŞ, Candan F, Hüzmeli C, Kayataş M, Alaygut D. Gitelman's syndrome associated with chondrocalcinosis: a case report. *Renal Failure* 35: 1285–1288, 2013.
63. Kotchen TA, Cowley AW, Frohlich ED. Salt in health and disease--a delicate balance. *N Engl J Med* 368: 1229–1237, 2013.
64. Krotkiewski M, Mandroukas K, Sjöström L, Sullivan L, Wetterqvist H, Björntorp P. Effects of long-term physical training on body fat, metabolism, and blood pressure in obesity. *Metab Clin Exp* 28: 650–658, 1979.
65. Lalioti MD, Zhang J, Volkman HM, Kahle KT, Hoffmann KE, Toka HR, Nelson-Williams C, Ellison DH, Flavell R, Booth CJ, Lu Y, Geller DS, Lifton RP. Wnk4 controls blood pressure and potassium homeostasis via regulation of mass and activity of the distal convoluted tubule. *Nat Genet* 38: 1124–1132, 2006.
66. Lazelle RA, McCully BH, Terker AS, Himmerkus N, Blankenstein K, Mutig K, Bleich M, Bachmann S, Yang C-L, Ellison DH. Renal Deletion of 12 kDa FK506-Binding Protein Attenuates Tacrolimus-Induced Hypertension. *J Am Soc Nephrol* 27: 1456–1464, 2015.
67. Lee DH, Maunsbach AB, Riquier-Brison AD, Nguyen MTX, Fenton RA, Bachmann S, Yu AS, McDonough AA. Effects of ACE inhibition and ANG II stimulation on renal Na-Cl cotransporter distribution, phosphorylation, and membrane complex properties. *Am J Physiol, Cell Physiol* 304: C147–C163, 2013.
68. Liu Y, Rafferty TM, Rhee SW, Webber JS, Song L, Ko B, Hoover RS, He B, Mu S. CD8(+) T cells stimulate Na-Cl co-transporter NCC in distal convoluted tubules leading to salt-sensitive hypertension. *Nat Commun* 8: 14037, 2017.
69. Loffing J, Kaissling B. Sodium and calcium transport pathways along the mammalian distal nephron: from rabbit to human. *Am J Physiol Renal Physiol* 284: F628–43, 2003.
70. Loffing J, Loffing-Cueni D, Valderrabano V, Kläusli L, Hebert SC, Rossier BC, Hoenderop JG, Bindels RJ, Kaissling B. Distribution of transcellular calcium and sodium transport pathways along mouse distal nephron. *Am J Physiol Renal Physiol* 281: F1021–7, 2001.
71. Louis-Dit-Picard H, Barc J, Trujillano D, Miserey-Lenkei S, Bouatia-Naji N, Pylypenko O, Beaurain G, Bonnefond A, Sand O, Simian C, Vidal-Petiot E, Soukaseum C, Mandet C, Broux F, Chabre O, Delahousse M, Esnault V, Fiquet B, Houillier P, Bagnis CI, Koenig J, Konrad M, Landais P, Mourani C, Niaudet P, Probst V, Thauvin C, Unwin RJ, Soroka SD, Ehret G, Ossowski S, Caulfield M, International Consortium for Blood Pressure ICBP, Bruneval P, Estivill X, Froguel P, Hadchouel J, Schott J-J, Jeunemaitre X. KLHL3 mutations cause familial hyperkalemic hypertension by impairing ion transport in the distal nephron. *Nat Genet* 44: 456–460, 2012.
72. Luft FC. Molecular genetics of human hypertension. *J. Hypertens.* 16: 1871–1878, 1998.
73. Margreiter R, European Tacrolimus vs Ciclosporin Microemulsion Renal Transplantation Study Group. Efficacy and safety of tacrolimus compared with ciclosporin microemulsion in renal transplantation: a randomised multicentre study. *Lancet* 359: 741–746, 2002.
74. Mastroianni N, Bettinelli A, Bianchetti M, Colussi G, De Fusco M, Sereni F, Ballabio A, Casari G. Novel molecular variants of the Na-Cl cotransporter gene are responsible for Gitelman syndrome. *Am J Hum Genet* 59: 1019–1026, 1996.
75. Mastroianni N, Fusco MD, Zollo M, Arrigo G, Zuffardi O, Bettinelli A, Ballabio A, Casari G. Molecular Cloning, Expression Pattern, and Chromosomal Localization of the Human Na–Cl Thiazide-Sensitive Cotransporter (SLC12A3). *Genomics* 35: 486–493, 1996.
76. Mattson DL, Dwinell MR, Greene AS, Kwitek AE, Roman RJ, Jacob HJ, Cowley AW. Chromosome substitution reveals the genetic basis of Dahl salt-sensitive hypertension and renal disease. *Am J Physiol Renal Physiol* 295: F837–42, 2008.
77. Mayan H, Vered I, Mouallem M, Tzadok-Witkon M, Pauzner R, Farfel Z. Pseudohypoaldosteronism type II: marked sensitivity to thiazides, hypercalciuria, normomagnesemia, and low bone mineral density. *J Clin Endocrinol Metab* 87: 3248–3254, 2002.
78. McCarron DA. Role of adequate dietary calcium intake in the prevention and management of salt-sensitive hypertension. *Am J Clin Nutr* 65: 712S–716S, 1997.

79. Melnikov S, Mayan H, Uchida S, Holtzman EJ, Farfel Z. Cyclosporine metabolic side effects: association with the WNK4 system. *European Journal of Clinical Investigation* 41: 1113–1120, 2011.
80. Messerli FH, Williams B, Ritz E. Essential hypertension. *The Lancet* 370: 591–603, 2007.
81. Mills KT, Bundy JD, Kelly TN, Reed JE, Kearney PM, Reynolds K, Chen J, He J. Global Disparities of Hypertension Prevalence and Control: A Systematic Analysis of Population-Based Studies From 90 Countries. *Circulation* 134: 441–450, 2016.
82. Miyata N, Park F, Li XF, Cowley AW. Distribution of angiotensin AT1 and AT2 receptor subtypes in the rat kidney. *Am J Physiol* 277: F437–46, 1999.
83. Moes AD, Lubbe N, Zietse R, Loffing J, Hoorn EJ. The sodium chloride cotransporter SLC12A3: new roles in sodium, potassium, and blood pressure regulation. *Pflugers Arch - Eur J Physiol* 466: 107–118, 2013.
84. Montani JP, Antic V, Yang Z, Dulloo A. Pathways from obesity to hypertension: from the perspective of a vicious triangle. *Int J Obes Relat Metab Disord* 26 Suppl 2: S28–38, 2002.
85. Morris RC, Sebastian A, Forman A, Tanaka M, Schmidlin O. Normotensive salt sensitivity: effects of race and dietary potassium. *Hypertension* 33: 18–23, 1999.
86. Mullins LJ, Bailey MA, Mullins JJ. Hypertension, kidney, and transgenics: a fresh perspective. *Physiological Reviews* 86: 709–746, 2006.
87. Murray CJL, Lopez AD. Measuring the Global Burden of Disease. *N Engl J Med* 369: 448–457, 2013.
88. Murthy M, Kurz T, O'Shaughnessy KM. WNK signalling pathways in blood pressure regulation. *Cell Mol Life Sci* 74: 1261–1280, 2016.
89. Na T, Wu G, Zhang W, Dong W-J, Peng J-B. Disease-causing R1185C mutation of WNK4 disrupts a regulatory mechanism involving calmodulin binding and SGK1 phosphorylation sites. *Am J Physiol Renal Physiol* 304: F8–F18, 2013.
90. Narayan KMV, Ali MK, Koplan JP. Global noncommunicable diseases – where worlds meet. *N Engl J Med* 363: 1196–1198, 2010.
91. Obermuller N, Bernstein P, Velazquez H, Reilly R, Moser D, Ellison DH, Bachmann S. Expression of the thiazide-sensitive Na-Cl cotransporter in rat and human kidney. *Am J Physiol Renal Physiol* 269: F900–F910, 1995.
92. Pacheco-Alvarez D, Cristobal PS, Meade P, Moreno E, Vazquez N, Munoz E, Diaz A, Juarez ME, Gimenez I, Gamba G. The Na+:Cl- cotransporter is activated and phosphorylated at the amino-terminal domain upon intracellular chloride depletion. *J Biol Chem* 281: 28755–28763, 2006.
93. Paver WK, Pauline GJ. Hypertension and hyperpotassaemia without renal disease in a young male. *Med J Aust* 2: 305–306, 1964.
94. Pedersen NB, Hofmeister MV, Rosenbaek LL, Nielsen J, Fenton RA. Vasopressin induces phosphorylation of the thiazide-sensitive sodium chloride cotransporter in the distal convoluted tubule. *Kidney Int* 78: 160–169, 2010.
95. Peng JF, Kimura B, Fregly MJ, Phillips MI. Reduction of cold-induced hypertension by antisense oligodeoxynucleotides to angiotensinogen mRNA and AT1-receptor mRNA in brain and blood. *Hypertension* 31: 1317–1323, 1998.
96. Petrella RJ. How effective is exercise training for the treatment of hypertension? *Clin J Sport Med* 8: 224–231, 1998.
97. Piala AT, Moon TM, Akella R, He H, Cobb MH, Goldsmith EJ. Chloride sensing by WNK1 kinase involves inhibition of autophosphorylation. *Science signaling* 7: ra41–ra41, 2014.
98. Pisitkun T, Shen RF, Knepper MA. Identification and proteomic profiling of exosomes in human urine. *Proc Natl Acad Sci* 101: 13368–13373, 2004.
99. Psaty BN, Lumley T, Furberg CD, Schellenbaum G, Pahor M, Alderman MH, Weiss NS. Health outcomes associated with various antihypertensive therapies used as first-line agents - A network meta-analysis. *JAMA* 289: 2534–2544, 2003.
100. Renfro JL. Water and ion transport by the urinary bladder of the teleost Pseudopleuronectes americanus. *Am J Physiol* 228: 52–61, 1975.
101. Renfro JL. Interdependence of Active Na+ and Cl- transport by the isolated urinary bladder of the teleost, Pseudopleuronectes americanus. *J Exp Zool* 199: 383–390, 1977.
102. Richardson C, Richardson C, Rafiqi FH, Rafiqi FH, Karlsson HKR, Karlsson HKR, Moleleki N,

Moleleki N, Vandewalle A, Vandewalle A, Campbell DG, Campbell DG, Morrice NA, Morrice NA, Alessi DR, Alessi DR. Activation of the thiazide-sensitive Na+-Cl- cotransporter by the WNK-regulated kinases SPAK and OSR1. *J Cell Sci* 121: 675–684, 2008.

103. Rinehart J, Kahle KT, de Los Heros P, Vazquez N, Meade P, Wilson FH, Hebert SC, Gimenez I, Gamba G, Lifton RP. WNK3 kinase is a positive regulator of NKCC2 and NCC, renal cation-Cl- cotransporters required for normal blood pressure homeostasis. *Proc Natl Acad Sci* 102: 16777–16782, 2005.
104. Ring AM, Leng Q, Rinehart J, Wilson FH, Kahle KT, Hebert SC, Lifton RP. An SGK1 site in WNK4 regulates Na+ channel and K+ channel activity and has implications for aldosterone signaling and K+ homeostasis. *Proc Natl Acad Sci* 104: 4025–4029, 2007.
105. Ronzaud C, Loffing-Cueni D, Hausel P, Debonneville A, Malsure SR, Fowler-Jaeger N, Boase NA, Perrier R, Maillard M, Yang B, Stokes JB, Koesters R, Kumar S, Hummler E, Loffing J, Staub O. Renal tubular NEDD4-2 deficiency causes NCC-mediated salt-dependent hypertension. *J Clin Invest* 123: 657–665, 2013.
106. Rosenbaek LL, Assentoft M, Pedersen NB, MacAulay N, Fenton RA. Characterization of a novel phosphorylation site in the sodium-chloride cotransporter, NCC. *The Journal of Physiology* 590: 6121–6139, 2012.
107. Rosenbaek LL, Kortenoeven MLA, Aroankins TS, Fenton RA. Phosphorylation decreases ubiquitylation of the thiazide-sensitive cotransporter NCC and subsequent clathrin-mediated endocytosis. *J Biol Chem* 289: 13347–13361, 2014.
108. Rossi GP, Ceolotto G, Caroccia B, Lenzini L. Genetic screening in arterial hypertension. *Nat Rev Endocrinol* 119: 694, 2017.
109. Rossier BC, Bochud M, Devuyst O. The Hypertension Pandemic: An Evolutionary Perspective. *Physiology (Bethesda)* 32: 112–125, 2017.
110. Rozansky DJ, Cornwall T, Subramanya AR, Rogers S, Yang Y-F, David LL, Zhu X, Yang C-L, Ellison DH. Aldosterone mediates activation of the thiazide-sensitive Na-Cl cotransporter through an SGK1 and WNK4 signaling pathway. *J Clin Invest* 119: 2601–2612, 2009.
111. Salih M, Gautschi I, van Bemmelen MX, Di Benedetto M, Brooks AS, Lugtenberg D, Schild L, Hoorn EJ. A Missense Mutation in the Extracellular Domain of αENaC Causes Liddle Syndrome. *J Am Soc Nephrol* (July 14, 2017). doi: 10.1681/ASN.2016111163.
112. Salih M, Zietse R, Hoorn EJ. Urinary extracellular vesicles and the kidney: biomarkers and beyond. *Am J Physiol Renal Physiol* 306: F1251–9, 2014.
113. San-Cristobal P, Pacheco-Alvarez D, Richardson C, Ring AM, Vazquez N, Rafiqi FH, Chari D, Kahle KT, Leng Q, Bobadilla NA, Hebert SC, Alessi DR, Lifton RP, Gamba G. Angiotensin II signaling increases activity of the renal Na-Cl cotransporter through a WNK4-SPAK-dependent pathway. *Proc Natl Acad Sci* 106: 4384–4389, 2009.
114. Sandberg MB, Riquier ADM, Pihakaski-Maunsbach K, McDonough AA, Maunsbach AB. ANG II provokes acute trafficking of distal tubule Na+-Cl cotransporter to apical membrane. *Am J Physiol Renal Physiol* 293: F662–F669, 2007.
115. Schmitt R, Ellison DH, Farman N, Rossier BC, Reilly RF, Reeves WB, Oberbäumer I, Tapp R, Bachmann S. Developmental expression of sodium entry pathways in rat nephron. *Am J Physiol* 276: F367–81, 1999.
116. Schwartz IL, Shlatz LJ, Kinne-Saffran E, Kinne R. Target cell polarity and membrane phosphorylation in relation to the mechanism of action of antidiuretic hormone. *Proc Natl Acad Sci* 71: 2595–2599, 1974.
117. Sepúlveda FV, Cid LP, Teulon J, Niemeyer MI. Molecular Aspects of Structure, Gating, and Physiology of pH-Sensitive Background K2P and Kir K+-Transport Channels. *Physiological Reviews* 95: 179–217, 2015.
118. Sever PS, Poulter NR. A hypothesis for the pathogenesis of essential hypertension: the initiating factors. *J Hypertens Suppl* 7: S9–12, 1989.
119. Shoda W, Nomura N, Ando F, Mori Y, Mori T, Sohara E, Rai T, Uchida S. Calcineurin inhibitors block sodium-chloride cotransporter dephosphorylation in response to high potassium intake. *Kidney International* 91: 402–411, 2017.
120. Simon DB, Karet FE, Hamdan JM, DiPietro A, Sanjad SA, Lifton RP. Bartter's syndrome, hypokalaemic alkalosis with hypercalciuria, is caused by mutations in the Na-K-2Cl cotransporter NKCC2. *Nat Genet* 13: 183–188, 1996.
121. Simon DB, Nelson-Williams C, Johnson Bia M, Ellison D, Karet FE, Molina AM, Vaara I, Iwata

F, Cushner HM, Koolen M, Gainza FJ, Gitelman HJ, Lifton RP. Gitelman“s variant of Barter”s syndrome, inherited hypokalaemic alkalosis, is caused by mutations in the thiazide-sensitive Na–Cl cotransporter. *Nat Genet* 12: 24–30, 1996.

122. Simon DB, Nelson-Williams C, Johnson Bia M, Ellison D, Karet FE, Morey Molina A, Vaara I, Iwata F, Cushner HM, Koolen M, Gainza FJ, Gitelman HJ, Lifton RP. Gitelman“s variant of Barter”s syndrome, inherited hypokalaemic alkalosis, is caused by mutations in the thiazide-sensitive Na–Cl cotransporter. *Nat Genet* 12: 24–30, 1996.
123. Staub O, Dho S, Henry P, Correa J, Ishikawa T, McGlade J, Rotin D. WW domains of Nedd4 bind to the proline-rich PY motifs in the epithelial Na+ channel deleted in Liddle's syndrome. *The EMBO Journal* 15: 2371–2380, 1996.
124. Stokes JB. Sodium chloride absorption by the urinary bladder of the winter flounder. A thiazide-sensitive, electrically neutral transport system. *J Clin Invest* 74: 7–16, 1984.
125. Subramanya AR, Ellison DH. Distal Convoluted Tubule. *Clin J Am Soc Nephrol* 9: 2147–2163, 2014.
126. Subramanya AR, Liu J, Ellison DH, Wade JB, Welling PA. WNK4 diverts the thiazide-sensitive NaCl cotransporter to the lysosome and stimulates AP-3 interaction. *J Biol Chem* 284: 18471–18480, 2009.
127. Talati G, Ohta A, Rai T, Sohara E, Naito S, Vandewalle A, Sasaki S, Uchida S. Effect of angiotensin II on the WNK-OSR1/SPAK-NCC phosphorylation cascade in cultured mpkDCT cells and in vivo mouse kidney. *Biochem Biophys Res Commun* 393: 844–848, 2010.
128. Tamari M, Daigo Y, Nakamura Y. Isolation and characterization of a novel serine threonine kinase gene on chromosome 3p22-21.3. *J Hum Genet* 44: 116–120, 1999.
129. Terker AS, Zhang C, Erspamer KJ, Gamba G, Yang C-L, Ellison DH. Unique chloride-sensing properties of WNK4 permit the distal nephron to modulate potassium homeostasis. *Kidney International* 89: 127–134, 2015.
130. Terker AS, Zhang C, McCormick JA, Lazelle RA, Zhang C, Meermeier NP, Siler DA, Park HJ, Fu Y, Cohen DM, Weinstein AM, Wang W-H, Yang C-L, Ellison DH. Potassium modulates electrolyte balance and blood pressure through effects on distal cell voltage and chloride. *Cell Metab* 21: 39–50, 2015.
131. The INTERSALT Co-operative Research Group. Sodium, potassium, body mass, alcohol and blood pressure: the INTERSALT Study. *J Hypertens Suppl* 6: S584–6, 1988.
132. The Trials of Hypertension Prevention Collaborative Research Group. Effects of weight loss and sodium reduction intervention on blood pressure and hypertension incidence in overweight people with high-normal blood pressure. The Trials of Hypertension Prevention, phase II. *Arch Intern Med* 157: 657–667, 1997.
133. Tutakhel OAZ, Jeleń S, Valdez-Flores M, Dimke H, Piersma SR, Jimenez CR, Deinum J, Lenders JW, Hoenderop JGJ, Bindels RJM. Alternative splice variant of the thiazide-sensitive NaCl cotransporter: a novel player in renal salt handling. *Am J Physiol Renal Physiol* 310: F204–F216, 2016.
134. Urbanová M, Reiterová J, Stěkrová J, Lněnička P, Ryšavá R. DNA analysis of renal electrolyte transporter genes among patients suffering from Bartter and Gitelman syndromes: summary of mutation screening. *Folia Biol (Praha)* 57: 65–73, 2011.
135. Valdez-Flores MA, Vargas-Poussou R, Verkaart S, Tutakhel OAZ, Valdez-Ortiz A, Blanchard A, Treard C, Hoenderop JGJ, Bindels RJM, Jeleń S. Functionomics of NCC mutations in Gitelman syndrome using a novel mammalian cell-based activity assay. *Am J Physiol Renal Physiol* 311: F1159–F1167, 2016.
136. Vallon V, Schroth J, Lang F, Kuhl D, Uchida S. Expression and phosphorylation of the Na+-Cl- cotransporter NCC in vivo is regulated by dietary salt, potassium, and SGK1. *Am J Physiol Renal Physiol* 297: F704–12, 2009.
137. van der Lubbe N, Jansen PM, Salih M, Fenton RA, van den Meiracker AH, Danser AHJ, Zietse R, Hoorn EJ. The phosphorylated sodium chloride cotransporter in urinary exosomes is superior to prostasin as a marker for aldosteronism. *Hypertension* 60: 741–748, 2012.
138. van der Lubbe N, Moes AD, Rosenbaek LL, Schoep S, Meima ME, Danser AHJ, Fenton RA, Zietse R, Hoorn EJ. K+-induced natriuresis is preserved during Na+ depletion and accompanied by inhibition of the Na+-Cl− cotransporter. *Am J Physiol Renal Physiol* 305: F1177–F1188, 2013.
139. Vargas-Poussou R, Dahan K, Kahila D, Venisse A, Riveira-Munoz E, Debaix H, Grisart B,

Bridoux F, Unwin R, Moulin B, Haymann J-P, Vantyghem M-C, Rigothier C, Dussol B, Godin M, Nivet H, Dubourg L, Tack I, Gimenez-Roqueplo A-P, Houillier P, Blanchard A, Devuyst O, Jeunemaitre X. Spectrum of mutations in Gitelman syndrome. *J Am Soc Nephrol* 22: 693–703, 2011.

140. Varshavsky A. The ubiquitin system, an immense realm. *Annu Rev Biochem* 81: 167–176, 2012.
141. Veiras LC, Han J, Ralph DL, McDonough AA. Potassium Supplementation Prevents Sodium Chloride Cotransporter Stimulation During Angiotensin II Hypertension. *Hypertension* 68: 904–912, 2016.
142. Weir MR, Dzau VJ. The renin-angiotensin-aldosterone system: a specific target for hypertension management. *Am J Hypertens* 12: 205S–213S, 1999.
143. Wilson FH, Disse-Nicodème S, Choate KA, Ishikawa K, Nelson-Williams C, Desitter I, Gunel M, Milford DV, Lipkin GW, Achard J-M, Feely MP, Dussol B, Berland Y, Unwin RJ, Mayan H, Simon DB, Farfel Z, Jeunemaitre X, Lifton RP. Human hypertension caused by mutations in WNK kinases. *Science* 293: 1107–1112, 2001.
144. Wolley MJ, Wu A, Xu S, Gordon RD, Fenton RA, Stowasser M. In Primary Aldosteronism, Mineralocorticoids Influence Exosomal Sodium-Chloride Cotransporter Abundance. *J Am Soc Nephrol* 28: 56–63, 2016.
145. Xin X, He J, Frontini MG, Ogden LG, Motsamai OI, Whelton PK. Effects of alcohol reduction on blood pressure: a meta-analysis of randomized controlled trials. *Hypertension* 38: 1112–1117, 2001.
146. Yang C-L, Zhu X, Ellison DH. The thiazide-sensitive Na-Cl cotransporter is regulated by a WNK kinase signaling complex. *J Clin Invest* 117: 3403–3411, 2007.
147. Yang C-L, Zhu X, Wang Z, Subramanya AR, Ellison DH. Mechanisms of WNK1 and WNK4 interaction in the regulation of thiazide-sensitive NaCl cotransport. *J Clin Invest* 115: 1379–1387, 2005.
148. Yang S-S, Fang Y-W, Tseng M-H, Chu P-Y, Yu I-S, Wu H-C, Lin S-W, Chau T, Uchida S, Sasaki S, Lin Y-F, Sytwu H-K, Lin S-H. Phosphorylation Regulates NCC Stability and Transporter Activity In Vivo. *J Am Soc Nephrol* 24: 1587–1597, 2013.
149. Yang S-S, Morimoto T, Rai T, Chiga M, Sohara E, Ohno M, Uchida K, Lin S-H, Moriguchi T, Shibuya H, Kondo Y, Sasaki S, Uchida S. Molecular Pathogenesis of Pseudohypoaldosteronism Type II: Generation and Analysis of a Wnk4D561A/+ Knockin Mouse Model. *Cell Metab* 5: 331–344, 2007.
150. Yue P, Sun P, Lin D-H, Pan C, Xing W, Wang W. Angiotensin II diminishes the effect of SGK1 on the WNK4-mediated inhibition of ROMK1 channels. *Kidney Int* 79: 423–431, 2011.
151. Zhou B, Zhuang J, Gu D, Wang H, Cebotaru L, Guggino WB, Cai H. WNK4 enhances the degradation of NCC through a sortilin-mediated lysosomal pathway. *J Am Soc Nephrol* 21: 82-92, 2010.

2

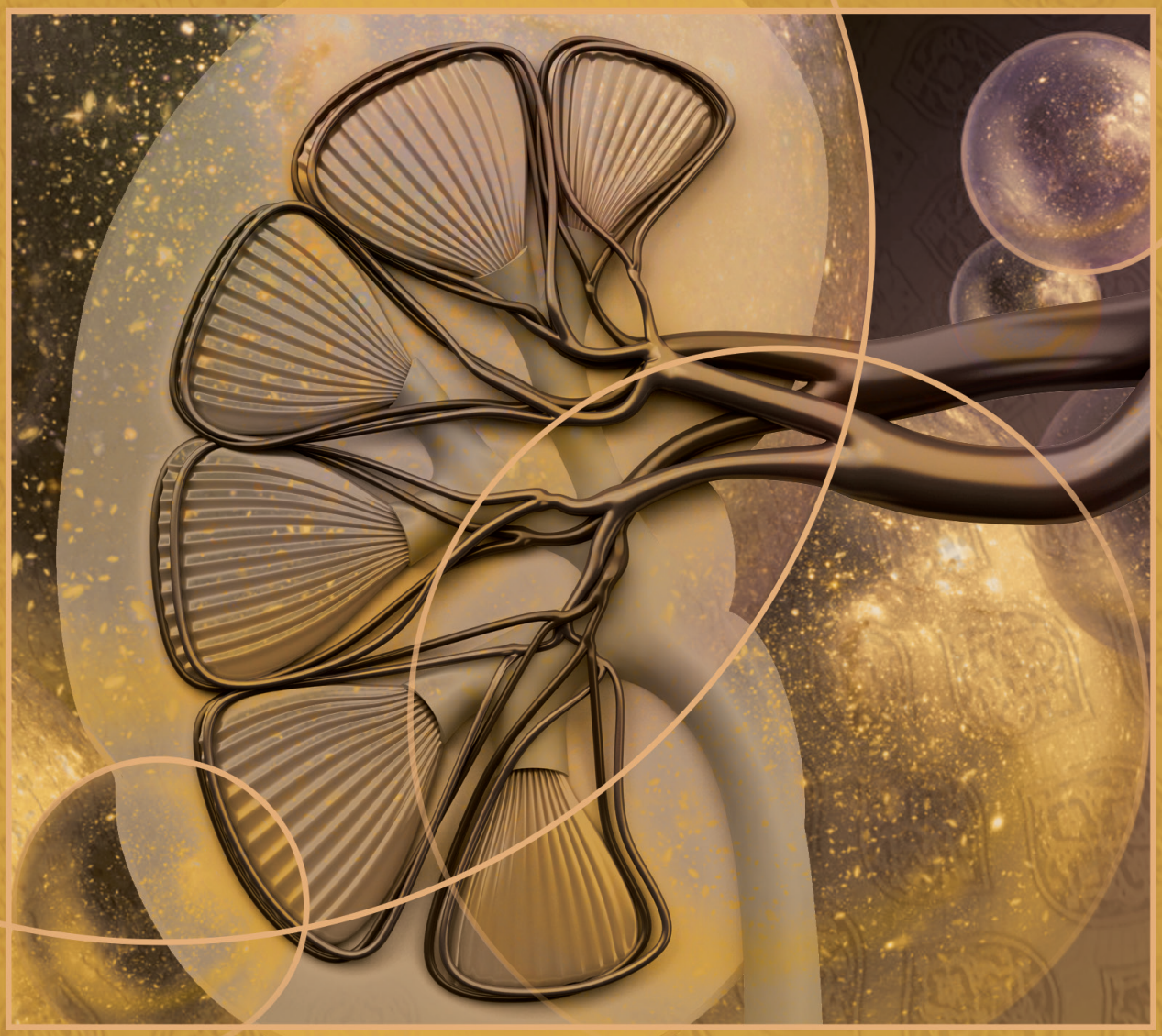

Alternative splice variant of the thiazidesensitive NaCl cotransporter: a novel player in renal salt handling

Omar A.Z. Tutakhel[1*], Sabina Jele[1*], Marco Valdez-Flores[1], Henrik Dimke[3], Sander R. Piersma[5], Connie R. Jimenez[5], Jaap Deinum[2], Jacques W. Lenders[2,4], Joost G.J. Hoenderop[1] and René J.M. Bindels[1]

Departments of [1]Physiology and [2]Internal Medicine, Radboud Institute for Molecular Life Sciences, Radboud university medical center, Nijmegen, The Netherlands; [3]Department of Cardiovascular and Renal Research, University of Southern Denmark, Odense, Denmark; [4]Department of Medicine III, University Hospital Carl Gustav Carus, Technische Universität, Dresden, Germany; [5]OncoProteomics Laboratory, Department of Medical Oncology, VU University Medical Center, Amsterdam, The Netherlands

* Authors contributed equally

Am J Physiol Renal Physiol, 310: F204-F216, 2016

Abstract

The thiazide-sensitive NaCl cotransporter (NCC) is an important pharmacological target in the treatment of hypertension. Human *SLC12A3* gene, encoding NCC, gives rise to three isoforms. Only the 3rd isoform has been extensively investigated. The aim of the present study was, therefore, to establish the abundance and localization of the almost identical isoforms 1 and 2 ($NCC_{1/2}$) in the human kidney and to determine their functional properties and regulation in physiological conditions. Immunohistochemical analysis of $NCC_{1/2}$ in the human kidney revealed that $NCC_{1/2}$ localizes to the apical plasma membrane of the distal convoluted tubule. Importantly, $NCC_{1/2}$ mRNA constitutes ~44% of all NCC isoforms in the human kidney. Functional analysis performed in the *Xenopus laevis* oocyte revealed that thiazide-sensitive $^{22}Na^{+}$ transport of NCC_1 was significantly increased in comparison to NCC_3. Mimicking a constitutively active phosphorylation site at residue 811 (S811D) in NCC_1 further augmented Na^{+} transport, while a non-phosphorylatable variant (S811A) of NCC_1 prevented this enhanced response. Analysis of human urinary exosomes demonstrated that water loading in human subjects significantly reduces the abundance of $NCC_{1/2}$ in urinary exosomes. The present study highlights that previously underrepresented $NCC_{1/2}$ is a fully functional thiazide-sensitive NaCl-transporting protein. Being significantly expressed in the kidney it may constitute a unique route of renal NaCl reabsorption and could, therefore, play an important role in blood pressure regulation.

Keywords: Hypertension / WNK4 / Aldosterone-sensitive distal part of the nephron / Sodium / Kidney

Introduction

Hypertension is a global disease with an overall prevalence around 30-45% in the general population (18, 21). The kidneys play a key role in chronic blood pressure homeostasis by maintaining appropriate renal salt reabsorption. It is of critical importance to understand the molecular mechanisms governing renal NaCl transport in physiological and pathophysiological conditions in order to exploit them as therapeutic targets.

The 2014 evidence-based guideline for the management of high blood pressure in adults recommends thiazide-type diuretics as initial therapy for hypertension (18). Thiazide-type diuretics act by blocking the NaCl cotransporter (NCC) in the distal convoluted tubule (DCT), highlighting the importance of NCC in blood pressure regulation. Mutations in NCC-encoding gene (*SLC12A3)* cause Gitelman's syndrome (OMIM 263800), a condition characterized by salt wasting and hypotension (13, 22). A mirror image of Gitelman's syndrome with increased renal reabsorption of NaCl and a resultant increase in systemic blood pressure can be observed in patients with Pseudohypoaldosteronism type II (PHAII, also known as Gordon syndrome (OMIM 145260) (10). PHAII results from mutations in the WNK [with-no-K(Lys)] kinases (members WNK1 and WNK4) (47), as well as kelch-like 3 (KLHL3) and cullin 3 (CUL3) (2, 14), which play an instrumental role in regulating NaCl reabsorption in the distal part of the nephron (20, 29, 31, 45, 47, 48). The amino- (N)-terminal domain of NCC contains several phosphorylation sites being of critical importance for NCC function. These residues are targets of the serine-threonine kinases, Ste20-related proline-alanine-rich kinase (SPAK) and oxidative stress response 1 (OSR1) (27, 31). In addition, kinases in the WNK family as well as the serum- and glucocorticoid-inducible kinase 1 (SGK1) interact within the network of SPAK and OSR1, thereby affecting the phosphorylation status of NCC (7, 38, 39, 49).

The *SLC12A3* gene encoding the human NCC yields three separate isoforms as a result of an alternative splicing. An mRNA sequence encoding a 1,030 amino acid NCC protein was first deposited in the GenBank by Simon *et al.* (35) representing isoform 1 (NCC_1) (accession no. NP_000330.2). Subsequently, Mastroianni *et al.* (23) reported an mRNA sequence encoding a protein of 1,021 amino acids representing isoform 3 (NCC_3) (accession no. NP_001119580.1), in which exon 20 is nine amino acids shorter than in NCC_1. Following studies confirmed the presence of both long and short form of the exon 20 (20a and 20b respectively) as a result of a possible cryptic splicing donor site (22). Moreover, cDNA analysis indicated that NCC_3 constitutes the predominant form in the human kidney (22). Isoform 2 (NCC_2) (accession no. NP_001119579.1) is only one amino acid shorter than NCC_1. Recently, Gonzales *et al.*(15) used a proteomic approach to analyze human urinary exosomes and identified a novel phosphorylation site at serine (Ser811). This

residue is present only in NCC_1 and NCC_2. Interestingly, mouse and rat *SLC12A3* genes do not contain the segment coded by human exon 20, hence NCC_1 and NCC_2 are not present in these animals. The lack of NCC_1 and NCC_2 in rodents hampered the progress and interest towards further investigations and until now NCC_3 has predominantly been studied (8, 12). At present, detailed localization of NCC_1 and NCC_2 proteins in human kidney, their regulatory network, and relevance in renal Na^+ handling remain to be elucidated.

The goal of the present study was, therefore, to determine the abundance and localization of previously underrepresented NCC isoforms in comparison to NCC_3 in the human kidney as well as their functional properties and regulation in physiological conditions. To this end, the presence of NCC_1, NCC_2, and NCC_3 in the human urinary exosomes was assessed by mass spectrometric analysis. The localization and regulation of NCC isoforms was investigated by immunohistochemical analysis in human kidney biopsies and by immunoblotting of kidney membrane fractions and urinary exosomes with newly developed isoform specific antibodies. Functional capacity to transport Na^+ by NCC_1 was determined using the *Xenopus* oocytes expression system. Furthermore, to evaluate physiological regulation of NCC isoforms during acute water loading of human subjects was chosen as a model, since hormones maintaining water balance are known to regulate NCC (5, 28, 30-34, 41, 42).

Materials and Methods

Isolation and sequencing of NCC variants from human kidney

Human kidney cDNA was amplified using primers against the C-terminal domain of NCC. The PCR product was isolated, cloned into the pGEM®-T Easy Vector System (Promega), and transformed into DH5-*E. Coli* bacteria. Colonies were isolated, plasmid DNA was extracted, and submitted for Sanger sequencing. The resulting chromatograms from the sequencing confirmed the presence of $NCC_{1/2}$ and NCC_3 in the human kidney.

Real-time relative RT-PCR quantification

All 7 donors gave permission for donating their kidneys after death. In case the kidney appeared not suitable for transplantation the donor gave permission to use the kidneys for research purposes, which is registered in the Dutch Donor registry. Relative amount of $NCC_{1/2}$ and $NCC_{1\text{-}3}$ mRNA in the human kidney was determined by a real-time RT-PCR based on the standard curve method (46). RNA from 7 healthy humans kidney cortex was isolated with Trizol Reagent (Life Technologies, Grand Island, NY, USA) and cDNA was synthesized with moloney murine leukemia virus (M-MLV) revers transcriptase (Invitrogen, Grand Island, NY, USA). Following primers amplifying specifically $NCC_{1/2}$ as well as primers

against N-terminal fragment recognizing both $NCC_{1/2}$ and NCC_3 combined (NCC_{1-3}) were used: $NCC_{1/2}$ Fw: GTGCCAGGCCATCAGTCT; $NCC_{1/2}$ Rev: TATGGTCTTCTTGCCCTGCT; NCC_{1-3} Fw: TGTTTGGGGCTATCATCTCC; NCC_{1-3} Rev: GAGGAGCCCCAATTTACCTC. Standard curve was prepared based on mixed DNA plasmids containing both $NCC_{1/2}$ and NCC_3 dilutions ranging from 2.5×10^5 – 5.12×10^8. Quantification was performed with iQ SYBR Green supermix system (Bio-Rad, Hercules, CA, USA) according to manufacturer's instructions. The products of the RT-PCR were verified by sequencing. The absolute copy number per µg of mRNA isolated form the human cortex was defined and the ratio of $NCC_{1/2}$ to NCC_{1-3} was determined.

Mutagenesis and constructs

Human NCC in pT7Ts has been previously described.(7) The human NCC_1 fragment was generated by site directed mutagenesis using the QuikChange site-directed mutagenesis kit (Stratagene, La Jolla, CA, USA) with the following primers: Fw GCGCCAGAGGTGCCAGGC CATCAGTCTCTGGCGCTTTGGACCCCAAGGC; Rev: GCCTTGGGGTCCAAAGCGCCAG AGACTGATGGCCTGGCACCTCTGGCGC; and subsequently inserted in the NCC_3-pT7Ts. The NCC_1 phosphomutants mimicking the active (S811D) and the inactive (S811A) phosphorylation sites were generated by site directed mutagenesis. Primers: S811D Fw: GTGCCAGGCCAGACGTCTCTGGCGCTTTG; Rev: CAAAGCGCCAGAGACGTCTGGCCT GGCAC; S811A Fw: GTGCCAGGCCAGCAGTCTCTGGCGCTTTG; Rev: CAAAGCGCCAG AGACTGCTGGCCTGGCAC. eGFP-NCC in pT7Ts was described previously.(7) The C-terminal part of human NCC_1 in pT7Ts was subcloned into the eGFP-NCC construct. For expression in mammalian systems, human eGFP-NCC_3 fragment described previously(7) was subcloned into empty pCMV-SPORT6 vector. Human NCC_1 and NCC_1 phosphorylation site mutants (S811A and S811D) fragments were subcloned to eGFP-NCC_3 pCMV SPORT6 construct. All the constructs were confirmed by sequence analyses.

In vitro cRNA translation for functional assays

Microinjection of cRNA and $^{22}Na^+$ uptake experiments were performed essentially as described previously (7). Briefly, constructs encoding the NCC variants were linearized, transcribed *in vitro* using the mMESSAGE mMACHINE® T7 Kit (Ambion, Austin, TX, USA). The integrity of the product was confirmed on 1% w/v agarose, 37% v/v formaldehyde gels and cRNA aliquots were stored at –80°C.

Oocyte harvesting and animal experimentation

All animal experiments received the approval from the animal ethics board of Radboud university medical center, Nijmegen, The Netherlands. *Xenopus laevis* oocytes were

processed based on previous established protocols (7). Mature oocytes were selected and microinjected with 5 ng of cRNA encoding the human NCC_1, NCC_3, NCC_1 S811D, NCC_1 S811A or co-injected with 10 ng of WNK4 cRNA. $^{22}Na^+$ uptake was corrected for the surface expression of the corresponding microinjected variant and expressed as a percent of WT uptake. All the experiments using $^{22}Na^+$ radioisotope were approved and monitored by the Environmental Health and Radiation Safety office, Radboud university medical center.

Quantification of eGFP-NCC in the oocyte membrane

Surface expression analyses were performed as described in detail previously (7). Briefly, oocytes were microinjected with 5 ng of cRNA encoding eGFP-NCC_1, eGFP-NCC_3, or eGFP-NCC_1 phosphorylation site mutants. All images were acquired on an Olympus FV1000 laser-scanning microscope (Center Valley, PA, USA) using a 10 x water objective. Densitometry analysis of fluorescence was done using Image J software (image processing program, NIH, Bethesda, MA, USA). Autofluorescence of water-injected oocytes was subtracted from the fluorescence of all injected variants.

Cell culture, transfection, and isolation of enriched plasma membrane

HEK293 cells were cultured on 100 mm dishes and grown in DMEM supplemented with 10% v/v fetal bovine serum, nonessential amino acids, and 2 mM L-glutamine. Cells were transfected with eGFP-NCC_3 pCMV SPORT6, eGFP-NCC_1 pCMV SPORT6, eGFP-NCC_1 S811D pCMV SPORT6 and eGFP-NCC_1 S811A pCMV SPORT6 vector using 32 μg of DNA and 96 μl of polyethylenimine (Polysciences, Inc., Warrington, PA, USA). Cells transfected with empty vector were used as controls (mock). At 48 hours post-transfection the cells were lysed in 1 ml of ice-cold dissection buffer per dish (300 mM sucrose, 25 mM imidazole, 1 mM EDTA, 1 μg/ml pepstatin, 1 mM phenylmethylsulfonyl fluoride (PMSF), 5 μg/ml leupeptin and 5 μg/ml apropotin). Lysed cells were centrifuged at 4,000 x g for 8 minutes and subsequently the supernatant was centrifuged at 16,000 x g for 40 minutes. The pellet was resuspended in ice-cold dissection buffer and 1x Laemmli (0.4% w/v SDS, 2% v/v glycerol, 12 mM Tris-HCl pH 6.8, 40 mM DTT and 0.002% w/v bromophenol blue) was added. Samples were incubated in 65°C for 15 minutes. BCA Protein Assay Kit (Pierce, Thermo Scientific, Rockford, IL, USA) was used to determine the protein concentration.

Kidney membrane preparations for NCC immunoblots

All three donors gave permission for donating their kidneys after death. In case the kidney appeared not suitable for transplantation the donor gave permission to use the kidneys for research purposes, which is registered in the Dutch Donor registry. Harvested kidneys were

snap-frozen immediately after isolation and homogenized in detergent-free lysis buffer containing 50 mM Tris-HCl pH 7.5, 1 mM EDTA, 1 mM EGTA, 1 mM sodium orthovanadate, 5 mM sodium fluoride, 5 mM sodium pyrophosphate, 0.27 M sucrose, 0.1% v/v 2-mercaptoethanol and protease inhibitors (Roche, 1 tablet per 50 ml) with a homogenizer (VWR VDI 12 Adaptable Homogenizers, OpticsPlanet, Inc., Commercial Avenue Northbrook, IL, USA). Nuclei and debris were pelleted by centrifugation at 1,500 x g for 5 minutes at 4°C. Next, supernatants were centrifuged at 100,000 x g for 1 hour at 4°C. The pellet was washed with 1 vol. of lysis buffer without reducing agent and centrifuged again at 100,000 x g for 15 minutes to remove any remaining cytosolic particles. The pellet was then resuspended in lysis buffer including 1% v/v Nonidet P40. BCA Protein Assay Kit (Pierce, Thermo Scientific, Rockford, IL, USA) was used to determine the protein concentration. Finally, samples were stored at -80°C for the immunoblotting.

Immunoblotting

Exosome and kidney membrane samples were loaded on a gradient SDS-PAGE gel (4-15% v/v Criterion™ TGX™ Precast Gel, Bio-Rad, The Netherlands) and cell membrane proteins (10 μg) were loaded on an 8% v/v SDS-PAGE gel. Proteins were transferred to PVDF membranes (Immobilon-P, Millipore Corporation, Bedford, MA, USA) by electroelution. PVDF membranes were incubated for 16 hours with primary antibodies in 4°C, washed and subsequently incubated with secondary antibody for two hours in room temperature. Proteins were visualized using enhanced chemiluminescence (Thermo Fischer Scientific, Waltham, MA, USA) and a gel imaging system (ChemiDoc XRS, Bio-Rad Laboratories, Hercules, CA, USA). Densitometry was performed using Image J software (image processing program, NIH, Bethesda, MA, USA).

Immunohistochemistry

Immunohistochemical staining was performed on cryosections of snap-frozen tissue. Briefly, 2 μm serial sections of frozen human kidney were fixed with acetone for 10 minutes at -20°C. The sections were incubated for 1 hour at room temperature with primary antibody diluted in TNB buffer (0.1 M Tris-HCl, pH 7.5, 0.15 M NaCl, 0.5% w/v, Blocking Reagent, #FP1020, Perkin Elmer, Groningen, The Netherlands). For detection, kidney sections were incubated with Alexa flour-conjugated secondary antibodies. Images were taken with an Axio Imager camera and ZEN Lite software (Zeiss, Sliedrecht, The Netherlands).

Antibodies

Anti $NCC_{1/2}$ rabbit polyclonal antibody was manufactured by 21st Century Biochemicals (Marlborough, MA, USA). Briefly, peptide corresponding to the sequence NH_2-

ARGARPSVSGALDP-COOH was manufactured by Fmoc chemistry and after cleavage/deprotection was HPLC purified to >90%, and the mass and sequence verified by nanospray MS and CID MS/MS, respectively. This peptide was conjugated to carrier protein and used to immunize two New Zealand rabbits. After multiple boosts and bleeds, the serum was immunodepleted by affinity purification of the antibody specific to $NCC_{1/2}$ with affinity column containing the immunizing peptide. The antibody was used at the following dilution rates: IB 1:1,000, IHC 1:50. Rabbit polyclonal antibody against the N-terminal portion of rat NCC (Millipore, Billerica, MA, USA, #AB3553; IB 1:2,000, IHC 1:50). Rabbit polyclonal antibody against rat (R7) AQP2 (kindly provided by Dr. Peter Deen; IB 1:3,000).(6) Mouse monoclonal antibody against amino acids 101-210 of CD9 of human origin (C4, Santa Cruz Biotechnology, Inc., CA, USA; IB 1:500). Secondary antibodies were as follows: peroxidase conjugated goat anti-rabbit (Sigma-Aldrich, St. Luis, MO, USA, #A4914; IB 1:10,000), goat anti-rabbit Alexa Fluor® 488 (Molecular Probes, Eugene, OR, USA, #A-11029, IHC 1:300).

Acute water loading

The study was conducted according to the principles expressed in the declaration of Helsinki. All participants gave written informed consent and the study protocol was approved by the Institutional Review Board of the Radboud university medical center, Nijmegen, The Netherlands (approval number NL47178.091.13). Healthy males between 25 to 35 years old and with a body weight below 100 kg body weight were included in the study. Subjects were asked to refrain from coffee, tea, alcohol intake and any vigorous exercise for 24 hours before and during the study. Subjects did not drink or eat for 12 hours before the first urine collection to achieve maximal urine concentration. Each subject ingested 20 ml/kg body weight of water in 30 minutes. Midstream urine was collected before (time 0 minutes) and after water ingestion in 30 minutes intervals up to 150 minutes. Collected urine samples were supplemented with a final concentrations of protease inhibitors of 50 μM phenylmethylsulfonyl (PMSF), 20 μM aprotinin, 10 μM pepstatin A, 20 μM leupeptin, and stored at -80°C.

Urinary exosome isolation

The urine samples were collected from healthy subjects after acute water loading (see Supplement). Ten ml of collected urine was centrifuged at 17,000 × g for 15 minutes at 24°C in ultracentrifuge (Sorvall™ WX Floor Ultra Centrifuges, Thermo Scientific, Asheville, NC, USA) with 70.1Ti rotor. Supernatant was stored at room temperature for 25 minutes. The pellet was resuspended in 200 μl isolation solution (250 mM sucrose and 10 mM triethanolamine-HCl, pH 7.6) and 50 μl 3.24 M dithiothreitol (DTT), subsequently centrifuged at 17,000 × g for 15 minutes at 24°C. Thereafter, the supernatant was collected, combined

with supernatant obtained from the previous step and centrifuged at 200,000 × g for 2 hours at 24°C. Exosome pellet was dissolved in 50 µl of 1.5 × Laemmli (0.6% w/v SDS, 3% v/v glycerol, 18 mM Tris-HCl pH 6.8 and 0.003% w/v bromophenol blue). All the samples were stored in -20°C for further use.

Mass spectrometry

Gel slices were cut from the Coomassie-stained and washed SDS PAGE gel on a clean glass plate and were further diced in 1 mm^3 cubes using a scalpel and were transferred to a 1.5 ml reaction tube for further processing. ¼ gelband equivalent was processed for trypsin digestion and ¾ gelband was processed for Lys-C digestion. Gel cubes were vortexed in 400 µl 50 mM NH_4HCO_3 for 10 minutes. Supernatant was removed and the gel cubes were vortexed in 400 µl 50 mM NH_4HCO_3, 50% v/v acetonitrile for 10 minutes. After removal of the supernatant this wash-step was repeated once. Gel cubes were reduced in 10 mM DTT in 50 mM NH_4HCO_3 at 56°C in a heating block for 60 minutes. After cooling down the supernatant was removed and gel cubes were alkylated with 54 mM iodoacetamide in 50 mM NH_4HCO_3 for 45 minutes in the dark at RT. Supernatant was removed and gel cubes were vortexed in 400 µl 50 mM NH_4HCO_3 for 10 minutes. Supernatant was removed and the gel cubes were vortexed in 50 mM NH_4HCO_3/50% v/v acetonitrile. After removal of the supernatant this wash-step was repeated once. Supernatant was removed and gel cubes were dried in a vacuum centrifuge at 50°C for 10 minutes. Dried gel slices were covered with trypsin solution or Lys-C solution (6.25 ng/µl in 50 mM NH_4HCO_3), after rehydration of the cubes excess protease was removed and gel cubes were covered with 50 mM NH_4HCO_3. Digestion proceeded overnight at 25°C in a heating block. After digestion, peptides were extracted from the gel cubes with 100 µl 1% v/v formic acid by vortexing. Supernatant was transferred to a 1.5 ml tube and gel cubes were extracted with 100 µl 5% v/v formic acid 50% v/v acetonitrile. Supernatant was pooled with the first eluate. The second extraction was repeated once and the supernatant was pooled with previous extracts. Extracts were concentrated in a vacuum centrifuge at 50°C and volumes were adjusted to 50 µl by adding 0.05% v/v formic acid.

LC-MS/MS

Peptides were separated by an Ultimate 3000 nanoLC-MS/MS system (Dionex LC-Packings, Amsterdam, The Netherlands) equipped with a 20 cm × 75 µm ID fused silica column custom packed with 1.9 µm 120 Å ReproSil Pur C18 aqua (Dr Maisch GMBH, Ammerbuch-Entringen, Germany). After injection (15/50 µl Lys-C digest; 20/50 µl trypsin digest), peptides were trapped at 6 µl/minute on a 10 mm × 100 µm ID trap column packed with 5 µm 120 Å ReproSil Pur C18 aqua at 2% buffer B (buffer A: 0.5% v/v acetic acid in

MQ; buffer B: 80% v/v ACN + 0.5% v/v acetic acid in MQ) and separated at 300 nl/minute in a 10–40% buffer B gradient in 60 minutes (90 minutes inject-to-inject) at 50˚C. Eluting peptides were ionized at a potential of +2 kVa into a Q Exactive mass spectrometer (Thermo Fisher, Bremen, Germany). Intact masses were measured at resolution 70.000 (at m/z 200) in the orbitrap using an AGC target value of 3×10^6 charges. The top 10 peptides signals (charge-states 2^+ and higher) were submitted to MS/MS in the HCD (higher-energy collision) cell (1.6 amu isolation width, 25% normalized collision energy). MS/MS spectra were acquired at resolution 17,500 (at m/z 200) in the orbitrap using an AGC target value of 1×10^6 charges, an underfill ratio of 0.1%, and a maximum injection time (IT) of 60 milliseconds. Dynamic exclusion was applied with a repeat count of 1 and an exclusion time of 30 seconds.

Protein identification

MS/MS spectra were searched against the Uniprot human reference proteome FASTA file, release January 2014, no fragments; 42104 entries using MaxQuant 1.5.2.8. Enzyme specificity was set to trypsin or Lys-C, depending on the protease used, and up to two missed cleavages were allowed. Cysteine carboxamidomethylation (Cys, +57.021464 Da) was treated as fixed modification and methionine oxidation (Met, +15.994915 Da), Gln->pyroglutamate (pyr-Gln, -17.026549 Da) and N-terminal acetylation (N-terminal, +42.010565 Da) as variable modifications. Peptide precursor ions were searched with a maximum mass deviation of 4.5 ppm and fragment ions with a maximum mass deviation of 20 ppm (default MaxQuant settings). Peptide and protein identifications were filtered at an FDR of 1% using the decoy database strategy. Proteins that could not be differentiated based on MS/MS spectra alone were grouped to protein groups (default MaxQuant settings).

Measurement of urinary creatinine and osmolality.

Urinary creatinine was measured according to Jaffe's method with the use of colorimetric assay (Labor und Technik, Berlin, Germany).(37) Osmolality of urine samples was measured by freezing point depression using a Micro-osmometer (Advanced Instrument model 3320, Nordwood, MA, USA).

Statistical analysis

In the oocyte analysis all depicted data are averages of at least 2 independent experiments, each containing a minimum of 10-15 oocytes per group. Overall statistics between groups was determined by one-way ANOVA. In case of significance, multiple comparisons between groups were performed by Bonferroni post-hoc tests. Immunoblot data were analyzed by comparing integrated optical densities of bands by one-way ANOVA followed by Dunnett's

Multiple Comparison post-hoc test. Values are mean ± SEM in acute water loading: normalized to time 0 minutes levels, n = 6. For all experiments P value <0.05 was considered statistically significant. All the data were analyzed using Prism 5 software (GraphPad Software Inc, La Jolla, CA, USA).

Results

NCC splicing and the S811 phosphorylation site

Fig. 1A displays the protein sequence alignment encompassing the fragment specific for NCC_1 and NCC_2. NCC_1 contains one extra amino acid as compared to NCC_2, which is localized outside the exon 20 region. Therefore, $NCC_{1/2}$ will refer to the combined presence of NCC_1 and NCC_2, as these are indistinguishable in several of the experimental assays performed in this study. The $NCC_{1/2}$ is present and preserved between some mammalian species (human and rabbit), but is not present in rodents (mouse and rat). In humans, the NCC splice site is encoded by exon 20 (Fig. 1B). Remarkably, this exon is absent in mouse and rat due to the lack of splice sites. Fig. 1B shows the exon prearrangement of $NCC_{1/2}$. Sequence analysis of cDNA fragments isolated from human kidney showed that both $NCC_{1/2}$ and NCC_3 are present (Fig. 1C). $NCC_{1/2}$ is longer than NCC_3 due to the presence of nine extra amino acid residues in the C-terminal domain (Fig. 1D). The phosphorylation site identified in the additional fragment corresponds to residue S811 (Fig. 1D). Constructs encoding NCC_3 and NCC_1 as well as the phosphorylation site mutants (S811D and S811A) (Fig. 1D) were subcloned into appropriate plasmid vectors for heterologous expression in Human Embryonic Kidney (HEK293) cells and *Xenopus laevis* oocytes. Quantitative PCR analysis revealed that $NCC_{1/2}$ mRNA constitute 44 ± 6% (n = 7) of all NCC isoforms present in the human kidney cortex biopsies (Table 1).

Mass spectrometric identification of human NCC isoforms

The presence of the NCC isoforms in the human urinary exosomes on the protein level was investigated by mass spectrometry. Data are available via ProteomeXchange with identifier PXD002279 (http://www.proteomexchange.org; Username: reviewer55274@ebi.ac.uk; Password: QI1g6xJe) (44). Overall 51 peptides were detected for SLC12A3 by tryptic digestion and 15 peptides by Lys-C digestion yielded sequence coverage of 14 and 39%, respectively. Two regions in the amino-acid sequence allow distinction between the isoforms: Peptides correlated to V807L and 9 amino-acid deletion peptides indicating the presence of both NCC_3 as well as $NCC_{1/2}$ were identified. Isoform-specific peptides spanning residues 781-838 are shown in Table 2. Specifically, Lys-C digestion yields MMQAHINPVFDPAEDGKEASARGARPSVSGALDPK ($NCC_{1/2}$ res 785-820, Andromeda

score 49.2) and MMQAHINPVFDPAEDGKEASA RVDPK (NCC_3 res 785-811, Andromeda score 70.3), as well as EASARGARPSVSGALDPK ($NCC_{1/2}$ res 802-820, Andromeda score 57.5) and EASARVDPKALVK (NCC_3 res 802-815, Andromeda score 32.9). Tryptic digestion additionally yielded GARPSVSGALDPK ($NCC_{1/2}$ res 807-820, Andromeda score 122.5) and PSVSGALDPK ($NCC_{1/2}$ res 810-820, Andromeda score 104.8). Identification of multiple overlapping peptides of both NCC_3 as well as $NCC_{1/2}$ firmly indicated that in exosomes, the *SCL12A3* gene product is present as a mixture of NCC_3 and at least one and possibly both NCC_1 and NCC_2.

Generation of specific antibodies against $NCC_{1/2}$

$NCC_{1/2}$-specific peptide epitope (ARGARPSVSGALDP) was used to generate anti-$NCC_{1/2}$ antibodies. Specificity of the antibody was tested using isolated membranes from HEK293 cells transfected with corresponding plasmids. A commercially available antibody against the N-terminal portion of NCC detected NCC_3 as well as $NCC_{1/2}$, as all are carrying the recognized epitope (Fig. 2A). Therefore, in the present study expression of NCC, detected by the antibody against the N-terminal NCC, refers to the combined expression of NCC_3 and $NCC_{1/2}$ hence denoted as $NCC_{1\text{-}3}$. The antibody specific for $NCC_{1/2}$ recognized only $NCC_{1/2}$, but not NCC_3 and $NCC_{1/2}$ mutants (S811A and S811D) (Fig. 2B). This demonstrates the high specificity of the newly generated antibody against the $NCC_{1/2}$ epitope. Immunoreactivity was not present in cells transfected with mock vector or in the presence of specific blocking peptides (Fig. 2C).

Immunoblot identification of human NCC isoforms

Immunoblots of kidney membrane fractions and urinary exosomes of three subjects showed two immunopositive protein bands of ~260 and 130 kDa, representing the dimeric and monomeric form of the $NCC_{1\text{-}3}$ transporter, respectively (Fig. 2D). Importantly, the $NCC_{1/2}$ protein was also detected in kidney membrane fractions and urinary exosomes as two bands of ~260 and 130 kDa as evidence for the dimeric and monomeric form, respectively (Fig. 2E). This indicates that NCC isoforms are present in oligomeric structures in the human kidney and urinary exosomes.

$NCC_{1/2}$ localizes to apical membrane of DCT

Immunohistochemical staining of human kidney serial sections revealed expression of $NCC_{1\text{-}3}$ (Fig. 3A and B) and $NCC_{1/2}$ (Fig. 3C and D) at the apical membrane of epithelial cells lining the DCT. Expression of both $NCC_{1\text{-}3}$ and $NCC_{1/2}$ was restricted to the same tubular sites.

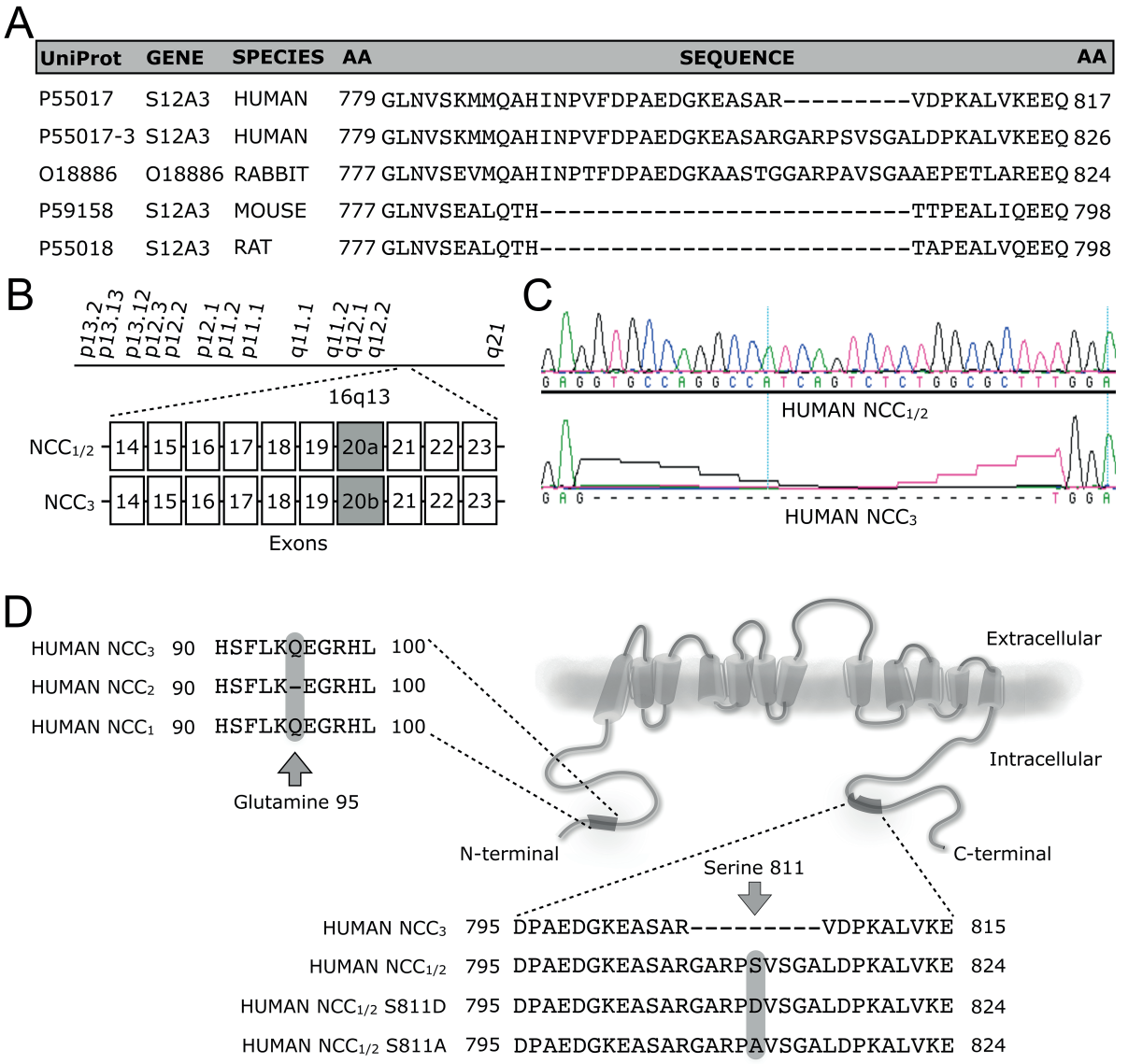

Figure 1 | Splicing of NaCl cotransporter (NCC) gene.

(**A**) Multiple protein alignment analysis of NCC against diverse species as stated. (**B**) Schematic representation of gene SLC12A3 and the exon 20a, in light grey box, that encodes for the splice variant. (**C**) DNA multiple alignment and chromatogram sequence analysis of the region encoding the human $NCC_{1/2}$ and NCC_3. (**D**) Topological representation of $NCC_{1/2}$ within the N-terminal domain, in light grey shadow, shows alignment of all three human NCC isoform sequences (NCC_3, NCC_2, and NCC_1) and carboxyl-terminal domain, in light grey shadow, shows the phosphorylation site at S811. Lower panel shows a multiple alignment of the human NCC protein sequence depicted the additional nine amino acids in $NCC_{1/2}$, including the phosphorylation mutant constructs (S811D and S811A).

Table 1 | Ratio of $NCC_{1/2}$ to NCC_{1-3} mRNA expression in seven human kidney cortex biopsies determined by Real-time relative RT-PCR quantification.

Volunteer #	% $NCC_{1/2}$
1	52
2	46
3	19
4	29
5	42
6	59
7	63
Average %	44
SEM	± 6

Table 2 | Peptides identified from the isoform-specific region of SLC12A3 aligned to the protein amino acid sequence.

Isoform	Nomen-clature	Protease	Sequence of identified peptides
		Lys-C	$^{811/820}$ALVKEEQATTIFQSEQGK$^{829/838}$
		Lys-C	^{785}MMQAHINPVFDPAEDGK^{802}
		Lys-C	^{785}MMQAHINPVFDPAEDGKEASAR ----------VDPK^{811}
		Lys-C	^{802}EASAR ----------VDPKALVK^{815}
SLC12A3-3	NCC_3		^{781}NVSKMMQAHINPVFDPAEDGKEASAR ----------VDPKALVKEEQATTIFQSEQGK^{829}
SLC12A3-1/2	$NCC_{1/2}$		^{781}NVSKMMQAHINPVFDPAEDGKEASARGARPSVSGALDPKALVKEEQATTIFQSEQGK^{838}
		Trypsin	^{785}MMQAHINPVFDPAEDGKEASAR^{807}
		Lys-C	^{785}MMQAHINPVFDPAEDGKEASARGARPSVSGALDPK^{820}
		Trypsin	^{802}EASARGARPSVSGALDPK^{820}
		Trypsin	^{807}GARPSVSGALDPK^{820}
		Trypsin	^{810}PSVSGALDPK^{820}

In red NCC_3 specific residues and in green $NCC_{1/2}$ specific residues. In the middle the aligned amino acid sequences of NCC_3 and $NCC_{1/2}$.

Functional characterization of NCC_1

In order to compare the functional abilities of NCC_1 and NCC_3, cRNA of the respective variants was microinjected into *Xenopus laevis* oocytes and thiazide-sensitive $^{22}Na^+$ uptake was measured (Fig. 4). It has been shown previously that cumulative amounts of eGFP-NCC correlate dose-dependently with the eGFP-NCC fluorescence at the oocyte membrane and with thiazide-sensitive $^{22}Na^+$ uptake (7). For the analysis, day 4 after cRNA injection was chosen. Thiazide-sensitive $^{22}Na^+$ transport was significantly increased in the NCC_1 compared to the NCC_3 (Fig. 4A). To further evaluate whether this increase in transport was dependent on the phosphorylation at S811 the effect of substituting the serine residue by an aspartic acid to mimic constitutive phosphorylation was tested. The S811D mutant exhibited a significant increase in thiazide-sensitive $^{22}Na^+$ uptake in comparison to NCC_3 and NCC_1. Moreover, the S811A mutant mimicking a constitutively inactive phosphorylation site showed a significant decrease in thiazide-sensitive $^{22}Na^+$ uptake, as compared to NCC_1 S811D variants (Fig. 4A).

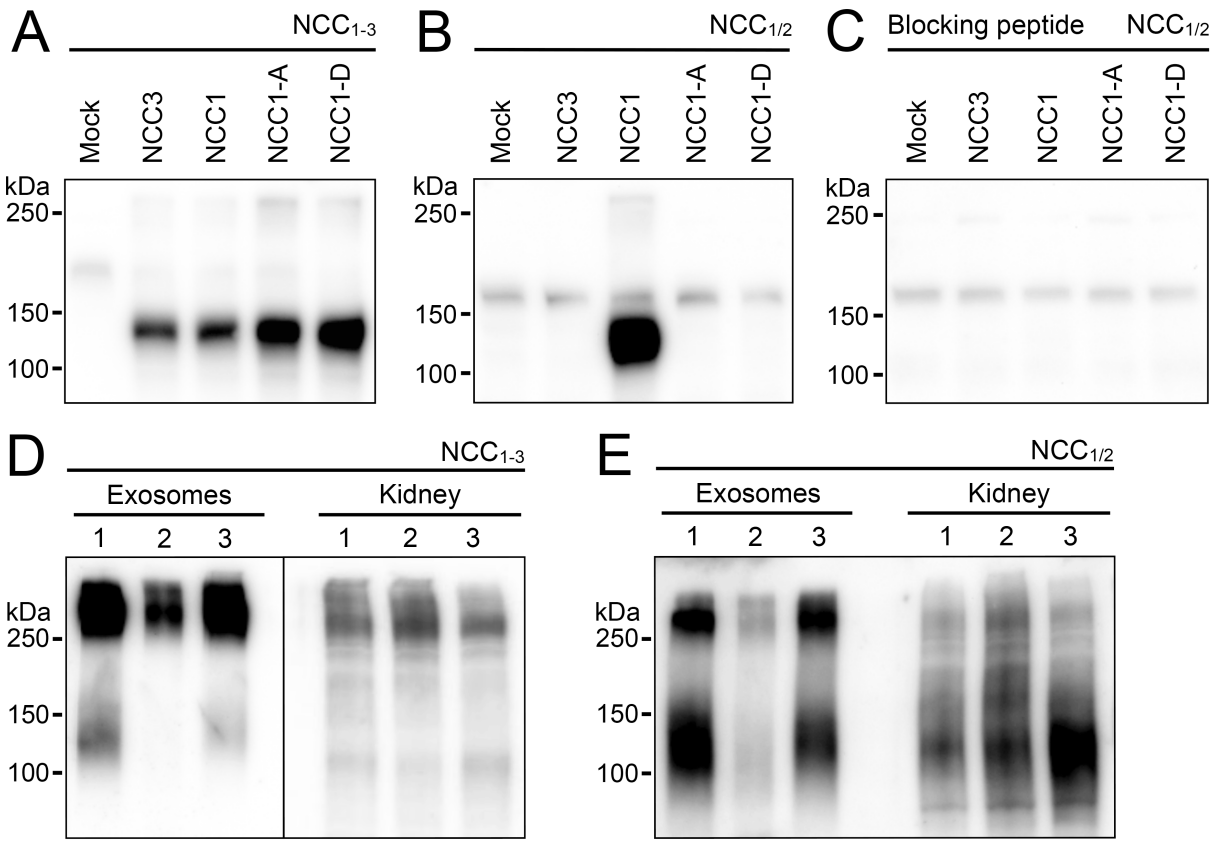

Figure 2 | Verification of $NCC_{1/2}$ antibody specificity.

(**A**) Immunoblot of total membrane fraction isolated from HEK293 cells transfected with empty vector (mock), NCC_3, NCC_1 and NCC_1 phosphorylation site mutants (S811A and S811D) probed with an antibody against NCC_{1-3}. (**B**) Immunoblot of total membrane fraction isolated from HEK293 cells transfected with empty vector (mock), NCC_3, NCC_1, and NCC_1 mutants (S811A and S811D) probed with an antibody recognizing specifically $NCC_{1/2}$. (**C**) Immunoblot of total membrane fraction isolated from HEK293 cells transfected with empty vector (mock), NCC_3, NCC_1 and NCC_1 mutants (S811A and S811D) probed with the $NCC_{1/2}$ antibody pre-absorbed with $NCC_{1/2}$ immunizing peptide. (**D**) Expression of NCC_{1-3} and (**E**) $NCC_{1/2}$ in kidney membrane fractions and urinary exosomes of three subjects depicting two bands of ~260 and 130 kDa.

WNK4 has previously been shown to reduce forward trafficking of NCC in the oocyte system, by diverting the cotransporter to the lysosomal compartment (38, 49). Additionally, WNK 4 modulates SPAK/OSR1 phosphorylation and hence NCC activity (4, 43). To elucidate whether WNK4 has similar effects on NCC_1, cRNA encoding the NCC variants were co-injected with WNK4. WNK4 reduced NCC-dependent $^{22}Na^+$ uptake to similar levels in all conditions, suggesting that the majority of NCC_1 activity is sensitive to WNK4 inhibition in S811 independent manner (Fig. 4A). In each condition $^{22}Na^+$ uptake was thiazide-sensitive (Fig. 4A, black bars). To determine surface expression of injected cRNA, fluorescent intensity of eGFP-tagged NCC_3, NCC_1, NCC_1 S811D or NCC_1 S811A was quantified (Fig. 4B and C).

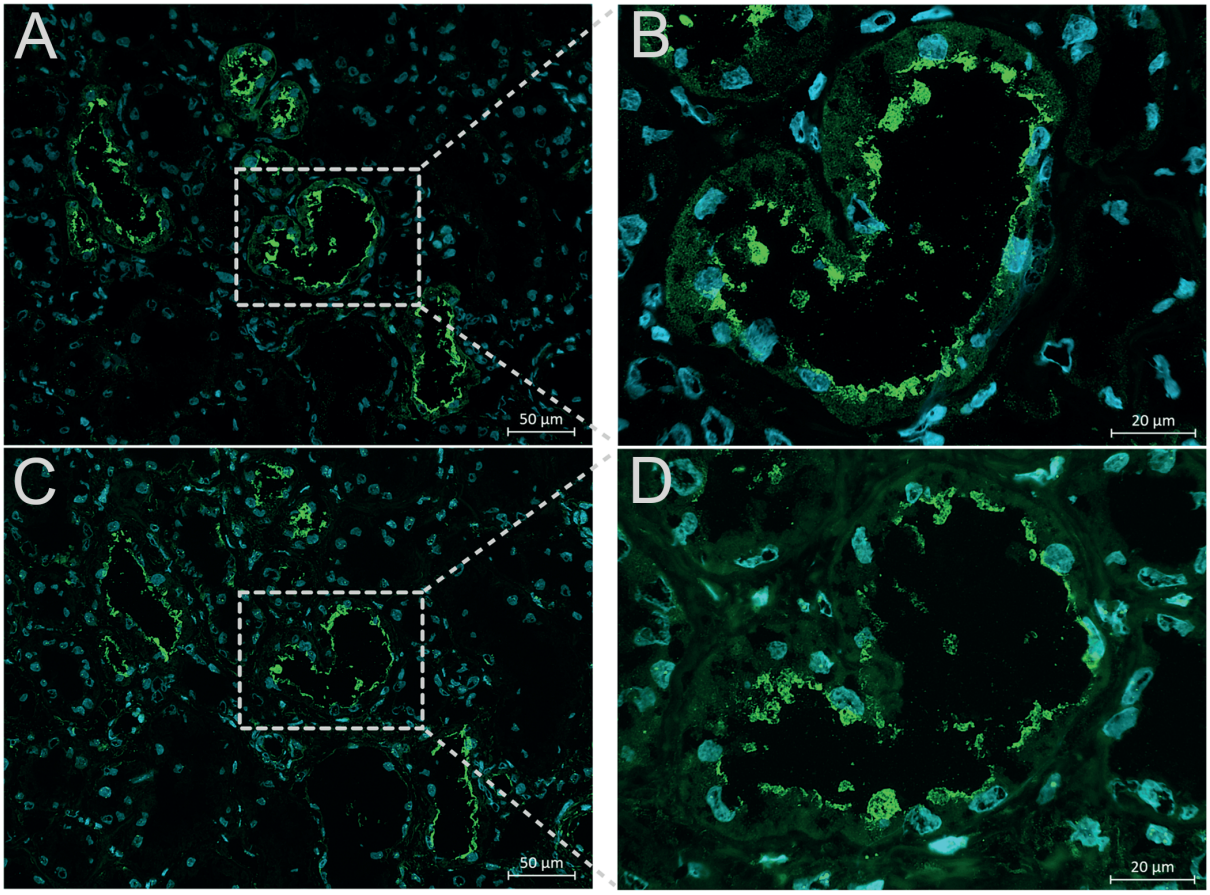

Figure 3 | Immunolocalization of $NCC_{1/2}$ in the human kidney.

Representative serial sections of human kidney depicting NCC_{1-3} (**A** and **B**) and $NCC_{1/2}$ (**C** and **D**). Immunofluorescence colocalizes at the apical membrane domains of epithelial cells lining DCT. As the antibody against NCC_{1-3} also binds to $NCC_{1/2}$, immunofluorescence in A and B may partially originate from $NCC_{1/2}$. The bar represents a scale of 20 or 50 µm as indicated.

Acute water loading

Acute water loading was performed in six healthy subjects to determine the effect of hypervolemia on the renal expression of NCC isoforms. Urine was collected before (time 0) and after acute water loading in 30-minute intervals up to 150 minutes. Urinary exosomes of each subject were loaded according to the urine creatinine concentration onto the gel and to confirm equal loading of the samples, the abundance of the exosomal marker CD9 was determined (1, 11). Our study demonstrated the existence of NCC in dimeric and monomeric forms in urinary exosomes using immunoblotting. Therefore, both dimeric and monomeric forms were analyzed separately. Immunoblots probed for $NCC_{1/2}$ showed a significant decrease of $NCC_{1/2}$ monomer and dimer expression 60 minutes after acute water loading, which returned to the baseline levels at 150 minutes (Fig. 5A, C and E). Expression of NCC_{1-3} monomer and dimer significantly dropped 60 minutes after acute water loading and restored after 150 minutes (Fig. 5B, D and F). The exosomes were also probed for the

expression of aquaporin 2 (AQP2) since water loading is known to downregulate AQP2 (36). Indeed, AQP2 expression in urinary exosomes was significantly reduced 60 minutes after acute water loading (Fig. 6A and B). CD9 expression levels within urinary exosomes did not change significantly at different time points, suggesting equal loading of exosomes (Fig. 5G, 5H, 6C, respectively). Urine osmolality decreased significantly 30 minutes after acute water loading (Fig. 6D).

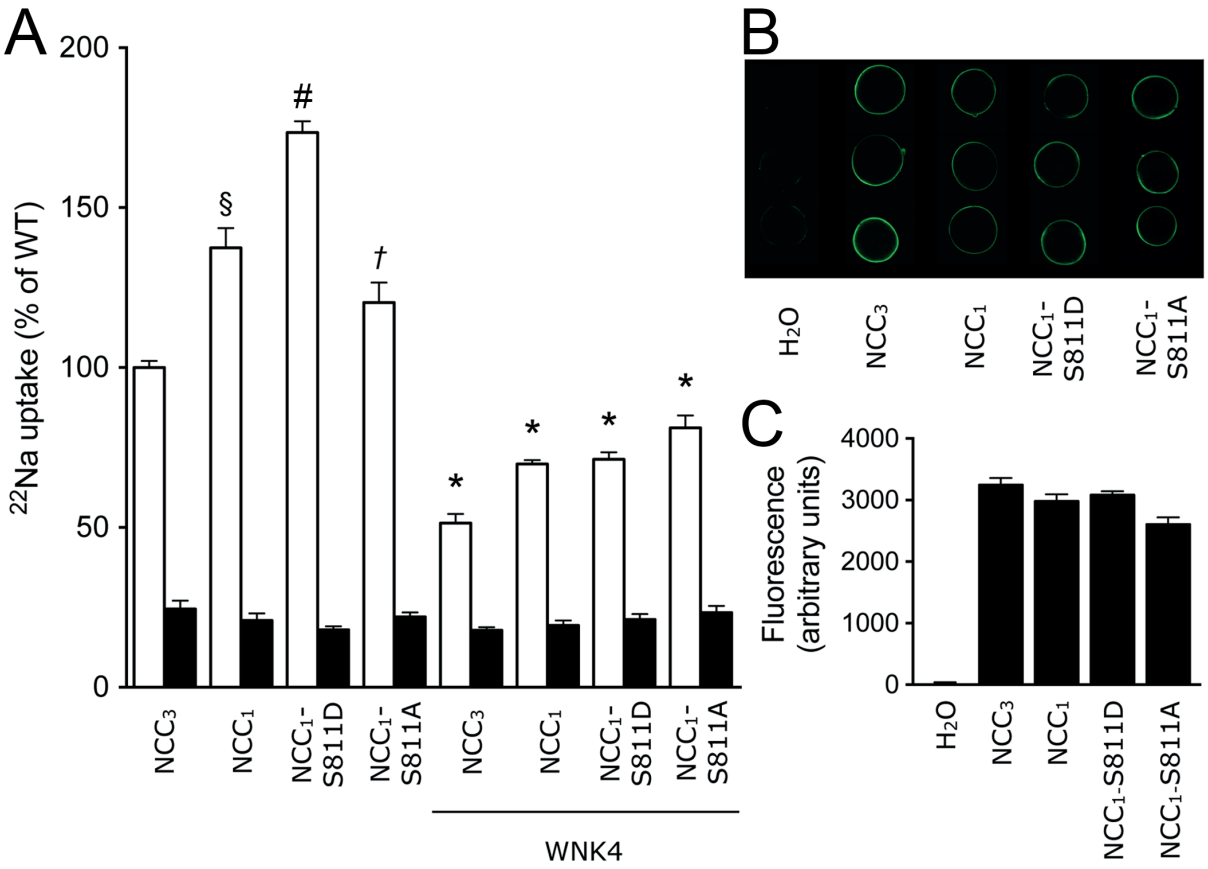

Figure 4 | Expression and functional analysis of eGFP tagged NCC variants in the oocyte membrane.

(**A**) $^{22}Na^{+}$ uptakes in *Xenopus laevis* oocytes microinjected with 5 ng of cRNA encoding the human NCC_3, NCC_1, NCC_1 S811D, NCC_1 S811A or co-injected with 10 ng of WNK4 cRNA. The $^{22}Na^{+}$ uptake experiments were performed in the absence (white bars) or presence (black bars) of 0.1 mM HCT. $^{22}Na^{+}$ uptakes were corrected for surface expression of the corresponding variants. NCC_1 vs. NCC_3 (§) as well as NCC_1 S811D vs. NCC_1 (#) had significantly increased $^{22}Na^{+}$ uptake. NCC_1 S811A had significantly reduced $^{22}Na^{+}$ uptake in comparison to NCC_1 S811D (*†*). Each variant co-injected with WNK4 had significantly decreased $^{22}Na^{+}$ uptake in comparison to its corresponding variant without WNK4 (*). (**B**) Three representative confocal images of oocytes that were injected with GFP-NCC_3, GFP-NCC_1, GFP-NCC_1 S811D or GFP-NCC_1 S811A cRNA. (**C**) Surface expression analyses were performed on oocytes four days after microinjection with corresponding cRNA. *P<0.05 was considered statistically significant.

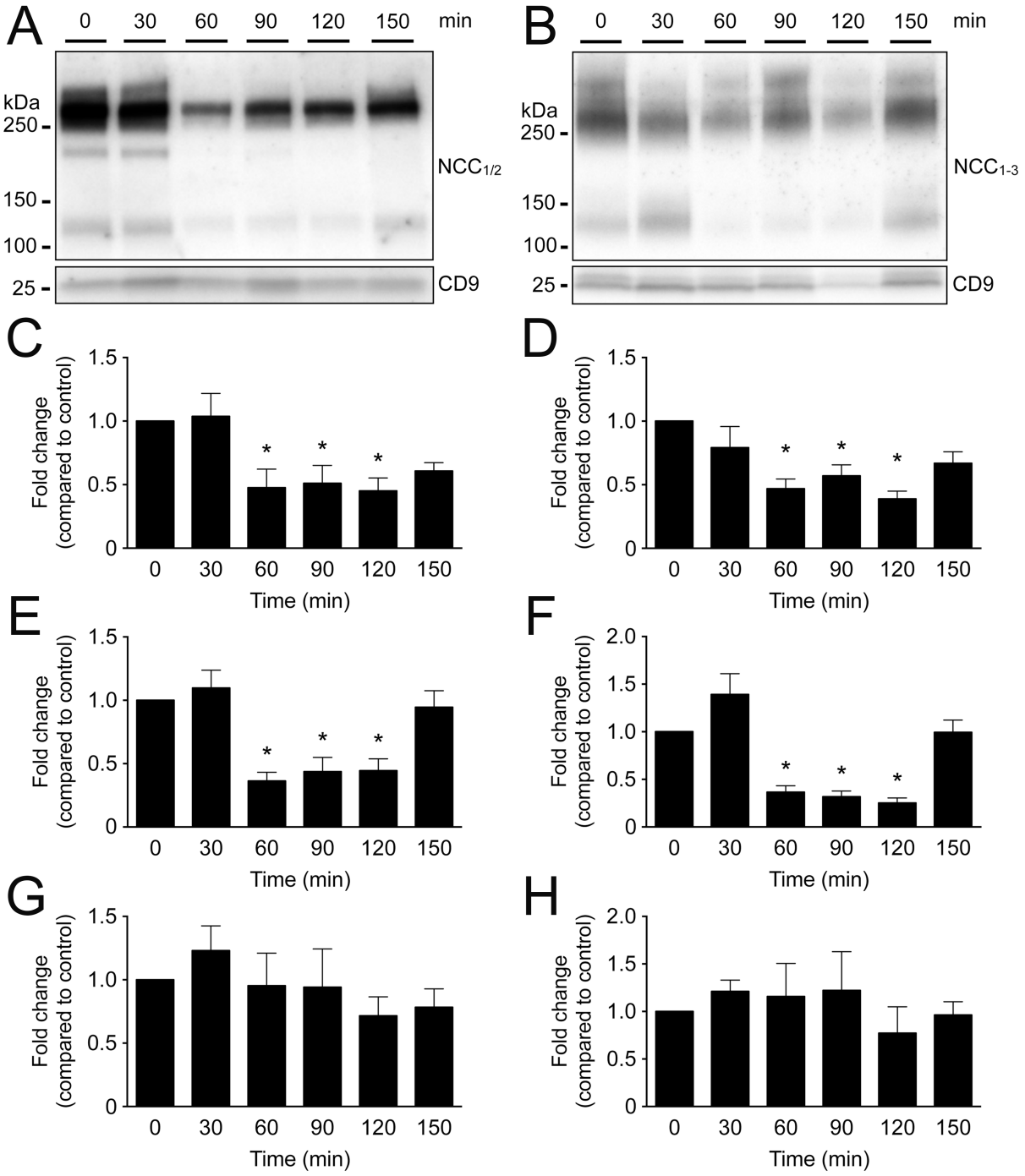

Figure 5 | Expression of $NCC_{1/2}$ and NCC_{1-3} in human urinary exosomes after acute water loading.

Immunoblot of urinary exosomes isolated before (0 minute) and after water loading probed for $NCC_{1/2}$ (**A**) and NCC_{1-3} (**B**). Both $NCC_{1/2}$ and NCC_{1-3} abundance was significantly reduced 60 minutes after acute water loading and returned to the baseline level after 150 minutes. Densitometry analysis of $NCC_{1/2}$ (**C**) and NCC_{1-3} (**D**) monomer abundance in urinary exosomes. Densitometry analysis of $NCC_{1/2}$ (**E**) and NCC_{1-3} (**F**) dimer abundance in urinary exosomes. (**G** and **H**) Densitometry analysis of CD9 expression levels showed no significant changes. Values are mean ± SEM (n = 6) normalized to time 0 levels. *P<0.05 was considered significant.

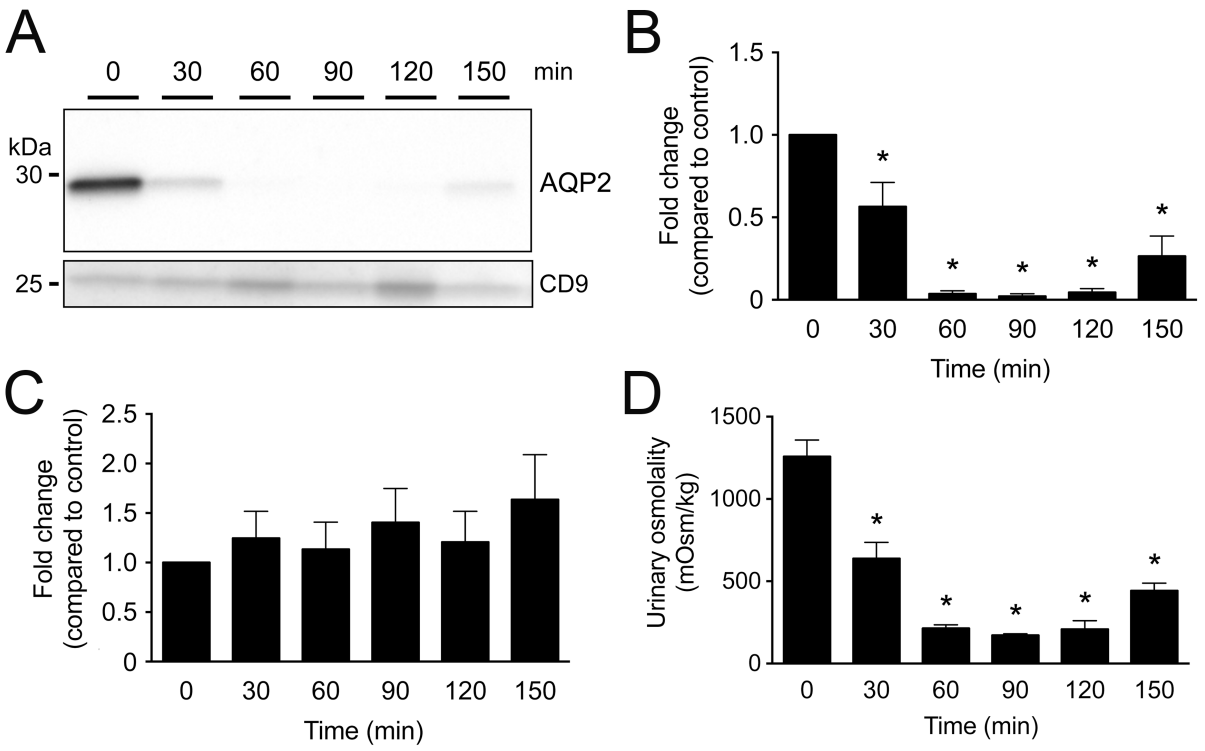

Figure 6 | Expression of AQP2 in human urinary exosomes after acute water loading.

(**A**) Immunoblot of urinary exosomes isolated before (0 minute) and after water loading probed for AQP2. AQP2 abundance was significantly decreased 60 minutes after acute water loading and maintained significantly lower levels up to 150 minutes. (**B**) Densitometry analysis of AQP2 abundance in urinary exosomes. (**C**) Densitometry analysis of CD9 expression levels corrected to urine creatinine concentration showed no significant changes. (**D**) Urinary osmolality was significantly decreased from 30 to 150 minutes after acute water loading. Values are mean ± SEM (n = 6) normalized to time 0 minute levels. *P<0.05 was considered significant.

Discussion

Since 1996, when human NCC was cloned, it has been shown that three isoforms of NCC are present in the human kidney (22, 23, 35). However, all NCC studies have focused on the shorter isoform, NCC_3, leaving the alternative splice variants unexplored. In the presented study, we delineated for the first time the localization, abundance, and functionality of $NCC_{1/2}$ in the human kidney by showing that: *i)* mRNA of $NCC_{1/2}$ constitutes ~44% of all NCC (NCC_{1-3}) transcripts in the human kidney; *ii)* $NCC_{1/2}$ is clearly detectable in human urinary exosomes by mass spectrometry and immunoblot analysis; *iii)* $NCC_{1/2}$ is, like the shorter NCC_3 isoform, present at the apical membrane of DCT; *iv)* phosphorylation at S811 regulates NCC_1 function; *v)* the abundance of $NCC_{1/2}$ is regulated in response to physiological stimuli such as acute water loading.

Generation of new antibodies specifically recognizing $NCC_{1/2}$ allowed us to demonstrate the presence of $NCC_{1/2}$ at the apical membrane of the DCT, present in the human kidney as well as monomeric and dimeric complexes in kidney membrane fractions and urinary exosomes. The presence of $NCC_{1/2}$ in the exosomes was confirmed by mass spectrometry. Noteworthy, all antibodies raised against NCC_3 recognize also $NCC_{1/2}$. Thus, in previously performed studies on endogenous human NCC also $NCC_{1/2}$ may have been detected. Because human NCC_1 and NCC_2 differ only by one amino acid it was impossible to differentiate between both isoforms with the immunodetection methods. Therefore, it was addressed as a combined expression of both isoforms, $NCC_{1/2}$. We demonstrated that $NCC_{1/2}$ mRNA constitutes a substantial amount (44%) of total NCC mRNA in the human kidney. Nevertheless, the relative protein abundance of each isoform depends on the translation and quality control of the proteins. Therefore, the expression level of mRNA does not always mirror the abundance of the protein. Moreover, presented mRNA analysis characterizes a combined expression of NCC_1 and NCC_2 since they were indistinguishable. Hence, the ratio of each isoform is not strictly determined.

Functional characterization of NCC_1 and the role of its phosphorylation site S811 were investigated by using *Xenopus* oocytes. As NCC_3, NCC_1 demonstrated thiazide-sensitive $^{22}Na^+$ transport. Additionally, NCC_1 activity can also be modified by changes in phosphorylation status. Splicing and subsequent single point directed mutagenesis to mimic constitutively active phosphorylation sites of NCC_1 (S811D) led to an increased activity of NCC_1 compared to NCC_3. We demonstrated that once the S811 residue is substituted by an alanine (S811A) mimicking inactive site, the activity of the splice variant is significantly decreased. The fact that inhibition of S811 phosphorylation reverts transporter capability only to basal levels implies that the $NCC_{1/2}$ and its phosphorylation is introduced in order to augment transport of NCC over the baseline level when needed. Our functional experiments demonstrated that WNK4 is a strong inhibitor of both NCC_1 and NCC_3. However, the effect of WNK4 is not mediated via S811 phosphorylation, since the constitutively active S811D mutant is not protected from the inhibitory effects of WNK4. This suggests that in both isoforms, NCC_1 and NCC_3, the effect of WNK4 is mediated via regulation at the N-terminus. Additionally, phosphorylation at S811 may depend on simultaneous regulation of the phosphorylation at the N-terminal residues.

In order to determine $NCC_{1/2}$ expression *in vivo,* human urinary exosomes were analyzed. Exosomes are frequently used as biomarkers for renal tubular disorders as they reflect changes in the expression of different proteins present in the tubular epithelial cells (16, 40). For instance, it has been demonstrated that patients with Gitelman syndrome do not express NCC in their urinary exosomes (19). In contrast, patients with familial hyperkalemic hypertension characterized by enhanced activity of NCC, have increased NCC

expression in their urinary exosomes (17, 24). This substantiates the notion that NCC abundance in urinary exosomes reflects the actual state of NCC expression in the DCT as postulated previously (16, 40). We hypothesized that the activity of $NCC_{1/2}$ can be modified by changes in the protein abundance at the plasma membrane. Depending on a stimulus (hormones, electrolyte concentration, etc.) NCC expression throughout the DCT can be altered by the insertion of a more potent isoform ($NCC_{1/2}$) into the apical membrane, in order to maximize NaCl transport and *vice versa*. Consequently, we showed that $NCC_{1/2}$ and NCC_{1-3} abundance in urinary exosomes is robustly down regulated in response to water loading (Fig. 5). Increased activity and expression of NCC in response to changes in the renin-angiotensin-aldosterone system and vasopressin has been well documented (5, 28, 30-34, 41, 42). Hence, decreased NCC abundance at the apical plasma membrane in water-loaded subjects is likely a result of hypervolemia, hyponatremia, and a subsequent decline in vasopressin release.

Thus far, signaling pathways regulating $NCC_{1/2}$ are unknown. However, prediction software (pkaPS) from the IMP-IMBA Bioinformatics group (26) suggested that the phosphorylated sequence around S811 of $NCC_{1/2}$ shows high similarity to a PKA consensus site. Therefore, potential hormones regulating the cAMP-PKA pathway might be involved in regulating transport via this kinase. Several hormonal systems have been shown to activate the cAMP-PKA pathway in the DCT (3, 9). Our water loading study substantiates the regulatory effect of vasopressin not only on NCC_{1-3} but also specifically on $NCC_{1/2}$ abundance in the kidney. Since S811 may contain PKA consensus site we hypothesized that a PKA-dependent mechanism could be occurring for the phosphorylation at S811 in response to vasopressin stimulation. Nevertheless, recent studies demonstrated a potential role for vasopressin in modulating NCC N-terminal phosphorylation in the DCT (25, 28, 34), which may constitute the main regulatory mechanism for all NCC isoforms since all variants contain the same N-terminal phosphorylation sites.

Our data clearly demonstrates that $NCC_{1/2}$ is not a redundant transcription product, but it merely constitutes a fully functional thiazide-sensitive NaCl-transporting protein. In parallel, we propose a novel way of NCC regulation by phosphorylation at the C-terminal S811 residue that adds to the complex system governing the regulation of NCC. Future experiments developing S811 phospho-specific antibodies and samples from different human pathological states could aid in determining the precise regulation of $NCC_{1/2}$. A better understanding of the regulation of NCC in the kidneys may be critical to help to elucidate the molecular events underlying the pathogenesis of essential hypertension.

Acknowledgements

The authors thank Pedro San-Cristobal, Ganesh Pathare, Mark J.J. de Graaf, Ron Engels, Henry Dijkman, and Marla Lavrijsen for technical assistance and helpful suggestions and discussions. The support of Johan van der Vlag supplying the human kidney cortex biopsies is greatly appreciated.

Grants

This study was supported by the European Society of Hypertension (2011-2013 Fellowship), the Netherlands, Organization for Scientific Research (VENI ZonMw 916.12.046), the Dutch Kidney Foundation (PHD12.14) and the European Union's Seventh Framework Programme (FP7/2007-2013) under grant agreement no. 305608 (EURenOmics). Henrik Dimke is funded by the Novo Nordisk Foundation (11749) and the Carlsberg Foundation (2013_01_0214).

Disclosures

The authors declare that they have no conflicts of interest with the contents of this article.

Author contribution

Author contributions: O.A.T., S.J., M.V.-F., H.D., and S.R.P. performed experiments; O.A.T., S.J., M.V.-F., H.D., S.R.P., C.R.J., J.G.H., and R.J.B. analyzed data; O.A.T., S.J., M.V.-F., H.D., S.R.P., C.R.J., J.D., J.W.L., J.G.H., and R.J.B. interpreted results of experiments; O.A.T. prepared figures; O.A.T., S.J., J.G.H., and R.J.B. drafted manuscript; O.A.T., S.J., M.V.-F., H.D., S.R.P., C.R.J., J.D., J.W.L., J.G.H., and R.J.B. edited and revised manuscript; O.A.T., S.J., M.V.-F., H.D., S.R.P., C.R.J., J.D., J.W.L., J.G.H., and R.J.B. approved final version of manuscript; J.G.H. and R.J.B. provided conception and design of research.

References

1. Alvarez ML, Khosroheidari M, Ravi RK, DiStefano JK. Comparison of protein, microRNA, and mRNA yields using different methods of urinary exosome isolation for the discovery of kidney disease biomarkers. *Kidney Int* 82: 1024–1032, 2012.
2. Boyden LM, Choi M, Choate KA, Nelson-Williams CJ, Farhi A, Toka HR, Tikhonova IR, Bjornson R, Mane SM, Colussi G, Lebel M, Gordon RD, Semmekrot BA, Poujol A, Valimaki MJ, De Ferrari ME, Sanjad SA, Gutkin M, Karet FE, Tucci JR, Stockigt JR, Keppler-Noreuil KM, Porter CC, Anand SK, Whiteford ML, Davis ID, Dewar SB, Bettinelli A, Fadrowski JJ, Belsha CW, Hunley TE, Nelson RD, Trachtman H, Cole TRP, Pinsk M, Bockenhauer D, Shenoy M, Vaidyanathan P, Foreman JW, Rasoulpour M, Thameem F, Al-Shahrouri HZ, Radhakrishnan J, Gharavi AG, Goilav B, Lifton RP. Mutations in kelch-like 3 and cullin 3 cause hypertension and electrolyte abnormalities. *Nature* 482: 98–U126, 2012.
3. Chabardes D, Gagnan-Brunette M, Imbert-Teboul M, Gontcharevskaia O, Montegut M, Clique A, Morel F. Adenylate cyclase responsiveness to hormones in various portions of the human nephron. *J Clin Invest* 65: 439–448, 1980.
4. Chiga M, Rafiqi FH, Alessi DR, Sohara E, Ohta A, Rai T, Sasaki S, Uchida S. Phenotypes of pseudohypoaldosteronism type II caused by the WNK4 D561A missense mutation are dependent on the WNK-OSR1/SPAK kinase cascade. *J Cell Sci* 124: 1391–1395, 2011.
5. Chiga M, Rai T, Yang S-S, Ohta A, Takizawa T, Sasaki S, Uchida S. Dietary salt regulates the phosphorylation of OSR1/SPAK kinases and the sodium chloride cotransporter through aldosterone. *Kidney Int* 74: 1403–1409, 2008.
6. Deen PM, Croes H, van Aubel RA, Ginsel LA, van Os CH. Water channels encoded by mutant aquaporin-2 genes in nephrogenic diabetes insipidus are impaired in their cellular routing. *Journal of Clinical Investigation* 95: 2291–2296, 1995.
7. Dimke H, San-Cristobal P, de Graaf M, Lenders JW, Deinum J, Hoenderop JGJ, Bindels RJM. γ-Adducin stimulates the thiazide-sensitive NaCl cotransporter. *J Am Soc Nephrol* 22: 508–517, 2011.
8. Dimke H. Exploring the intricate regulatory network controlling the thiazide-sensitive NaCl cotransporter (NCC). *Pflügers Archiv European Journal of Physiology* 462: 767–777, 2011.
9. Elalouf JM, Roinel N, de Rouffignac C. Stimulation by human calcitonin of electrolyte transport in distal tubules of rat kidney. *Pflügers Arch* 399: 111–118, 1983.
10. Farfel Z, Iaina A, Rosenthal T, Waks U, Shibolet S, Gafni J. Familial hyperpotassemia and hypertension accompanied by normal plasma aldosterone levels: possible hereditary cell membrane defect. *Arch Intern Med* 138: 1828–1832, 1978.
11. Fernandez-Llama P, Khositseth S, Gonzales PA, Star RA, Pisitkun T, Knepper MA. Tamm-Horsfall protein and urinary exosome isolation. *Kidney Int* 77: 736–742, 2010.
12. Gamba G. Regulation of the renal Na+-Cl- cotransporter by phosphorylation and ubiquitylation. *Am J Physiol-Renal* 303: F1573–83, 2012.
13. Gitelman HJ, Graham JB, Welt LG. A new familial disorder characterized by hypokalemia and hypomagnesemia. *Trans Assoc Am Physicians* 79: 221–235, 1966.
14. Glover M, Ware JS, Henry A, Wolley M, Walsh R, Wain LV, Xu S, Van't Hoff WG, Tobin MD, Hall IP, Cook S, Gordon RD, Stowasser M, O'Shaughnessy KM. Detection of mutations in KLHL3 and CUL3 in families with FHHt (familial hyperkalaemic hypertension or Gordon's syndrome). *Clin Sci* 126: 721–726, 2014.
15. Gonzales PA, Pisitkun T, Hoffert JD, Tchapyjnikov D, Star RA, Kleta R, Wang NS, Knepper MA. Large-scale proteomics and phosphoproteomics of urinary exosomes. *J Am Soc Nephrol* 20: 363–379, 2009.
16. Hoorn EJ, Pisitkun T, Zietse R, Gross P, Frokiaer J, Wang NS, Gonzales PA, Star RA, Knepper MA. Prospects for urinary proteomics: Exosomes as a source of urinary biomarkers. *Nephrology* 10: 283–290, 2005.
17. Isobe K, Mori T, Asano T, Kawaguchi H, Nonoyama S, Kumagai N, Kamada F, Morimoto T, Hayashi M, Sohara E, Rai T, Sasaki S, Uchida S. Development of enzyme-linked immunosorbent assays for urinary thiazide-sensitive Na-Cl cotransporter measurement. *Am J Physiol-Renal* 305: F1374–F1381, 2013.
18. James PA, Oparil S, Carter BL, Cushman WC, Dennison-Himmelfarb C, Handler J, Lackland DT, LeFevre ML, MacKenzie TD, Ogedegbe O, Smith SC, Svetkey LP, Taler SJ, Townsend

RR, Wright JT, Narva AS, Ortiz E. 2014 Evidence-Based Guideline for the Management of High Blood Pressure in Adults: Report From the Panel Members Appointed to the Eighth Joint National Committee (JNC 8). *JAMA* 311: 507–520, 2014.

19. Joo KW, Lee JW, Jang HR, Heo NJ, Jeon US, Oh YK, Lim CS, Na KY, Kim J, Cheong HI, Han JS. Reduced urinary excretion of thiazide-sensitive Na-Cl cotransporter in Gitelman syndrome: preliminary data. *Am J Kidney Dis* 50: 765–773, 2007.
20. Lalioti MD, Zhang J, Volkman HM, Kahle KT, Hoffmann KE, Toka HR, Nelson-Williams C, Ellison DH, Flavell R, Booth CJ, Lu Y, Geller DS, Lifton RP. Wnk4 controls blood pressure and potassium homeostasis via regulation of mass and activity of the distal convoluted tubule. *Nat Genet* 38: 1124–1132, 2006.
21. Mancia G, Fagard R, Narkiewicz K, Redon J, Zanchetti A, Böhm M, Christiaens T, Cifkova R, De Backer G, Dominiczak A, Galderisi M, Grobbee DE, Jaarsma T, Kirchhof P, Kjeldsen SE, Laurent S, Manolis AJ, Nilsson PM, Ruilope LM, Schmieder RE, Sirnes PA, Sleight P, Viigimaa M, Waeber B, Zannad F, Task Force Members. 2013 ESH/ESC Guidelines for the management of arterial hypertension: the Task Force for the management of arterial hypertension of the European Society of Hypertension (ESH) and of the European Society of Cardiology (ESC). *J. Hypertens.* 31: 1281–1357, 2013.
22. Mastroianni N, Bettinelli A, Bianchetti M, Colussi G, DeFusco M, Sereni F, Ballabio A, Casari C. Novel molecular variants of the Na-Cl cotransporter gene are responsible for Gitelman syndrome. *Am J Hum Genet* 59: 1019–1026, 1996.
23. Mastroianni N, Fusco MD, Zollo M, Arrigo G, Zuffardi O, Bettinelli A, Ballabio A, Casari G. Molecular Cloning, Expression Pattern, and Chromosomal Localization of the Human Na–Cl Thiazide-Sensitive Cotransporter (SLC12A3). *Genomics* 35: 486–493, 1996.
24. Mayan H, Attar-Herzberg D, Shaharabany M, Holtzman EJ, Farfel Z. Increased urinary Na-Cl cotransporter protein in familial hyperkalaemia and hypertension. *Nephrol Dial Transplant* 23: 492–496, 2008.
25. Mutig K, Saritas T, Uchida S, Kahl T, Borowski T, Paliege A, Bohlick A, Bleich M, Shan Q, Bachmann S. Short-term stimulation of the thiazide-sensitive Na+-Cl- cotransporter by vasopressin involves phosphorylation and membrane translocation. *Am J Physiol-Renal* 298: F502–9, 2010.
26. Neuberger G, Schneider G, Eisenhaber F. pkaPS: prediction of protein kinase A phosphorylation sites with the simplified kinase-substrate binding model. *Biol Direct* 2: 1, 2007.
27. Pacheco-Alvarez D, Cristobal PS, Meade P, Moreno E, Vazquez N, Munoz E, Diaz A, Juarez ME, Gimenez I, Gamba G. The Na+:Cl- cotransporter is activated and phosphorylated at the amino-terminal domain upon intracellular chloride depletion. *J Biol Chem* 281: 28755–28763, 2006.
28. Pedersen NB, Hofmeister MV, Rosenbaek LL, Nielsen J, Fenton RA. Vasopressin induces phosphorylation of the thiazide-sensitive sodium chloride cotransporter in the distal convoluted tubule. *Kidney Int* 78: 160–169, 2010.
29. Ponce-Coria J, San-Cristobal P, Kahle KT, Vazquez N, Pacheco-Alvarez D, de los Heros P, Juarez P, Munoz E, Michel G, Bobadilla NA, Gimenez I, Lifton RP, Hebert SC, Gamba G. Regulation of NKCC2 by a chloride-sensing mechanism involving the WNK3 and SPAK kinases. *Proc Natl Acad Sci USA* 105: 8458–8463, 2008.
30. Rieg T, Tang T, Uchida S, Hammond HK, Fenton RA, Vallon V. Adenylyl cyclase 6 enhances NKCC2 expression and mediates vasopressin-induced phosphorylation of NKCC2 and NCC. *Am J Pathol* 182: 96–106, 2013.
31. Rozansky DJ, Cornwall T, Subramanya AR, Rogers S, Yang Y-F, David LL, Zhu X, Yang C-L, Ellison DH. Aldosterone mediates activation of the thiazide-sensitive Na-Cl cotransporter through an SGK1 and WNK4 signaling pathway. *J Clin Invest* 119: 2601–2612, 2009.
32. San-Cristobal P, Pacheco-Alvarez D, Richardson C, Ring AM, Vazquez N, Rafiqi FH, Chari D, Kahle KT, Leng Q, Bobadilla NA, Hebert SC, Alessi DR, Lifton RP, Gamba G. Angiotensin II signaling increases activity of the renal Na-Cl cotransporter through a WNK4-SPAK-dependent pathway. *Proc Natl Acad Sci USA* 106: 4384–4389, 2009.
33. Sandberg MB, Riquier ADM, Pihakaski-Maunsbach K, McDonough AA, Maunsbach AB. ANG II provokes acute trafficking of distal tubule Na+-Cl cotransporter to apical membrane. *Am J Physiol-Renal* 293: F662–F669, 2007.
34. Saritas T, Borschewski A, McCormick JA, Paliege A, Dathe C, Uchida S, Terker A, Himmerkus

N, Bleich M, Demaretz S, Laghmani K, Delpire E, Ellison DH, Bachmann S, Mutig K. SPAK Differentially Mediates Vasopressin Effects on Sodium Cotransporters. *J Am Soc Nephrol* 24: 407–418, 2013.

35. Simon DB, Nelson-Williams C, Johnson Bia M, Ellison D, Karet FE, Morey Molina A, Vaara I, Iwata F, Cushner HM, Koolen M, Gainza FJ, Gitelman HJ, Lifton RP. Gitelman's variant of Bartter's syndrome, inherited hypokalaemic alkalosis, is caused by mutations in the thiazide-sensitive Na-Cl cotransporter. *Nat Genet* 12: 24–30, 1996.
36. Soodvilai S, Jia Z, Wang M-H, Dong Z, Yang T. mPGES-1 deletion impairs diuretic response to acute water loading. *Am J Physiol-Renal* 296: F1129–F1135, 2009.
37. Spierto FW, Macneil ML, Burtis CA. The effect of temperature and wavelength on the measurement of creatinine with the jaffe procedure. *Clinical Biochemistry* 12: 18–21, 1979.
38. Subramanya AR, Liu J, Ellison DH, Wade JB, Welling PA. WNK4 Diverts the Thiazide-sensitive NaCl Cotransporter to the Lysosome and Stimulates AP-3 Interaction. *Journal of Biological Chemistry* 284: 18471–18480, 2009.
39. Vallon V, Schroth J, Lang F, Kuhl D, Uchida S. Expression and phosphorylation of the Na^+-Cl^- cotransporter NCC in vivo is regulated by dietary salt, potassium, and SGK1. *Am J Physiol-Renal* 297: F704–12, 2009.
40. van der Lubbe N, Jansen PM, Salih M, Fenton RA, van den Meiracker AH, Danser AHJ, Zietse R, Hoorn EJ. The Phosphorylated Sodium Chloride Cotransporter in Urinary Exosomes Is Superior to Prostasin as a Marker for Aldosteronism. *Hypertension* 60: 741–748, 2012.
41. van der Lubbe N, Lim CH, Fenton RA, Meima ME, Danser AHJ, Zietse R, Hoorn EJ. Angiotensin II induces phosphorylation of the thiazide-sensitive sodium chloride cotransporter independent of aldosterone. *Kidney Int* 79: 66–76, 2011.
42. van der Lubbe N, Lim CH, Meima ME, van Veghel R, Rosenbaek LL, Mutig K, Danser AHJ, Fenton RA, Zietse R, Hoorn EJ. Aldosterone does not require angiotensin II to activate NCC through a WNK4–SPAK–dependent pathway. *Pflügers Archiv - European Journal of Physiology* 463: 853–863, 2012.
43. Vitari AC, Deak M, Morrice NA, Alessi DR. The WNK1 and WNK4 protein kinases that are mutated in Gordon's hypertension syndrome phosphorylate and activate SPAK and OSR1 protein kinases. *Biochem J* 391: 17–24, 2005.
44. Vizcaíno JA, Deutsch EW, Wang R, Csordas A, Reisinger F, Ríos D, Dianes JA, Sun Z, Farrah T, Bandeira N, Binz P-A, Xenarios I, Eisenacher M, Mayer G, Gatto L, Campos A, Chalkley RJ, Kraus H-J, Albar JP, Martinez-Bartolomé S, Apweiler R, Omenn GS, Martens L, Jones AR, Hermjakob H. ProteomeXchange provides globally coordinated proteomics data submission and dissemination. *Nat Biotechnol* 32: 223–226, 2014.
45. Wakabayashi M, Mori T, Isobe K, Sohara E, Susa K, Araki Y, Chiga M, Kikuchi E, Nomura N, Mori Y, Matsuo H, Murata T, Nomura S, Asano T, Kawaguchi H, Nonoyama S, Rai T, Sasaki S, Uchida S. Impaired KLHL3-mediated ubiquitination of WNK4 causes human hypertension. *Cell Rep* 3: 858–868, 2013.
46. Whelan JA, Russell NB, Whelan MA. A method for the absolute quantification of cDNA using real-time PCR. *J Immunol Methods* 278: 261–269, 2003.
47. Wilson FH, Disse-Nicodeme S, Choate KA, Ishikawa K, Nelson-Williams C, Desitter I, Gunel M, Milford DV, Lipkin GW, Achard JM, Feely MP, Dussol B, Berland Y, Unwin RJ, Mayan H, Simon DB, Farfel Z, Jeunemaitre X, Lifton RP. Human hypertension caused by mutations in WNK kinases. *Science* 293: 1107–1112, 2001.
48. Yang CL, Zhu X, Ellison DH. The thiazide-sensitive Na-Cl cotransporter is regulated by a WNK kinase signaling complex. *J Clin Invest* 117: 3403–3411, 2007.
49. Zhou B, Zhuang J, Gu D, Wang H, Cebotaru L, Guggino WB, Cai H. WNK4 enhances the degradation of NCC through a sortilin-mediated lysosomal pathway. *J Am Soc Nephrol* 21: 82–92, 2010.

3

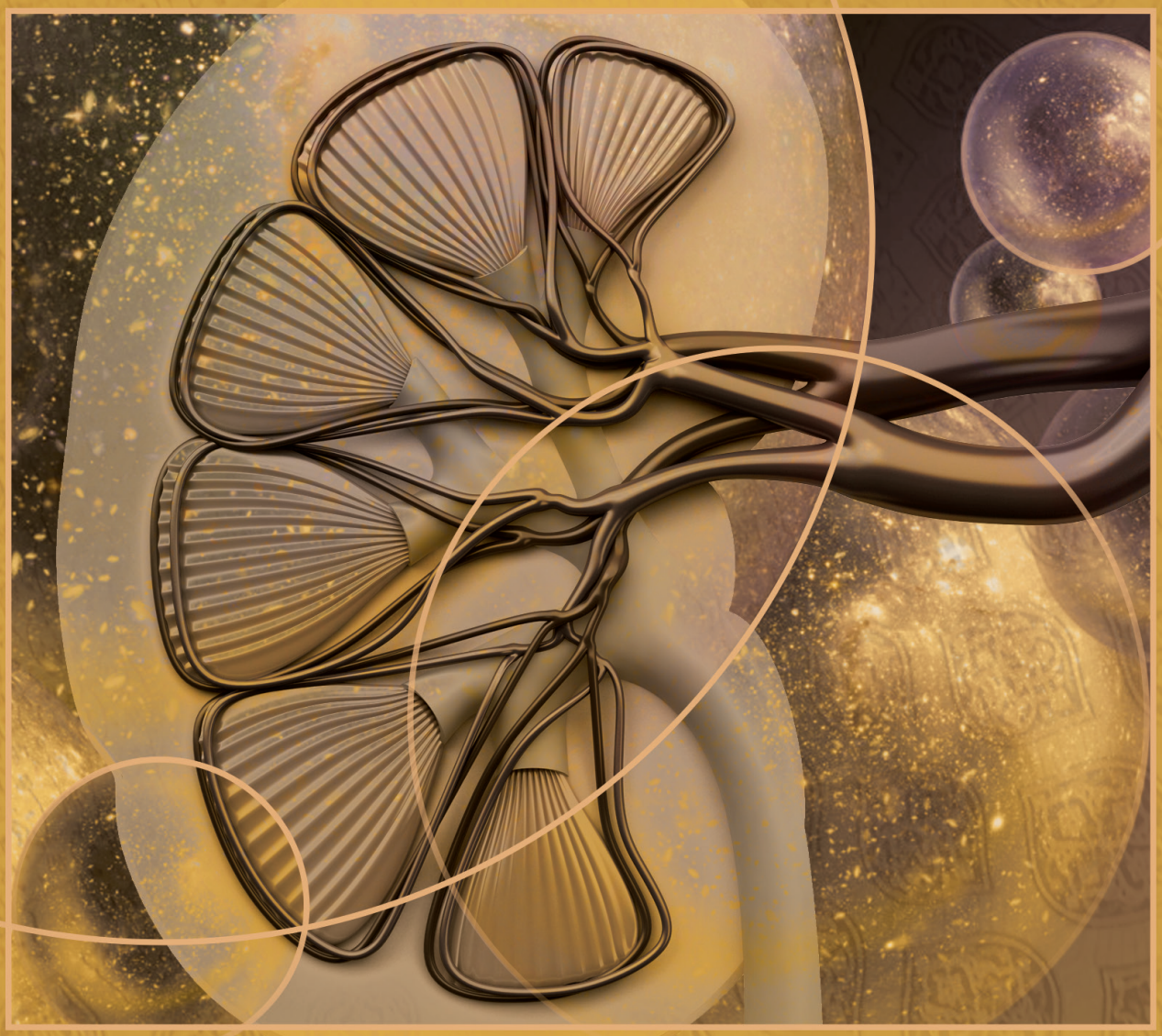

Hydrochlorothiazide treatment increases the abundance of the NaCl cotransporter in urinary extracellular vesicles of essential hypertensive patients

Ganesh Pathare[1]*, Omar A.Z. Tutakhel[1]*, Mark C. van der Wel[2], Luke M. Shelton[1], Jaap Deinum[3], Jacques W.M. Lenders[3,4], Joost G.J. Hoenderop[1] and René J.M. Bindels[1]

Departments of [1]Physiology, [2]Primary and Community Care, and [3]Internal Medicine, Radboud Institute for Molecular Life Sciences, Radboud university medical center, Nijmegen, The Netherlands; [4]Department of Medicine III, University Hospital Carl Gustav Carus, Technische Universität Dresden, Germany

* Authors contributed equally

Am J Physiol Renal Physiol, 312: F1063-F1072, 2017

Abstract

The thiazide-sensitive NaCl cotransporter (NCC), located apically in distal convoluted tubule epithelia, regulates the fine-tuning of renal sodium excretion. Three isoforms of NCC are generated through alternative splicing of the transcript, of which the third isoform has been the most extensively investigated in pathophysiological conditions. The aim of this study was to investigate the effect of different anti-hypertensive treatments on the abundance and phosphorylation of all three NCC isoforms in urinary extracellular vesicles (uEVs) of essential hypertensive patients. In uEVs isolated from patients (n=23) before and after hydrochlorothiazide or valsartan treatment the abundance and phosphorylation of the NCC isoforms was determined. Additionally, clinical biochemistry and blood pressure of the patients was assessed. Our results show that NCC detected in human uEVs has a glycosylated and oligomeric structure, comparable to NCC present in human kidney membrane fractions. Despite the inhibitory action of hydrochlorothiazide on NCC activity, immunoblot analysis of uEVs showed significantly increased abundance of NCC isoforms 1 and 2 ($NCC_{1/2}$), total NCC (NCC_{1-3}), and the phosphorylated form of total NCC ($pNCC_{1-3}$-T55/T60) in essential hypertensive patients treated with hydrochlorothiazide, but not with valsartan. This study highlights that $NCC_{1/2}$, NCC_{1-3}, and $pNCC_{1-3}$-T55/T60 are upregulated by hydrochlorothiazide, and the increase in NCC abundance in uEVs of essential hypertensive patients correlates with the blood pressure response to hydrochlorothiazide.

Keywords: Hypertension / NaCl cotransporter / Thiazide diuretics / Urinary extracellular vesicles / kidney

Introduction

Hypertension is a major risk factor for stroke, myocardial infarction, heart failure and chronic kidney disease (CKD) (16). According to the latest report from the American Heart Association, 78 million American adults (representing 33 % of the population) have increased blood pressure (16), of which ~90 % present with primary or essential hypertension (4, 28). Anti-hypertensive medications, such as valsartan (Val) and thiazide-type diuretics are, therefore, prescribed to achieve blood pressure control. Although the pathogenesis of essential hypertension is multifactorial, the kidneys play a key role in blood pressure regulation by modulating renal sodium excretion (24). Several guidelines for management of hypertension in adults consider thiazide-type diuretics as a fundamental therapeutic tool (21, 36). Thiazide-type diuretics act by blocking the thiazide-sensitive NaCl cotransporter (NCC), apically localized in epithelial cells lining the distal convoluted tubule (DCT) (20). Loss of function mutations in NCC cause Gitelman syndrome (OMIM 263800), a condition characterized by sodium wasting, hypokalemic metabolic alkalosis, hypomagnesemia, hypocalciuria and hypotension when compared to their age-matched unaffected relatives (15, 39). Activation of NCC, through mutations in WNK [with no lysine (K)] kinases, mainly WNK1 and WNK4 (45), KLHL3 or Cullin3 (3) results in pseudohypoaldosteronism type II (PHAII) (also known as familial hyperkalemic hypertension (OMIM 145260)), which is characterized by increased renal sodium reabsorption, hyperkalemic metabolic acidosis, hypercalciuria and hypertension (32). The known involvement of NCC in these disease states suggests a role in the physiological regulation of blood pressure.

In humans, alternate splicing of the *SLC12A3* gene gives rise to three separate isoforms of the NCC (43); namely NCC_1 (39), NCC_2 (17), and NCC_3 (26). Our previous work delineated the abundance and localization of NCC_1 and NCC_2 ($NCC_{1/2}$) in the human kidney as well as its functional properties in physiological conditions (43). Significantly expressed in human kidney, $NCC_{1/2}$ may constitute a unique route of renal NaCl reabsorption and therefore might play an important role in human blood pressure regulation (43). Rodents express NCC_3, but they lack $NCC_{1/2}$ (43), which has hampered progress towards further investigating the role of $NCC_{1/2}$ in the pathophysiology of hypertension.

In humans, urinary extracellular vesicles (uEVs) can be used as a non-invasive tool to study the regulation of NCC in the kidney (17, 44, 46). uEVs, including exosomes, are nanosized vesicles (30-120 nm) that form when multivesicular bodies within the cell merge with the cell membrane and release internal vesicles into the extracellular space or pro-urine (35). The cargo of uEVs reflects changes in the expression of different proteins present in the epithelial cells of the DCT, including total NCC (NCC_{1-3}) and phosphorylated form of total

NCC ($pNCC_{1-3}$-T55/T60) (43, 44). It has been shown that patients with Gitelman syndrome have decreased NCC abundance in uEVs (7, 22), while patients with PHAII have increased NCC abundance in uEVs (27, 44).

Val reduces blood pressure by antagonizing angiotensin II type I receptors and thereby prevents the actions of angiotensin II (47). Despite the divergent mechanisms of action of thiazides and Val, both anti-hypertensive medications result in a reduction of blood pressure (18). Importantly, angiotensin II is a well-known direct activator of NCC (38), making Val a suitable anti-hypertensive drug to compare with thiazides. Unlike thiazides, Val does not directly bind to NCC, but it might alter NCC activity by effects on NCC phosphorylation and abundance. The anti-hypertensive effects of these drugs are well investigated; however, in humans their response to NCC expression has not been studied. The aim of this study was, therefore, to investigate the effect of different anti-hypertensive treatments on the abundance and phosphorylation of all three NCC isoforms in uEVs of essential hypertensive patients, and to explore the relationship between NCC abundance in uEVs and changes in blood pressure.

Materials and Methods

Patients, design and setting

The study was conducted according to the principles expressed in the Declaration of Helsinki. The Nijmegen Anti-hypertensive Management Improvement Study (NAMIS) was approved by the local Ethics Committee of the Radboud university medical center, Nijmegen, The Netherlands (clinicaltrials.gov; trial registration no. NCT00457483). Patients with newly diagnosed hypertension, aged 18-65 years and listed in general practices affiliated with the Radboud university medical center were screened for eligibility to participate in a prospective open-label and blinded end-point (PROBE) crossover study. Patients with a confirmed diagnosis of hypertension and who gave written consent were included in the study (n=23). Exclusion criteria were the following: use of anti-hypertensive medication; blood pressure higher than 200 mmHg systolic or 120 mmHg diastolic; presence of cardiovascular co-morbidity (diabetes mellitus, peripheral arterial disease, ischemic heart disease, stroke, transient ischemic attack and atrial fibrillation) and the inability to speak or understand Dutch.

Figure 1 shows a schematic view of the study design. After a two weeks run-in period, untreated (Unt) patients used hydrochlorothiazide (HCT) for four weeks (12.5 mg, once daily), followed by a four weeks washout period and then Val treatment for four weeks (80 mg, once daily). At the run-in, age, sex and menopausal state were also recorded. After the run-in period and at the end of each medication, ambulatory blood pressure, plasma sodium,

potassium and renin concentrations, amino (N)-terminal of the prohormone brain natriuretic peptide (NT-proBNP), estimated glomerular filtration rate (eGFR), urinary albumin excretion, body mass index and waist circumference were measured.

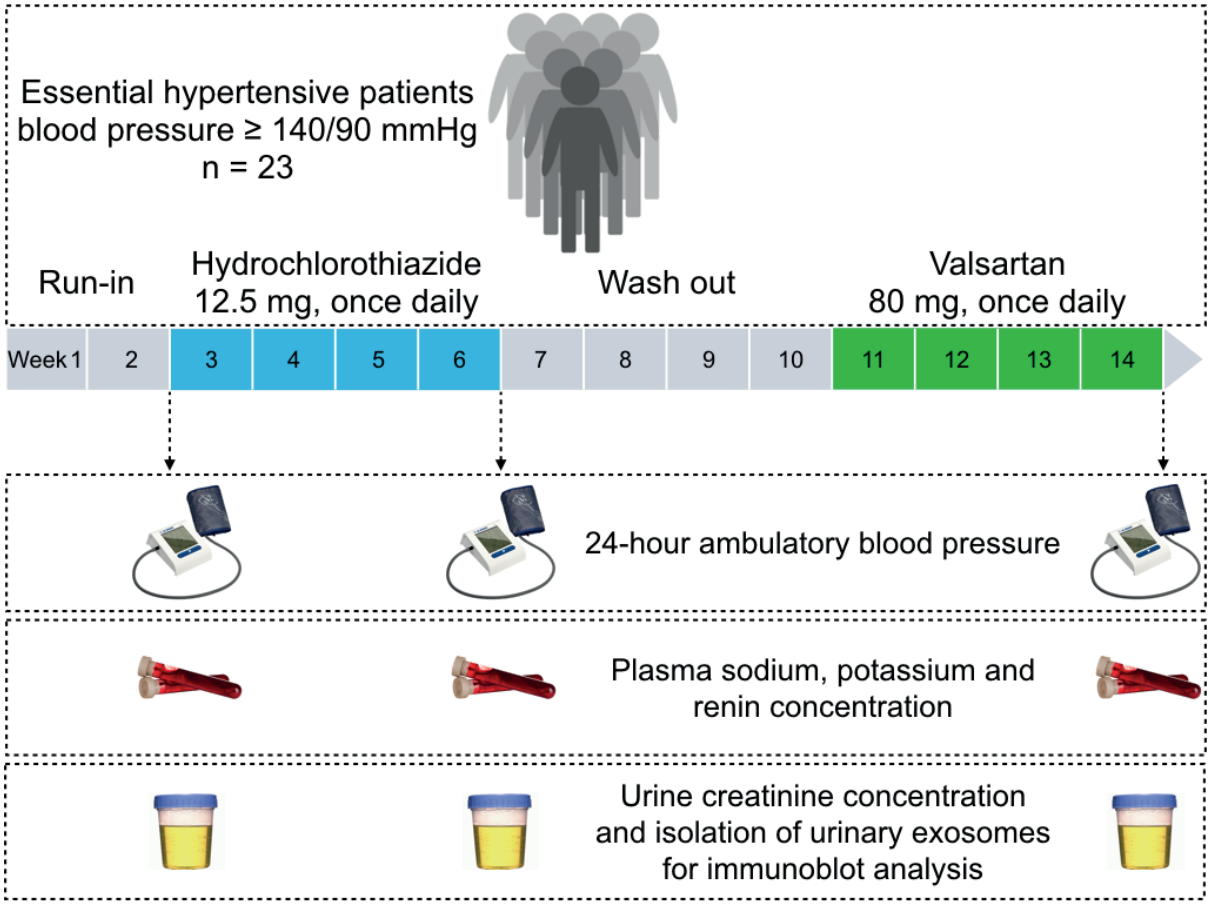

Figure 1 | Schematic view of the Nijmegen Anti-hypertensive Management Improvement Study (NAMIS) design.

Twenty-three patients with blood pressure ≥ 140/90 mmHg were included in the study. After a two weeks run-in period (Unt), patients used HCT for four weeks (12.5 mg, once daily), followed by a four weeks washout period and then Val treatment for four weeks (80 mg, once daily). After the run-in and at the end of each medication, ambulatory blood pressure, plasma sodium, plasma potassium, plasma renin and urine creatinine concentrations were measured and urinary extracellular vesicles of patients were isolated for immunoblot analysis.

Blood pressure measurements and laboratory tests

During eligibility screening performed by the local staff of the general practices, a diagnosis of hypertension (≥ 140/90 mmHg) was given based on the mean of all blood pressure measurements taken by trained practice nurses at three different clinic visits. The data of the blood pressure levels were presented as mean arterial pressure (MAP). All practices were provided with oscillometric blood pressure monitors (Stabil-O-Graph, I.E.M. GMBH, Stolberg, Germany).

All 24-hour ambulatory blood pressure recordings were taken on weekdays and patients were asked to keep a standardized diary of their daily activities. Practices used the same 24-hour ambulatory blood pressure monitor device (Mobil-O-Graph, I.E.M. GMBH, Stolberg, Germany) for each patient. The measurement interval was 20 minutes from 7 a.m. to 11 p.m. and 1 hour from 11 p.m. to 7 a.m. We defined the mean day ambulatory blood pressure from 9 a.m. to 9 p.m. and used this as our primary blood pressure outcome. Only recordings with 70 % or more valid readings were used. Ambulatory blood pressure values were not communicated to the patient, prescribing physician and researcher until after completion of the study protocol. Furthermore, the following laboratory tests were used: creatinine (CREA plus, Roche Diagnostics, IN, USA), renin (DSL-25100 ACTIVE Renin IRMA kit, Diagnostic Systems Laboratories, TX, USA), NT-proBNP (Elecsys, Roche Diagnostics, Zug, Switzerland), potassium (ISE Indirect, Roche Diagnostics, IN, USA) and urinary albumin (COBAS, Roche Diagnostics, Zug, Switzerland). For comparison of NCC abundance with blood pressure, patients were considered responders if they exhibited a decrease of ≥5 mmHg in blood pressure, n=14. The remainder were considered non-responders, n=9.

Urine collection and measurement of urinary creatinine

For the patient study, second morning mid-stream urine was collected after the run-in period, and at the termination of both HCT and Val treatment. Urine samples were collected between 8.30 a.m. and 9.30 a.m. to minimize the effects of circadian rhythm on NCC abundance. Additionally, second morning mid-stream urine was collected from 4 healthy subjects (males, aged 25-35 years old) solely for the purpose to characterize NCC. uEVs of healthy subjects were subjected to *N*-glycosidase F (PNGase F) and endoglycosidase H (Endo H) treatment. All healthy subjects gave written informed consent, and the study protocol was approved by the Institutional Review Board of the Radboud University Medical Center (approval no. NL47178.091.13). Protease inhibitors (50 µmol/L phenylmethylsulfonyl fluoride (PMSF), 20 µmol/L aprotinin, 10 µmol/L pepstatin A and 20 µmol/L leupeptin) were added immediately after collecting urine samples to prevent degradation of proteins in uEVs. Urinary creatinine was measured according to Jaffe's method, via a colorimetric assay (Labor und Technik, Berlin, Germany) (40). The urine samples were subsequently stored at -80 °C until required.

Urinary extracellular vesicle isolation

uEVs were isolated as previously described (43). Briefly, 5 ml of collected urine was centrifuged at 17,000 × g for 15 minutes at 24 °C in a Sorvall™ WX Floor Ultra Centrifuge (Thermo Scientific, Asheville, NC, USA) with a 70.1Ti rotor. 4 ml of the supernatant was removed and incubated at room temperature for 25 minutes. The pellet with remaining 1 ml

of the supernatant was resuspended in 200 µl isolation solution (250 mmol/L sucrose and 10 mmol/L triethanolamine-HCl, pH 7.6) and 50 µl 3.24 mol/L dithiothreitol (DTT), and subsequently centrifuged at 17,000 × g for 15 minutes at 24 °C. This supernatant was collected and combined with supernatant obtained from the previous step and centrifuged at 200,000 × g for 2 hours at 24 °C. The uEV pellet was dissolved in 50 µl of Laemmli buffer (0.6 % w/v SDS, 3 % v/v glycerol, 18 mmol/L Tris-HCl pH 6.8 and 0.003 % w/v bromophenol blue), and stored at -20 °C for further use.

Kidney membrane preparations

Kidneys were obtained for research purposes through either donation after death, or due to unsuitability for transplantation. Membrane fractions of human kidney were isolated as described previously (43). In brief, harvested kidneys were snap-frozen immediately after isolation and homogenized in detergent-free lysis buffer, containing 50 mmol/L, Tris-HCl pH 7.5, 1 mmol/L ethylene diamine tetraacetic acid (EDTA), 1 mmol/L ethylene glycol tetra-acetic acid (EGTA), 1 mmol/L sodium orthovanadate, 5 mmol/L sodium fluoride, 5 mmol/L sodium pyrophosphate, 0.27 mol/L sucrose, 0.1 % v/v β-mercaptoethanol (β-met) and protease inhibitors (Roche, 1 tablet per 50 ml), with a homogenizer (VWR VDI 12 Adaptable Homogenizers, OpticsPlanet, Inc., Commercial Avenue Northbrook, IL, USA). Nuclei and debris were pelleted by centrifugation at 1,500 x g for 5 minutes at 4°C. Next, supernatants were centrifuged at 100,000 x g for 1 hour at 4°C. The pellet was washed with 1 volume of lysis buffer without reducing agent and centrifuged again at 100,000 x g for 15 minutes to remove any remaining cytosolic particles. The pellet was subsequently resuspended in lysis buffer including 1 % v/v nonidet P40. Bicinchoninic acid protein assay kit (Pierce, Thermo Scientific, Rockford, IL, USA) was used to determine the protein concentration. Finally, samples were stored at -80°C for the immunoblotting.

Immunoblotting

uEV pellets resuspended in Laemmli buffer were incubated at 60 °C for 15 minutes. The volume of uEV suspension per lane was adjusted according to the urinary creatinine concentration and loaded on 4–15 % v/v Criterion™ TGX™ Precast Gels (Bio-Rad, The Netherlands) for protein separation. Proteins were subsequently transferred to polyvinylidene difluoride (PVDF) membranes (Immobilon-P, Millipore Corporation, Bedford, MA, USA) and incubated with the appropriate primary antibody overnight at 4 °C. After washing, the PVDF membrane was incubated with the appropriate secondary antibody for one hour at room temperature, and immunoreactive bands were visualized using chemiluminescence (Thermo Fischer Scientific, Waltham, MA, USA). Immunoblots of uEVs from hypertensive patients were first probed for the presence of $NCC_{1\text{-}3}$. Subsequently,

PVDF membranes were stripped using stripping buffer (100 mmol/L β-met, 2 % w/v SDS, 62.5 mmol/L Tris-HCl pH 6.8, and 0.1 % v/v Tween-20) and reprobed for $pNCC_{1-3}$-T55/T60. Membrane stripping was performed once for each PVDF membrane that was probed for NCC_{1-3}. Immunoreactive band volumes were quantified using Quantity One software (Bio-Rad, CA, USA).

Dithiothreitol and β-mercaptoethanol treatment

To reduce dimeric NCC into the monomeric form, the reducing agents DTT and β-met were used, in addition to incubation of uEV-samples at 100 °C for 5 minutes. uEV-samples of healthy subjects in Laemmli buffer were treated with 0.1 mol/L DTT or 5, 10 and 20 % v/v β-met. This mixture was continuously mixed for 2 hours at 37 °C with agitation at 0.3 x g in a benchtop orbital shaker (Eppendorf, Thermomixer Compact, Gelderland, The Netherlands). Subsequently, uEV-samples were incubated at 100 °C for 5 minutes and/or at 60 °C for 15 minutes (control) and then used for immunoblotting, as previously described in this section.

N-glycosidase F and endoglycosidase H treatment

Two µl glycoprotein denaturing buffer (New England Biolabs, MA, USA) was added to 18 µl of uEVs of healthy subjects in Laemmli buffer. The samples were heated at 60 °C for 15 minutes and treated with either *N*-glycosidase F (PNGase F) or endoglycosidase H (Endo H) (New England Biolabs, MA, USA) at the final concentration of 9,800 units/ml and 9,800 units/ml, respectively. This mixture was continuously mixed for 2 hours at 37 °C with agitation at 0.3 x g in a benchtop orbital shaker (Eppendorf, Thermomixer Compact, Gelderland, The Netherlands) and subsequently used for immunoblotting, as previously described in this section.

Antibodies

The following primary antibodies were used: anti-N-terminal human total NCC (Millipore, Billerica, MA, USA, #AB3553; 1:2,000); anti-carboxy (C)-terminal human $NCC_{1/2}$, generated by one of the authors (RJMB, 1:2,000) (43); anti-N-terminal phosphorylated total NCC (anti-pT55/T60-NCC in human or anti-pT53/T58-NCC in mice; 1:2,000) kindly provided by Prof. R. Fenton, Aarhus University, Denmark (33) and anti-amino acid 101-210 of the uEV marker CD9 of human origin (C4, Santa Cruz Biotechnology, Inc., CA, USA; 1:500). Secondary antibodies used were peroxidase-conjugated goat anti-rabbit (Sigma-Aldrich, St. Louis, MO, USA; 1:10,000), and anti-mouse (Sigma-Aldrich, St. Louis, MO, USA; 1:10,000).

Statistical analysis

All data are expressed as mean ± standard error of the mean (SEM). Comparisons were made between groups using one-way ANOVA with Tukey's multiple comparisons test as *post hoc* test. Comparisons between responders and non-responders were made by non-parametric Student's *t*-tests. A *P*-value of < 0.05 was considered statistically significant. All data were analyzed using Prism 5 software (GraphPad Software Inc, La Jolla, CA, USA).

Results

Structural characterization of NCC in uEVs of healthy subjects

Figure 2 shows representative immunoblots of uEVs from a healthy subject probed for the presence of $NCC_{1\text{-}3}$. In uEVs, NCC protein is present in oligomeric structures, shown in Figure 2 as two immunoreactive bands of ~260 (dimer) and ~130 kDa (monomer). The molecular size of NCC in uEVs is in agreement with NCC expressed in human kidney (Fig. 2C) and mouse renal tissue (19). Treatment with the reducing agents β-met, and DTT and/or incubation at 100 °C did not reduce the dimeric NCC into the monomeric form (Fig. 2, A and B), indicative of the complex oligomeric structure of NCC in human uEVs.

Resuspended uEV pellets were subjected to Endo H and PNGase F treatment to determine glycosylation. Endo H cleaves high-mannose and a limited number of hybrid oligosaccharides from *N*-linked glycoproteins, but does not cleave complex glycans, whereas PNGase F removes all *N*-glycans from glycoproteins, and was used as a control (9, 19). Both dimeric and monomeric immunoreactive bands of NCC were insensitive to Endo H treatment (Fig. 2C). However, PNGase F treatment resulted in migration of both dimeric and monomeric immunoreactive bands of NCC to a lower molecular weight (Fig. 2C), demonstrating the complex glycosylated structure of NCC.

Table 1 depicts the clinical and laboratory characteristics of the study population of patients with essential hypertension, demonstrating no significant differences in any of these parameters between groups. Both HCT and Val treatment significantly reduce arterial blood pressure of hypertensive patients (Fig. 3A). Plasma sodium levels did not change after both treatments (Fig. 3B). Plasma potassium concentrations were significantly reduced after HCT treatment, but not following Val treatment (Fig. 3C), and plasma renin levels were significantly increased after both HCT and Val treatment (Fig. 3D).

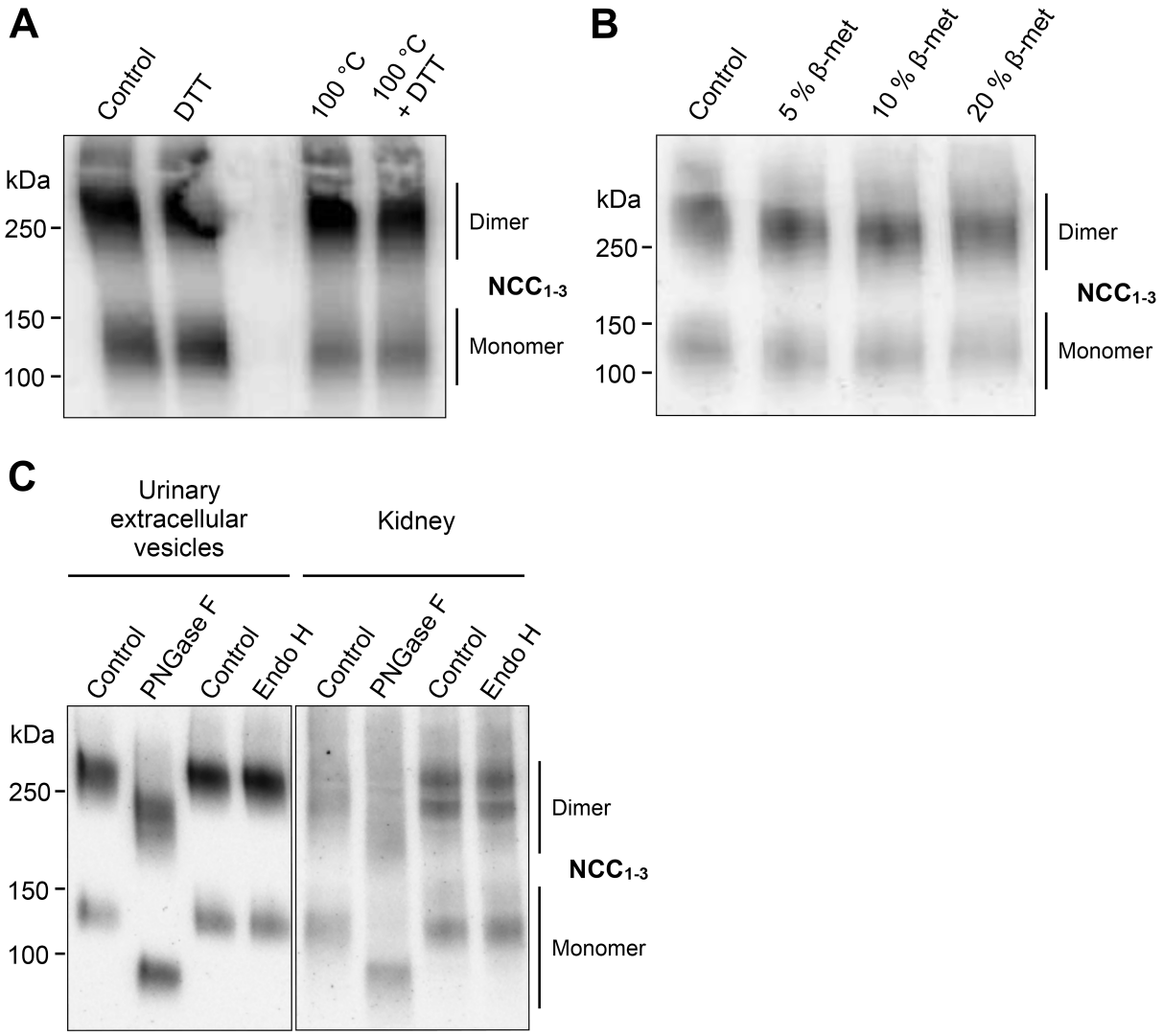

Figure 2 | The structure of NCC in human uEVs and human kidney membrane fractions is presented as an oligomeric and glycosylated complex.

Representative immunoblots of NCC_{1-3} within uEVs of a healthy subject show band sizes of ~260 and ~130 kDa. (**A**) Lane 1- Control (uEVs incubated at 60 °C for 15 minutes prior to immunoblotting); Lane 2- Samples treated with dithiothreitol (DTT) (0.1 mol/L) prior to incubation at 60 °C for 15 minutes; Lane 3- Samples incubated at 100 °C for 5 minutes; Lane 4- Samples treated with DTT (0.1 mol/L) prior to incubation at 100 °C for 5 minutes. (**B**) Lane 1- Control; Lane 2, 3 and 4- Samples treated with 5, 10 and 20 % v/v β-mercaptoethanol (β-met) respectively prior to incubation at 60 °C for 15 minutes. (**C**) Lane 1- untreated uEVs (Control); Lane 2- uEVs treated with *N*-glycosidase F (PNGase F) 9,800 units/mL; Lane 3- untreated uEVs (Control); Lane 4- uEVs treated with endoglycosidase H (Endo H) 9,800 units/mL; Lane 5- untreated human kidney membrane fractions (Control); Lane 6- human kidney membrane fractions treated with PNGase F 9,800 units/ml; Lane 7- untreated human kidney membrane fractions (Control) and Lane 8- human kidney membrane fractions treated with Endo H 9,800 units/mL.

Efficacy of anti-hypertensive medications

Table 1 | Clinical and laboratory characteristics of 23 patients with essential hypertension.

Physiological parameters	Unt	HCT	Val
Body Weight (Kg)	81 ± 3	81 ± 3	81 ± 3
Body Mass Index (Kg/m^2)	27.8 ± 0.7	27.9 ± 0.8	27.9 ± 0.8
Men/women	17/6	17/6	17/6
Menopause	4	4	4
Serum creatinine (µmol/L)	75 ± 3	73 ± 3	74 ± 3
eGFR (mL/min/1.73 m^2)	81 ± 3	81 ± 3	82 ± 3
HDL (mmol/L)	1.2 ± 0.1	1.2 ± 0.1	1.1 ± 0.1
LDL (mmol/L)	4.0 ± 0.2	4.2 ± 0.2	4.1 ± 0.2
Blood glucose (mmol/L)	5.9 ± 0.2	5.8 ± 0.2	5.9 ± 0.2
Blood NT-ProBNP (pmol/L)	7 ± 1	6 ± 1	14 ± 8
Urinary creatinine (mmol/L)	11 ± 1	12 ± 1	11 ± 1
Urinary albumin (mg/L)	15 ± 5	12 ± 3	11 ± 2
Urinary albumin/Urinary creatinine (mg/mmol)	1.1 ± 0.2	0.9 ± 0.2	1.0 ± 0.2

Average age of the patients summarized above was 52 ± 2 years. Data are presented as the mean ± SEM. All parameters in HCT or valsartan groups are compared with untreated and found statistically not significant.

Unt: untreated; HCT: hydrochlorothiazide; Val: valsartan (treatment protocol depicted in Fig. 1); Menopause 4: 4 out of 6 women were in menopausal state; eGFR: Estimated glomerular filtration rate; HDL: High-density lipoprotein in blood; LDL: Low-density lipoprotein in blood; NT-ProBNP: amino (N)-terminal of the prohormone brain natriuretic peptide.

NCC abundance in uEVs of hypertensive patients is increased by the treatment of HCT, but not Val

The volume of uEV suspension per sample was adjusted according to urinary creatinine concentration prior to immunoblot analysis. Figure 4A shows representative immunoblots of uEVs from three hypertensive patients probed for the presence of $NCC_{1/2}$, NCC_{1-3}, $pNCC_{1-3}$-T55/T60, and the uEV marker CD9, to confirm equal loading (1, 35, 43). Densitometric analysis of the immunoreactive bands of 23 hypertensive patients representing dimeric and monomeric NCC isoforms and $pNCC_{1-3}$-T55/T60 was performed together (Fig. 4). The abundance of $NCC_{1/2}$, NCC_{1-3}, and $pNCC_{1-3}$-T55/T60 was significantly increased in uEVs of HCT, but not Val-treated patients (Fig. 4). No difference in CD9 abundance was observed between the three groups suggesting that normalization by urinary creatinine results in comparable uEV-numbers (Fig. 4, E and F). Finally, the ratio of $pNCC_{1-3}$-T55/T60 to NCC_{1-3} was not significantly different after HCT or Val treatment (Fig. 5G). Additional normalization by CD9 abundance led to similar results (data not shown).

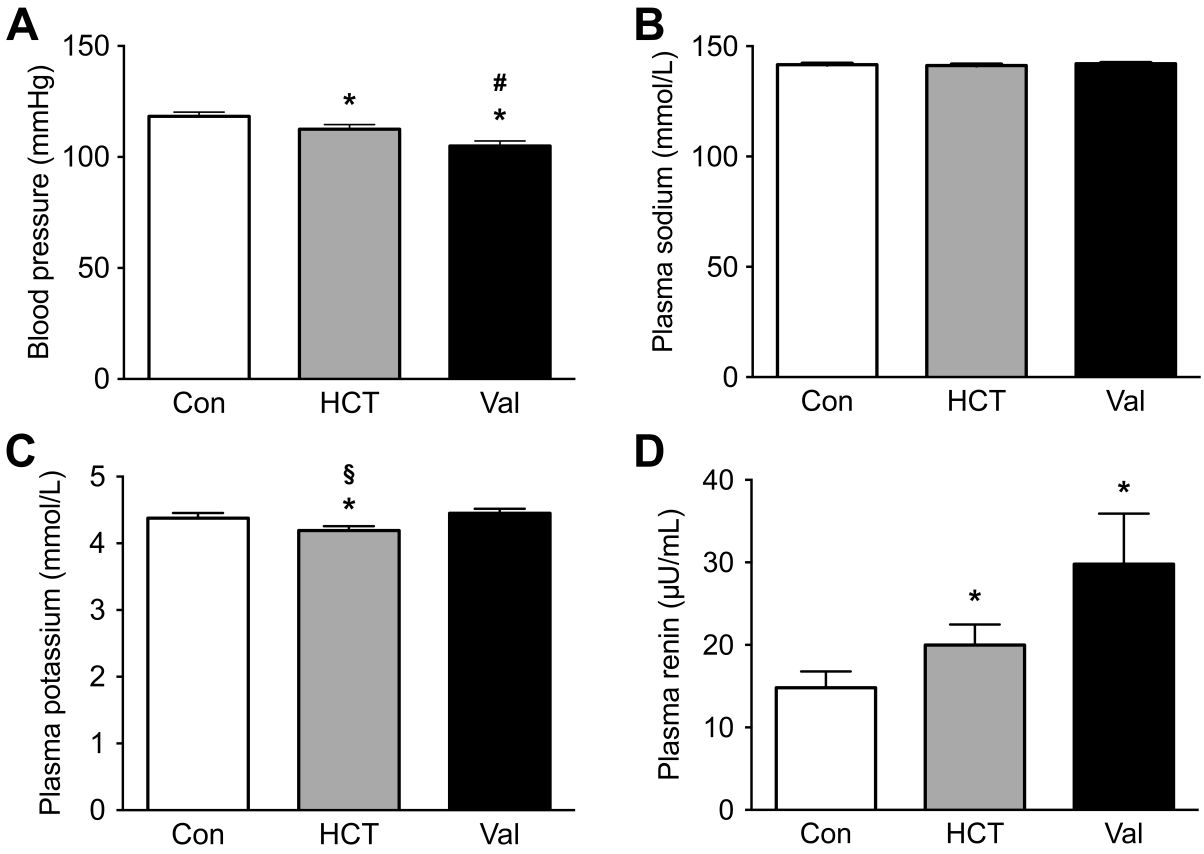

Figure 3 | Effect of anti-hypertensive drugs on systolic blood pressure, plasma sodium, potassium, and renin levels in patients with essential hypertension.

White bars represent, untreated (Unt), grey bars following four weeks of hydrochlorothiazide (HCT) treatment and black bars following four weeks of valsartan (Val) treatment. (**A**) Both HCT and Val treatment vs. Unt (*) as well as HCT vs. Val treatment ($^{\#}$) significantly reduced arterial blood pressure. (B) Plasma sodium levels did not significantly change after HCT or Val treatment. (**C**) HCT vs. both Unt (*) and Val (§) treatment significantly decreased plasma potassium levels. (**D**) Plasma renin levels were significantly increased following both treatments. The data on arterial blood pressure levels are presented as mean arterial pressure (MAP). Values are mean ± SEM. Comparisons were made between groups using one-way ANOVA with Tukey's multiple comparisons test as *post hoc* test. $^{*,\#,\S}P<0.05$, n=23.

Efficacy of anti-hypertensive medications in responders and non-responders

During analysis of the data presented in Figure 3, we observed that with respect to HCT administration, the subjects could be divided into responders (Fig. 5, A-E) and non-responders (Fig. 5, F-J). Responders displayed a decrease of ≥5 mmHg in blood pressure, with the remainder considered non-responders. In responders (Fig. 5A), compared to non-responders (Fig. 5F), the abundance of $NCC_{1/2}$, NCC_{1-3}, and $pNCC_{1-3}$-T55/T60 was significantly increased (3-4 fold higher) upon HCT, but not Val treatment. In responders, arterial blood pressure was significantly reduced after HCT as well as Val treatment, and in the non-responder group, arterial blood pressure was significantly reduced in only the Val treated group (Fig. 5, B and G). Plasma sodium levels were not significantly different

between the responders and non-responders of the treatment groups (Fig. 5, C and H). In the responder group, plasma potassium levels of HCT treated patients significantly decreased when compared to both Unt and Val treatment, however in the non-responder group no significant change in plasma potassium levels were observed between the three treatment groups (Fig. 5, D and I). Plasma renin levels were significantly increased in the responder group following both HCT and Val treatment and in the non-responder group plasma renin concentrations were significantly increased after Val, but not HCT treatment (Fig. 5, E and J).

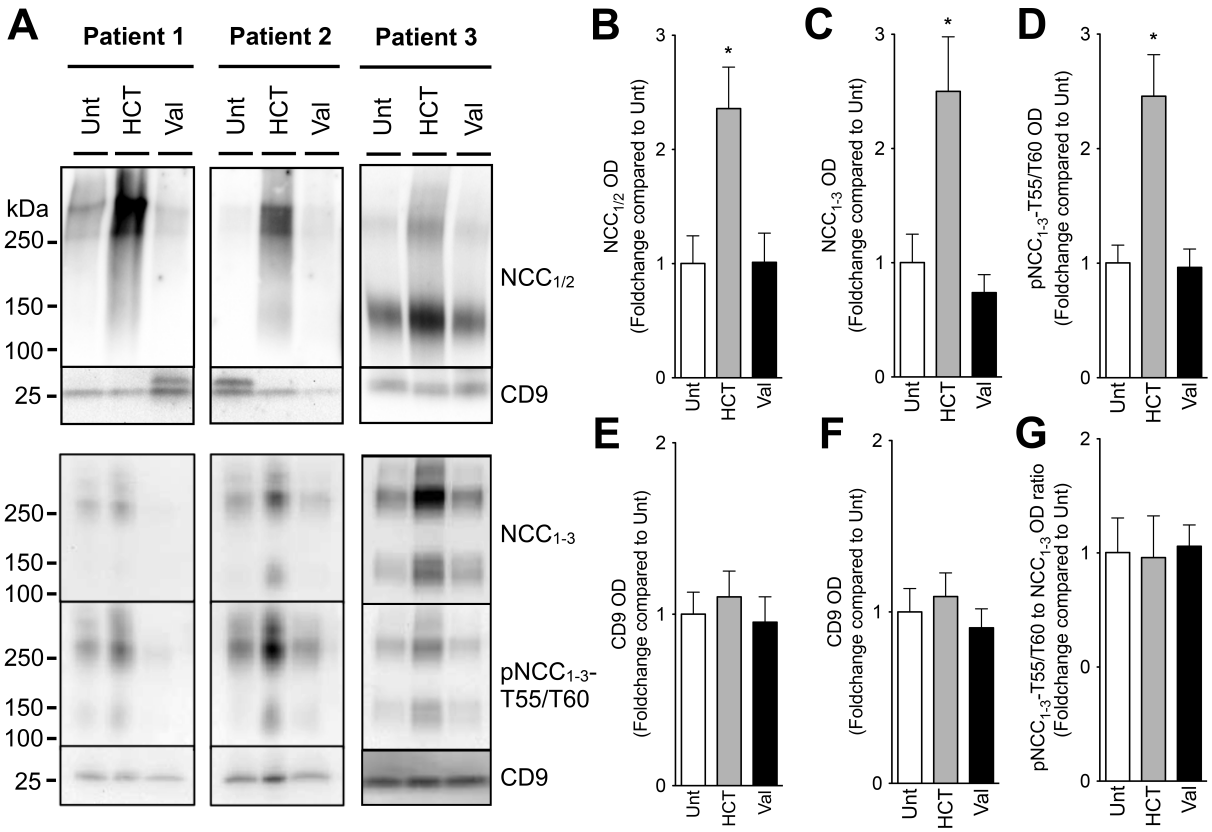

Figure 4 | Expression of $NCC_{1/2}$, NCC_{1-3}, $pNCC_{1-3}$-T55/T60, and CD9 in uEVs of patients with essential hypertension before (Unt) and after treatment with hydrochlorothiazide (HCT) or valsartan (Val).

(**A**) Representative immunoblots of 3 patients depicting abundance of $NCC_{1/2}$, NCC_{1-3}, $pNCC_{1-3}$-T55/T60, and CD9 in uEVs. In all immunoblots, lane 1 represents protein expression prior to the treatment (Unt), and lanes 2 and lane 3 represent protein expression after HCT and Val treatment, respectively. Densitometric analysis of the immunoblots of 23 patients depicting the abundance of $NCC_{1/2}$ (**B**), NCC_{1-3} (**C**), $pNCC_{1-3}$-T55/T60 (**D**) and the ratio of $pNCC_{1-3}$-T55/T60 to NCC_{1-3} (**G**). Densitometric analysis of CD9 expression of the immunoblots of 23 patients for $NCC_{1/2}$ (**E**) and NCC_{1-3} and $pNCC_{1-3}$-T55/T60 (**F**) showed no significant difference between the three groups. Values are mean ± SEM (n=23) normalized to Unt levels. Comparisons were made between groups using one-way ANOVA with Tukey's multiple comparisons test as *post hoc* test. **P*<0.05, n=23.

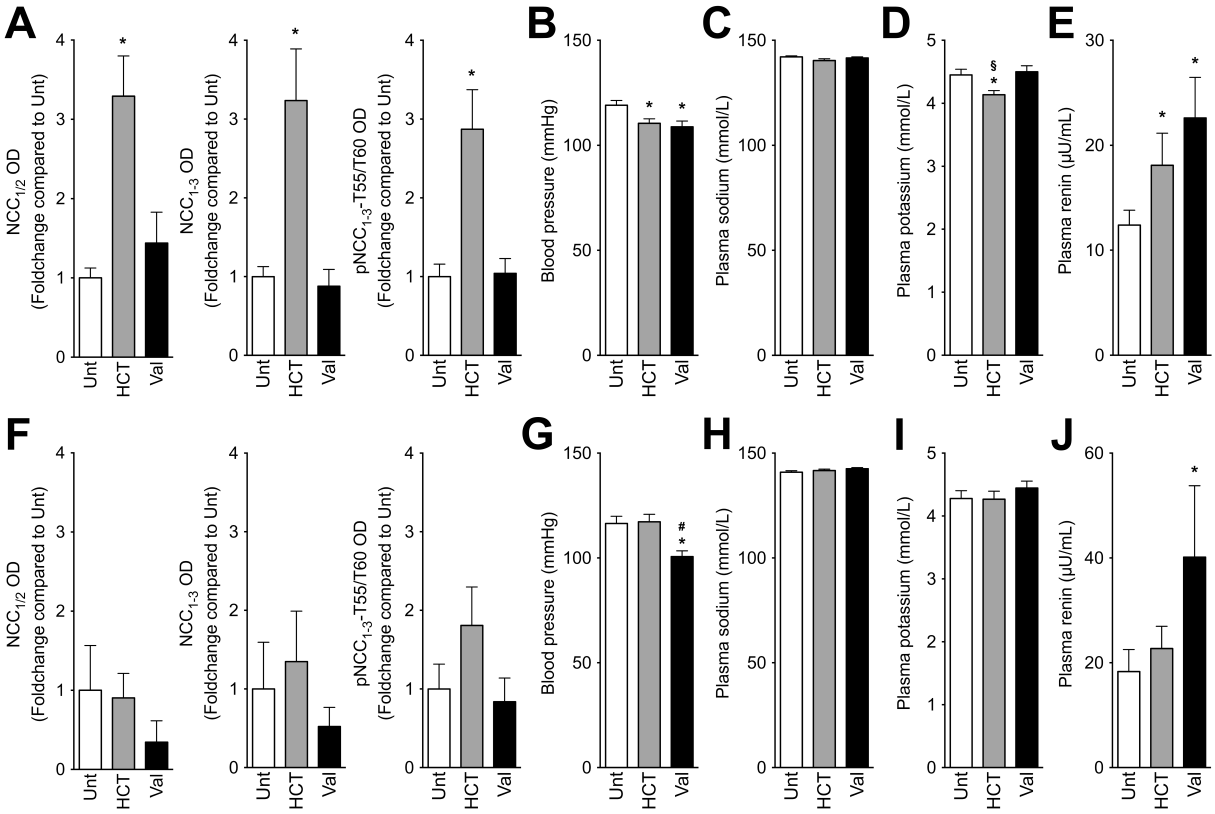

Figure 5 | Effect of anti-hypertensive drugs on the expression of $NCC_{1/2}$, NCC_{1-3} and $pNCC_{1-3}$-T55/T6 and systolic blood pressure, plasma sodium, potassium, and renin levels in responders compared to non-responders.

Densitometric analysis of the immunoblots of 23 patients depicting the abundance of $NCC_{1/2}$, NCC_{1-3} and $pNCC_{1-3}$-T55/T60 and arterial blood pressure, plasma sodium levels, plasma potassium levels and plasma renin levels of hypertensive patients after treatment with hydrochlorothiazide (HCT) of responders (**A**-**E**, n=14) and non-responders (**F**-**J**, n=9) have been analyzed separately. White bars represent untreated (Unt), grey bars following four weeks of hydrochlorothiazide (HCT) treatment and black bars following four weeks of valsartan (Val) treatment. The abundance of $NCC_{1/2}$, NCC_{1-3}, and $pNCC_{1-3}$-T55/T60 was significantly increased in uEVs of responders (**A**), compared to non-responders (**F**), upon HCT-, but not Val-treatment. In responders (**B**), both HCT and Val treatment vs. Unt (*) significantly reduced arterial blood pressure, while in non-responders (**G**) only Val treatment vs. Unt (*) and HCT treatment ($^{\#}$) significantly reduced arterial blood pressure. Plasma sodium levels showed no significant difference in both responders (**C**) and non-responders (**H**) between the groups. (**D**) In responders, plasma potassium levels of HCT vs. both Unt (*) and Val (§) treatment significantly decreased, however (**I**) in the non-responder group plasma potassium levels did not significantly change after HCT or Val treatment. (**E**) In the responder group plasma renin levels were significantly increased following both treatments however (**J**) in non-responder group plasma renin concentrations were significantly increased only after Val treatment. The data on arterial blood pressure levels are presented as mean arterial pressure (MAP). Values are mean ± SEM. Comparisons were made between groups using one-way ANOVA with Tukey's multiple comparisons test as *post hoc* test. $^{*,\#,\S}P<0.05$, n=23.

Blood pressure correlates with NCC abundance in uEVs and plasma potassium of hypertensive patients treated with HCT

To determine if HCT-induced reduction in blood pressure is correlated with NCC abundance, the blood pressure response of hypertensive patients to HCT was plotted against NCC

abundance for both responder and non-responder groups. As shown in Figure 6, A and B, both NCC_{1-2} and NCC_{1-3} abundance was significantly higher in patients who responded to HCT treatment than non-responders, after normalization to pretreatment. There was no significant difference of $pNCC_{1-3}$-T55/T60 abundance between responders and non-responders (Fig. 6C, *P*>0.2).

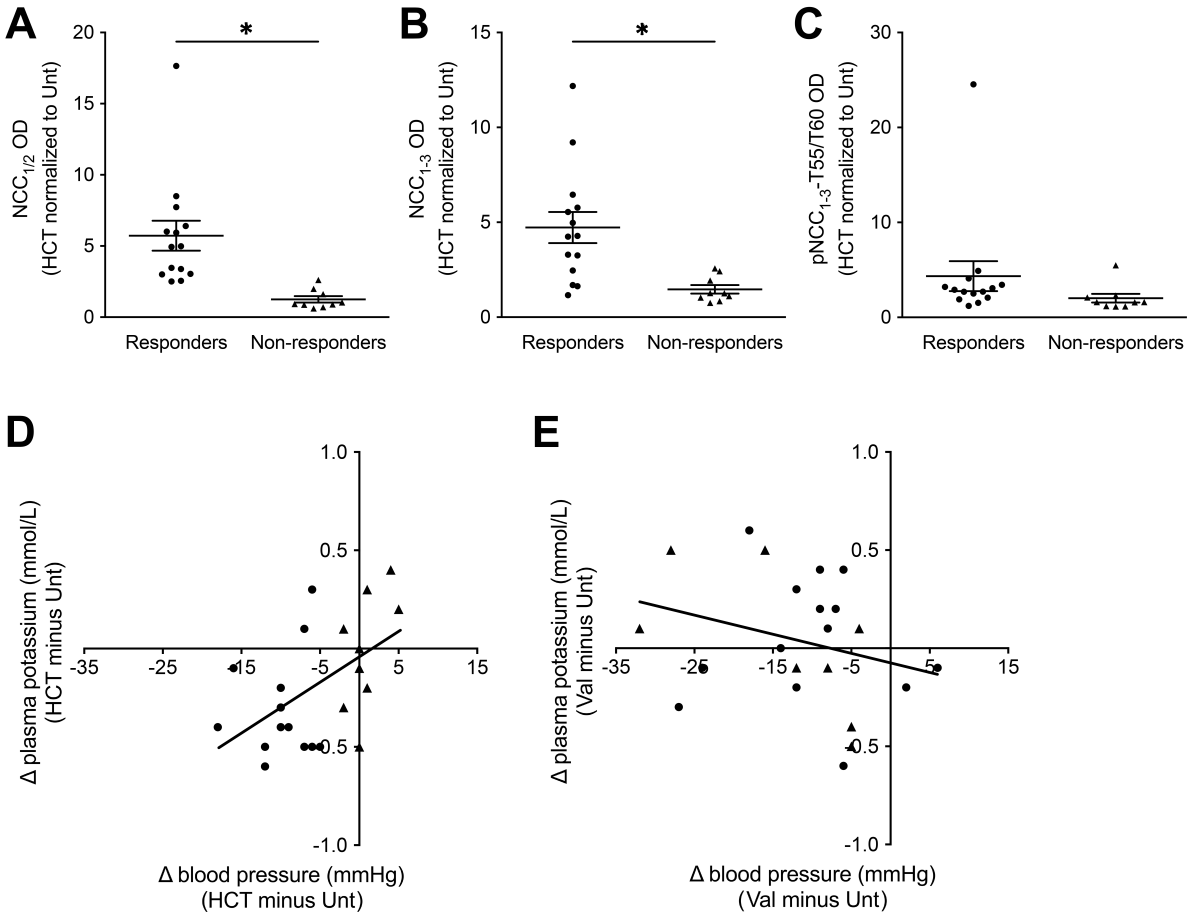

Figure 6 | Blood pressure correlates with plasma potassium and NCC abundance in uEVs of essential hypertensive patients treated with HCT.

The abundance of $NCC_{1/2}$ (**A**), NCC_{1-3} (**B**) and $pNCC_{1-3}$-T55/T60 (**C**) in uEVs of hypertensive patients after treatment with hydrochlorothiazide (HCT) of both responders (n=14) and non-responders (n=9) normalized to untreated (Unt). The increase of both $NCC_{1/2}$ (**A**) and NCC_{1-3} (**B**) in uEVs was significantly higher in responders compared to non-responders. (**C**) $pNCC_{1-3}$-T55/T60 abundance in uEVs showed no significant difference between responders and non-responders. Correlation of Δ blood pressure with Δ plasma potassium levels of HCT minus Unt (**D**, r=0.32, *P*<0.05) or Val minus Unt (**E**, r=0.07, *P*>0.2). Circles represent responders and triangles represent non-responders. Correlation data from one responding patient from panel D, and one non-responding patient from panel E is not shown as plasma potassium values are not available. Values are mean ± SEM normalized to untreated (Unt) levels. Comparisons between responders and non-responders were made by using non-parametric *t*-test. **P*<0.05, n=23.

To determine if changes in plasma potassium levels are associated with a reduction in blood pressure following anti-hypertensive treatment, the correlation between plasma potassium and blood pressure was assessed. Positive correlation (r=0.32, *P*<0.05) was

observed between plasma potassium and blood pressure when hypertensive patients were treated with HCT (Fig. 6D). As depicted in Figure 6E, similar correlation was not observed in the group of patients treated with valsartan.

Discussion

This study demonstrates that chronic HCT treatment, in contrast to Val, enhances the abundance of $NCC_{1/2}$, NCC_{1-3}, and $pNCC_{1-3}$-T55/T60 in uEVs derived from essential hypertensive patients (Fig. 4), indicative of such changes in the DCT (43, 44). Additionally, we show that blood pressure correlates with NCC abundance in uEVs and plasma potassium levels of essential hypertensive patients treated with HCT, but not with Val. As in human kidney membrane fractions, in uEVs NCC is present in a glycosylated and oligomeric structure.

In both uEVs and human kidney membrane fractions NCC is present in oligomeric structures as demonstrated by the presence of NCC protein as complex bands of ~260 and ~130 kDa (Fig. 2), representing the dimeric and monomeric forms, respectively. It was not possible to dissociate the dimeric NCC complex in a monomeric form by incubating the uEVs at 100 °C or exposing them to the reducing agents DTT and β-met. The NCC complexes of ~260 and ~130 kDa detected in the human uEVs are comparable to NCC expression in human kidney membrane fractions, indicative of detection of NCC derived from distal tubule epithelia, in line with our previously published studies (10, 43).

Previously, it has been demonstrated that NCC is *N*-glycosylated in rat kidney and that *N*-glycosylation is essential for the cell surface expression of NCC, thiazide sensitivity and NCC activity (19). Our study demonstrates that in uEVs of healthy subjects and kidney membrane fractions of healthy donors both dimeric and monomeric NCC bands were sensitive to digestion with PNGase F, suggesting that NCC protein in uEVs, similarly to kidney membrane fractions, is glycosylated.

Proteins that are sensitive to Endo H digestion are suggested to be retained in the endoplasmic reticulum and pre-Golgi complex without further processing (9, 14, 37). Our results demonstrate that in uEVs and human kidney membrane fractions both the dimeric and monomeric NCC bands were insensitive to Endo H digestion, indicating that NCC in uEVs is present as a matured protein with complex glycosylation. In an overexpression system, immunoblots of total membranes isolated from *Xenopus* oocytes injected with cRNAs coding for human NCC showed that the NCC immunoreactive band at ~130 kDa (monomer) is insensitive to Endo H treatment, while the NCC immunoreactive band at ~110 kDa (monomer) is sensitive to Endo H digestion (9, 19), suggesting the presence of unprocessed NCC. The presence of an Endo H-insensitive NCC immunoreactive band at

~130 kDa (monomer) and the absence of an immunoreactive band of ~110 kDa (monomer) in uEVs, as in human kidney membrane fractions, suggests that NCC protein in uEVs represents a mature plasma membrane protein with complex glycosylation. Therefore, in humans, uEVs can be used as a non-invasive tool to study the regulation of NCC in the kidney.

It has previously been shown that prolonged HCT treatment increases NCC abundance in the rodent kidney, in agreement with our results (29, 30). Additionally, the binding density of [^{3}H] metolazone, an indirect measure of NCC abundance, is augmented by chronic HCT treatment in rat kidney membrane fractions (6). The increased abundance of NCC in the DCT, which is reflected by an increase abundance of NCC in uEVs, upon chronic HCT treatment, may be a compensatory effect to counteract reduced NCC activity as a result of thiazide-mediated inhibition of NCC (11). This compensatory response could, therefore, partly contribute to diuretic resistance (12). The upstream stimulator pathways of NCC, such as that of angiotensin II, are still intact upon HCT treatment (38), thus Val treatment blocks the angiotensin II dependent stimulation of NCC (47), which might explain why there is no enhancement of NCC abundance in uEVs after Val treatment.

Sodium reabsorption along the distal nephron plays an important role in potassium homeostasis (42). Due to the inhibitory effect of HCT on NCC activity, sodium delivery to the collecting duct will increase, and these latter segments will therefore reabsorb more sodium. As a consequence more potassium is excreted, ultimately resulting in decreased plasma potassium levels (41). Conversely, Terker *et al*. demonstrated that a modest decrease in plasma potassium levels, within the narrow physiological range of 3.5–5.0 mmol/L, increases NCC abundance and activity (41). The reduced plasma potassium levels observed in this study may help to explain the increase in abundance of $NCC_{1/2}$, NCC_{1-3}, and $pNCC_{1-3}$-T55/T60 in uEVs of hypertensive patients following HCT treatment (Figs. 3C, 4 and 5, A and D). Additionally, Val treatment, in contrast to HCT, did not enhance the abundance of $NCC_{1/2}$, NCC_{1-3}, and $pNCC_{1-3}$-T55/T60 in uEVs derived from essential hypertensive patients. The lack of NCC response to Val treatment may indicate NCC activation to be partly dependent on angiotensin II stimulation (5), whereas thiazides block NCC directly by interfering with chloride binding to NCC (20). Indeed, angiotensin II is also known to increase the abundance and activity of NCC through the WNK pathways (38). The upstream regulatory pathways of NCC stimulation (such as RAAS) are still intact during HCT treatment and may stimulate NCC abundance and phosphorylation, while its function is still blocked by HCT. When the dataset is separated into responders and non-responders, it becomes observable that in responders HCT or Val treatment reduces blood pressure of the hypertensive patients to a similar degree (Fig. 5B). Previously, it has been shown that high dietary sodium ingestion contributes to diuretic resistance (34). Patients with resistant

hypertension who were on a reduced sodium diet compared to those on an increased sodium diet showed significantly increased plasma renin levels (34). In this study, higher dietary sodium intake may have been a contributory factor to non-responsiveness to the HCT treatment (diuretic resistance).

Here, we show that blood pressure correlates with the differential NCC abundance and plasma potassium levels of essential hypertensive patients treated with HCT, but not with Val (Fig. 6). NCC abundance was increased in the group of patients that responded to HCT treatment, as defined by a significant reduction in blood pressure, however, there was no difference in NCC abundance of non-responders.

Loffing *et al.* have previously demonstrated in rats that 3 days HCT administration of 40 mg/kg/day reduces NCC expression in the DCT and induces apoptosis of DCT cells (25). In contrast, 7 days HCT administration in mice increased NCC abundance in the kidney, measured by immunoblot and immunostaining (29), in agreement with our findings using human uEVs. Moreover, in mice HCT administration of 25 mg/kg/day for 6 days did not induce apoptosis of DCT cells or a decrease in NCC expression (30), while hypocalciuria, renal Mg^{2+} wasting and hypomagnesemia were observed (a phenotype resembling the effects of chronic thiazide administration and Gitelman syndrome) (8, 13, 15, 23). Subsequent experiments by Loffing *et al.* failed to reproduce the observed DCT cell apoptotic changes in mice, when using several mouse strains, both sexes of mice, and different thiazide-type diuretics and application protocols (30). Indeed, they found chronic HCT treatment in mice to increase NCC abundance in the kidney (30). Different doses of HCT administration, inter-species variation in transporter expression (2, 31) and the length of treatment regimen of the study may help to answer this discrepancy.

Our study demonstrates that chronic HCT treatment, in contrast to Val, enhances the abundance of $NCC_{1/2}$, $NCC_{1\text{-}3}$, and $pNCC_{1\text{-}3}$-T55/T60 in uEVs derived from essential hypertensive patients, indicative of such changes in the DCT (43, 44). NCC in uEVs is present in a glycosylated and oligomeric structure, as found in human kidney membrane fractions.

Acknowledgements

We thank Pedro San-Cristobal, Marco Valdez-Flores, Sjoerd Verkaart, Vera M. Poort and Ferruh Artunc for their helpful suggestions.

Grants

This study was supported by the European Society of Hypertension (2011-2013 Fellowship), the EURenOmics project from the European Union seventh Framework Programme (FP7/2007–2013, agreement no. 305608), the Netherlands Organization for Scientific Research (VENI ZonMw 916.12.046) and the Dutch Kidney Foundation (PHD12.14 and 16OI04).

Disclosure

No conflicts of interest, financial or otherwise, are declared by the authors.

Author contribution

G.P., O.A.T., and M.C.v.d.W. performed experiments; G.P., O.A.T., and M.C.v.d.W. analyzed data; G.P., O.A.T., M.C.v.d.W., L.M.S., J.D., J.W.L., J.G.H., and R.J.B. interpreted results of experiments; G.P. and O.A.T. prepared figures; G.P., O.A.T., J.G.H., and R.J.B. drafted manuscript; G.P., O.A.T., M.C.v.d.W., L.M.S., J.D., J.W.L., J.G.H., and R.J.B. edited and revised manuscript; G.P., O.A.T., M.C.v.d.W., L.M.S., J.D., J.W.L., J.G.H., and R.J.B. approved final version of manuscript; J.D., J.W.L., J.G.H., and R.J.B. con- ceived and designed research.

References

1. Alvarez ML, Khosroheidari M, Ravi RK, DiStefano JK. Comparison of protein, microRNA, and mRNA yields using different methods of urinary exosome isolation for the discovery of kidney disease biomarkers. *Kidney Int* 82: 1024–1032, 2012.
2. Bachmann S, Velazquez H, Obermuller N, Reilly RF, Moser D, Ellison DH. Expression of the thiazide-sensitive Na-Cl cotransporter by rabbit distal convoluted tubule cells. *J Clin Invest* 96: 2510–2514, 1995.
3. Boyden LM, Choi M, Choate KA, Nelson-Williams CJ, Farhi A, Toka HR, Tikhonova IR, Bjornson R, Mane SM, Colussi G, Lebel M, Gordon RD, Ben A Semmekrot, Poujol A, Välimäki MJ, De Ferrari ME, Sanjad SA, Gutkin M, Karet FE, Tucci JR, Stockigt JR, Keppler-Noreuil KM, Porter CC, Anand SK, Whiteford ML, Davis ID, Dewar SB, Bettinelli A, Fadrowski JJ, Belsha CW, Hunley TE, Nelson RD, Trachtman H, Cole TRP, Pinsk M, Bockenhauer D, Shenoy M, Vaidyanathan P, Foreman JW, Rasoulpour M, Thameem F, Al-Shahrouri HZ, Radhakrishnan J, Gharavi AG, Goilav B, Lifton RP. Mutations in kelch-like 3 and cullin 3 cause hypertension and electrolyte abnormalities. *Nature* 482: 98–102, 2012.
4. Carretero OA, Oparil S. Essential hypertension. Part I: definition and etiology. *Circulation* 101: 329–335, 2000.
5. Castañeda-Bueno M, Gamba G. Mechanisms of sodium-chloride cotransporter modulation by angiotensin II. *Curr Opin Nephrol Hypertens* 21: 516–522, 2012.
6. Chen ZF, Vaughn DA, Beaumont K, Fanestil DD. Effects of diuretic treatment and of dietary sodium on renal binding of 3H-metolazone. *J Am Soc Nephrol* 1: 91–98, 1990.
7. Corbetta S, Raimondo F, Tedeschi S, Syren M-L, Rebora P, Savoia A, Baldi L, Bettinelli A, Pitto M. Urinary exosomes in the diagnosis of Gitelman and Bartter syndromes. *Nephrol Dial Transplant* 30: 621–630, 2015.
8. Dai LJ, Ritchie G, Kerstan D, Kang HS, Cole DE, Quamme GA. Magnesium transport in the renal distal convoluted tubule. *Physiological Reviews* 81: 51–84, 2001.
9. de Jong JC, Van Der Vliet WA, van den Heuvel LPWJ, Willems PHGM, Knoers NVAM, Bindels RJM. Functional expression of mutations in the human NaCl cotransporter: evidence for impaired routing mechanisms in Gitelman's syndrome. *J Am Soc Nephrol* 13: 1442–1448, 2002.
10. de Jong JC, Willems PHGM, Mooren FJM, van den Heuvel LPWJ, Knoers NVAM, Bindels RJM. The structural unit of the thiazide-sensitive NaCl cotransporter is a homodimer. *J Biol Chem* 278: 24302–24307, 2003.
11. Ellison DH, Velazquez H, Wright FS. Thiazide-sensitive sodium chloride cotransport in early distal tubule. *Am J Physiol* 253: F546–54, 1987.
12. Ellison DH. Diuretic resistance: physiology and therapeutics. *Semin Nephrol* 19: 581–597, 1999.
13. Ellison DH. Divalent cation transport by the distal nephron: insights from Bartter's and Gitelman's syndromes. *Am J Physiol Renal Physiol* 279: F616–F625, 2000.
14. Freeze HH, Kranz C. Endoglycosidase and glycoamidase release of N-linked glycans. *Curr Protoc Protein Sci* Chapter 12: Unit12.4–12.4.25, 2010.
15. Gitelman HJ, Graham JB, Welt LG. A new familial disorder characterized by hypokalemia and hypomagnesemia. *Trans Assoc Am Physicians* 79: 221–235, 1966.
16. Go AS, Mozaffarian D, Roger VL, Benjamin EJ, Berry JD, Blaha MJ, Dai S, Ford ES, Fox CS, Franco S, Fullerton HJ, Gillespie C, Hailpern SM, Heit JA, Howard VJ, Huffman MD, Judd SE, Kissela BM, Kittner SJ, Lackland DT, Lichtman JH, Lisabeth LD, Mackey RH, Magid DJ, Marcus GM, Marelli A, Matchar DB, McGuire DK, Mohler ER, Moy CS, Mussolino ME, Neumar RW, Nichol G, Pandey DK, Paynter NP, Reeves MJ, Sorlie PD, Stein J, Towfighi A, Turan TN, Virani SS, Wong ND, Woo D, Turner MB, American Heart Association Statistics Committee and Stroke Statistics Subcommittee. Heart disease and stroke statistics-2014 update: a report from the American Heart Association. *Circulation* 129: e28–e292, 2014.
17. Gonzales PA, Pisitkun T, Hoffert JD, Tchapyjnikov D, Star RA, Kleta R, Wang NS, Knepper MA. Large-scale proteomics and phosphoproteomics of urinary exosomes. *J Am Soc Nephrol* 20: 363–379, 2009.
18. Hegner G, Faust G, Freytag F, Meilenbrock S, Sullivan J, Bodin F. Valsartan, a new

angiotensin II antagonist for the treatment of essential hypertension: efficacy and safety compared to hydrochlorothiazide. *Eur J Clin Pharmacol* 52: 173–177, 1997.

19. Hoover RS, Poch E, Monroy A, Vazquez N, Nishio T, Gamba G, Hebert SC. N-Glycosylation at two sites critically alters thiazide binding and activity of the rat thiazide-sensitive Na(+):Cl(-) cotransporter. *J Am Soc Nephrol* 14: 271–282, 2003.
20. Hughes AD. How do thiazide and thiazide-like diuretics lower blood pressure? *J Renin Angiotensin Aldosterone Syst* 5: 155–160, 2004.
21. James PA, Oparil S, Carter BL, Cushman WC, Dennison-Himmelfarb C, Handler J, Lackland DT, LeFevre ML, MacKenzie TD, Ogedegbe O, Smith SC, Svetkey LP, Taler SJ, Townsend RR, Wright JT, Narva AS, Ortiz E. 2014 Evidence-Based Guideline for the Management of High Blood Pressure in Adults: Report From the Panel Members Appointed to the Eighth Joint National Committee (JNC 8). *JAMA* 311: 507–520, 2014.
22. Joo KW, Lee JW, Jang HR, Heo NJ, Jeon US, Oh YK, Lim CS, Na KY, Kim J, Cheong HII, Han JS. Reduced urinary excretion of thiazide-sensitive Na-Cl cotransporter in Gitelman syndrome: Preliminary data. *Am J Kidney Dis* 50: 765–773, 2007.
23. Lemmink HH, van den Heuvel LPWJ, van Dijk HA, Merkx GFM, Smilde TJ, Taschner PEM, Monnens LAH, Hebert SC, Knoers NVAM. Linkage of Gitelman syndrome to the thiazide-sensitive sodium-chloride cotransporter gene with identification of mutations in Dutch families. *Pediatr Nephrol* 10: 403–407, 1996.
24. Lifton RP, Gharavi AG, Geller DS. Molecular Mechanisms of Human Hypertension. *Cell* 104: 545–556, 2001.
25. Loffing J, Loffing-Cueni D, Hegyi I, Kaplan MR, Hebert SC, Le Hir M, Kaissling B. Thiazide treatment of rats provokes apoptosis in distal tubule cells. *Kidney Int* 50: 1180–1190, 1996.
26. Mastroianni N, Fusco MD, Zollo M, Arrigo G, Zuffardi O, Bettinelli A, Ballabio A, Casari G. Molecular Cloning, Expression Pattern, and Chromosomal Localization of the Human Na–Cl Thiazide-Sensitive Cotransporter (SLC12A3). *Genomics* 35: 486–493, 1996.
27. Mayan H, Attar-Herzberg D, Shaharabany M, Holtzman EJ, Farfel Z. Increased urinary Na-Cl cotransporter protein in familial hyperkalaemia and hypertension. *Nephrol Dial Transplant* 23: 492–496, 2008.
28. Messerli FH, Williams B, Ritz E. Essential hypertension. *The Lancet* 370: 591–603, 2007.
29. Na KY, Oh YK, Han JS, Joo KW, Lee JS, Earm J-H, Knepper MA, Kim G-H. Upregulation of Na+ transporter abundances in response to chronic thiazide or loop diuretic treatment in rats. *Am J Physiol Renal Physiol* 284: F133–F143, 2003.
30. Nijenhuis T, Vallon V, van der Kemp AWCM, Loffing J, Hoenderop JGJ, Bindels RJM. Enhanced passive Ca2+ reabsorption and reduced Mg2+ channel abundance explains thiazide-induced hypocalciuria and hypomagnesemia. *J Clin Inves* 115: 1651–1658, 2005.
31. Obermuller N, Bernstein P, Velazquez H, Reilly R, Moser D, Ellison DH, Bachmann S. Expression of the thiazide-sensitive Na-Cl cotransporter in rat and human kidney. *Am J Physiol Renal Physiol* 269: F900–F910, 1995.
32. Pathare G, Hoenderop JGJ, Bindels RJM, San-Cristobal P. A molecular update on pseudohypoaldosteronism type II. *Am J Physiol Renal Physiol* 305: F1513–F1520, 2013.
33. Pedersen NB, Hofmeister MV, Rosenbaek LL, Nielsen J, Fenton RA. Vasopressin induces phosphorylation of the thiazide-sensitive sodium chloride cotransporter in the distal convoluted tubule. *Kidney Int* 78: 160–169, 2010.
34. Pimenta E, Gaddam KK, Oparil S, Aban I, Husain S, Dell'Italia LJ, Calhoun DA. Effects of dietary sodium reduction on blood pressure in subjects with resistant hypertension: results from a randomized trial. *Hypertension* 54: 475–481, 2009.
35. Pisitkun T, Shen RF, Knepper MA. Identification and proteomic profiling of exosomes in human urine. *Proc Natl Acad Sci USA* 101: 13368–13373, 2004.
36. Psaty BN, Lumley T, Furberg CD, Schellenbaum G, Pahor M, Alderman MH, Weiss NS. Health outcomes associated with various antihypertensive therapies used as first-line agents - A network meta-analysis. *JAMA* 289: 2534–2544, 2003.
37. Robbins PW, Trimble RB, Wirth DF, Hering C, Maley F, Maley GF, Das R, Gibson BW, Royal N, Biemann K. Primary structure of the Streptomyces enzyme endo-beta-N-acetylglucosaminidase H. *J Biol Chem* 259: 7577–7583, 1984.
38. San-Cristobal P, Pacheco-Alvarez D, Richardson C, Ring AM, Vazquez N, Rafiqi FH, Chari D, Kahle KT, Leng Q, Bobadilla NA, Hebert SC, Alessi DR, Lifton RP, Gamba G. Angiotensin II

signaling increases activity of the renal Na-Cl cotransporter through a WNK4-SPAK-dependent pathway. *Proc Natl Acad Sci USA* 106: 4384–4389, 2009.

39. Simon DB, Nelson-Williams C, Johnson Bia M, Ellison D, Karet FE, Morey Molina A, Vaara I, Iwata F, Cushner HM, Koolen M, Gainza FJ, Gitelman HJ, Lifton RP. Gitelman's variant of Barter's syndrome, inherited hypokalaemic alkalosis, is caused by mutations in the thiazide-sensitive Na–Cl cotransporter. *Nat Genet* 12: 24–30, 1996.
40. Spierto FW, MacNeil ML, Burtis CA. The effect of temperature and wavelength on the measurement of creatinine with the Jaffe procedure. *Clin Biochem* 12: 18–21, 1979.
41. Terker AS, Zhang C, Erspamer KJ, Gamba G, Yang C-L, Ellison DH. Unique chloride-sensing properties of WNK4 permit the distal nephron to modulate potassium homeostasis. *Kidney Int* 89: 127–134, 2015.
42. Terker AS, Zhang C, McCormick JA, Lazelle RA, Zhang C, Meermeier NP, Siler DA, Park HJ, Fu Y, Cohen DM, Weinstein AM, Wang W-H, Yang C-L, Ellison DH. Potassium modulates electrolyte balance and blood pressure through effects on distal cell voltage and chloride. *Cell Metab* 21: 39–50, 2015.
43. Tutakhel OAZ, Jeleń S, Valdez-Flores M, Dimke H, Piersma SR, Jimenez CR, Deinum J, Lenders JW, Hoenderop JGJ, Bindels RJM. Alternative splice variant of the thiazide-sensitive NaCl cotransporter: a novel player in renal salt handling. *Am J Physiol Renal Physiol* 310: F204–F216, 2016.
44. van der Lubbe N, Jansen PM, Salih M, Fenton RA, van den Meiracker AH, Danser AHJ, Zietse R, Hoorn EJ. The phosphorylated sodium chloride cotransporter in urinary exosomes is superior to prostasin as a marker for aldosteronism. *Hypertension* 60: 741–748, 2012.
45. Wilson FH, Disse-Nicodème S, Choate KA, Ishikawa K, Nelson-Williams C, Desitter I, Gunel M, Milford DV, Lipkin GW, Achard J-M, Feely MP, Dussol B, Berland Y, Unwin RJ, Mayan H, Simon DB, Farfel Z, Jeunemaitre X, Lifton RP. Human hypertension caused by mutations in WNK kinases. *Science* 293: 1107–1112, 2001.
46. Wolley MJ, Wu A, Xu S, Gordon RD, Fenton RA, Stowasser M. In Primary Aldosteronism, Mineralocorticoids Influence Exosomal Sodium-Chloride Cotransporter Abundance. *J Am Soc Nephrol* 28: 56-63, 2016.
47. Wood JM, Schnell CR, Levens NR. Kidney is an important target for the antihypertensive action of an angiotensin II receptor antagonist in spontaneously hypertensive rats. *Hypertension* 21: 1056–1061, 1993.

4

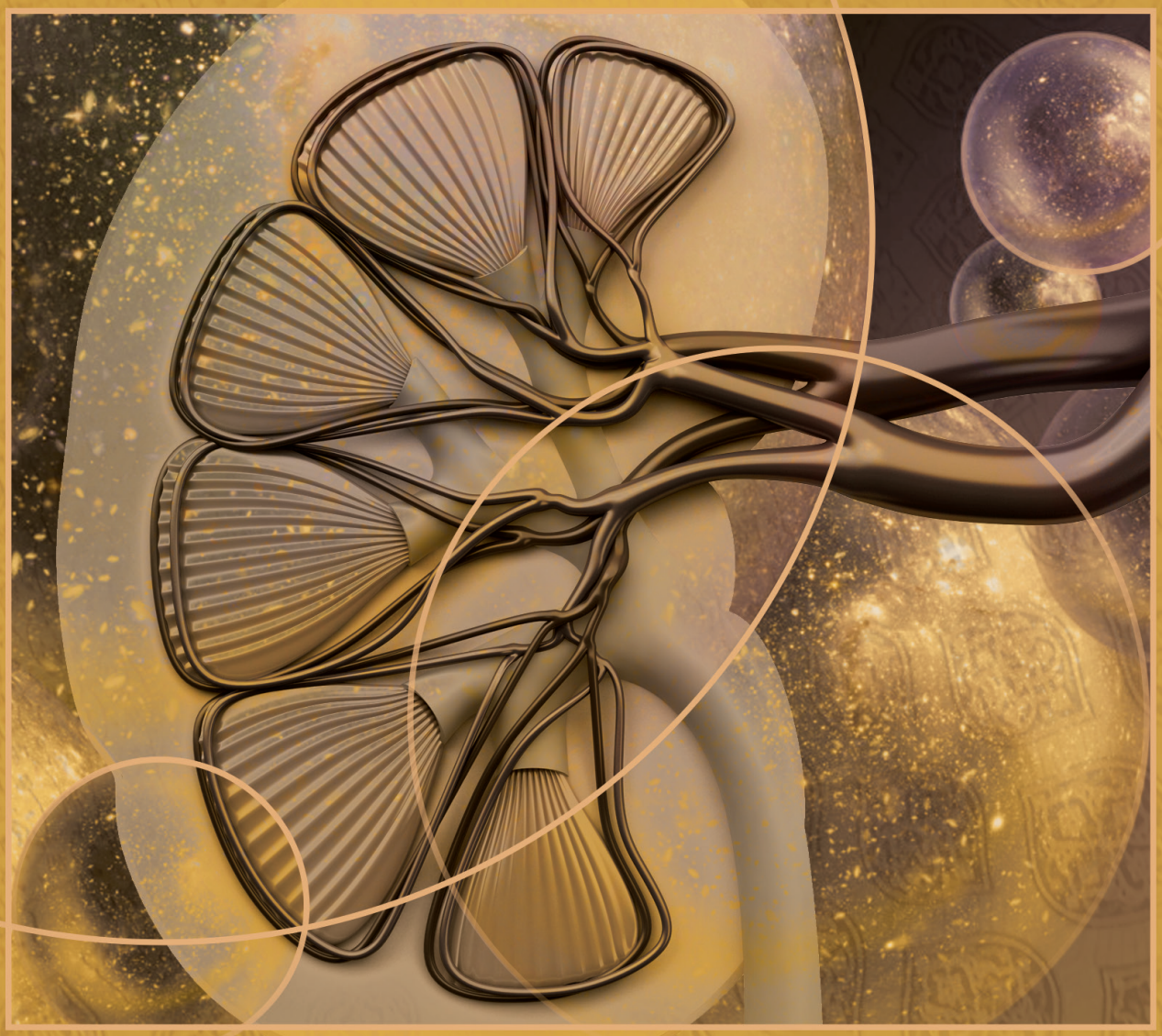

Dominant functional role of the novel phosphorylation site S811 in the human renal NaCl cotransporter

Omar A.Z. Tutakhel[1], Frans Bianchi[1], Daniël A. Smits[1], René J.M. Bindels[1], Joost G.J. Hoenderop[1] and Jenny van der Wijst[1]

[1]Department of Physiology, Radboud Institute for Molecular Life Sciences, Radboud university medical center, Nijmegen, The Netherlands

Submitted, 2017

Abstract

The NaCl cotransporter, NCC, is essential for electrolyte homeostasis and blood pressure control. The human *SLC12A3* gene, encoding NCC, gives rise to three isoforms, of which only the shortest isoform (NCC_3) has been studied extensively. All NCC isoforms share key phosphorylation sites at threonine 55 (T55) and 60 (T60) that are essential mediators of NCC function. Recently, a novel phosphorylation site at serine 811 (S811) was identified in isoforms 1 and 2 (NCC_{SV}), only present in humans and higher primates. The aim of this study is, therefore, to investigate the role of S811 phosphorylation in the regulation of NCC by a combination of biochemical and fluorescent microscopy analyses. We show that the phosphorylation-deficient S811A mutant hinders phosphorylation at T55 and T60 in NCC_{SV}, as well as in NCC_3. NCC_{SV} S811A impairs NCC_3 activity in a dominant negative fashion, while it does not affect plasma membrane abundance. This effect may be explained by heterodimerization of NCC_{SV} with NCC_3. Taken together, our study highlights a dominant negative effect of NCC_{SV} on T55 and T60 phosphorylation and NCC activity. Hereby, we reveal a new function of NCC_{SV} in humans that broadens the understanding on NCC regulation in blood pressure control.

Keywords: Hypertension / Kidney / NCC / Splice variant

Introduction

Hypertension (high blood pressure) affects over 1.3 billion people worldwide, and can lead to severe cardiovascular complications, including cerebrovascular disease, heart failure, ischemic heart disease and renal failure (6, 9, 19, 35, 39, 41). This makes hypertension the greatest contributing risk factor to morbidity and mortality worldwide. The cause of hypertension is identified in only ~10% of the cases (secondary hypertension) (10, 34). It is of critical importance to increase our understanding of the pathophysiology of hypertension. The kidneys play a key role in blood pressure control by regulating sodium (Na^+) excretion (5, 7, 12, 13, 38). Fine-tuning (5-10%) of Na^+ excretion primarily takes place in the distal convoluted tubule (DCT) by Na^+ reabsorption through the NaCl cotransporter (NCC) (16, 17, 59).

Since the cloning of NCC, three splice isoforms of NCC have been identified, which are the result of alternative splicing of the *SLC12A3* gene (59). So far, most research has focused on the shortest NCC isoform (NCC_3), as the other two isoforms are not present in rodents (20). NCC isoforms 1 and 2 that result from alternative splicing of exon 20 are nine amino acids longer than NCC_3 (20, 55). Subsequent studies confirmed the presence of both long and short forms of the exon 20 (20a and 20b respectively), which possibly indicates a splicing donor site (33). Compared to NCC isoform 1, isoform 2 lacks one amino acid at glutamine residue 95 within amino (N)-terminal domain. Therefore, NCC isoform 1 and 2 are practically indistinguishable and are, in this study, collectively referred to as NCC splice variant (NCC_{SV}). Interestingly, NCC_{SV} is only present in humans and higher primates. In the human kidney, NCC_{SV} mRNA comprises ~44% of the total NCC content (59).

The importance of NCC in blood pressure regulation is illustrated by diseases such as Gitelman Syndrome (OMIM #263800) (60-62) and Familial Hyperkalemic Hypertension (FHHt; OMIM #145260) (28, 50, 66, 68). Gitelman Syndrome is caused by loss of function mutations in the *SLC12A3* gene, encoding NCC (60-62), resulting in renal Na^+ wasting and hypotension (23, 55). In contrast, FHHt is a form of hypertension that results from gain of function of NCC, as a consequence of mutations in genes encoding for key signaling molecules (8, 66). In FHHt, mutations have been identified in *WNK1* and *WNK4* encoding the with no lysine (WNK) kinases (66), or in *KLHL3* and *CUL3*, coding for Kelch-like 3 and Cullin 3, respectively (8). WNK kinases phosphorylate and activate Ste20-related proline-alanine-rich kinase (SPAK) and oxidative stress response 1 (OSR1), which in turn phosphorylate threonine residues 55 and 60 (T55 and T60) in NCC (1, 43, 59). Phosphorylation of these sites is essential for NCC activity (16, 43, 57, 71) and plasma membrane abundance (27, 69).

Interestingly, Gonzales *et al.* described a novel phosphorylation site on serine residue 811 (S811), which is only present in NCC_{SV} (20). Our group has previously shown that NCC_{SV} plays a role in physiological (59) and pathophysiological (45) processes. However, the importance of NCC_{SV} S811 phosphorylation in NCC_{SV} and NCC_3 function remains unknown. Therefore, the present study aims to investigate the role of NCC_{SV} S811 in the phosphorylation and activity of NCC_{SV} as well as NCC_3. A combinational approach of immunoblotting with phospho-specific antibodies, cell surface biotinylation, and fluorescence microscopy was used to examine the influence of S811 on the phosphorylation, membrane abundance and activity of NCC. In addition, the interaction of NCC_{SV} with NCC_3 was assessed by fluorescence lifetime imaging microscopy (FLIM).

Materials and Methods

Mutagenesis and constructs.

NCC isoform 1 (accession no. NP_000330.2) was used in all experiments to represent NCC_{SV}. For co-immunoprecipitation, enhanced green fluorescent protein (eGFP) carboxy (C)-terminal-coupled human NCC_3-eGFP, NCC_{SV}-eGFP, and the phospho-mutants of NCC_{SV}-eGFP (constitutively phosphorylated S811D and non-phosphorylated S811A) in pCMV-SPORT6 were generated as previously described (16, 59). In addition, human NCC_3, NCC_{SV}, and NCC_{SV} phospho-mutants were cloned into the HA pCINeo-IRES-mCherry vector using standard PCR and restriction cloning. For the FLIM and co-immunoprecipitation experiments, NCC_{SV} and NCC_3 were cloned into the pCINeo vector and human codon optimized mCitrine and mCherry tags were fused to the C-terminal end separated by a 15 residues long linker region (3x GGGGS) using PCR and uracil excision based cloning (42). For the fluorescence microscopy measurements, NCC_3, NCC_{SV}, NCC_{SV} phospho-mutants (S811D and S811A) and NCC_3 phospho-mutant (T55A/T60A) were cloned into the pCINeo-IRES-eCFP vector using restriction cloning. The vector carrying halide-sensitive yellow fluorescent protein (YFP) and mKate gene was described previously (64) and was kindly provided by Dr. Jeffrey M. Beekman (University Medical Center Utrecht, the Netherlands).

Cell culture and transfection.

Cell culture and transfection was performed as described previously (59). In brief, human embryonic kidney (HEK293) cells were grown in DMEM medium supplemented with 10% v/v fetal bovine serum, non-essential amino acids and 2 mM L-glutamine. The cells were transiently transfected using polyethylenimine (Polysciences, Warrington, PA, USA) in DNA:polyethylenimine ratio of 1:6. Cells transfected with empty vectors were used as control (mock). For co-transfection, cells were transfected in a DNA ratio of 1:1.

Buffers.

The following buffers were used: isotonic control buffer contained (in mM) 135 NaCl, 5 KCl, 0.5 $CaCl_2$, 0.5 $MgCl_2$, 0.5 Na_2HPO_4, 0.5 Na_2SO_4, 15 HEPES/Tris pH 7.4; hypotonic low Cl^- buffer contained (in mM) 67.5 Na-Gluconate, 2.5 K-gluconate, 0.25 $CaCl_2$, 0.25 $MgCl_2$, 0.5 Na_2HPO_4, 0.5 Na_2SO_4, 7.5 HEPES/Tris pH 7.4; dissection buffer contained (in mM) 300 sucrose, 25 imidazole, 1 EDTA, HCl pH 7.2 and freshly added protease inhibitors (in µM) 50 phenylmethylsulfonyl, 20 aproptinin, 20 leupeptin, 10 pepstatin A; PBS-CM, PBS supplemented with (in mM) 1 $MgCl_2$, 0.5 $CaCl_2$, NaOH pH 8.0; Lysis buffer contained (in mM) 50 Tris/HCl pH 7.5, 1 EGTA, 1 EDTA, 10 Na^+ β-glycerophosphate, 1 Na-orthovanadate, 50 Na-fluoride, 10 Na-pyrophosphate, 270 sucrose, 150 NaCl, 1% v/v Triton X-100 and freshly added protease inhibitors (in µM) 50 phenylmethylsulfonyl, 20 aproptinin, 20 leupeptin, 10 pepstatin A; 1x Laemmli sample buffer contained (in mM) 40 DTT, 12 Tris/HCl pH 6.8, 0.4% w/v SDS, 2% v/v glycerol, 0.002% w/v bromophenol blue; TBS-T contained (in mM) 140 NaCl, 20 Tris/HCl pH 7.5, 0.1% v/v Tween-20. NaI solution contained (in mM) 140 NaI, 4.2 KCl, 1.4 $CaCl_2$, 1 $MgCl_2$, 5.5 D-glucose, 10 HEPES/Tris pH 7.4, 300 mosmol/kg H_2O.

Cell treatment.

At 48 h post-transfection, the HEK293 cells were washed once with PBS. Next, cells were incubated for 30 min at 37ºC with isotonic control buffer or hypotonic low Cl^- buffer. Subsequently, the cells were used for isolation of total cell membrane fractions, cell surface biotinylation, or co-immunoprecipitation.

Isolation of total cell membrane fractions.

HEK293 cells were lysed with ice-cold dissection buffer. Lysed cells were centrifuged at 4,000 g for 8 min at 4ºC, after which the supernatant was centrifuged at 16,000 g for 40 min at 4ºC. The pellet was resuspended in ice-cold dissection buffer and protein concentration was determined using the Bradford method (Sigma-Aldrich, St. Louis, MO, USA). Proteins were eluted in 1x Laemmli sample buffer. Samples were incubated for 15 min at 65ºC prior to immunoblotting.

Cell surface biotinylation.

Cells surface biotinylation was performed as described previously (14). Subsequently, HEK293 cells were lysed in ice-cold lysis buffer and centrifuged at 16,000 g at 4°C. Protein concentrations were determined using the Bradford method (Sigma-Aldrich, St. Louis, MO, USA). Equal amounts of protein were incubated with neutravidin beads (Pierce

Biotechnology, Rockfort, IL, USA) for 2 h at 4°C. The beads were washed three times with lysis buffer and eluted in 1x Laemmli sample buffer. Samples were incubated for 15 min at 65ºC prior to immunoblotting.

Fluorescence lifetime imaging microscopy.

FLIM images were generated from HEK293 cells 16 h after transfection with NCC_3 and NCC_{SV} containing mCitrine and/or mCherry C-terminal fusion plasmids. Total amount of DNA per transfection was 2 µg (1:1 donor acceptor ratio) in WillCo-dish (diameter 35 mm, WillCo Wells B.V. Amsterdam, Noord-Holland, NL) with 1.2 X 10^6 cell density. Imaging and measurements were performed as previously described (63). In brief, samples were washed and imaged in Live Cell imaging solution (HEPES buffered saline solution; Thermo Scientific, Rockford, IL, USA). Photon traces in Picoquant Photon Trace version (PT3) format were used to construct FLIM images in Image Cytometry Standard (ICS). Conversion of PT3 files to ICS was performed using PT32ICS conversion software (63). For FLIM statistics of single cells, photons were pooled for each individual cell and fitted with exponential decay functions de-convoluted with the instrument response function (IRF) using OriginPro2016 (Originlab, Northampton, MA, USA). Single pixel-fitted FLIM images were generated for individual cells (with at least 1,000,000 photons per cell) using the TRI2 software (version 2.8.6.2; Gray institute, Oxford, OXF, UK) (3, 4). Settings used for TRI2 were: 7 x 7 pixel circular binning and thresholding 15%-100% intensity. Lifetime imaging pictures were generated using FIJI ImageJ (52).

Co-immunoprecipitation.

Transfected HEK293 cells were lysed in ice-cold lysis buffer for 1 h at 4ºC. Subsequently, cell lysate was collected and centrifuged at 16,000 g at 4ºC. Protein concentrations were determined using the Bradford method. The anti-green fluorescent protein (GFP) or anti-HA antibodies were coupled to protein A/G plus agarose beads (Santa Cruz Biotechnology, Santa Cruz, CA, USA) by gentle agitation for 2 h at 4ºC. Subsequently, equal amounts of protein were incubated with GFP- or HA-conjugated beads for 2 h at 4ºC. GFP-conjugated beads were used for co-immunoprecipation of mCitrine-tagged NCC to demonstrate binding to mCherry-tagged NCC. Co-immunoprecipation of HA-tagged NCC was performed with the HA-conjugated beads to detect interaction with eGFP-tagged NCC. Beads were washed three times with ice-cold lysis buffer and proteins were eluted in 1x Laemmli sample buffer. Samples were incubated for 15 min at 65ºC prior to immunoblotting. The co-immunoprecipitation was analyzed by anti-GFP, anti-HA, anti-mCherry antibodies.

Immunoblotting.

Samples in Laemmli buffer were loaded on an 8% w/v SDS-PAGE gel, transferred to polyvinylidene difluoride membranes (Immobilon-P, Millipore Corporation, Bedford, MA, USA) that were subsequently blocked for 30 min with TBS-T containing 5% w/v skimmed dried milk powder. Subsequently, membranes were incubated with primary antibodies dissolved in 5% w/v in non-fat dry milk (NFDM) in TBS-T overnight at 4ºC. Next, membranes were incubated with horseradish peroxidase (HRP) conjugated secondary antibodies diluted in 1% w/v NFDM in TBS-T for 1 h at room temperature and visualized with the imaging system (ChemiDoc XRS, Bio-Rad Laboratories, Hercules, CA, USA) using enhanced chemiluminescence (Thermo Fischer Scientific, Waltham, MA, USA). Immunoreactive bands were quantified with Image Studio Lite software (LI-COR biosciences, Lincoln, NE, USA).

Antibodies.

The following antibodies were used: anti-total NCC (Millipore, Billerica, MA, USA, #AB3553; 1:2,000); anti-NCC pT55 and anti-NCC pT60 (equivalent mouse NCC pT53 and pT58; 1:2,000) as previously described (46), anti-HA (Cell Signaling Technology, Beverly, MA, USA, #2367; 1:5,000), anti-GFP (generated in house, detects eGFP and mCitrine, 1:5,000), anti-mCherry (Abcam, Cambridge, UK, #ab167453; 1:1,000) and anti-β-actin (Sigma-Aldrich, St. Louis, MO, USA, #A5441; 1:20,000). Secondary antibodies were as follows: horseradish peroxidase-conjugated goat-anti-rabbit (Sigma-Aldrich, St. Louis, MO, USA, #A4914; 1:10,000) and goat-anti-mouse (Jackson Immunoresearch laboratories, West Grove, PA, USA, #515-035-003; 1:10,000).

NCC activity measurements using YFP-mKate.

NCC activity was performed as described previously (61). In brief, HEK293 cells were co-transfected with the halide-sensitive YFP-mKate construct (64) and the appropriate human NCC pCINeo-IRES-eCFP construct or pCINeo-IRES-eCFP mock. Total amount of DNA per transfection was 2 µg (0.2 µg YFP-mKate + 1.8 µg NCC) in WillCo-dish with 1.2 X 10^6 cell density. 19 h after transfection and prior to the measurements, cells were incubated with hypotonic low Cl^- buffer for 10 min at 37°C. Next, cells were placed in an incubation chamber containing hypotonic low Cl^- buffer (500 µL) and attached to the stage of an inverted microscope (Axiovert 200M, Carl Zeiss, Jena, Germany). NCC-expressing HEK293 cells were identified by detecting eCFP fluorescence using a monochromator at 430-nm excitation, and subsequently the emitted light was directed by a 480AF30 dichroic mirror. After 30 s, an equal volume of NaI solution was added to the incubation chamber (final concentration of Na^+ 105 mM and I^- 70 mM). Changes in intracellular halide concentrations were monitored by simultaneous measurements of halide-sensitive YFP fluorescence and

the halide-insensitive fluorescence of mKate (64). Halide-sensitive YFP was excited at 488 nm using a monochromator. The fluorescence-emitted light was directed by a 505DRLPXR dichroic mirror (Omega Optical, Brattleboro, VT) through a 535af26 emission filter. mKate was excited at 543 nm, and fluorescence-emitted light was directed by a 560DRLP dichroic mirror (Omega Optical) through a 565ALP emission filter onto a Cool-SNAP HQ monochrome CCD camera. The integration time of the CCD camera was set at 200 ms for both YFP and mKate, with a sampling interval of 3 s. All measurements were performed at 37°C. Quantitative image analysis was performed with Metamorph 6.0 (Molecular Devices, Sunnyvale, CA). For each wavelength, the mean fluorescence intensity was monitored in an intracellular region and, for purpose of background correction, an extracellular region of identical size. After background correction, the fluorescence emission ratio of the green and red fluorescence of YFP and mKate, respectively, was used to determine changes in intracellular halide content as a measure for NCC activity. NCC is able to transport NaI as NaCl in a hydrochlorothiazide (HCTZ)-sensitive manner (61). Signal specificity was assessed by addition of 100 µM HCTZ or an equivalent amount of its solvent DMSO together to the hypotonic low Cl^- buffer incubation for 10 min at 37°C. The thiazide-sensitive uptake was determined by the difference of the measurements with and without HCTZ.

Statistics.

The immunoblot data were analyzed by comparing integrated optical densities of bands by one-way ANOVA with Tukey's multiple comparisons *post hoc* test if multiple groups were compared. In the FLIM and NCC activity measurements, all depicted data are averages of at least 3 independent experiments, and all statistical analyses were performed using a one-way ANOVA with Dunnett's multiple comparison *post hoc* test comparing the control condition versus all other conditions. Depicted values are means ± SEM of at least three independent experiments, and $P<0.05$ was considered statistically significant. All data were analyzed using Prism 6 software (Graph- Pad Software, La Jolla, CA).

Results

Effect of S811 on NCC_{SV} phosphorylation at T55 and T60.

To examine the role of phosphorylation at S811 in NCC_{SV}, the NCC_{SV} S811D and S811A plasmids were generated that represent the constitutively phosphorylated and non-phosphorylated form of S811, respectively. HEK293 cells transfected with the respective plasmids were subjected to hypotonic low Cl^- buffer, which is a known stimulus of NCC phosphorylation at T55 and T60 (Fig. 1A) (43, 48). Interestingly, NCC_{SV} S811A did not show a significant stimulation of T55 and T60 phosphorylation upon hypotonic low Cl^- buffer,

compared to the isotonic control buffer (Fig. 1). Moreover, T55 and T60 phosphorylation of NCC_{SV} S811A was significantly lower compared to NCC_3, NCC_{SV} or NCC_{SV} S811D under hypotonic low Cl^- condition (Fig. 1, white bars). NCC_3, NCC_{SV} and NCC_{SV} S811D demonstrated significantly higher phosphorylation at T55 and T60 upon hypotonic low Cl^- buffer treatment, compared to the isotonic control buffer (Fig. 1). No difference in T55 and T60 phosphorylation was observed between NCC_{SV} and NCC_3 after treatment with hypotonic low Cl^- buffer. Isotonic control buffer did not result in T55 and T60 phosphorylation in any of the conditions tested. Immunoreactive bands were not observed in cells transfected with the empty vector (mock) (Fig. 1A).

Effect of S811 phosphorylation on phosphorylation of NCC_3 at T55 and T60.

As NCC_{SV} and NCC_3 are co-expressed at the apical membrane of epithelial cells lining the DCT (59), we hypothesized that S811 phosphorylation could affect the phosphorylation at T55 and T60 of NCC_3. Co-expression of NCC_{SV} S811A and NCC_3 resulted in significantly less phosphorylation at T55 and T60 compared to co-expression of NCC_{SV} and NCC_3, when treated with hypotonic low Cl^- buffer. Interestingly, this decrease was more than 50% for both T55 and T60 (Fig. 2B, C, white bars). Co-expression of NCC_3 with NCC_{SV} or NCC_{SV} S811D showed significantly higher phosphorylation at T55 and T60 when treated with hypotonic low Cl^- buffer, compared to isotonic control buffer (Fig. 2). Similar to Fig. 1, NCC_{SV} S811A alone did not show significant difference in T55 and T60 phosphorylation between the isotonic control and hypotonic low Cl^- buffer treatment (Fig. 2). In isotonic control buffer, there was no difference in T55 and T60 phosphorylation levels in any of the conditions tested (Fig. 2B and C, black bars). Cells transfected with the mock vector did not show immunoreactive bands (Fig. 2A).

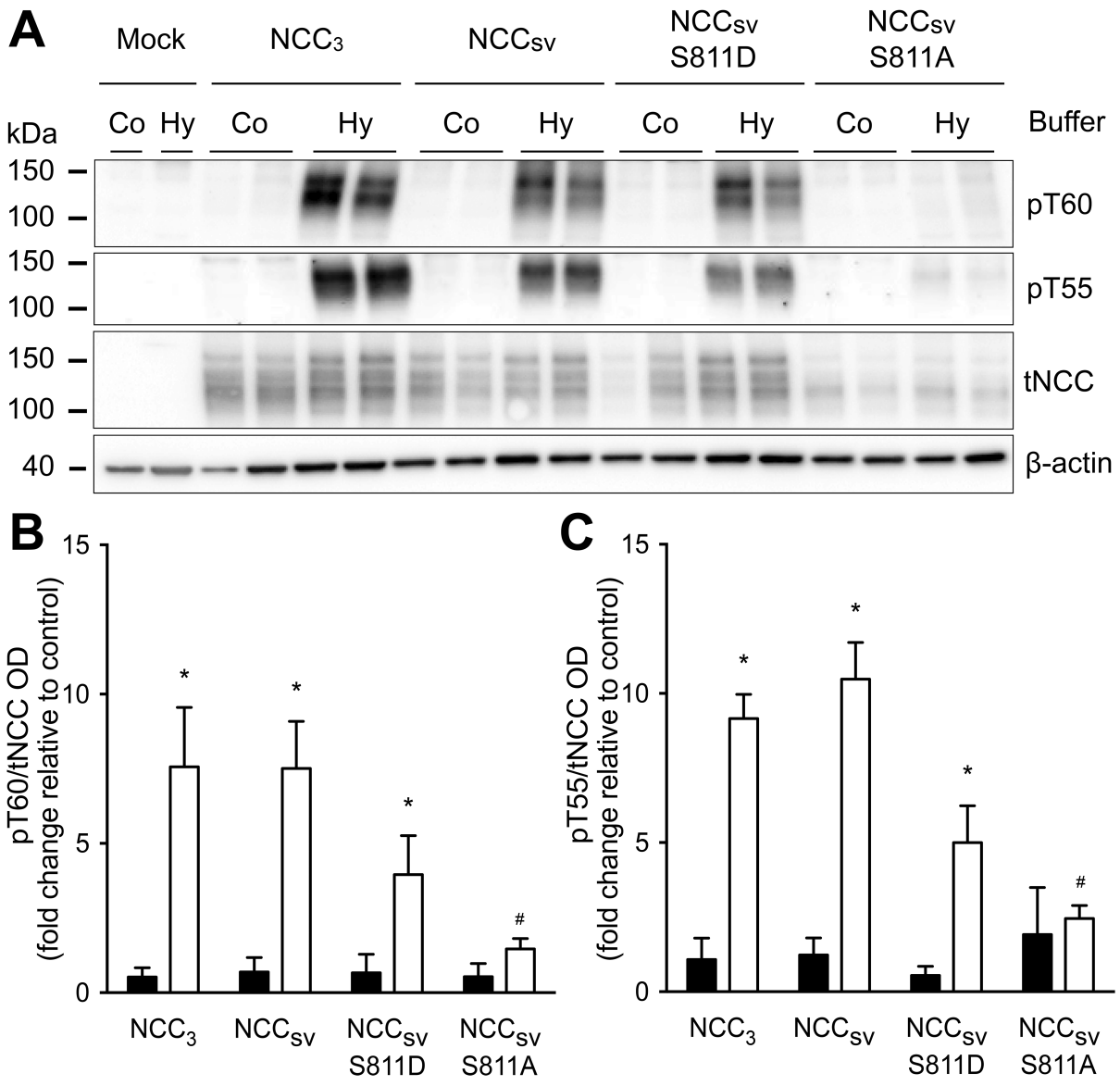

Figure 1 | S811A mutant of NCC_{SV}, but not S811D, prevents the phosphorylation at T55 and T60.

(**A**) Representative immunoblot of total cell membrane fractions isolated from HEK293 cells transfected with mock, indicated NCC isoforms and NCC_{SV} mutants, treated with isotonic control (Co) or hypotonic low Cl^- (Hy) buffer. Immunoblots were probed with anti-total NCC (tNCC), anti-phosphorylated T55 (pT55) and T60 (pT60) NCC antibodies, depicting the immunoreactive band of ~130 kDa. β-actin was used as a sample loading control. (**B** and **C**) Densitometry analysis of immunoreactive bands of pT55 and pT60 to tNCC ratio. The abundance of tNCC and pT55 and pT60 upon the treatment with hypotonic low Cl^- buffer relative to the treatment with isotonic control buffer was determined. Subsequently, this relative abundance in hypotonic low Cl^- condition of NCC_{SV}, NCC_{SV} S811D, and NCC_{SV} S811A was compared to the relative abundance of NCC_3. Values are expressed as mean ± SEM of at least 3 independent experiments. *indicates the significance of hypotonic low Cl^- buffer compared to its own control. #indicates significance compared to NCC_{SV}. $^{*\#}P<0.05$ was considered statistically significant.

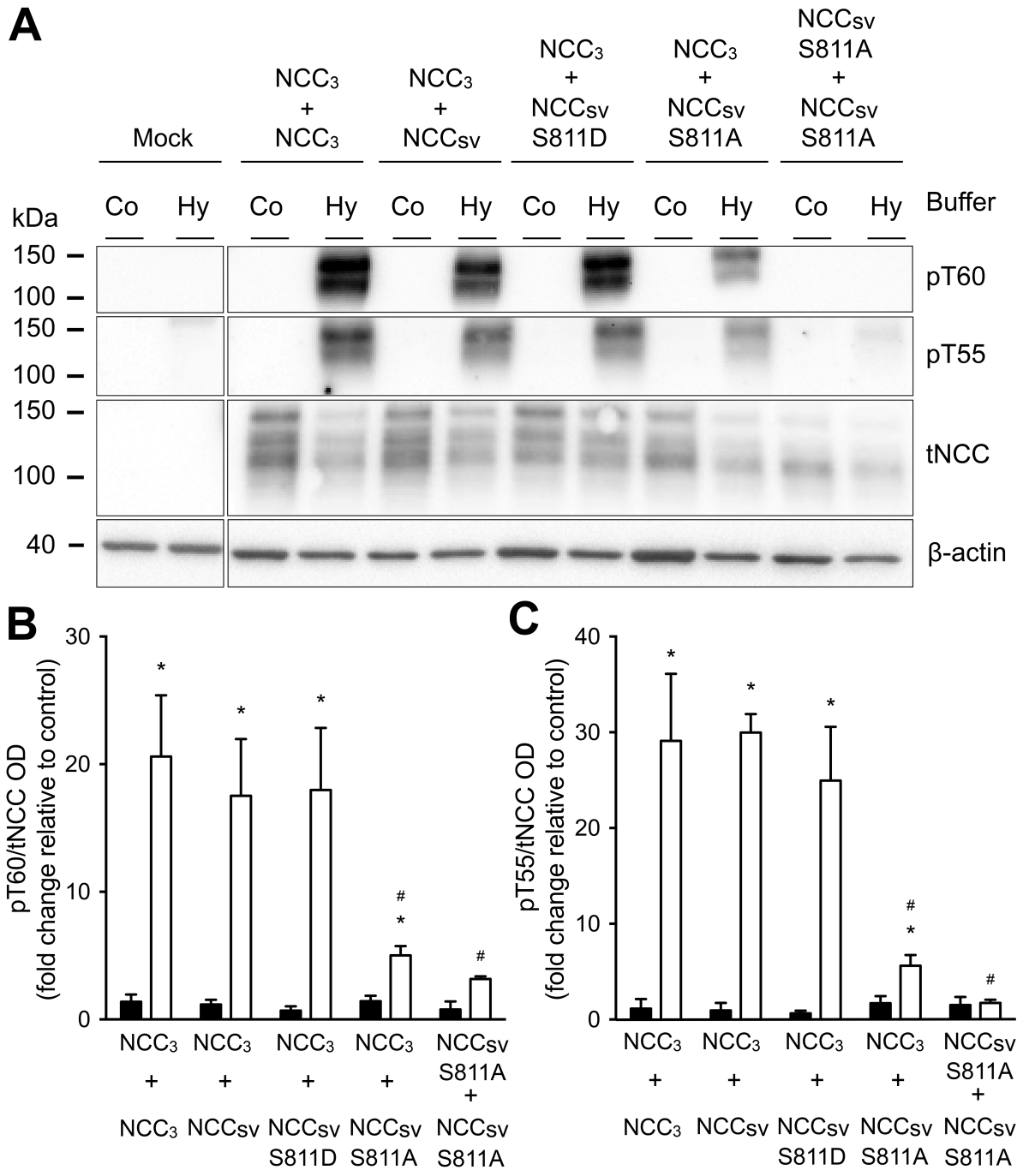

Figure 2 | NCC_{SV} S811A inhibits the phosphorylation at T55 and T60 of NCC_3.

(**A**) Representative immunoblot of total cell membrane fractions isolated from HEK293 cells co-transfected with NCC_3 and NCC_{SV} or NCC_{SV} mutants in a 1:1 ratio, treated with isotonic control (Co) or hypotonic low Cl^- (Hy) buffer. Immunoblots were probed with anti-total NCC (tNCC), anti-phosphorylated T55 (pT55) and T60 (pT60) NCC antibodies, depicting the immunoreactive band of ~130 kDa. β-actin was used as a sample loading control. (**B** and **C**) Densitometry analysis of immunoreactive bands of pT55 and pT60 divided by immunoreactive bands of tNCC. The abundance of tNCC and pT55 and T60 upon the treatment with hypotonic low Cl^- buffer relative to the treatment with isotonic control buffer was determined. This relative abundance in hypotonic low Cl^- condition of each combination was compared with the relative abundance of NCC_3 co-transfected with NCC_{SV}. Values are expressed as mean ± SEM of at least 3 independent experiments. *indicates the significance of hypotonic low Cl^- buffer compared to its own control. #indicates significant compared to NCC_3 + NCC_{SV}. *# $P<0.05$ was considered statistically significant.

NCC_{SV} and NCC_3 form hetero- and homo-dimers.

To assess whether the effect of NCC_{SV} S811 phosphorylation on NCC_3 T55 and T60 phosphorylation could be exerted via dimerization of NCC_{SV} with NCC_3, a Förster resonance energy transfer (FRET) based microscopy approach was used with C-terminal mCitrine and mCherry fusions of NCC_{SV} and NCC_3, respectively. FRET was measured using FLIM microscopy, which has the advantage that the lifetime (τ) is not dependent on excitation power and probe concentration, thereby being technically less challenging than ratiometric FRET analysis (65). The amount of FRET, which represents the interaction between the donor and acceptor pair, is measured as lifetime of the mCitrine fluorescent signal. This signal shortens due to the energy transfer to the mCherry probe in case of protein dimerization (26, 63). Co-expression of NCC_{SV}-mCitrine with either NCC_{SV}-mCherry or NCC_3-mCherry in HEK293 cells resulted in a significant decrease in lifetime as shown by the phasor plots (Fig. 3B) and single-cell analysis (Fig. 3A), indicating the formation of both hetero- and homo-dimers of NCC_{SV} with NCC_{SV} and NCC_3, respectively. The dimerization of NCC_{SV} and NCC_3 was further tested by a competition experiment, where NCC_{SV}-mCitrine was co-expressed with unlabeled NCC_3 as competitor together with NCC_3-mCherry. Competition with unlabeled NCC_3 resulted in an increase of the donor lifetime, compared to HEK293 cells co-expressing NCC_{SV}-mCitrine and NCC_{SV}-mCherry (Fig. 3B). In addition, SLC41A1 is used as a negative control. This is a Mg^{2+} transporter that localizes to the apical membrane of the DCT (21, 25), but does not interact with NCC_{SV}. Therefore, NCC_{SV}-mCitrine and SLC41A1-mCherry were co-expressed in HEK293 cells, which did not co-localize (Fig. 4A) and showed no significant lifetime decrease in line with two proteins that do not interact (Fig. 4A and B). The dimerization, as observed by FRET/FLIM, was further established by co-immunoprecipitation experiments, where NCC_{SV}-mCitrine was co-expressed with NCC_{SV}-mCherry and NCC_3-mCherry in HEK293 cells. As the GFP antibody binds to mCitrine, our results demonstrated that NCC_{SV}-mCitrine (bound to GFP-coupled beads) interacted with both NCC_{SV}- and NCC_3-mCherry (Fig. 3C). As a negative control, NCC_{SV}-mCitrine and mock were co-expressed in HEK293 cells and did not show interaction between mCitrine and mCherry (Fig. 3C). In addition, a co-immunoprecipitation was performed with HA- and eGFP-tagged plasmids to confirm the dimerization of NCC_{SV} mutants and NCC_3. eGFP-tagged NCC_3 plasmid was co-expressed with HA-tagged NCC_3, NCC_{SV}, NCC_{SV} S811D, or NCC_{SV} S811A in HEK293 cells. NCC_3 showed an interaction between NCC_3 and NCC_{SV}, NCC_{SV} S811D, or NCC_{SV} S811A (Fig. 4C). No immunoreactive bands were observed in any of the samples of HEK293 cells co-transfected with mock-eGFP or mock-HA (Fig. 4C). Input samples demonstrated equal expression under all conditions (Figs. 3C and 4C). Immunoblots with β-actin were used as a sample loading control.

Effect of S811 phosphorylation on the NCC function.

Since NCC activity is regulated by its phosphorylation (43), a functional assay was used to study the effect of S811 phosphorylation on the transport activity of NCC_{SV} and NCC_3. The respective plasmids were co-transfected in HEK293 cells with halide-sensitive YFP coupled to halide-insensitive fluorescent red protein mKate. Prior to the measurements, transfected HEK293 cells were incubated in hypotonic low Cl^- buffer to maximally increase NCC phosphorylation and activity (61). After 30 s, NaI was added to the medium, which induced a significant reduction in YFP/mKate ratio in NCC_3-expressing cells, indicative of NCC transport activity (Fig. 5A and B). Pretreatment with HCTZ (40 min, 100 µM), a well-known inhibitor of NCC, completely abrogated this response (Fig. 5B). As described previously (61), NCC activity is measured as the difference in the YFP/mKate ratio (Δ YFP/mKate ratio) between *t*=0 and *t*=180 s after NaI addition. This is plotted as the HCTZ-specific NCC activity: Δ YFP/mKate ratio without HCTZ minus Δ YFP/mKate ratio with HCTZ (Fig. 5C). Cells expressing NCC_{SV} S811A alone or in combination with NCC_3 displayed significantly reduced NCC activity compared to NCC_3 (Fig. 5C). The NCC_3 phospho-deficient T55A/T60A mutant (NCC_3 T55A/T60A) was included as negative control and displayed significantly reduced NCC activity compared to wild-type NCC_3 (Fig. 5C). Of note, the basal YFP/mKate ratio at *t*=0 s was not significantly different between the various conditions tested (Fig. 5B).

The effect of S811 on the abundance of NCC at the plasma membrane.

To determine the effect of S811 phosphorylation on the localization of NCC at the plasma membrane, HEK293 cells transfected with mock, NCC_3, NCC_{SV}, NCC_{SV} S811D or S811A mutants, were subjected to cell surface protein biotinylation. NCC protein was demonstrated in the total cell lysate (input) and the biotinylated fraction upon both isotonic control and hypotonic low Cl^- conditions (Fig. 5D). The optical density of biotinylated fraction was corrected for input fraction to assess NCC protein abundance at the plasma membrane. No significant difference was observed between the conditions tested, indicating equal amount of NCC protein abundance at the plasma membrane (Fig. 5E). Cells transfected with the mock vector did not show immunoreactive bands of NCC in biotinylated fractions or the input (Fig. 5D).

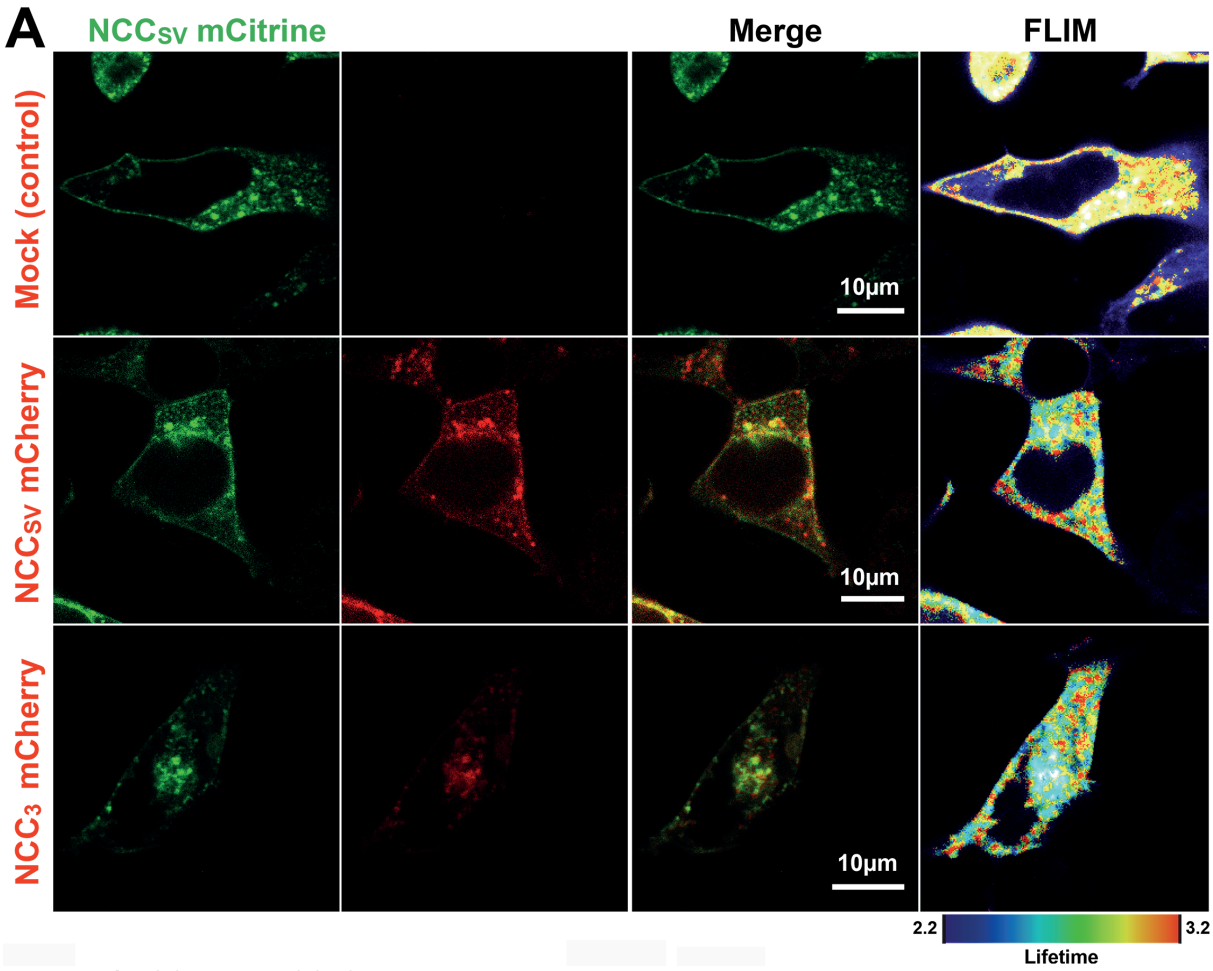

Figure 3 | NCC_{SV} and NCC_3 form hetero- and homo-dimers.

(**A**) NCC_{SV}-mCitrine was transiently co-transfected with NCC_3-mCherry or NCC_{SV}-mCherry in HEK293 cells. Förster resonance energy transfer between the labels was monitored by fluorescence lifetime imaging. Representative confocal microscopy (left) and convoluted FLIM (right) images of NCC_{SV}-mCitrine (green) with NCC_3-mCherry (red) or NCC_{SV}-mCherry (red) with scale bars of 10 µm.

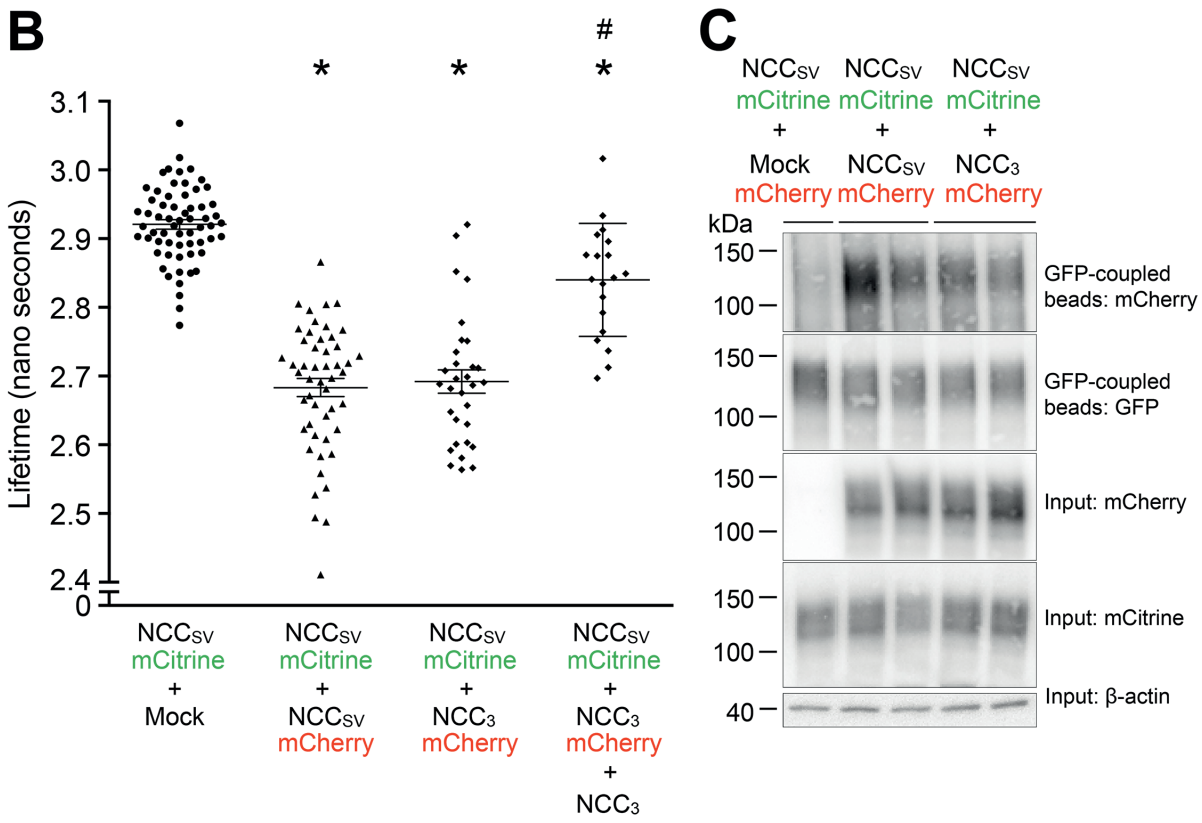

Figure 3 | Continued.

(**B**) Whole cell apparent fluorescence lifetimes demonstrating hetero- and homo-dimerization of NCC_{SV} and NCC_3 proteins in live cells. Significant difference between NCC_{SV}-mCitrine + mock and other conditions is denoted by * and their difference from NCC_{SV}-mCitrine + NCC_3-mCherry + NCC_3 is denoted by #. $N \geq 3$; $n > 20$/condition. $^{\#*}P < 0.05$ was considered statistically significant. (**C**) Co-immunoprecipitation with mCitrine-labelled NCC_{SV} and mCherry-labelled mock, NCC_{SV} and NCC_3. GFP-coupled beads represent the immunoprecipitated NCC_{SV}-mCitrine fraction and the immublots were probed with anti-mCherry and anti-GFP antibodies, depicting the immunoreactive NCC band of ~130 kDa. The total cell lysate (input) was probed with anti-mCherry, anti-GFP or anti-β-actin antibodies. β-actin was used as a sample loading control.

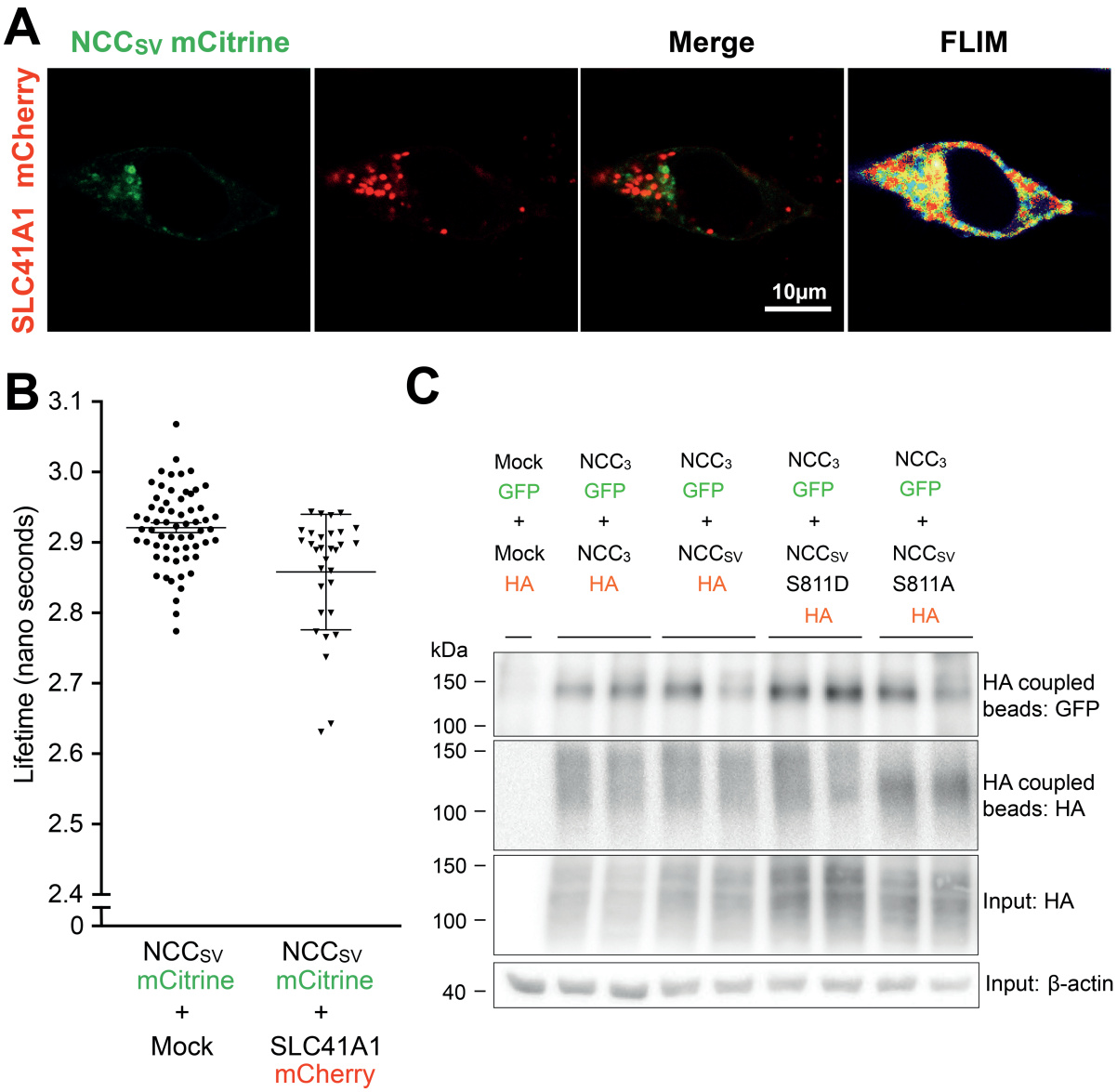

Figure 4 | NCC_{SV} and NCC_3 form hetero- and homo-dimers.

(**A**) As control for a specific background FRET/FLIM, NCC_{SV}-mCitrine (green) and SLC41A1-mCherry (red) were transiently co-transfected in human embryonic kidney (HEK)293 cells. Förster resonance energy transfer between the labels was monitored by fluorescence lifetime imaging. Representative confocal microscopy (left) and convoluted FLIM (right) images of NCC_{SV}-mCitrine (green) with SLC41A1-mCherry (red). Scale bars are 10 µm. (**B**) Whole cell apparent fluorescence lifetimes demonstrated for NCC_{SV}-mCitrine plus mock or SLC41A1-mCherry. (**C**) Representative immunoblots of co-immunoprecipitation with NCC isoforms and NCC_{SV} phospho-mutants. Co-immunoprecipitation with eGFP-tagged NCC_3 and HA-tagged mock, NCC_3, NCC_{SV}, NCC_{SV} S811D and NCC_{SV} S811A. The HA-coupled beads fraction represents the immunoprecipitated fraction and probed with anti-GFP and anti-HA antibodies, depicting the immunoreactive NCC band of ~130 kDa. The total cell lysate (input) was probed with anti-HA and anti-β-actin antibodies. β-actin was used as a sample loading control.

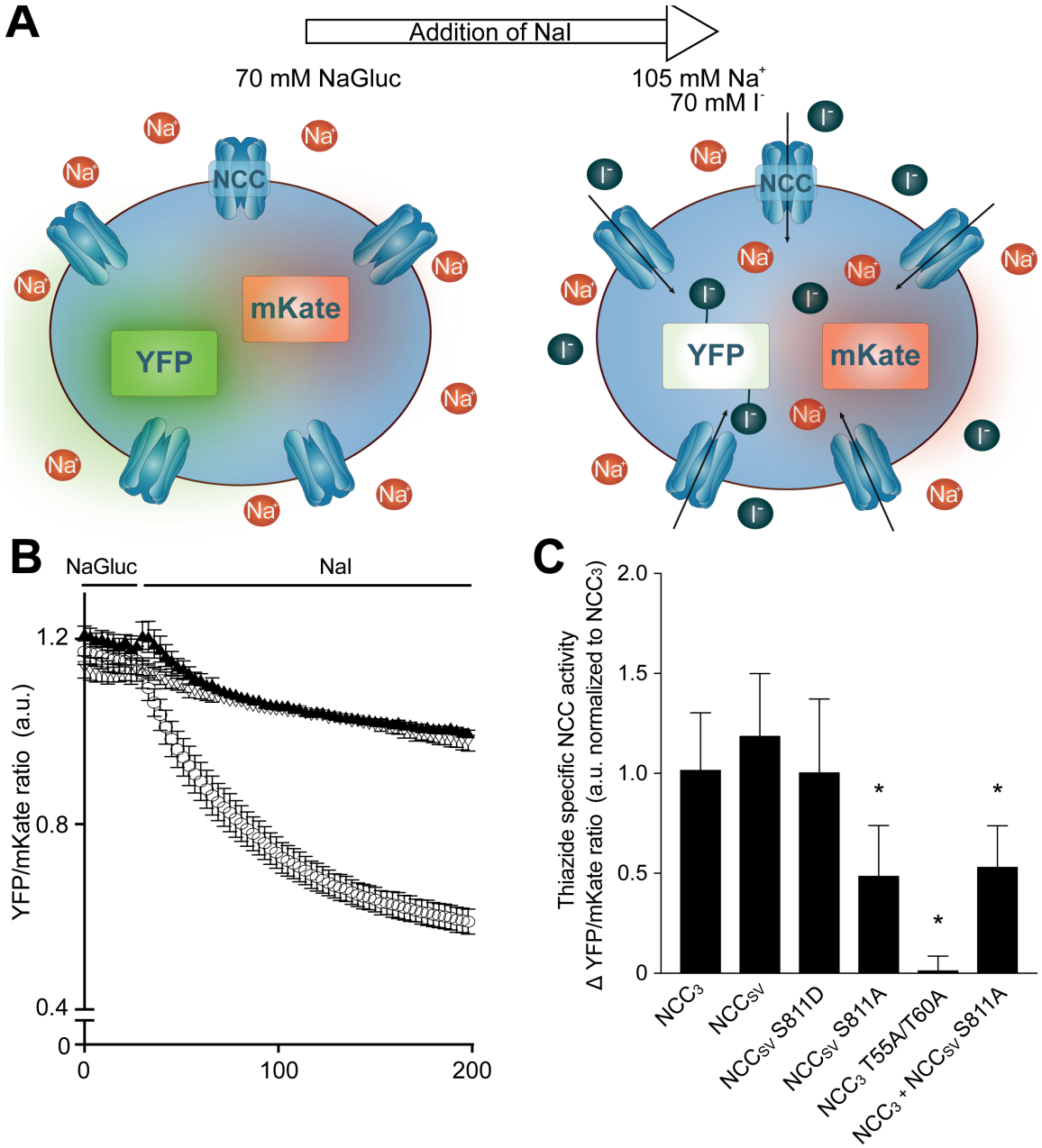

Figure 5 | S811A exhibits significantly impaired NCC activity.

(**A**) Model of NCC activity assay in HEK293 cells depicting the co-expression of an NCC isoform with a halide-sensitive yellow fluorescent protein (YFP) that is coupled to the red fluorescent protein mKate. The latter is insensitive to changes in intracellular halide concentrations. Pre-incubation of these cells in hypotonic low Cl^- solution containing 70 mM Na-Gluconate (NaGluc) for 40 min and subsequent addition of NaI (final Na^+ and I^- concentration 105 and 70 mM, respectively) resulted in a change in YFP fluorescence, which is corrected for the red fluorescent iodide-insensitive (mKate) signal. This allows the determination of changes in intracellular iodide concentrations using the YFP/mKate ratio as a measure of NCC activity. (**B**) NaI was added 30 s after the start (*t*=0) and the YFP/mKate ratio was plotted over time for mock and NCC_3 expressing HEK293 cells treated with or without thiazide (HCTZ, 100 µM); [*N*=3, mock (DMSO, ▽), *N*=3; NCC_3 HCTZ (▲), *N*=3; NCC_3 DMSO (○)]. (**C**) Activity of NCC_3, NCC_{SV}, NCC_{SV} S811D, NCC_{SV} S811A and NCC_3 T55A/T60A is expressed as the difference in the YFP/mKate ratio (Δ YFP/mKate ratio, *t*=0 s minus *t*=180 s). The thiazide-specific NCC activity was determined by the ratio difference of the measurements with and without HCTZ. Significant difference in activity between NCC_3 and all other constructs is denoted by *. *N*=3; *n*>65/condition. *P<0.05 was considered statistically significant.

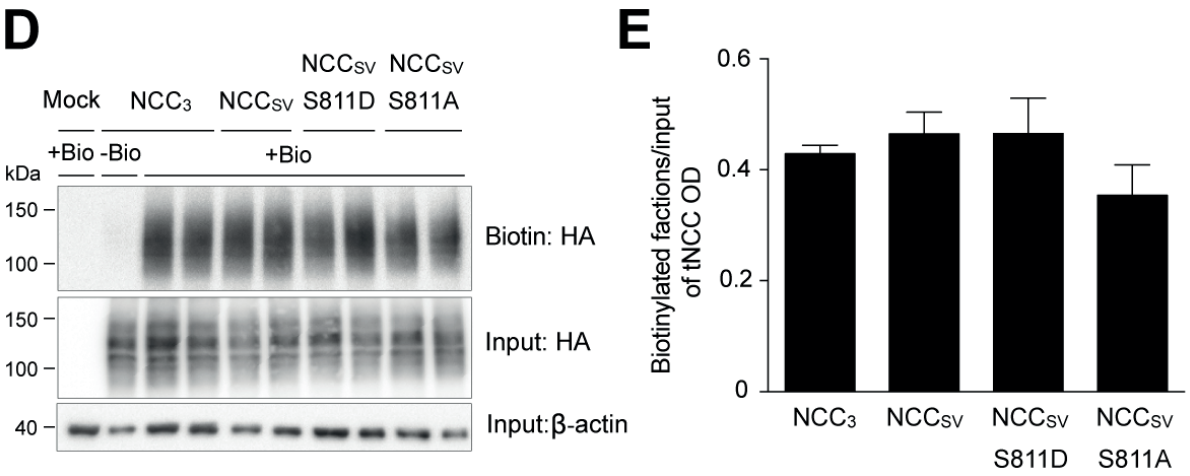

Figure 5 | Continued.

(**D**) Representative immunoblot of total lysate (input) and biotinylated fractions of HEK293 cells transfected with NCC_3, NCC_{SV} or the indicated mutants, probed with anti-HA and β-actin antibodies. β-actin was used as a sample loading control. (**E**) Densitometry analysis of cell surface biotinylation. The optical densities of the beads fractions were divided by corresponding optical densities of the input samples. *N*=3. Values are expressed as mean ± SEM. **P*<0.05 was considered statistically significant.

Discussion

This study shows that S811 acts as a dominant regulatory site for phosphorylation of T55 and T60 in NCC_{SV} as well as in NCC_3. Moreover, our findings demonstrate that the phosphorylation-deficient S811A mutant decreases the transport activity of both NCC_{SV} and NCC_3. The effect of S811 phosphorylation on NCC_3 activity likely occurs through the formation of heterodimers. Together, this provides strong evidence that S811, present only in NCC_{SV}, is a crucial new residue involved in NCC regulation.

Our findings demonstrate that S811 has a dominant-negative effect on T55 and T60 phosphorylation. Richardson *et al*. previously showed that mutation of T60 to alanine in NCC_3 markedly inhibits phosphorylation of neighboring residues, such as T55, induced by hypotonic low Cl^- treatment (48). Additionally, the T60A mutant strongly inhibited NCC activity, while this was less prominent for the T55A mutant (48). This implies that T60 can exert a dominant-negative role over other phosphorylation sites in NCC_3 (48). Several other studies have shown that T60 is a key phosphorylation site for NCC activity (43, 48, 69). This is highlighted by a loss of function mutation at T60 in NCC that is linked to Gitelman Syndrome (29, 69). Previously, it has also been shown that defective T60 phosphorylation corrects the phenotype of FHHt in mice (69). Our study adds a new important site solely present in NCC_{SV} at S811. Importantly, this site could have a regulatory role on NCC, as the S811A mutant prevented the T55 and T60 phosphorylation and inhibited the activity in both NCC_{SV} and NCC_3 (Fig. 6). The inhibitory effect of S811A on NCC function is in line with our

previous data showing that *Xenopus laevis* oocytes expressing NCC_{SV} S811A exhibited decreased $^{22}Na^{+}$-uptake compared to oocytes expressing wild-type NCC_{SV} (59). Furthermore, it was shown that WNK4 inhibits both NCC_3 and NCC_{SV} function independent of S811, since the NCC_{SV} S811D mutant was not protected from the inhibitory effects of WNK4 (59). While it is known that T55 and T60 are phosphorylated via activation of WNK-SPAK signaling pathway (1, 43), the kinase involved in S811 phosphorylation remains to be elucidated. Notably, prediction software suggested that the S811 phosphorylation site shows high similarity to a protein kinase A (PKA) consensus site. Therefore, hormones regulating the PKA pathway could potentially be involved in regulating NCC_{SV}-mediated Na^{+} transport in DCT. There is a growing body of evidence demonstrating that NCC abundance and phosphorylation is affected by protein kinase C or PKA downstream of angiotensin II or vasopressin signaling, respectively (11, 40, 46, 51).

It has previously been shown that NCC mRNA in the human kidney comprises 55% of NCC_3 and 45% of NCC_{SV} (59). To mimic the physiological distribution, a co-transfection experiment was performed with NCC_{SV} S811A and NCC_3, demonstrating significantly less phosphorylation at T55 and T60 compared to cells co-transfected with NCC_{SV} and NCC_3. We show that NCC_3 and NCC_{SV} can dimerize resulting in a mixture of hetero- and homo-dimers of the two variants. Interestingly, the observed decrease in phosphorylation levels was more than 50% for both T55 and T60, which suggests that NCC_{SV} S811A not only affected NCC_{SV} but also blocked T55 and T60 phosphorylation in NCC_3 (Fig. 6). Furthermore, cells co-expressing NCC_{SV} S811A and NCC_3 showed significantly impaired NCC activity, confirming the dominant-negative effect of NCC_{SV} S811 on NCC_3 function. The observations that NCC_{SV} is significantly expressed in the kidney (59) together with the fact that S811 can affect T55 and T60 phosphorylation and function in NCC_{SV} and NCC_3, implicates a potential key role of S811 in NCC-mediated renal salt handling.

Although the NCC_{SV} to NCC_3 mRNA ratio in the human kidney is 45% on average , this ratio of NCC_{SV} to NCC_3 expression varied from 19% to 63% in 7 human kidneys (59). This large difference in NCC_{SV} to NCC_3 ratio suggests that splicing of NCC is highly regulated in humans (33). In humans, it has been shown that ~95% of genes are alternatively spliced (44). The production of alternatively spliced mRNAs is diversely regulated by a variety of external stimuli or/and genetic make-up. Between human individuals, altered splicing can lead to differences in alternative spliced mRNAs that can consequently impact abundance or function of a protein (31, 47). Mechanisms of alternative splicing machinery are highly variable and not well understood (31). In several well-documented examples, such natural variation of alternative splicing has indeed been shown to contribute to the development of various diseases, such as cancer and diabetes (2, 24, 56, 58, 70). Moreover, altered splicing of genes are suggested to influence drug response (22). Therefore, unravelling the

mechanism behind the splicing ratio of NCC_{SV} to NCC_3 in the kidney might revise our understanding of salt transport and response to diuretics in the distal part of the nephron.

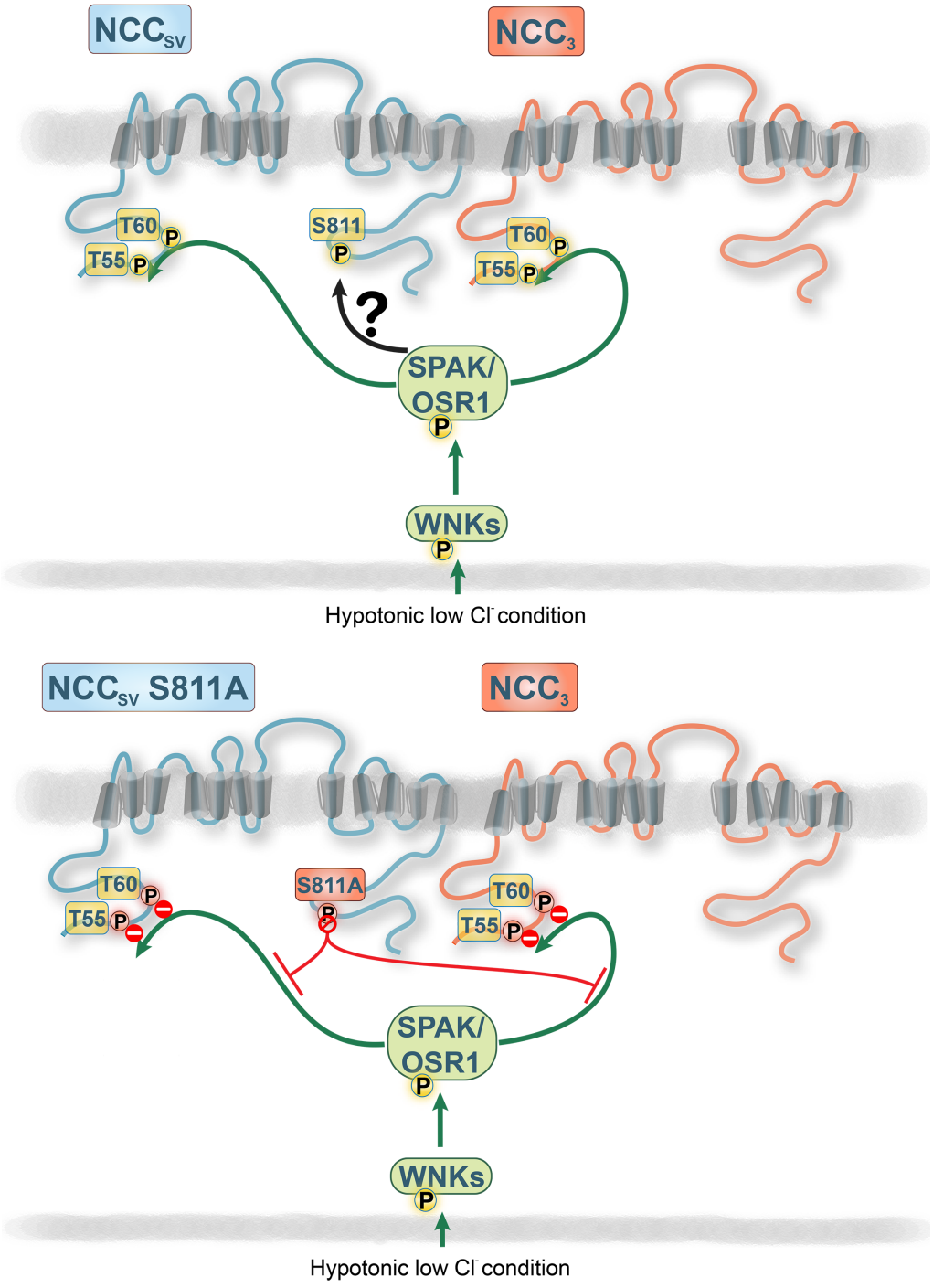

Figure 6 | Schematic model for NCC_{SV} S811 regulation.

The NCC_{SV} S811A mutant not only abolishes the hypotonic low Cl^--induced phosphorylation at T55 and T60 in NCC_{SV}, but also prevents the phosphorylation at T55 and T60 in NCC_3. With no lysine (WNK) kinases are auto-phosphorylated (activated) when the intracellular Cl^- concentration decreases. WNKs can phosphorylate and activate Ste20-related proline-alanine-rich kinase (SPAK) and oxidative stress response 1 (OSR1), which in turn phosphorylate threonine residues 55 and 60 (T55 and T60) in NCC (top panel). The dominant-negative effect of NCC_{SV} S811A on the phosphorylation of T55 and T60 in NCC_{SV} and NCC_3 may occur through the formation of heterodimers between NCC_{SV} and NCC_3 (bottom panel).

To explore the molecular mechanism by which NCC_{SV} S811 exerts a dominant-negative effect on NCC_3, FLIM and co-immunoprecipitation experiments were conducted. Here, we showed that both the constitutively phosphorylated and non-phosphorylated NCC_{SV} S811 mutants form heterodimers with NCC_3, indicating that the effect of S811 on phosphorylation of NCC_3 can occur through interaction between the two isoforms. The phosphorylation status of S811 did not affect the interaction between NCC_{SV} and NCC_3. Importantly, our findings show for the first time that NCC_{SV} and NCC_3 form hetero- and homo-dimers in living cells and that NCC_{SV} competes with NCC_3 on the functional level. Homodimerization of two NCC_3 has been proposed in previous studies using immunoblotting (15, 18, 49, 61), and it was also found that NCC is present at the plasma membrane in a dimerized form (15, 18). While it has been shown for other proteins that dimerization occurs at the surface of plasma membrane (30), our data now suggests that the dimerization of NCC already occurs in the cytosol as decreased lifetime of NCC_3 was observed in organellar membranes. Dimerization of transmembrane proteins is a common mechanism that precedes advanced functional regulation of a protein. For example, in the tyrosine kinase pathway, Erb2/Erb3 cross-phosphorylate each other after dimerization (32, 53). From its dimeric nature, NCC resembles NaKCl cotransporter (NKCC2) (18, 37), suggesting that other members of the family of electroneutral cation-chloride cotransporters form similar oligomeric structures. Interestingly, it has recently been shown that NCC can interact with the epithelial Na^+ channel (ENaC) (54). Moreover, inhibition of NCC also affected the function of ENaC, probably through direct interaction of both proteins (36). As NCC and ENaC are co-expressed along the later part of the DCT, it has been suggested that this interaction can regulate Na^+ reabsorption in the DCT (36, 67). The heterodimerization of NCC_{SV} with NCC_3 suggests that NCC_{SV} phosphorylation adds an additional regulatory mechanism by affecting the phosphorylation of the N-terminal T55 and T60 of NCC_3 via dimerization.

NCC abundance at the plasma membrane is a powerful mechanism to modulate Na^+ reabsorption in the kidney. In our study, cell surface biotinylation of NCC-transfected cells revealed that a change in S811 phosphorylation of NCC_{SV} does not affect the abundance of NCC_{SV} at the plasma membrane, where NCC is functionally active. Moreover, there is no change in plasma membrane abundance of NCC in any of the NCC isoforms or mutants when cells are exposed to hypotonic low Cl^- stress. Our findings indicate that, upon hypotonic low Cl^- stress, translocation of NCC to the plasma membrane is not affected. Rather, intrinsic T55 and T60 phosphorylation of NCC at the plasma membrane is increased. Our findings are in correspondence with previous studies demonstrating that NCC surface expression is not affected by the phosphorylation status of T60 or S811 in *Xenopus laevis* oocytes (43, 59). Similarly, the triple mutation of T55, T60 and serine 73 to alanine did not significantly change the NCC abundance at the plasma membrane (27).

Previously, the relation between the T60 phosphorylation and membrane stability of NCC has been suggested (69). Although, several studies demonstrated a decreased abundance of NCC_3 T60A in both the biotinylated fractions and input fraction, suggesting unaltered abundance at the plasma membrane (27, 69).

Taking together, our results show that S811 of NCC_{SV} plays a crucial role in NCC function, and could therefore be a key factor in renal salt handling. Further experiments are needed to find the kinases that regulate S811 phosphorylation, which can provide more insight in the influence of S811 on NCC activity and might be crucial in elucidating the pathogenesis of essential hypertension.

Acknowledgements

The authors thank Marco A. Valdez-Flores, Sjoerd Verkaart, Geert v.d. Bogaart, Danielle R.J. Verboogen for technical assistance and advice.

Grants

This study was financially supported by the Netherlands Organization for Scientific Research (VENI 863.13.010 and VICI 016.130.668) and the Dutch Kidney Foundation (PHD12.14 and 16OI04). The authors declare no conflicts of interest.

Disclosures

The authors declare that they have no conflicts of interest with the contents of this article.

Author contribution

O.A.T., F.B., R.J.M.B., J.G.J.H., and J.W. conceived and designed the research; O.A.T., F.B., D.A.S., and J.W. performed the research; O.A.T., F.B., and D.A.S. analyzed the data. O.A.T., F.B., D.A.S., and J.W. drafted the manuscript; all authors read and approved the final manuscript.

References

1. Alessi DR, Zhang J, Khanna A, Hochdörfer T, Shang Y, Kahle KT. The WNK-SPAK/OSR1 pathway: master regulator of cation-chloride cotransporters. *Science signaling* 7: re3–re3, 2014.
2. Allagnat F, Christulia F, Ortis F, Pirot P, Lortz S, Lenzen S, Eizirik DL, Cardozo AK. Sustained production of spliced X-box binding protein 1 (XBP1) induces pancreatic beta cell dysfunction and apoptosis. *Diabetologia* 53: 1120–1130, 2010.
3. Barber PR, Ameer-Beg SM, Gilbey J, Carlin LM, Keppler M, Ng TC, Vojnovic B. Multiphoton time-domain fluorescence lifetime imaging microscopy: practical application to protein–protein interactions using global analysis. *Journal of The Royal Society Interface* 6: S93–S105, 2009.
4. Barber PR, Ameer-Beg SM, Gilbey JD, Edens RJ. Global and pixel kinetic data analysis for FRET detection by multi-photon time-domain FLIM. *Proc SPIE*.
5. Bianchi G, Fox U, Di Francesco GF, Bardi U, Radice M. The hypertensive role of the kidney in spontaneously hypertensive rats. *Clin Sci Mol Med Suppl* 45 Suppl 1: 135s–9, 1973.
6. Bloch MJ. Worldwide prevalence of hypertension exceeds 1.3 billion. *J Am Soc Hypertens* 10: 753–754, 2016.
7. Boudoulas KD, Triposkiadis F, Parissis J, Butler J, Boudoulas H. The Cardio-Renal Interrelationship. *Prog Cardiovasc Dis* 59: 636–648, 2016.
8. Boyden LM, Choi M, Choate KA, Nelson-Williams CJ, Farhi A, Toka HR, Tikhonova IR, Bjornson R, Mane SM, Colussi G, Lebel M, Gordon RD, Semmekrot BA, Poujol A, Välimäki MJ, De Ferrari ME, Sanjad SA, Gutkin M, Karet FE, Tucci JR, Stockigt JR, Keppler-Noreuil KM, Porter CC, Anand SK, Whiteford ML, Davis ID, Dewar SB, Bettinelli A, Fadrowski JJ, Belsha CW, Hunley TE, Nelson RD, Trachtman H, Cole TRP, Pinsk M, Bockenhauer D, Shenoy M, Vaidyanathan P, Foreman JW, Rasoulpour M, Thameem F, Al-Shahrouri HZ, Radhakrishnan J, Gharavi AG, Goilav B, Lifton RP. Mutations in kelch-like 3 and cullin 3 cause hypertension and electrolyte abnormalities. *Nature* 482: 98–102, 2012.
9. Cameron AC, Lang NN, Touyz RM. Drug Treatment of Hypertension: Focus on Vascular Health. *Drugs* 76: 1529–1550, 2016.
10. Carretero OA, Oparil S. Essential hypertension. Part I: definition and etiology. *Circulation* 101: 329–335, 2000.
11. Castañeda-Bueno M, Arroyo JP, Zhang J, Puthumana J, Yarborough O III, Shibata S, Rojas-Vega L, Gamba G, Rinehart J, Lifton RP. Phosphorylation by PKC and PKA regulate the kinase activity and downstream signaling of WNK4. *Proc Natl Acad Sci* 114: E879–E886, 2017.
12. Coffman TM, Crowley SD. Kidney in hypertension: guyton redux. *Hypertension* 51: 811–816, 2008.
13. Dahl LK, Heine M. Primary role of renal homografts in setting chronic blood pressure levels in rats. *Circ Res* 36: 692–696, 1975.
14. de Groot T, Lee K, Langeslag M, Xi Q, Jalink K, Bindels RJM, Hoenderop JGJ. Parathyroid Hormone Activates TRPV5 via PKA-Dependent Phosphorylation. *J Am Soc Nephrol* 20: 1693–1704, 2009.
15. de Jong JC, Willems PHGM, Mooren FJM, van den Heuvel LPWJ, Knoers NVAM, Bindels RJM. The structural unit of the thiazide-sensitive NaCl cotransporter is a homodimer. *J Biol Chem* 278: 24302–24307, 2003.
16. Dimke H, San-Cristobal P, de Graaf M, Lenders JW, Deinum J, Hoenderop JGJ, Bindels RJM. γ-Adducin stimulates the thiazide-sensitive NaCl cotransporter. *J Am Soc Nephrol* 22: 508–517, 2011.
17. Ellison DH, Velazquez H, Wright FS. Thiazide-sensitive sodium chloride cotransport in early distal tubule. *Am J Physiol* 253: F546–54, 1987.
18. Frindt G, Palmer LG. Surface expression of sodium channels and transporters in rat kidney: effects of dietary sodium. *Am J Physiol Renal Physiol* 297: F1249–55, 2009.
19. Go AS, Mozaffarian D, Roger VL, Benjamin EJ, Berry JD, Blaha MJ, Dai S, Ford ES, Fox CS, Franco S, Fullerton HJ, Gillespie C, Hailpern SM, Heit JA, Howard VJ, Huffman MD, Judd SE, Kissela BM, Kittner SJ, Lackland DT, Lichtman JH, Lisabeth LD, Mackey RH, Magid DJ, Marcus GM, Marelli A, Matchar DB, McGuire DK, Mohler ER, Moy CS, Mussolino ME, Neumar

RW, Nichol G, Pandey DK, Paynter NP, Reeves MJ, Sorlie PD, Stein J, Towfighi A, Turan TN, Virani SS, Wong ND, Woo D, Turner MB, American Heart Association Statistics Committee and Stroke Statistics Subcommittee. Heart disease and stroke statistics-2014 update: a report from the American Heart Association. *Circulation* 129: e28–e292, 2014.

20. Gonzales PA, Pisitkun T, Hoffert JD, Tchapyjnikov D, Star RA, Kleta R, Wang NS, Knepper MA. Large-scale proteomics and phosphoproteomics of urinary exosomes. *J Am Soc Nephrol* 20: 363–379, 2009.
21. Goytain A, Quamme GA. Functional characterization of human SLC41A1, a Mg2+ transporter with similarity to prokaryotic MgtE Mg2+ transporters. *Physiol Genomics* 21: 337–342, 2005.
22. Heinzen EL, Yoon W, Tate SK, Sen A, Wood NW, Sisodiya SM, Goldstein DB. Nova2 interacts with a cis-acting polymorphism to influence the proportions of drug-responsive splice variants of SCN1A. *Am J Hum Genet* 80: 876–883, 2007.
23. HJ G, JB G, LG W. A new familial disorder characterized by hypokalemia and hypomagnesemia. *Trans Assoc Am Physicians* 79: 221–235, 1965.
24. Hull J, Campino S, Rowlands K, Chan M-S, Copley RR, Taylor MS, Rockett K, Elvidge G, Keating B, Knight J, Kwiatkowski D. Identification of common genetic variation that modulates alternative splicing. *PLoS Genet* 3: e99, 2007.
25. Hurd TW, Otto EA, Mishima E, Gee HY, Inoue H, Inazu M, Yamada H, Halbritter J, Seki G, Konishi M, Zhou W, Yamane T, Murakami S, Caridi G, Ghiggeri G, Abe T, Hildebrandt F. Mutation of the Mg2+ transporter SLC41A1 results in a nephronophthisis-like phenotype. *Journal of the American Society of Nephrology* 24: 967–977, 2013.
26. Jares-Erijman EA, Jovin TM. FRET imaging. *Nat Biotechnol* 21: 1387–1395, 2003.
27. Khan MZH, Sohara E, Ohta A, Chiga M, Inoue Y, Isobe K, Wakabayashi M, Oi K, Rai T, Sasaki S, Uchida S. Phosphorylation of Na-Cl cotransporter by OSR1 and SPAK kinases regulates its ubiquitination. *Biochem Biophys Res Commun* 425: 456–461, 2012.
28. Lalioti MD, Zhang J, Volkman HM, Kahle KT, Hoffmann KE, Toka HR, Nelson-Williams C, Ellison DH, Flavell R, Booth CJ, Lu Y, Geller DS, Lifton RP. Wnk4 controls blood pressure and potassium homeostasis via regulation of mass and activity of the distal convoluted tubule. *Nat Genet* 38: 1124–1132, 2006.
29. Lin S-H, Shiang J-C, Huang C-C, Yang S-S, Hsu Y-J, Cheng C-J. Phenotype and genotype analysis in Chinese patients with Gitelman's syndrome. *J Clin Endocrinol Metab* 90: 2500–2507, 2005.
30. Lin W-C, Iversen L, Tu H-L, Rhodes C, Christensen SM, Iwig JS, Hansen SD, Huang WYC, Groves JT. H-Ras forms dimers on membrane surfaces via a protein-protein interface. *Proc Natl Acad Sci* 111: 2996–3001, 2014.
31. Lu Z-X, Jiang P, Xing Y. Genetic variation of pre-mRNA alternative splicing in human populations. *Wiley Interdiscip Rev RNA* 3: 581–592, 2012.
32. Maruyama IN. Mechanisms of activation of receptor tyrosine kinases: monomers or dimers. *Cells* 3: 304–330, 2014.
33. Mastroianni N, Bettinelli A, Bianchetti M, Colussi G, De Fusco M, Sereni F, Ballabio A, Casari G. Novel molecular variants of the Na-Cl cotransporter gene are responsible for Gitelman syndrome. *Am J Hum Genet* 59: 1019–1026, 1996.
34. Messerli FH, Williams B, Ritz E. Essential hypertension. *The Lancet* 370: 591–603, 2007.
35. Mills KT, Bundy JD, Kelly TN, Reed JE, Kearney PM, Reynolds K, Chen J, He J. Global Disparities of Hypertension Prevalence and Control: A Systematic Analysis of Population-Based Studies From 90 Countries. *Circulation* 134: 441–450, 2016.
36. Mistry AC, Wynne BM, Yu L, Tomilin V, Yue Q, Zhou Y, Al-Khalili O, Mallick R, Cai H, Alli AA, Ko B, Mattheyses A, Bao H-F, Pochynyuk O, Theilig F, Eaton DC, Hoover RS. The sodium chloride cotransporter (NCC) and epithelial sodium channel (ENaC) associate. *Biochem J* 473: 3237–3252, 2016.
37. Moore-Hoon ML, Turner RJ. The structural unit of the secretory Na+-K+-2Cl- cotransporter (NKCC1) is a homodimer. *Biochemistry* 39: 3718–3724, 2000.
38. Mullins LJ, Bailey MA, Mullins JJ. Hypertension, kidney, and transgenics: a fresh perspective. *Physiological Reviews* 86: 709–746, 2006.
39. Murray CJL, Lopez AD. Measuring the Global Burden of Disease. *N Engl J Med* 369: 448–457, 2013.
40. Mutig K, Saritas T, Uchida S, Kahl T, Borowski T, Paliege A, Bohlick A, Bleich M, Shan Q,

Bachmann S. Short-term stimulation of the thiazide-sensitive Na+-Cl- cotransporter by vasopressin involves phosphorylation and membrane translocation. *Am J Physiol Renal Physiol* 298: F502–9, 2010.

41. Narayan KMV, Ali MK, Koplan JP. Global noncommunicable diseases – where worlds meet. *N Engl J Med* 363: 1196–1198, 2010.
42. Nørholm MHH. A mutant Pfu DNA polymerase designed for advanced uracil-excision DNA engineering. *BMC Biotechnol* 10: 21, 2010.
43. Pacheco-Alvarez D, Cristobal PS, Meade P, Moreno E, Vazquez N, Munoz E, Diaz A, Juarez ME, Gimenez I, Gamba G. The Na+:Cl- cotransporter is activated and phosphorylated at the amino-terminal domain upon intracellular chloride depletion. *J Biol Chem* 281: 28755–28763, 2006.
44. Pan Q, Shai O, Lee LJ, Frey BJ, Blencowe BJ. Deep surveying of alternative splicing complexity in the human transcriptome by high-throughput sequencing. *Nat Genet* 40: 1413–1415, 2008.
45. Pathare G, Tutakhel OAZ, V D Wel MC, Shelton LM, Deinum J, Lenders JW, Hoenderop JGJ, Bindels RJM. Hydrochlorothiazide treatment increases the abundance of the NaCl cotransporter in urinary extracellular vesicles of essential hypertensive patients. *Am J Physiol Renal Physiol* 312: F1063–F1072, 2017.
46. Pedersen NB, Hofmeister MV, Rosenbaek LL, Nielsen J, Fenton RA. Vasopressin induces phosphorylation of the thiazide-sensitive sodium chloride cotransporter in the distal convoluted tubule. *Kidney Int* 78: 160–169, 2010.
47. Pickrell JK, Marioni JC, Pai AA, Degner JF, Engelhardt BE, Nkadori E, Veyrieras J-B, Stephens M, Gilad Y, Pritchard JK. Understanding mechanisms underlying human gene expression variation with RNA sequencing. *Nature* 464: 768–772, 2010.
48. Richardson C, Richardson C, Rafiqi FH, Rafiqi FH, Karlsson HKR, Karlsson HKR, Moleleki N, Moleleki N, Vandewalle A, Vandewalle A, Campbell DG, Campbell DG, Morrice NA, Morrice NA, Alessi DR, Alessi DR. Activation of the thiazide-sensitive Na+-Cl- cotransporter by the WNK-regulated kinases SPAK and OSR1. *J Cell Sci* 121: 675–684, 2008.
49. Rieg T, Tang T, Uchida S, Hammond HK, Fenton RA, Vallon V. Adenylyl Cyclase 6 Enhances NKCC2 Expressionand Mediates Vasopressin-Induced Phosphorylation of NKCC2 and NCC. *The American Journal of Pathology* 182: 96–106, 2013.
50. Rozansky DJ, Cornwall T, Subramanya AR, Rogers S, Yang Y-F, David LL, Zhu X, Yang C-L, Ellison DH. Aldosterone mediates activation of the thiazide-sensitive Na-Cl cotransporter through an SGK1 and WNK4 signaling pathway. *J Clin Invest* 119: 2601–2612, 2009.
51. Saritas T, Borschewski A, McCormick JA, Paliege A, Dathe C, Uchida S, Terker A, Himmerkus N, Bleich M, Demaretz S, Laghmani K, Delpire E, Ellison DH, Bachmann S, Mutig K. SPAK differentially mediates vasopressin effects on sodium cotransporters. *Journal of the American Society of Nephrology* 24: 407–418, 2013.
52. Schindelin J, Arganda-Carreras I, Frise E, Kaynig V, Longair M, Pietzsch T, Preibisch S, Rueden C, Saalfeld S, Schmid B, Tinevez J-Y, White DJ, Hartenstein V, Eliceiri K, Tomancak P, Cardona A. Fiji: an open-source platform for biological-image analysis. *Nat Methods* 9: 676–682, 2012.
53. Schlessinger J. Common and distinct elements in cellular signaling via EGF and FGF receptors. *Science* 306: 1506–1507, 2004.
54. Schmitt R, Ellison DH, Farman N, Rossier BC, Reilly RF, Reeves WB, Oberbäumer I, Tapp R, Bachmann S. Developmental expression of sodium entry pathways in rat nephron. *Am J Physiol* 276: F367–81, 1999.
55. Simon DB, Nelson-Williams C, Johnson Bia M, Ellison D, Karet FE, Molina AM, Vaara I, Iwata F, Cushner HM, Koolen M, Gainza FJ, Gitelman HJ, Lifton RP. Gitelman"s variant of Barter"s syndrome, inherited hypokalaemic alkalosis, is caused by mutations in the thiazide-sensitive Na–Cl cotransporter. *Nat Genet* 12: 24–30, 1996.
56. Skotheim RI, Nees M. Alternative splicing in cancer: noise, functional, or systematic? *Int J Biochem Cell Biol* 39: 1432–1449, 2007.
57. Subramanya AR, Liu J, Ellison DH, Wade JB, Welling PA. WNK4 diverts the thiazide-sensitive NaCl cotransporter to the lysosome and stimulates AP-3 interaction. *J Biol Chem* 284: 18471–18480, 2009.
58. Sveen A, Kilpinen S, Ruusulehto A, Lothe RA, Skotheim RI. Aberrant RNA splicing in cancer;

expression changes and driver mutations of splicing factor genes. *Oncogene* 35: 2413–2427, 2016.

59. Tutakhel OAZ, Jeleń S, Valdez-Flores M, Dimke H, Piersma SR, Jimenez CR, Deinum J, Lenders JW, Hoenderop JGJ, Bindels RJM. Alternative splice variant of the thiazide-sensitive NaCl cotransporter: a novel player in renal salt handling. *Am J Physiol Renal Physiol* 310: F204–F216, 2016.
60. Urbanová M, Reiterová J, Stěkrová J, Lněnička P, Ryšavá R. DNA analysis of renal electrolyte transporter genes among patients suffering from Bartter and Gitelman syndromes: summary of mutation screening. *Folia Biol (Praha)* 57: 65–73, 2011.
61. Valdez-Flores MA, Vargas-Poussou R, Verkaart S, Tutakhel OAZ, Valdez-Ortiz A, Blanchard A, Treard C, Hoenderop JGJ, Bindels RJM, Jeleń S. Functionomics of NCC mutations in Gitelman syndrome using a novel mammalian cell-based activity assay. *Am J Physiol Renal Physiol* 311: F1159–F1167, 2016.
62. Vargas-Poussou R, Dahan K, Kahila D, Venisse A, Riveira-Munoz E, Debaix H, Grisart B, Bridoux F, Unwin R, Moulin B, Haymann J-P, Vantyghem M-C, Rigothier C, Dussol B, Godin M, Nivet H, Dubourg L, Tack I, Gimenez-Roqueplo A-P, Houillier P, Blanchard A, Devuyst O, Jeunemaitre X. Spectrum of mutations in Gitelman syndrome. *Journal of the American Society of Nephrology* 22: 693–703, 2011.
63. Verboogen DRJ, González Mancha N, Beest Ter M, van den Bogaart G. Fluorescence Lifetime Imaging Microscopy reveals rerouting of SNARE trafficking driving dendritic cell activation. *Elife* 6: 3289, 2017.
64. Vijftigschild LAW, van der Ent CK, Beekman JM. A novel fluorescent sensor for measurement of CFTR function by flow cytometry. *Cytometry A* 83: 576–584, 2013.
65. Wallrabe H, Periasamy A. Imaging protein molecules using FRET and FLIM microscopy. *Curr Opin Biotechnol* 16: 19–27, 2005.
66. Wilson FH, Disse-Nicodème S, Choate KA, Ishikawa K, Nelson-Williams C, Desitter I, Gunel M, Milford DV, Lipkin GW, Achard J-M, Feely MP, Dussol B, Berland Y, Unwin RJ, Mayan H, Simon DB, Farfel Z, Jeunemaitre X, Lifton RP. Human hypertension caused by mutations in WNK kinases. *Science* 293: 1107–1112, 2001.
67. Wynne BM, Mistry AC, Al-Khalili O, Mallick R, Theilig F, Eaton DC, Hoover RS. Aldosterone Modulates the Association between NCC and ENaC. *Sci Rep* 7: 4149, 2017.
68. Yang C-L, Zhu X, Ellison DH. The thiazide-sensitive Na-Cl cotransporter is regulated by a WNK kinase signaling complex. *J Clin Invest* 117: 3403–3411, 2007.
69. Yang S-S, Fang Y-W, Tseng M-H, Chu P-Y, Yu I-S, Wu H-C, Lin S-W, Chau T, Uchida S, Sasaki S, Lin Y-F, Sytwu H-K, Lin S-H. Phosphorylation Regulates NCC Stability and Transporter Activity In Vivo. *J Am Soc Nephrol* 24: 1587–1597, 2013.
70. Zhang W, Duan S, Bleibel WK, Wisel SA, Huang RS, Wu X, He L, Clark TA, Chen TX, Schweitzer AC, Blume JE, Dolan ME, Cox NJ. Identification of common genetic variants that account for transcript isoform variation between human populations. *Hum Genet* 125: 81–93, 2009.
71. Zhou B, Zhuang J, Gu D, Wang H, Cebotaru L, Guggino WB, Cai H. WNK4 enhances the degradation of NCC through a sortilin-mediated lysosomal pathway. *J Am Soc Nephrol* 21: 82–92, 2010.

5

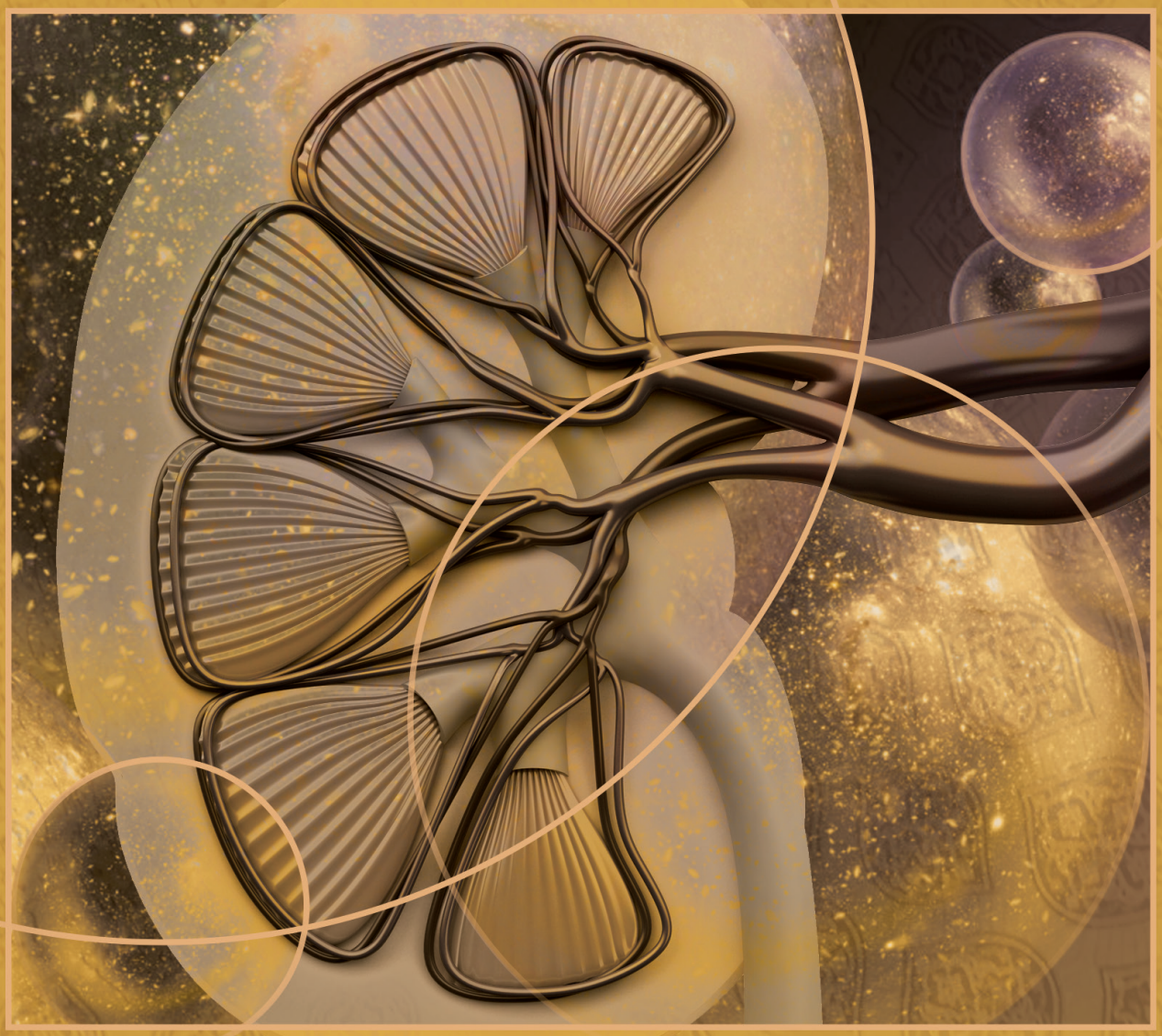

Calcineurin inhibitors increase the NaCl cotransporter in urinary vesicles and predicts thiazide sensitivity

Omar A.Z. Tutakhel[1*], Arthur D. Moes[3*], Marco A. Valdez-Flores[1,5], Marleen L. A. Kortenoeven[4], Mathijs v. d. Vrie[2], Sabina Jele[1], Robert A. Fenton[4], Robert Zietse[3], Joost G.J. Hoenderop[1], Ewout J. Hoorn[3], Luuk Hilbrands[2], and René J.M. Bindels[1]

[1]Department of Physiology, Radboud Institute for Molecular Life Sciences, Radboud university medical center, Nijmegen, The Netherlands; [2]Department of Nephrology, Radboud Institute for Molecular Life Sciences, Radboud university medical center, Nijmegen, The Netherlands; [3]Department of Internal Medicine, Nephrology and Transplantation, Erasmus Medical Center, Rotterdam, The Netherlands; [4]Department of Biomedicine, Center for Interaction of Proteins in Epithelial Transport, Aarhus University, Aarhus, Denmark; [5]Programa Regional en Doctorado en Biotecnología, Universidad Autónoma de Sinaloa, Sinaloa, Mexico.

* Authors contributed equally

PLOS ONE, 12: e0176220, 2017

Abstract

Animal studies have shown that the calcineurin inhibitors (CNIs) cyclosporine and tacrolimus can activate the thiazide-sensitive NaCl cotransporter (NCC). A common side effect of CNIs is hypertension. Renal salt transporters such as NCC are excreted in urinary extracellular vesicles (uEVs) after internalization into multivesicular bodies. Human studies indicate that CNIs also increase NCC abundance in uEVs, but results are conflicting and no relationship with NCC function has been shown. Therefore, we investigated the effects of CsA and Tac on the abundance of both total NCC (tNCC) and phosphorylated NCC at Thr60 phosphorylation site (pNCC) in uEVs, and assessed whether NCC abundance in uEVs predicts the blood pressure response to thiazide diuretics. Our results show that in kidney transplant recipients treated with cyclosporine (n=9) or tacrolimus (n=23), the abundance of both tNCC and pNCC in uEVs is 4-5 fold higher than in CNI-free kidney transplant recipients (n=13) or healthy volunteers (n=6). In hypertensive kidney transplant recipients, higher abundances of tNCC and pNCC prior to treatment with thiazides predicted the blood pressure response to thiazides. During thiazide treatment, the abundance of pNCC in uEVs increased in responders (n=10), but markedly decreased in non-responders (n=8). Thus, our results show that CNIs increase the abundance of both tNCC and pNCC in uEVs, and these increases correlate with the blood pressure response to thiazides. This implies that assessment of NCC in uEVs could represent an alternate method to guide anti-hypertensive therapy in kidney transplant recipients.

Keywords: Hypertension / Calcineurin inhibitors / NaCl cotransporter / Thiazide diuretics / Urinary extracellular vesicles

Introduction

The calcineurin inhibitors (CNIs) cyclosporine A (CsA) and tacrolimus (Tac) are widely used to prevent rejection of transplanted organs. CNIs inhibit the calcineurin-mediated immune response in T-cells (13). Although both CsA and Tac exert their principal immunosuppressive effects through inhibition of the same target protein, calcineurin, they differ in cytoplasmic-binding proteins, namely cyclophilins and FKBP12 for CsA and Tac, respectively. CsA and Tac also vary with respect to their immunosuppressive potency (40, 58) and side effects (14, 25, 29). A common side effect of CNIs is hypertension, although CsA appears more hypertensinogenic than Tac (4, 5, 29). CNI-induced hypertension may be accompanied by hyperkalemia and metabolic acidosis (17, 21). The clinical characteristics of CNI-treated patients sometimes resemble that of familial hyperkalemic hypertension (FHHt) (2, 37), also known as Gordon syndrome (12) or pseudohypoaldosteronism type II (50) (OMIM 145260). FHHt results from mutations in WNK [with no lysine (K)] kinases WNK1 and WNK4 (59), KLHL3 (26), or Cullin3 (3), which all lead to a gain-of-function in the thiazide-sensitive NaCl cotransporter (NCC) resulting in salt retention in the distal part of the nephron (23, 47, 59, 61). Several studies have shown that CNIs increase NCC activity possibly contributing to hypertension (16, 24). Melnikov *et al*. demonstrated that rats treated with CsA develop a phenotype similar to that of FHHt, which they attributed to an increase in WNK4 abundance in the kidney (31). This phenomenon is supported by *in vitro* studies showing that the abundance of WNK4 and ultimately of total NCC (tNCC) and phosphorylated, or active, NCC (pNCC), is increased in immortalized mouse distal convoluted tubule (mDCT) cells treated with CsA (31). Hoorn *et al*. revealed that Tac-induced hypertension in mice is predominantly mediated by an increase in pNCC abundance, possibly through an effect of the NCC-regulating kinases WNK3, WNK4, and STE20/SPS1-related proline/alanine-rich kinase (SPAK) (16). Recent evidence suggests that in mice, Tac prevents the high potassium stimulated NCC dephosphorylation (53). Additionally, it has been demonstrated that Tac acts directly on kidney tubule cells expressing NCC to cause hypertension, and that inhibition of calcineurin is required for this effect (24).

In humans, urinary extracellular vesicles (uEVs), including exosomes, have been extensively characterized and studied as non-invasive biomarkers for renal tubular disorders (7, 11, 15, 49). uEVs are nanosized membranous vesicles released from all cells lining the nephron. Alterations in the expression of different proteins present in the epithelial cells of the distal convoluted tubule (DCT), including NCC, are reflected in the composition of uEVs (18, 55, 56). Patients with FHHt have an increased NCC abundance in uEVs (18, 30, 56), while patients with Gitelman syndrome exhibit a decreased NCC abundance in uEVs (7, 20). In humans, mineralocorticoid administration rapidly increased the abundance of tNCC and

pNCC in uEVs, possibly via the WNK pathway (60). This suggests that NCC abundance in uEVs reflects the actual state of NCC expression in the epithelial cells of the DCT. Accordingly, we previously showed that in patients with primary aldosteronism, pNCC increased similarly in kidney and uEVs (56).

Although protein abundance and characterization in uEVs can potentially be used as biomarkers for some diseases (7, 18, 20, 30, 56), only a few studies have been conducted to investigate the role of NCC in CNI-induced hypertension in humans. Esteva-Font *et al.* found a positive correlation between plasma CsA levels and NCC abundance in uEVs of CsA-treated kidney transplant recipients (9). Rojas-Vega *et al*. showed an increased abundance of NCC in uEVs of Tac-treated hypertensive kidney transplant recipients (45). Although these studies showed the stimulatory effect of CNIs on NCC abundance in uEVs of kidney transplant recipients, they did not explore the relationship between NCC abundance and blood pressure in kidney transplant recipients. Therefore, in the present study, we performed a large-scale study to investigate the effect of CsA and Tac on the abundance of both tNCC and pNCC in uEVs, and assessed whether NCC abundance in uEVs predicts the blood pressure response to thiazide diuretics. Finally, in order to confirm the effect of CNIs on NCC in the kidney, an *ex vivo* study was conducted in mice cortical tubules exposed to CsA.

Materials and Methods

Study Design and Population

Two groups of kidney transplant recipients using CNIs were studied. Group 1 was recruited at the Radboud university medical center, in Nijmegen, The Netherlands, and consisted of a randomly selected cohort of 45 kidney transplant recipients and 6 healthy volunteers of whom uEVs were isolated and analyzed. The kidney transplant recipients used CsA (n=9), Tac (n=23) or a CNI-free immunosuppressive regimen (n=13) for at least 6 months and were matched for age and gender. Kidney transplant recipients who had been using thiazide diuretics or aldosterone antagonists after transplantation were excluded. Group 2 consisted of Tac-treated hypertensive kidney transplant recipients (median of 2.4 years after kidney transplantation), recruited from a clinical trial studying the anti-hypertensive effect of thiazide-type diuretic chlorthalidone at the Erasmus Medical Center, in Rotterdam, The Netherlands (32). Patients with an office blood pressure >140/90 mmHg were invited for ambulatory blood pressure measurement. In this group, 18 patients with an average daytime systolic blood pressure >140 mmHg were enrolled and followed for 8 weeks chlorthalidone (12-25 mg once daily) treatment. Patients who responded to chlorthalidone (‘responders’, decrease of ≥10 mmHg in average daytime systolic blood pressure, n=10) were compared with patients who did not respond to chlorthalidone (‘non-responders’, no change or an

increase in average daytime systolic blood pressure, n=8). All participants gave written informed consent and both cohorts were approved by Medical Ethics Committee (CMO09/073 for Radboud university medical center and MEC-2012-417 for Erasmus Medical Center) and this study was conducted according to the principles expressed in the Declaration of Helsinki.

Urine collection and isolation of extracellular vesicles

In Group 1, second-morning mid-stream urine sample was collected. In Group 2, second-morning mid-stream urine was collected just before starting and after 8 weeks of chlorthalidone treatment. In both groups, immediately after urine collection, the protease inhibitors (50 µmol/L phenylmethylsulfonyl fluoride, 20 µmol/L aprotinin, 10 µmol/L pepstatin A, and 20 µmol/L leupeptin) were added to the urine to reduce protein degradation. All samples were directly stored at -80°C. uEVs were isolated as reported previously (41, 55, 56). In brief, 10 to 40 mL of the collected urine samples were centrifuged at 17,000 × g for 15 minutes at 24°C in an ultracentrifuge (Sorvall™ WX Floor Ultra Centrifuges, Thermo Scientific, Asheville, NC, USA) with a 70.1Ti rotor. The supernatant was stored at room temperature for 25 minutes. The pellet was resuspended in 50 µL of 3.24 mol/L dithiothreitol and 200 µL isolation solution (10 mmol/L triethanolamine, 250 mmol/L sucrose, HCl pH 7.6) and centrifuged at 17,000 × g for 15 minutes at 24°C. Next, the supernatant was collected and combined with the supernatant obtained from the previous centrifugation, and the combined supernatants were centrifuged at 170,000 × g for 2.5 hours at 24°C. Pellets containing uEVs were solubilized in Laemmli sample buffer (0.6% w/v SDS, 3% v/v glycerol, 18 mmol/L Tris-HCl pH 6.8 and 0.003% w/v bromophenol blue). All the samples were preheated for 15 minutes at 65°C before immunoblotting. Urinary creatinine was measured according to Jaffe's method with the use of a colorimetric assay (Labor und Technik, Berlin, Germany).

Mouse cortical tubule suspension

Animal protocols were approved by the board of the Institute of Biomedicine, University of Aarhus. The animal protocols comply with the European Community guidelines for the use of experimental animals, were approved and performed under a license issued for the use of experimental animals by the Danish Ministry of Justice (Dyreforsøgstilsynet). For this study mice were anesthetized using isoflurane inhalation, followed by cervical dislocation. Both kidneys from a male wildtype C57BL/6J mouse were removed and dissected into approximately 1 mm pieces and placed into 4 mL of enzyme solution containing 1.5 mg/mL collagenase type B (Worthington Labs, Lakewood, NJ, USA) in basic buffer (125 mmol/L NaCl, 30 mmol/L glucose, 0.4 mmol/L KH_2PO_4, 1.6 mmol/L K_2HPO_4, 1 mmol/L $MgSO_4$, 10

mmol/L Na-acetate, 1 mmol/L α-ketoglutarate, 1.3 mmol/L Ca-gluconate, 5 mmol/L glycine, 48 µg/mL trypsin inhibitor, and 50 µg/mL DNase, Tris-HCl pH 7.4). Samples were mixed continuously at 37°C using a benchtop orbital mixer. Samples were incubated for 15 minutes at 22°C to let the large fragments sink down to the bottom of the tube. Next, 2 mL of the enzyme solution was removed and replaced with 2 mL of basic buffer. After 10 minutes' incubation at 4°C, an additional 2 mL of basic buffer was added, and samples were incubated for an additional 10 minutes at 22°C. Large fragments were allowed to settle, the supernatant was removed and centrifuged at 200 × g for 2 minutes. The pellet was resuspended in 5 mL of basic buffer (buffer B) (120 mmol/L NaCl, 30 mmol/L glucose, 1 mmol/L $CaCl_2$, 1 mmol/L $MgCl_2$, 1 mmol/L Na_2HPO_4, 1 mmol/L Na_2SO_4, 15 mmol/L Na-HEPES, Tris-HCl pH 7.4) and centrifuged at 200 × g for 2 minutes. The tubular suspensions were resuspended in buffer B and 500 µL was transferred into individual tubes containing either DMSO (negative control) or different concentrations of CsA (final concentrations of 5, 10, or 20 µmol/L). Hypotonic low chloride (buffer H), which stimulates NCC (36, 44), was used as a positive control. Suspensions were incubated with continuous mixing for 30 and 90 minutes at 37°C. Tubules were centrifuged for 10 minutes at 3,000 × g at 4°C and pellets were resuspended in 300 µL Laemmli sample buffer containing dithiothreitol (50 mg/mL). Finally, the samples were heated for 15 minutes at 60°C before immunoblotting.

Immunoblotting

uEV-samples were loaded on a gradient SDS-PAGE gel (4-15% v/v Criterion™ TGX™ Precast Gel, Bio-Rad, The Netherlands). The volume of uEV-suspension per lane was adjusted according to the urinary creatinine concentration to account for concentration differences between the uEV-samples (49). Loading was not dependent on the fraction of the total protein in uEV-samples. The volume of uEV-suspension was lowest in the sample with the lowest urinary creatinine concentration, and the samples with a higher urinary creatinine concentration were diluted according to the ratio compared to that of the lowest urinary creatinine concentration. Subsequently, immunoblotting was performed on polyvinylidene difluoride membranes (Immobilon-P, Millipore Corporation, Bedford, MA, USA), which were blocked and probed with antigen-specific primary antibodies. Blots were incubated with species-specific fluorescent secondary antibodies and visualized using enhanced chemiluminescence (Thermo Fischer Scientific, Waltham, MA, USA) and gel imaging system (ChemiDoc XRS, Bio-Rad Laboratories, Hercules, CA, USA). Finally, both the dimeric and monomeric forms of the NCC bands on the blots were quantified together with Image Studio Lite software (LI-COR Biosciences, NE, USA) or ImageQuant TL (GE Healthcare Life Sciences, PA, USA). To analyze whether normalization by urinary creatinine

resulted in a similar number of uEVs loaded on a gel, the abundance of the uEV-marker CD9 was measured (1, 49, 55).

Antibodies

The following antibodies were used: anti-total NCC (Millipore, Billerica, MA, USA, #AB3553; 1:2,000); anti-human phosphorylated NCC at Thr60 or (anti-mouse phosphorylated NCC at Thr58; 1:2,000) as previously described (38) and anti-uEV marker CD9 of human origin (C4, Santa Cruz Biotechnology, Inc., CA, USA; 1:500). Secondary antibodies used were peroxidase-conjugated goat anti-rabbit (Sigma-Aldrich, St. Louis, MO, USA; 1:10,000), and anti-mouse (Sigma-Aldrich, St. Louis, MO, USA; 1:10,000).

Statistical analysis

Values are expressed as mean ± SEM. In Group 1 the immunoblot data were analyzed by comparing integrated optical densities of bands by one-way ANOVA with Dunnett multiple comparisons *post hoc* test. In Group 2 the immunoblot data were analyzed using a non-parametric Student's *t*-test (comparing responders to non-responders). Two-way ANOVA was used to assess changes in uEV protein abundance before and after the chlorthalidone treatment. In the mouse study the immunoblot data were analyzed by comparing integrated optical densities of bands after 30 and 90 minutes exposure to CsA separately compared to its negative control (basic buffer without CsA) by one-way ANOVA with Dunnett multiple comparisons *post hoc* test. In this study, fold-change of 1 means no change. $P<0.05$ was considered statistically significant. All data were analyzed using Prism 5 software (GraphPad Software Inc, La Jolla, CA, USA).

Results

CNIs increase NCC in uEVs of kidney transplant recipients

Table 1 shows the clinical and laboratory characteristics of 9 CsA, 23 Tac and 13 CNI-free immunosuppressive regimens treated kidney transplant recipients (Group 1). The effect of CNI on NCC abundance in uEVs was assessed using immunoblot analysis. Two immunoreactive bands of ~260 and ~130 kDa representing the dimeric and monomeric forms of the NCC protein were detected in uEVs (Fig. 1). Both forms were included in the analysis to determine the effect of CNI treatment on NCC abundance in uEVs. The abundances of tNCC and pNCC in uEVs of both CsA and Tac-treated kidney transplant recipients were significantly increased compared to uEVs isolated from kidney transplant recipients treated with CNI-free immunosuppressive regimens or healthy volunteers (Fig. 2, A and C). No significant difference in tNCC and pNCC abundance was detected between

CsA and Tac-treated kidney transplant recipients. The ratio of pNCC to tNCC did not differ between kidney transplant recipients treated with CsA, Tac, CNI-free immunosuppressive regimens, and healthy volunteers (Fig. 2E). Females may express more NCC (46), but in our study a gender difference in the abundance of NCC in the uEVs was not demonstrated (supplemental Fig. S3 available online). No significant differences in CD9 abundance were observed between the four experimental groups, suggesting comparable uEV numbers (Fig. 2, B and D). Additional normalization by CD9 abundance showed that both tNCC and pNCC abundance in both CsA- and Tac-treated kidney transplant recipients was significantly increased in comparison to kidney transplant recipients treated with CNI-free immunosuppressive regimens, but not healthy volunteers (supplemental Fig. S4, A and B available online).

NCC abundance in uEVs predicts the anti-hypertensive response to thiazides

Subsequently, we investigated whether the blood pressure response to thiazide diuretics in hypertensive kidney transplant recipients treated with Tac correlates with NCC abundance in uEVs. To this end, we compared tNCC and pNCC abundances in uEVs of patients with a blood pressure response to a thiazide in comparison to those who did not respond. Table 2 shows the clinical and laboratory characteristics of these patients (Group 2). Pre-treatment abundances of both tNCC and pNCC in uEVs were significantly higher in chlorthalidone responders compared to non-responders (Fig. 3). Furthermore, both pNCC and tNCC abundance in uEVs correlated with the blood pressure response (R^2=0.27 and 0.30 using log-tranformed densitometry data because of non-normal distribution, P<0.05 for both, Fig. 3). Subsequently, the change in NCC abundance before and after treatment with chlorthalidone in uEVs of both responders and non-responders was compared (Fig. 4 and supplemental Figs. S5 and S6 available online, show original immunoblots). The increase of tNCC in uEVs was larger in non-responders than in responders (P<0.05). While pNCC in uEVs also increased in most responders, there was a decrease in pNCC in the majority of non-responders (P<0.05). As a result, the pNCC to tNCC ratio remained constant in the responders, but markedly decreased in non-responders (P<0.05). This suggests that phospho-occupancy at the measured site was lower in non-responders. No gender differences were found (supplemental Fig. S9 available online). Again, no significant differences were found in the abundances of CD9 between groups, suggesting comparable uEV-numbers (Fig. 3 and supplemental Fig. S7 available online). Additional normalization by CD9 abundance led to similar results (supplemental Fig. S8 available online).

Table 1 | Clinical and laboratory characteristics of the patients in study Group 1.

Characteristic (mean ± SEM)	CNI-free group (n=13)	CsA group (n=9)	Tac group (n=23)	*P*-value
Age	53 ± 3	51 ± 2	52 ± 3	0.90[a], 0.96[b]
Male (n (%))	7 (54)	5 (56)	12 (52)	
Body mass index, Kg/m^2	25 ± 1	27 ± 2	27 ± 1	0.53[a], 0.38[b]
Cause of ESRD (n)				
Polycystic kidney disease	3	1	5	
Diabetes	0	2	2	
Glomerular disease	2	0	0	
Hypertension/Vascular	0	0	2	
Other	8	6	14	
Plasma Na, mmol/L	140 ± 1	138 ± 1	139 ± 1	0.44[a], 0.72[b]
Plasma K, mmol/L	4.0 ± 0.1	4.1 ± 0.1	4.1 ± 0.1	0.80[a], 0.72[b]
Plasma Cl, mmol/L	106 ± 1	105 ± 1	108 ± 1	0.80[a], 0.29[b]
Plasma creatinine, mg/dL	1.6 ± 0.1	1.5 ± 0.1	1.7 ± 0.1	0.80[a], 0.72[b]
eGFR, mL/min/1.73 m^2	46 ± 2	42 ± 3	45 ± 4	0.76[a], 0.97[b]
Systolic blood pressure, mmHg	135 ± 3	137 ± 4	142 ± 3	0.91[a], 0.22[b]
Diastolic blood pressure, mmHg	80 ± 2	84 ± 4	82 ± 2	0.52[a], 0.77[b]
CsA pre-dose level, µg/L		127 ± 14		
Tac pre-dose level, µg/L			6.7 ± 0.4	

SEM = standard error of the mean; ESRD = end stage renal disease; data are presented as mean ± SEM. [a] = *P*-value for difference between CsA and CNI-free; [b] = *P*-value for difference between Tac and CNI-free, 95% CI, 95% confidence interval.

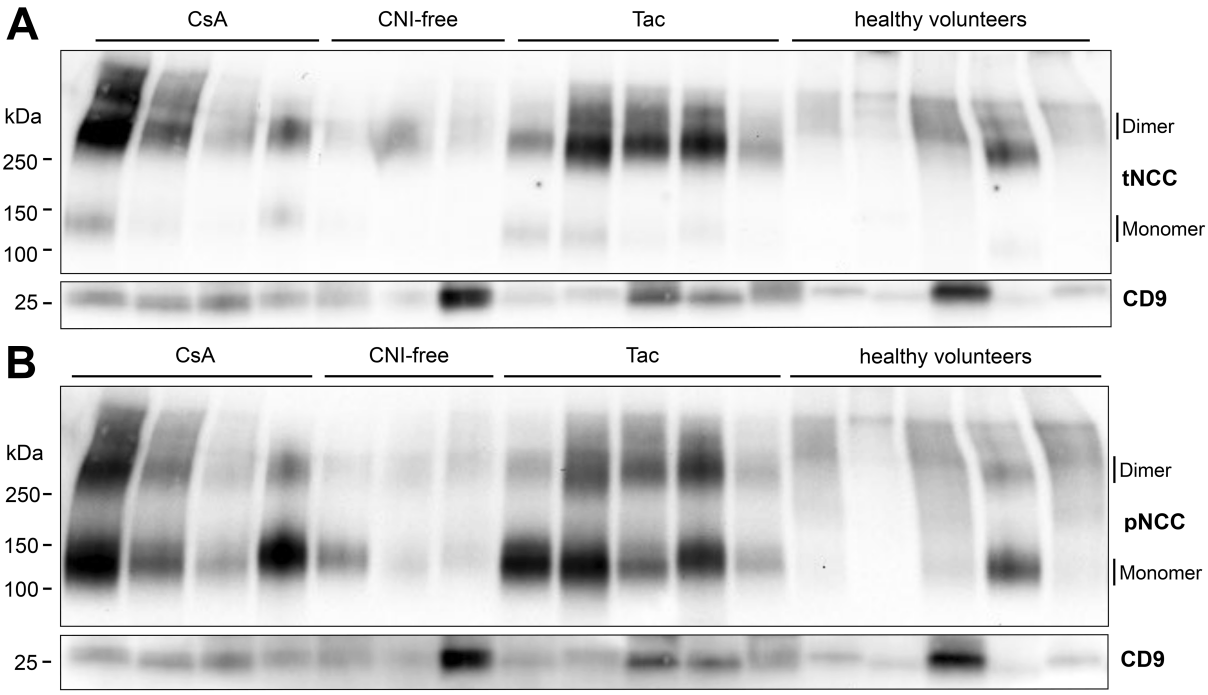

Figure 1 | Representative immunoblots of tNCC and pNCC abundance in uEVs of kidney transplant recipients treated with CsA, Tac or CNI-free immunosuppressive regimens and healthy volunteers.

Panels **A** and **B** show the immunoreactive bands in uEVs of patients treated with CsA (n=4), Tac (n=5), CNI-free immunosuppressive regimens (n=3), and healthy volunteers (n=5). tNCC (**A**) and pNCC (**B**) immunoreactive bands in uEVs of both CsA- and Tac-treated kidney transplant recipients were stronger compared to kidney transplant recipients treated with CNI-free immunosuppressive regimens and healthy volunteers.

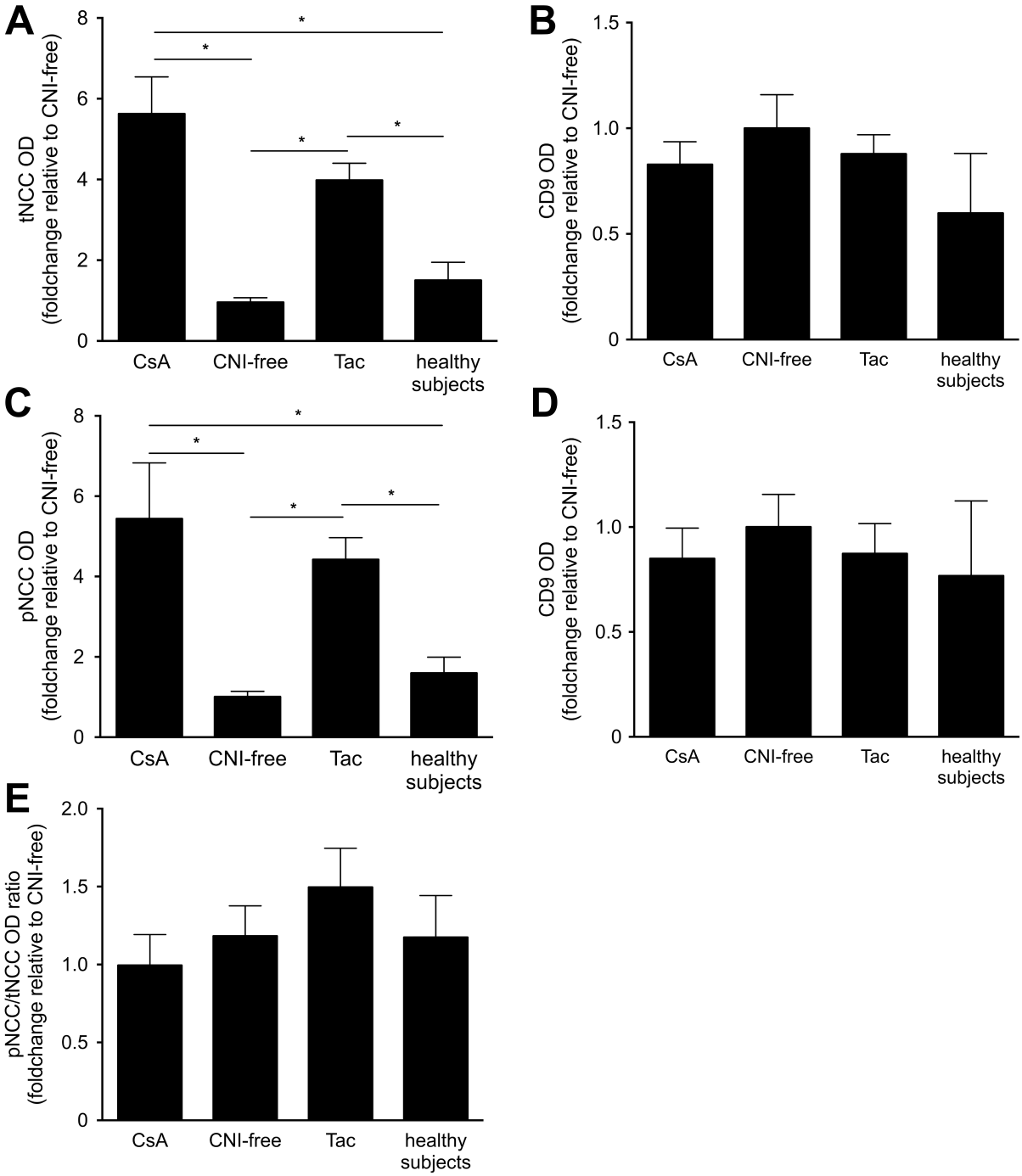

Figure 2 | Densitometry of tNCC and pNCC immunoreactive bands in uEVs of all kidney transplant recipients treated with CsA (n=9), Tac (n=23) or CNI-free immunosuppressive regimens (n=13) and healthy volunteers (n=6).

Both tNCC (**A**) and pNCC (**C**) abundance in both CsA- and Tac-treated kidney transplant recipients was significantly increased in comparison to kidney transplant recipients treated with CNI-free immunosuppressive regimens and healthy volunteers. Densitometry analysis of CD9 expression of the immunoblots for tNCC (**B**) and pNCC (**D**) showed no significant differences between the four groups. The ratio of pNCC to tNCC abundance in uEVs of CsA- and Tac-treated group was not significantly increased in comparison to kidney transplant recipients treated with CNI-free immunosuppressive regimens and healthy volunteers (**E**). The original immunoblots are shown in Fig. 1 and supplemental Figs. S1 and S2 available online. Values are mean ± SEM normalized to kidney transplant recipients treated with CNI-free immunosuppressive regimens (one-way ANOVA, **P*<0.05, n=51).

Table 2 | Clinical and laboratory characteristics of the patients in study Group 2.

Characteristic (mean ± SEM)	Responders (n=10)	Non-responders (n=8)	*P*-value
Age	61 ± 2	57 ± 3	0.15
Males (n (%))	6 (60)	6 (75)	0.27
Body mass index, Kg/m^2	27 ± 2	30 ± 2	0.14
Cause of ESRD (n)			
Polycystic kidney disease	1	0	
Diabetes	2	3	
Glomerular disease	0	3	
Hypertension/vascular	6	1	
Other	1	1	
Plasma Na, mmol/L	140 ± 1	140 ± 1	0.40
Plasma K, mmol/L	4.5 ± 0.1	5.1 ± 0.2*	<0.01
Plasma Cl, mmol/L	103 ± 1	105 ± 1	0.07
Plasma creatinine, mg/dL	1.2 ± 0.1	1.7 ± 0.2*	0.01
eGFR, mL/min/1.73 m^2	55 ± 5	43 ± 6	0.06
Urine K/creatinine, mmol/mmol	5.2 ± 2.1	4.6 ± 1.9	0.28
Systolic blood pressure, mmHg	158 ± 4	151 ± 5	0.15
Diastolic blood pressure, mmHg	86 ± 2	80 ± 3	0.07
Tac pre-dose level, µg/L	5.5 ± 0.4	5.8 ± 0.5	0.30

SEM = standard error of the mean; ESRD = end stage renal disease; data are presented as mean ± SEM. *P*-value for difference between responders and non-responders, 95% CI, 95% confidence interval.

Increased pNCC in mouse cortical tubule suspensions exposed to CsA

To study the acute effect of CsA on NCC abundance in kidney, mouse cortical tubules were isolated and exposed to CsA. All mouse cortical tubule suspensions were incubated in basic buffer for 30 or 90 minutes in the absence or presence of CsA (at final concentrations of 5, 10, and 20 µmol/L). No significant changes were observed in tNCC, while the pNCC abundance and the ratio of pNCC to tNCC were significantly increased after 30 minutes of exposure to 10 or 20 µmol/L of CsA, and after 90 minutes of exposure to 5, 10, or 20 µmol/L of CsA (Fig. 5). Hypotonic low chloride, which decreases the intracellular chloride concentration thereby activating the WNK-SPAK and OSR1 pathways (36, 44), was used as a positive control. pNCC and the ratio of pNCC to tNCC were significantly increased in hypotonic low chloride buffer, whereas tNCC remained unchanged (Fig. 5).

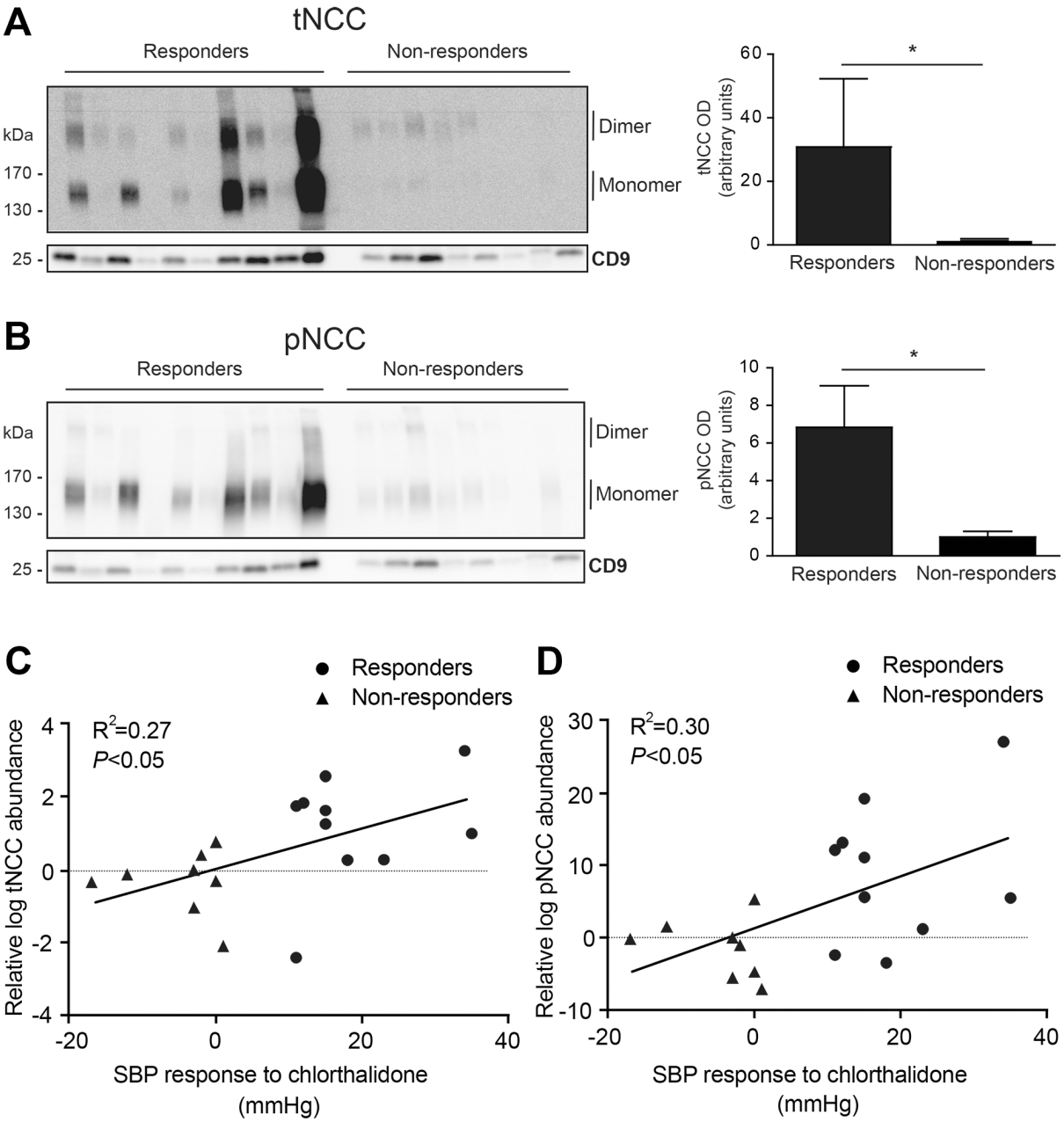

Figure 3 | Pre-treatment tNCC and pNCC abundances in uEVs isolated from hypertensive kidney transplant recipients who did or did not respond to chlorthalidone.

Shown are immunoblots of tNCC (panel **A**) and pNCC (panel **B**) together with CD9 in uEVs of hypertensive kidney transplant recipients using Tac. 'Responders' (n=10) refer to patients who subsequently had a significant anti-hypertensive response (≥10 mmHg reduction in systolic blood pressure) to 8-week treatment with chlorthalidone. Non-responders (n=8) did not have an anti-hypertensive response to chlorthalidone (no change or increase in systolic blood pressure). uEVs were isolated before the treatment with chlorthalidone. Both tNCC and pNCC abundance were significantly higher in responders compared to non-responders (non-parametric t-test, **P*<0.05, n=18). Both pNCC and tNCC abundance in uEVs correlated with the blood pressure response (panel **C**, R^2=0.27 and panel **D**, R^2=0.30 using log-tranformed densitometry data because of non-normal distribution, *P*<0.05 for both). Abbreviations: SBP, ambulatory systolic blood pressure.

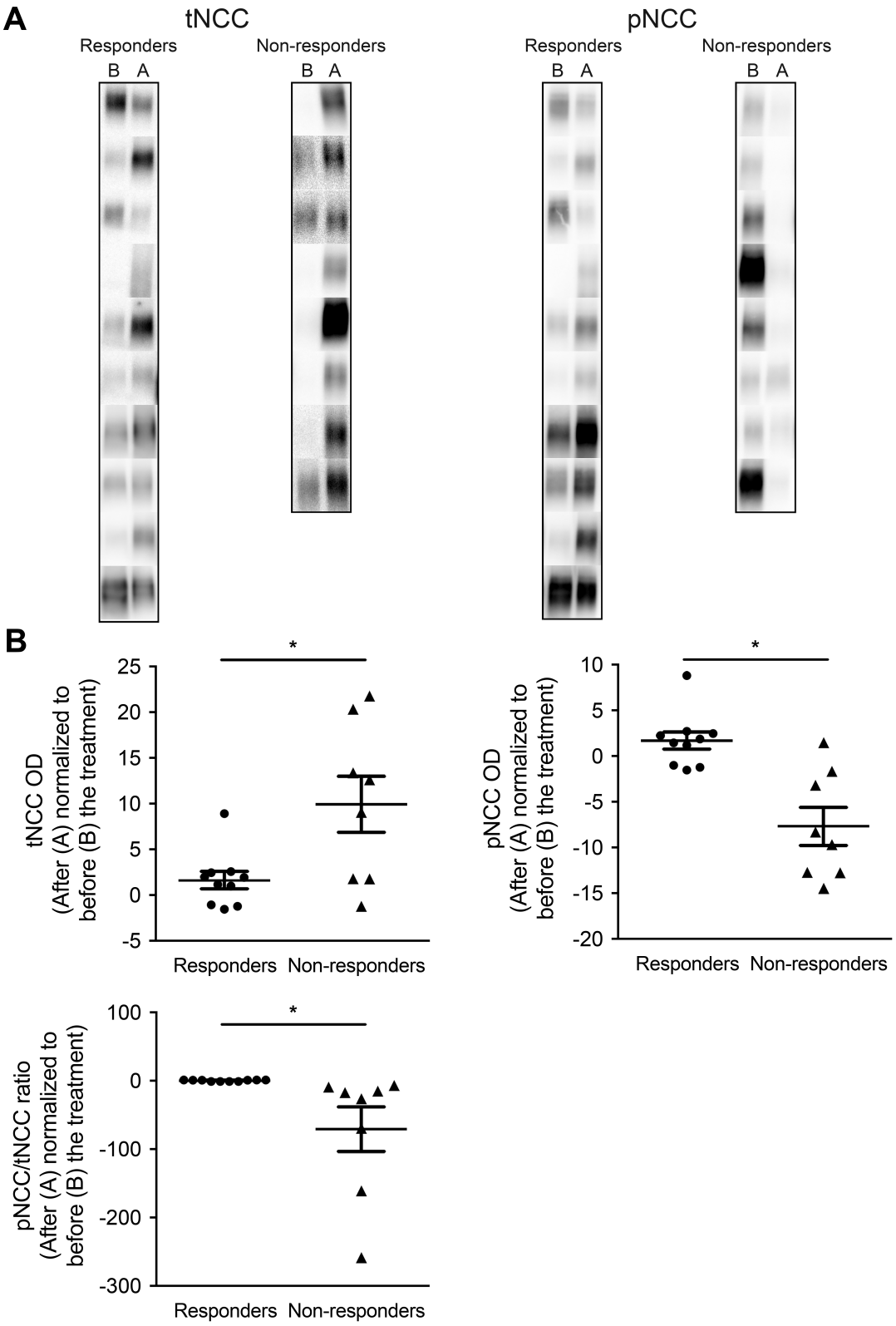

Figure 4 | pNCC and tNCC abundances in uEVs before and after treatment with chlorthalidone.

Panel **A** shows pNCC and tNCC abundances in uEVs before (B) and after (A) the 8-week treatment period with chlorthalidone in both responders (n=10) and non-responders (n=8). The fold-changes in the before-after abundances of pNCC and tNCC in uEVs (as measured by densitometry) of both responders and non-responders are shown in panel **B** (Fold-change of 1 means no change, **P*<0.05). The scatter plots represent the fold change in tNCC, pNCC or their ratio after treatment with chlorthalidone (densitometry values before treatment with chlorthalidone were set to 1).

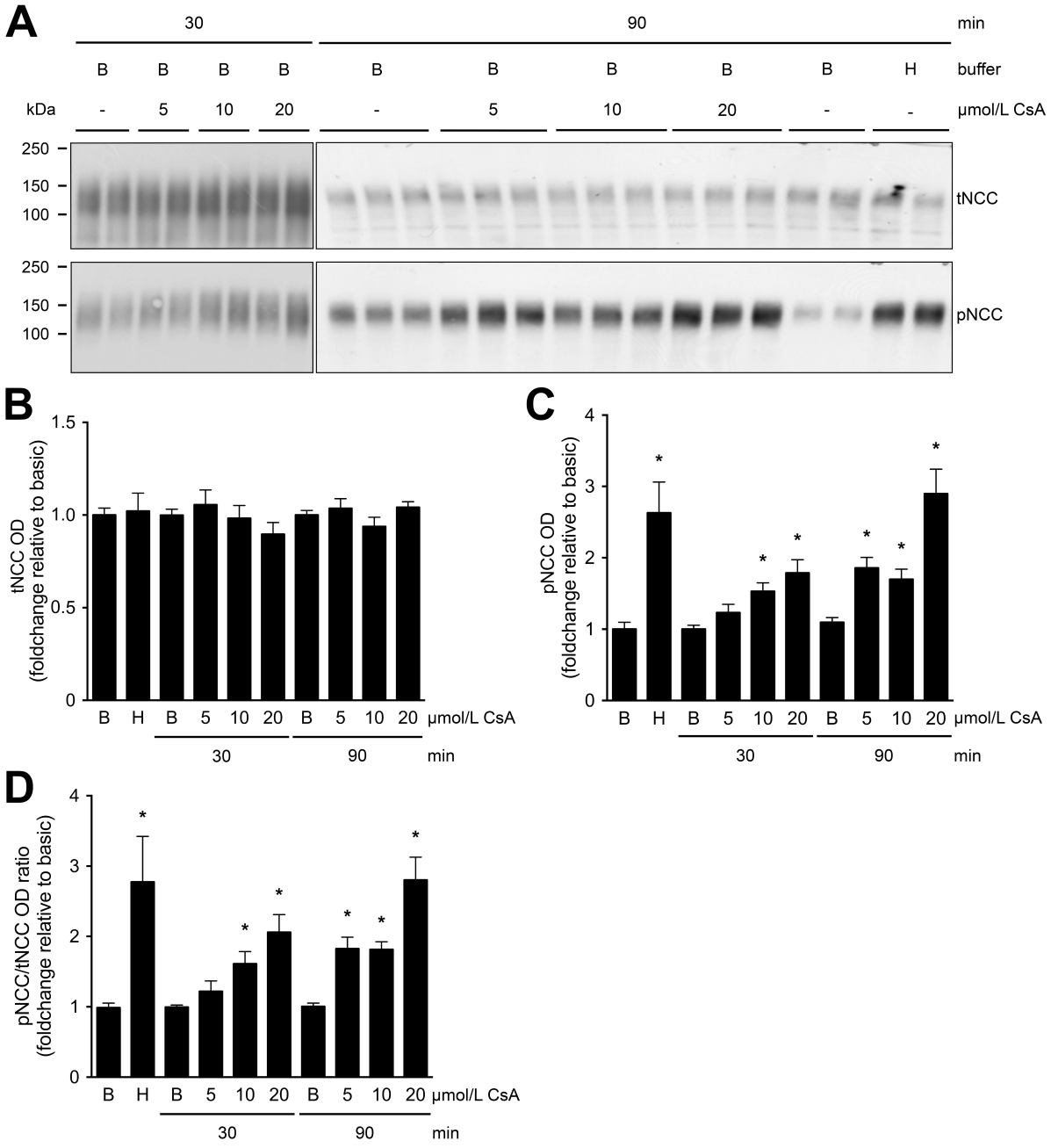

Figure 5 | tNCC and pNCC abundance in mouse cortical tubule suspension exposed to CsA.

Panel **A** shows representative immunoblots of tNCC and pNCC abundance in mouse cortical tubule suspension exposed to CsA. Immunoblots of protein homogenates of mouse cortical tubule suspensions were incubated in basic (B) buffer for 30 and 90 minutes, in the absence (-) or presence of CsA at final concentrations of 5, 10, or 20 µmol/L (**A**). tNCC remained at baseline levels (**B**), while pNCC (**C**) and ratio of pNCC to tNCC (**D**) were significantly increased in the mouse cortical tubule suspension after 30 minutes of exposure to 10 and 20 µmol/L of CsA and 90 minutes of exposure to 5, 10, and 20 µmol/L of CsA. Similarly, pNCC and the ratio of pNCC to tNCC were significantly increased in hypotonic low chloride (H) buffer (**C** and **D**). The original immunoblots for 30 and 90 minutes, in the absence (-) or presence of CsA at final concentrations of 5, 10, or 20 µmol/L are shown in Fig. 5 and supplemental Fig. S10 available online. Values are mean ± SEM normalized to basic (B) condition (one-way ANOVA, **P*<0.05, 30 minutes exposure n=3, 90 minutes exposure n=4).

Discussion

Our study demonstrates that chronic treatment with CNIs increases both tNCC and pNCC abundance in uEVs of kidney transplant recipients, suggesting increased Na reabsorption in the distal part of the nephron. Additionally, we show that the increase in pNCC abundance in uEVs of kidney transplant recipients correlates with the blood pressure response to NCC-inhibiting thiazide diuretics. Lastly, we corroborate that CNIs affect the NCC level in the kidney by showing that short-term exposure to cyclosporine increases pNCC but not tNCC abundance in mouse cortical tubules suspensions. Collectively, these observations indicate that the CNI-induced increase in NCC abundance and activity are involved in the pathogenesis of hypertension in kidney transplant recipients, and suggest that pNCC abundance in uEVs could be used as a biomarker to predict the blood pressure response to thiazide diuretics.

Since the introduction of CNIs in the 1980s, there has been a steep increase in the prevalence of hypertension after kidney transplantation (10, 28). In a study using a kidney specific 12 kDa FK506-binding protein, FKBP12, knockout mice, Tac caused hypertension by inhibiting calcineurin directly in DCT cells expressing NCC (24). Moreover, NCC knockout mice were protected from tacrolimus-induced hypertension (16), confirming the role of NCC in CNI-induced hypertension. Although both CsA and Tac inhibit calcineurin, they differ in structure and cytoplasmic binding protein, which might explain why hypertension is less common and less severe in patients using Tac than in those using CsA (4, 5, 17, 29, 39, 58). However, it is still not known whether the higher incidence of hypertension in CsA-treated kidney transplant recipients is due to a stronger tNCC and pNCC upregulation in CsA- compared to Tac-treated kidney transplant recipients. Our study demonstrates that CsA does not increase tNCC and pNCC abundances in uEVs of kidney transplant recipients more than Tac (Fig. 2). This suggests that factors other than NCC might contribute to the discrepancy in the increased blood pressure between patient groups using CsA and Tac. It is known that CNIs affect tissues other than the kidney, which are also involved in the development of hypertension (24). CsA and Tac might differ in their ability to cause vasoconstriction (33, 51), activate the renin-angiotensin-aldosterone system (RAAS) (16, 33), or the sympathetic nervous system (27), all of which can contribute to the development of hypertension.

Several guidelines recommend thiazide-type diuretics as first-line treatment for the management of hypertension in adults (19, 42). Thiazide-type diuretics act by blocking NCC, thus increasing Na excretion by the kidney (8). Given the role of NCC in CNI-induced hypertension, thiazide diuretics might be especially effective drugs for hypertensive transplant recipients using CNIs and NCC abundance in their uEVs might predict the blood

pressure response to thiazide diuretics. Indeed, uEV analysis in patients selected from our crossover study demonstrates that pre-treatment abundances of tNCC and pNCC in uEVs predict the blood pressure response to thiazide diuretics (Fig. 3). This implies that the abundance of pNCC in uEVs of hypertensive kidney transplant recipients using CNIs could be used to predict thiazide sensitivity. Although it may be more pragmatic to simply test the response to a trial of thiazide diuretics, urinary biomarkers may help individualize anti-hypertensive treatment, especially with the development of high-throughput assays (48). However, acute regulators of NCC activity such as the RAAS and potassium status should also be taken into account when interpreting the obtained results (see below). A relevant question is what explains the higher pNCC and tNCC in uEVs of responders prior to treatment, and the decrease in ratio of pNCC to tNCC in non-responders after thiazide treatment. One could argue that CNI-induced NCC activation was greater in responders. An alternative possibility is that the potassium balance determined thiazide sensitivity. A high potassium diet and hyperkalemia have recently been shown to inhibit NCC (43, 54). Indeed, serum potassium concentrations were higher in non-responders compared to responders. Here, we show that NCC abundance was increased in the majority of “responders” after thiazide treatment (Fig. 4), which is consistent with data obtained in animal models (34, 35). Na *et al*. showed with immunoblot analysis and immunostaining that chronic hydrochlorothiazide treatment in rats increased the abundance of NCC (34). Moreover, chronic hydrochlorothiazide infusion in mice increased the binding density of [^{3}H] metolazone, an indirect measure of NCC activity, which confirms the increase of NCC after hydrochlorothiazide (6). Similarly, chronic administration of the diuretics furosemide and amiloride (which blocks the Na-K-Cl cotransporter and the epithelial Na channel, respectively), increased the abundance of these proteins in rodent kidney (22, 34). These effects might be the result of compensatory mechanisms, potentially mediated by the RAAS or/and potassium balance, which counteract reduced NCC function by the thiazide treatment (52). Of interest, non-responders had a completely different pattern during thiazide treatment with a decrease in pNCC and ratio of pNCC to tNCC (Fig. 4). The explanation for this difference is unclear, but one might speculate that a blood pressure response to thiazides is accompanied by RAAS activation resulting in different NCC excretion patterns in uEVs. Alternatively, differences in potassium balance may explain these results, because a recent study showed that pNCC stimulation by angiotensin II occurs as a compensatory response to renal potassium loss (57).

To further confirm the effect of CNIs on NCC in the kidney, we performed an *ex vivo* study using mice cortical tubules. This experiment demonstrated that short-term exposure to CsA increases pNCC abundance, while tNCC remained stable (Fig. 5). This phenomenon was previously reported by Hoorn *et al.* (16) in mice and human embryonic kidney 293 cells

treated with Tac, and by Melnikov *et al*. (31) in mDCT cells treated with CsA. Recently, it was demonstrated in mice that treatment with Tac prevents the acute high potassium induced NCC dephosphorylation, while tNCC remained unaffected (53). In contrast to previous studies, this acute regulatory system mediated by calcineurin is shown to be independent of the WNK-SPAK signaling cascade (53). Our study demonstrated that chronic administration of CNIs increases the abundance of both tNCC and pNCC in uEVs of kidney transplant recipients. This suggests that the difference in tNCC increase between mice cortical tubules and uEVs might be dependent on the time of stimulation or another signaling molecule involved in the *in vivo* situation.

A number of limitations of our study should be mentioned. First, several other factors, in addition to CNIs, may regulate NCC, which may also explain differences in expression of NCC and in thiazide sensitivity. Second, an unresolved question in the uEV-field remains whether the abundance of protein per uEV varies, or that the number of uEVs is regulated. Although we included the uEV-marker CD9, techniques that allow uEV counting will be necessary to address this point more conclusively.

Our findings demonstrate that CNI treatment increases both tNCC and pNCC abundance in uEVs isolated from kidney transplant recipients. We also show that the blood pressure response to chlorthalidone in Tac-treated hypertensive kidney transplant recipients was related to the pNCC abundance in uEVs. This implies that pNCC in uEVs of kidney transplant recipients treated with a CNI might be used to predict blood pressure response to thiazide diuretics. In addition, uEV analysis may have clinical utility as a non-invasive biomarker for a variety of physiological and pathological conditions.

Supplemental information

Supplemental information for this article is available online at http://journals.plos.org/plosone/article?id=10.1371/journal.pone.0176220. All the dataset underlying the findings in this chapter of the thesis are uploaded as supporting information files. Supporting information files contain supplemental figures and densitometry data of all figures. To calculate the ratio of pNCC to tNCC, the obtained optical density of pNCC was divided by the optical density of tNCC of the same sample.

Acknowledgements

Authors thank Hamed Qaderdan for technical assistance and Drs Sjoerd Verkaart and Luke Shelton for critical reading of the manuscript.

Grants

This study was supported by Dutch Kidney Foundation (PHD12.14 and 16OI04) and EURenOmics funding from European Union seventh Framework Program (FP7/2007–2013, agreement no 305608). M.A.V. was funded by Consejo-Nacional de Ciencia-y-Tecnología (CONACYT-México) and “Doctores-Jóvenes” program, Universidad Autónoma de Sinaloa in Mexico. E.J.H. was supported by grants from Netherlands Organisation for Scientific Research (NWO, Veni 916.12.140) and Dutch Kidney Foundation (KSP-14OK19). R.A.F. was supported by Danish Medical Research Foundation, Lundbeck Foundation and Novo Nordisk Foundation. M.L.A.K. was supported by Danish Medical Research Council.

Disclosures

The authors declare that they have no conflicts of interest with the contents of this article.

Author contributions

Author contributions: O.A.T., A.D.M, M.A.V-F., M.L.A.K., M.V.D.V., S.J., R.A.F., R.Z., J.G.J.H., E.J.H., L.H., and R.J.M.B. Conceived and designed the experiments: R.A.F., R.Z., J.G.J.H., E.J.H., L.H., R.J.M.B.. Performed the experiments: O.A.T., A.D.M., M.L.A.K. Analyzed the data: O.A.T., A.D.M., M.A.V-F., M.L.A.K., M.V.D.V., S.J., R.A.F., R.Z., J.G.J.H., E.J.H., L.H., R.J.M.B.; Contributed reagents/materials/analysis tools: J.G.J.H., R.A.F., R.Z., E.J.H., L.H., R.J.M.B. Wrote the paper: O.A.T., A.D.M., J.G.J.H., E.J.H. and R.J.M.B. take responsibility that this study has been reported honestly, accurately, and transparently; that no important aspects of the study have been omitted; and that any discrepancies from the study as planned have been explained.

References

1. Alvarez ML, Khosroheidari M, Ravi RK, DiStefano JK. Comparison of protein, microRNA, and mRNA yields using different methods of urinary exosome isolation for the discovery of kidney disease biomarkers. *Kidney International* 82: 1024–1032, 2012.
2. Arnold JE, Healy JK. Hyperkalemia, hypertension and systemic acidosis without renal failure associated with a tubular defect in potassium excretion. *Am J Med* 47: 461–472, 1969.
3. Boyden LM, Choi M, Choate KA, Nelson-Williams CJ, Farhi A, Toka HR, Tikhonova IR, Bjornson R, Mane SM, Colussi G, Lebel M, Gordon RD, Semmekrot BA, Poujol A, Välimäki MJ, De Ferrari ME, Sanjad SA, Gutkin M, Karet FE, Tucci JR, Stockigt JR, Keppler-Noreuil KM, Porter CC, Anand SK, Whiteford ML, Davis ID, Dewar SB, Bettinelli A, Fadrowski JJ, Belsha CW, Hunley TE, Nelson RD, Trachtman H, Cole TRP, Pinsk M, Bockenhauer D, Shenoy M, Vaidyanathan P, Foreman JW, Rasoulpour M, Thameem F, Al-Shahrouri HZ, Radhakrishnan J, Gharavi AG, Goilav B, Lifton RP. Mutations in kelch-like 3 and cullin 3 cause hypertension and electrolyte abnormalities. *Nature* 482: 98–102, 2012.
4. Canzanello V. Evolution of cardiovascular risk after liver transplantation: A comparison of cyclosporine A and tacrolimus (FK506). *Liver Transplantation* 3: 1–9, 1997.
5. Canzanello VJ, Textor SC, Taler SJ, Schwartz LL, Porayko MK, Wiesner RH, Krom RAF. Late hypertension after liver transplantation: A comparison of cyclosporine and tacrolimus (FK 506). *Liver Transplantation and Surgery* 4: 328–334, 1998.
6. Chen ZF, Vaughn DA, Beaumont K, Fanestil DD. Effects of diuretic treatment and of dietary sodium on renal binding of 3H-metolazone. *J Am Soc Nephrol* 1: 91–98, 1990.
7. Corbetta S, Raimondo F, Tedeschi S, Syren M-L, Rebora P, Savoia A, Baldi L, Bettinelli A, Pitto M. Urinary exosomes in the diagnosis of Gitelman and Bartter syndromes. *Nephrology Dialysis Transplantation* 30: 621–630, 2015.
8. Ellison DH, Velazquez H, Wright FS. Thiazide-sensitive sodium chloride cotransport in early distal tubule. *Am J Physiol* 253: F546–54, 1987.
9. Esteva-Font C, Guillen-Gomez E, Manuel Diaz J, Guirado L, Facundo C, Ars E, Ballarin JA, Fernández-Llama P. Renal Sodium Transporters Are Increased in Urinary Exosomes of Cyclosporine-Treated Kidney Transplant Patients. *American Journal of Nephrology* 39: 528–535, 2014.
10. First MR, Neylan JF, Rocher LL, Tejani A. Hypertension after renal transplantation. *J Am Soc Nephrol* 4: S30, 1994.
11. Gonzales PA, Pisitkun T, Hoffert JD, Tchapyjnikov D, Star RA, Kleta R, Wang NS, Knepper MA. Large-scale proteomics and phosphoproteomics of urinary exosomes. *J Am Soc Nephrol* 20: 363–379, 2009.
12. Gordon RD. The syndrome of hypertension and hyperkalaemia with normal GFR. A unique pathophysiological mechanism for hypertension? *Clin Exp Pharmacol Physiol* 13: 329–333, 1986.
13. Halloran PF. Immunosuppressive Drugs for Kidney Transplantation. *N Engl J Med* 351: 2715–2729, 2004.
14. Holt S, Moore K. Different effects of tacrolimus and cyclosporine on renal hemodynamics and blood pressure in healthy subjects. *Transplantation* 73: 673–674, 2002.
15. Hoorn EJ, Pisitkun T, Zietse R, GROSS P, FROKIAER J, WANG NS, Gonzales PA, Star RA, Knepper MA. Prospects for urinary proteomics: exosomes as a source of urinary biomarkers. *Nephrology (Carlton)* 10: 283–290, 2005.
16. Hoorn EJ, Walsh SB, McCormick JA, Fürstenberg A, Yang C-L, Roeschel T, Paliege A, Howie AJ, Conley J, Bachmann S, Unwin RJ, Ellison DH. The calcineurin inhibitor tacrolimus activates the renal sodium chloride cotransporter to cause hypertension. *Nat Med* 17: 1304–1309, 2011.
17. Hoorn EJ, Walsh SB, McCormick JA, Zietse R, Unwin RJ, Ellison DH. Pathogenesis of calcineurin inhibitor–induced hypertension. *J Nephrol* 25: 269–275, 2012.
18. Isobe K, Mori T, Asano T, Kawaguchi H, Nonoyama S, Kumagai N, Kamada F, Morimoto T, Hayashi M, Sohara E, Rai T, Sasaki S, Uchida S. Development of enzyme-linked immunosorbent assays for urinary thiazide-sensitive Na-Cl cotransporter measurement. *Am J Physiol Renal Physiol* 305: F1374–81, 2013.

19. James PA, Oparil S, Carter BL, Cushman WC, Dennison-Himmelfarb C, Handler J, Lackland DT, LeFevre ML, MacKenzie TD, Ogedegbe O, Smith SC, Svetkey LP, Taler SJ, Townsend RR, Wright JT, Narva AS, Ortiz E. 2014 evidence-based guideline for the management of high blood pressure in adults: report from the panel members appointed to the Eighth Joint National Committee (JNC 8). *JAMA* 311 American Medical Association: 507–520, 2014.
20. Joo KW, Lee JW, Jang HR, Heo NJ, Jeon US, Oh YK, Lim CS, Na KY, Kim J, Cheong HII, Han JS. Reduced urinary excretion of thiazide-sensitive Na-Cl cotransporter in Gitelman syndrome: Preliminary data. *American Journal of Kidney Diseases* 50: 765–773, 2007.
21. Kamel KS, Ethier JH, Quaggin S, Levin A, Albert S, Carlisle EJ, Halperin ML. Studies to determine the basis for hyperkalemia in recipients of a renal transplant who are treated with cyclosporine. *J Am Soc Nephrol* 2: 1279–1284, 1992.
22. Kim GH. Long-Term Adaptation of Renal Ion Transporters to Chronic Diuretic Treatment. *Am J Nephrol* 24: 595–605, 2005.
23. Lalioti MD, Zhang J, Volkman HM, Kahle KT, Hoffmann KE, Toka HR, Nelson-Williams C, Ellison DH, Flavell R, Booth CJ, Lu Y, Geller DS, Lifton RP. Wnk4 controls blood pressure and potassium homeostasis via regulation of mass and activity of the distal convoluted tubule. *Nat Genet* 38: 1124–1132, 2006.
24. Lazelle RA, McCully BH, Terker AS, Himmerkus N, Blankenstein K, Mutig K, Bleich M, Bachmann S, Yang C-L, Ellison DH. Renal Deletion of 12 kDa FK506-Binding Protein Attenuates Tacrolimus-Induced Hypertension. *J Am Soc Nephrol* 27: 1456–1464, 2015.
25. Ligtenberg G, Hené RJ, Blankestijn PJ, Koomans HA. Cardiovascular risk factors in renal transplant patients: cyclosporin A versus tacrolimus. *J Am Soc Nephrol* 12: 368–373, 2001.
26. Louis-Dit-Picard H, Barc J, Trujillano D, Miserey-Lenkei S, Bouatia-Naji N, Pylypenko O, Beaurain G, Bonnefond A, Sand O, Simian C, Vidal-Petiot E, Soukaseum C, Mandet C, Broux F, Chabre O, Delahousse M, Esnault V, Fiquet B, Houillier P, Bagnis CI, Koenig J, Konrad M, Landais P, Mourani C, Niaudet P, Probst V, Thauvin C, Unwin RJ, Soroka SD, Ehret G, Ossowski S, Caulfield M, International Consortium for Blood Pressure ICBP, Bruneval P, Estivill X, Froguel P, Hadchouel J, Schott J-J, Jeunemaitre X. KLHL3 mutations cause familial hyperkalemic hypertension by impairing ion transport in the distal nephron. *Nat Genet* 44: 456–460, 2012.
27. Lyson T, Ermel LD, Belshaw PJ, Alberg DG, Schreiber SL, Victor RG. Cyclosporine- and FK506-induced sympathetic activation correlates with calcineurin-mediated inhibition of T-cell signaling. *Circ Res* 73: 596–602, 1993.
28. Mangray M, Vella JP. Hypertension After Kidney Transplant. *American Journal of Kidney Diseases* 57: 331–341, 2011.
29. Margreiter R, European Tacrolimus vs Ciclosporin Microemulsion Renal Transplantation Study Group. Efficacy and safety of tacrolimus compared with ciclosporin microemulsion in renal transplantation: a randomised multicentre study. *Lancet* 359: 741–746, 2002.
30. Mayan H, Attar-Herzberg D, Shaharabany M, Holtzman EJ, Farfel Z. Increased urinary Na-Cl cotransporter protein in familial hyperkalaemia and hypertension. *Nephrology Dialysis Transplantation* 23: 492–496, 2008.
31. Melnikov S, Mayan H, Uchida S, Holtzman EJ, Farfel Z. Cyclosporine metabolic side effects: association with the WNK4 system. *European Journal of Clinical Investigation* 41: 1113–1120, 2011.
32. Moes AD, Hesselink DH, van den Meiracker AH, Zietse R, Hoorn EJ. Chlorthalidone Versus Amlodipine for Hypertension in Kidney Transplant Recipients Treated With Tacrolimus: A Randomized Crossover Trial. *Am. J. Kidney Dis.*
33. Murray BM, Paller MS, Ferris TF. Effect of Cyclosporine Administration on Renal Hemodynamics in Conscious Rats. *Kidney International* 28: 767–774, 1985.
34. Na KY, Oh YK, Han JS, Joo KW, Lee JS, Earm J-H, Knepper MA, Kim G-H. Upregulation of Na+ transporter abundances in response to chronic thiazide or loop diuretic treatment in rats. *Am J Physiol Renal Physiol* 284: F133–F143, 2003.
35. Nijenhuis T, Vallon V, van der Kemp AWCM, Loffing J, Hoenderop JGJ, Bindels RJM. Enhanced passive Ca2+ reabsorption and reduced Mg2+ channel abundance explains thiazide-induced hypocalciuria and hypomagnesemia. *Journal of Clinical Investigation* 115: 1651–1658, 2005.
36. Pacheco-Alvarez D, Cristobal PS, Meade P, Moreno E, Vazquez N, Munoz E, Diaz A, Juarez

ME, Gimenez I, Gamba G. The Na+:Cl- cotransporter is activated and phosphorylated at the amino-terminal domain upon intracellular chloride depletion. *J Biol Chem* 281: 28755–28763, 2006.

37. Paver WK, Pauline GJ. Hypertension and hyperpotassaemia without renal disease in a young male. *Med J Aust* 2: 305–306, 1964.
38. Pedersen NB, Hofmeister MV, Rosenbaek LL, Nielsen J, Fenton RA. Vasopressin induces phosphorylation of the thiazide-sensitive sodium chloride cotransporter in the distal convoluted tubule. *Kidney Int* 78: 160–169, 2010.
39. Pham SM, Kormos RL, Hattler BG, Kawai A, Tsamandas AC, Demetris AJ, Murali S, Fricker FJ, Chang HC, Jain AB, Starzl TE, Hardesty RL, Griffith BP. A prospective trial of tacrolimus (FK 506) in clinical heart transplantation: Intermediate-term results. *The Journal of Thoracic and Cardiovascular Surgery* 111: 764–772, 1996.
40. Pirsch JD, Miller J, Deierhoi MH, Vincenti F, Filo RS. A comparison of tacrolimus (FK506) and cyclosporine for immunosuppression after cadaveric renal transplantation. FK506 Kidney Transplant Study Group. *Transplantation* 63: 977–983, 1997.
41. Pisitkun T, Shen RF, Knepper MA. Identification and proteomic profiling of exosomes in human urine. *Proc Natl Acad Sci* 101: 13368–13373, 2004.
42. Psaty BN, Lumley T, Furberg CD, Schellenbaum G, Pahor M, Alderman MH, Weiss NS. Health outcomes associated with various antihypertensive therapies used as first-line agents - A network meta-analysis. *JAMA* 289: 2534–2544, 2003.
43. Rengarajan S, Lee DH, Oh YT, Delpire E, Youn JH, McDonough AA. Increasing plasma [K+] by intravenous potassium infusion reduces NCC phosphorylation and drives kaliuresis and natriuresis. *Am J Physiol Renal Physiol* 306: F1059–F1068, 2014.
44. Richardson C, Rafiqi FH, Karlsson HKR, Moleleki N, Vandewalle A, Campbell DG, Morrice NA, Alessi DR. Activation of the thiazide-sensitive Na+-Cl– cotransporter by the WNK-regulated kinases SPAK and OSR1. *J Cell Sci* 121: 675–684, 2008.
45. Rojas-Vega L, Jimenez AR, Bazua-Valenti S, Arroyo-Garza I, Jimenez JV, Gomez-Ocadiz R, Carrillo-Perez DL, Moreno E, Morales-Buenrostro LE, Alberú J, Gamba G. Increased phosphorylation of the renal Na+-Cl- cotransporter in male kidney transplant recipient patients with hypertension: a prospective cohort. *Am. J. Physiol. Renal Physiol.* (September 2, 2015). doi: 10.1152/ajprenal.00326.2015.
46. Rojas-Vega L, Reyes-Castro LA, Ramirez V, Bautista-Perez R, Rafael C, Castañeda-Bueno M, Meade P, de los Heros P, Arroyo-Garza I, Bernard V, Binart N, Bobadilla NA, Hadchouel J, Zambrano E, Gamba G. Ovarian hormones and prolactin increase renal NaCl cotransporter phosphorylation. *Am J Physiol Renal Physiol* 308: F799–F808, 2015.
47. Rozansky DJ, Cornwall T, Subramanya AR, Rogers S, Yang Y-F, David LL, Zhu X, Yang C-L, Ellison DH. Aldosterone mediates activation of the thiazide-sensitive Na-Cl cotransporter through an SGK1 and WNK4 signaling pathway. *J Clin Invest* 119: 2601–2612, 2009.
48. Salih M, Fenton RA, Knipscheer J, Janssen JW, van den Berg MSV, Jenster G, Zietse R, Hoorn EJ. An Immunoassay for Urinary Extracellular Vesicles. *Am. J. Physiol. Renal Physiol.* (January 28, 2016). doi: 10.1152/ajprenal.00463.2015.
49. Salih M, Zietse R, Hoorn EJ. Urinary extracellular vesicles and the kidney: biomarkers and beyond. *Am J Physiol Renal Physiol* 306: F1251–9, 2014.
50. Schambelan M, Sebastian A, Rector FC. Mineralocorticoid-resistant renal hyperkalemia without salt wasting (type II pseudohypoaldosteronism): role of increased renal chloride reabsorption. *Kidney International* 19: 716–727, 1981.
51. Schwertfeger E, Wehrens J, Oberhauser V, Katzenwadel A, Rump LC. Contractile effects of tacrolimus in human and rat isolated renal arteries. *Journal of Autonomic Pharmacology* 21: 205–210, 2001.
52. Sevá Pessôa B, van der Lubbe N, Verdonk K, Roks AJM, Hoorn EJ, Danser AHJ. Key developments in renin-angiotensin-aldosterone system inhibition. *Nat Rev Nephrol* 9: 26–36, 2013.
53. Shoda W, Nomura N, Ando F, Mori Y, Mori T, Sohara E, Rai T, Uchida S. Calcineurin inhibitors block sodium-chloride cotransporter dephosphorylation in response to high potassium intake. *Kidney International* 91: 402–411, 2017.
54. Sorensen MV, Grossmann S, Roesinger M, Gresko N, Todkar AP, Barmettler G, Ziegler U, Odermatt A, Loffing-Cueni D, Loffing J. Rapid dephosphorylation of the renal sodiumchloride

cotransporter in response to oral potassiumintake in mice. *Kidney Int* 83: 811–824, 2013.

55. Tutakhel OAZ, Jeleń S, Valdez-Flores M, Dimke H, Piersma SR, Jimenez CR, Deinum J, Lenders JW, Hoenderop JGJ, Bindels RJM. Alternative splice variant of the thiazide-sensitive NaCl cotransporter: a novel player in renal salt handling. *Am J Physiol Renal Physiol* 310: F204–F216, 2016.
56. van der Lubbe N, Jansen PM, Salih M, Fenton RA, van den Meiracker AH, Danser AHJ, Zietse R, Hoorn EJ. The phosphorylated sodium chloride cotransporter in urinary exosomes is superior to prostasin as a marker for aldosteronism. *Hypertension* 60: 741–748, 2012.
57. Veiras LC, Han J, Ralph DL, McDonough AA. Potassium Supplementation Prevents Sodium Chloride Cotransporter Stimulation During Angiotensin II Hypertension. *Hypertension* 68: 904–912, 2016.
58. Vincenti F, Jensik SC, Filo RS, Miller J, Pirsch J. A long-term comparison of tacrolimus (FK506) and cyclosporine in kidney transplantation: evidence for improved allograft survival at five years. *Transplantation* 73: 775–782, 2002.
59. Wilson FH, Disse-Nicodème S, Choate KA, Ishikawa K, Nelson-Williams C, Desitter I, Gunel M, Milford DV, Lipkin GW, Achard J-M, Feely MP, Dussol B, Berland Y, Unwin RJ, Mayan H, Simon DB, Farfel Z, Jeunemaitre X, Lifton RP. Human hypertension caused by mutations in WNK kinases. *Science* 293: 1107–1112, 2001.
60. Wolley MJ, Wu A, Xu S, Gordon RD, Fenton RA, Stowasser M. In Primary Aldosteronism, Mineralocorticoids Influence Exosomal Sodium-Chloride Cotransporter Abundance. *Journal of the American Society of Nephrology* (July 5, 2016). doi: 10.1681/ASN.2015111221.
61. Yang C-L, Zhu X, Ellison DH. The thiazide-sensitive Na-Cl cotransporter is regulated by a WNK kinase signaling complex. *J Clin Invest* 117: 3403–3411, 2007.

6

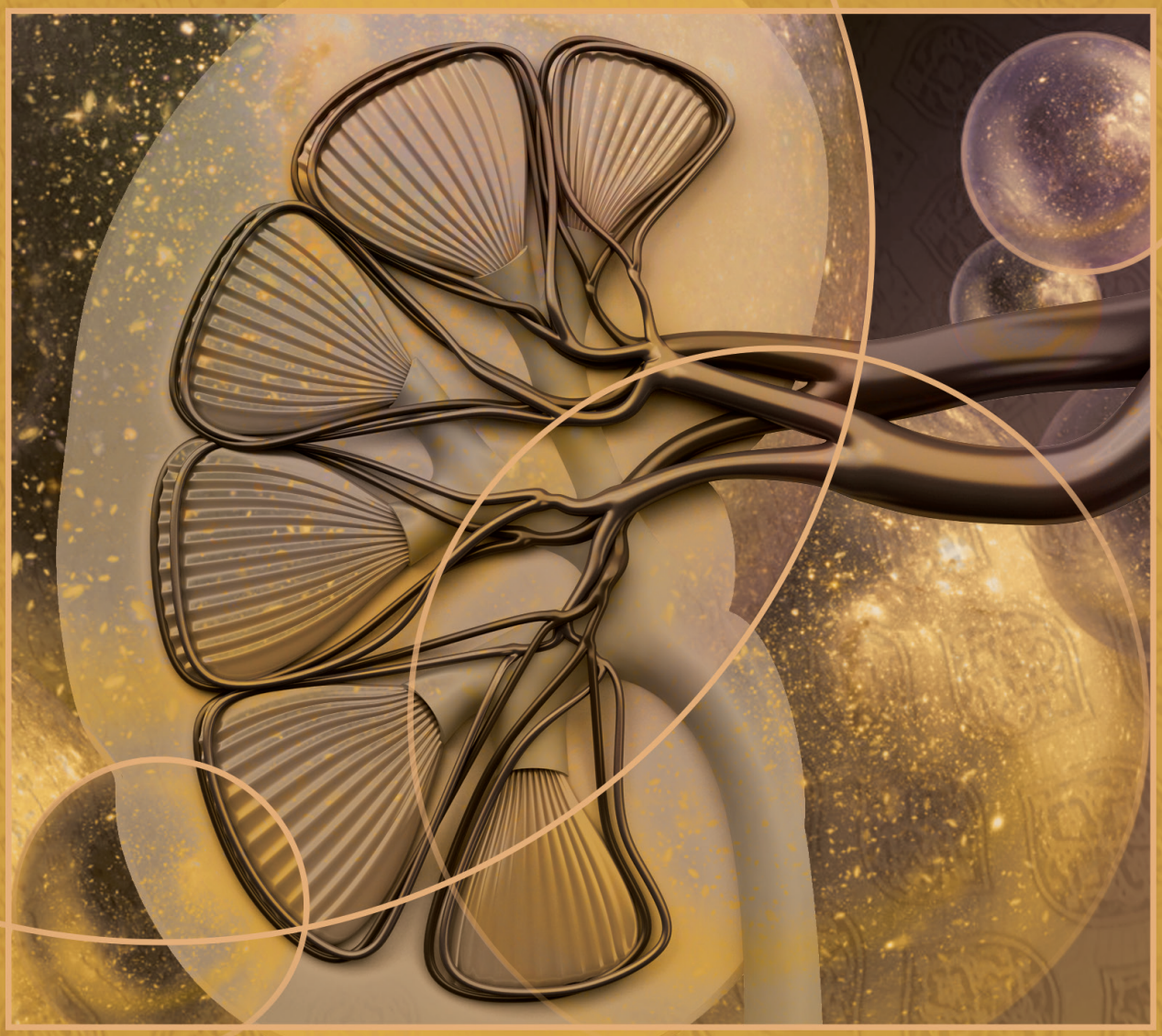

Effects of a high sodium-low potassium diet on renal calcium, magnesium, and phosphate handling

Jenny van der Wijst[1*], Omar A.Z. Tutakhel[1*], Caro Bos[1], Alexander H.J. Danser[2], Ewout J. Hoorn[3], Joost G.J. Hoenderop[1], René J.M. Bindels[1]

[1]Department of Physiology, Radboud Institute for Molecular Life Sciences, Radboud university medical center, Nijmegen, The Netherlands; [2]Division of Pharmacology and Vascular Medicine, Department of Internal Medicine, Erasmus MC, Rotterdam, The Netherlands; [3]Division of Nephrology and Transplantation, Department of Internal Medicine, Erasmus University Medical Center Rotterdam, Rotterdam, the Netherlands

* Authors contributed equally

Am J Physiol Renal Physiol, in press

Abstract

The distal convoluted tubule (DCT) of the kidney plays an important role in blood pressure regulation by modulating Na^+ reabsorption via the Na^+-Cl^- cotransporter (NCC). A diet containing high salt (NaCl) and low K^+ activates NCC, thereby causing Na^+ retention and a rise in blood pressure. Since high blood pressure, hypertension, is associated with changes in serum calcium (Ca^{2+}) and magnesium (Mg^{2+}) levels, we hypothesized that dietary Na^+ and K^+ intake affects Ca^{2+} and Mg^{2+} transport in the DCT. Therefore, the present study aimed to investigate the effect of a high Na^+/low K^+ diet on renal Ca^{2+} and Mg^{2+} handling. Mice were divided in 4 groups and fed a normal Na^+/normal K^+, normal Na^+/low K^+, high Na^+/normal K^+, or high Na^+/low K^+ diet for 4 days. Serum and urine were collected for electrolyte and hormone analysis. Gene and protein expression of electrolyte transporters were assessed in kidney and intestine by qPCR and immunoblotting. While Mg^{2+} homeostasis was not affected, the mice had elevated urinary Ca^{2+} and phosphate (Pi) excretion upon high Na^+ intake, as well as significantly lower serum Ca^{2+} levels in the high Na^+/low K^+ group. Alterations in the gene and protein expression of players involved in Ca^{2+} and Pi transport indicate that reabsorption in the proximal tubular and TAL is affected, while inducing a compensatory response in the DCT. These effects may contribute to the negative health impact of a high salt diet, including kidney stone formation, chronic kidney disease, and loss of bone mineral density.

Keywords: Potassium / Salt / Kidney / Calcium / Phosphate

Introduction

The majority of people worldwide consume a diet containing high salt (NaCl) and low potassium (K^+) levels, which is associated with increased blood pressure (hypertension) (44). Hypertension is one of the most important public health issues due to its increased risk of cardiovascular-renal disease, resulting in an overall elevated mortality (24). While mechanisms for salt-dependent hypertension have been mainly related to the consumption of Na^+, it has recently been shown that K^+ intake plays an essential role in blood pressure regulation. Dietary K^+ intake is inversely correlated to the risk of hypertension and cardiovascular-related mortality (31, 34). A K^+-rich diet is expected to have a protective effect and can reduce blood pressure in hypertensive patients (1).

The kidney is the central organ for maintaining the body's Na^+ balance by controlling Na^+ reabsorption along different nephron segments. Specifically, the aldosterone-sensitive distal part of the nephron, consisting of the distal convoluted (DCT), connecting tubule (CNT), and collecting duct (CD), is essential for Na^+ reabsorption (50). The DCT can be further subdivided into the early and late DCT, DCT1 and DCT2 respectively. Na^+ reabsorption is mediated by the Na^+-Cl^--cotransporter (NCC) in DCT1 and DCT2, as well as by the epithelial Na^+ channel (ENaC) in DCT2, CNT and CD. Here, Na^+ reabsorption through ENaC is coupled to K^+ secretion via the renal outer medullary K^+ channel (ROMK). In short, Na^+ reabsorption in the DCT1 determines the amount of Na^+ delivery to the downstream segments and thereby has an indirect role in K^+ secretion. This is highlighted by the molecular mechanisms underlying Gitelman syndrome and pseudohypoaldosteronism type 2 (familial hyperkalemic hypertension, FHHt). Gitelman syndrome results from inactivating mutations in the *NCC* gene (48), which leads to reduced NCC function. Patients suffer from hypokalemia that can partly be explained by enhanced Na^+ delivery to ENaC and subsequent K^+ secretion by ROMK due to disturbed NCC-mediated Na^+ reabsorption in the DCT. On the contrary, FHHt patients suffer from hyperkalemia as a result of mutations in the genes encoding for proteins regulating NCC, including Cullin3, KLHL3, and the with-no-lysine kinases WNK1 and WNK4 (7, 60). Activation of the WNK kinases leads to phosphorylation and thereby activation of two related proteins, SPAK (STE20/SPS1-related proline/alanine-rich kinase) and OSR1 (oxidative stress–responsive kinase 1) (58). Activated SPAK and OSR1 kinases then phosphorylate key residues in the amino-terminal region of NCC, resulting in enhanced Na^+ reabsorption by either increased transport activity or enriched NCC abundance at the apical membrane (35). Hence, Na^+ reabsorption and subsequent K^+ secretion are diminished in downstream segments, which can explain the hyperkalemia in FHHt. In addition, WNK kinases have also been shown to directly alter ENaC and ROMK function (23).

Interestingly, a recent study by Terker *et al.* postulated an additional relationship between K^+ and Na^+ in which dietary K^+ can regulate renal Na^+ handling through plasma K^+ levels (53). They suggested that lower plasma K^+ induces a Cl^- efflux from the DCT cell, thereby releasing the Cl^--dependent inhibition of WNK1. Subsequently, this results in WNK1 autophosphorylation and activation (38), which in turn phosphorylates and activates NCC through the SPAK/OSR1 kinases (53). Conversely, increasing dietary K^+ intake was shown to reduce NCC phosphorylation (and activity) in a linear range (40, 49, 56).

In addition to regulating renal Na^+ and K^+ handling, the distal part of the nephron also determines the final urinary Ca^{2+} and Mg^{2+} excretion since no Ca^{2+} or Mg^{2+} reabsorption takes place beyond the DCT/CNT. Interestingly, hypertension is associated with altered serum Ca^{2+} and Mg^{2+} levels (41, 42). However, the underlying molecular mechanisms are not well understood. Since renal Na^+ and K^+ handling plays a key role in the pathogenesis of hypertension, we hypothesized that the disturbances in the Ca^{2+} and Mg^{2+} balance can be explained by Na^+ and/or K^+-induced changes in Ca^{2+} and Mg^{2+} reabsorption in the distal part of the nephron. The present study aimed to identify the molecular players involved in the effect of dietary Na^+ and K^+ intake on renal Ca^{2+} and Mg^{2+} handling in wild-type mice fed a high Na^+ diet combined with normal or low K^+. Furthermore, we examined renal phosphate (Pi) handling.

Materials and Methods

Antibodies

The following primary antibodies were used: NCC (Millipore, Billerica, MA, USA; #AB3553; immunoblotting (IB) 1:2,000; immunohistochemistry (IHC) 1:200), pNCC-T58 (kindly provided by Dr. Robert Fenton (36); IB 1:2,000), β-actin (Sigma-Aldrich, St. Louis, MO, USA; #A5441; IB 1:10,000), $CaBP_{28k}$ (Sigma; #C9848; IB 1:5,000), NaPi-2a (kind gift of Dr. Jürg Biber (15); IB 1:2,000), NaPi-2c (Lifespan BioSciences Inc., Seattle, WA, USA; #LS-C101349; IB 1:2,000) and TRPV5 ((25), IHC 1:2,000). Secondary antibodies were as follows: peroxidase conjugated goat anti-rabbit (Sigma-Aldrich; #A4914; IB 1:10,000); peroxidase conjugated sheep anti-mouse (Jackson ImmunoResearch Laboratories Inc., West Grove, PA, USA; #515-035-003; IB 1:10,000); Anti-guinea pig Biotin-SP-conjugated secondary antibody (Jackson ImmunoResearch Laboratories Inc.; #106-065-003; IHC 1:2,000); anti-rabbit Alexa Fluor® 594 conjugated secondary antibody (Invitrogen; #A11012; IHC 1:300).

Buffers

Lysis buffer: 50 mM Tris-HCl (pH 7.5), 150 mM NaCl, 1 mM EDTA, 1 mM EGTA, 1% (v/v) Triton X-100, 1 mM sodium-orthovanadate, 10 mM sodium-glycerophosphate, 50 mM sodium fluoride, 10 mM sodium pyrophosphate, 0.27 M sucrose, containing freshly added tablet of complete protease inhibitor cocktail (Roche, Basel, Switzerland) and 0.1% (v/v) β-mercaptoethanol. TBS-T (Tris-buffered saline, 0.1% Tween 20): Tris-HCL (200 mM, pH 7.5), 0.15 M NaCl, and 0.2% v/v Tween-20. SDS-PAGE sample buffer: 5x 10% w/v SDS, 10 mM β-mercaptoethanol, 50% v/v glycerol, 0.3 M Tris-HCl (pH 7.5), 0.05% w/v bromophenol blue.

Animals

Studies were approved by the Central Animal Laboratory Nijmegen and the animal ethics board of the Radboud University Nijmegen (CCD #AVD103002016382). All mice were 10-12 weeks old males, 20–25 g, and had a C57Bl/6 background. Prior to dietary intervention, they were housed in standard cages in a temperature- and light-controlled room, with control synthetic pellet chow and drinking water available *ad libitum* for 4 days. Following, the mice were randomly divided in 4 groups of 10 mice and fed their respective diet for 4 days. At the last day, they were housed in metabolic cages for 24 hours to collect urine and feces. After anesthetizing with 4% (v/v) isoflurane, the mice were sacrificed and blood, kidneys, and intestines were collected and snap frozen in liquid nitrogen.

Animal diets

All diets were prepared by SSNIFF Spezialdiäten GmbH, Soest, Germany. High Na^+ was obtained by adding NaCl to make a 6% (w/w) NaCl diet. Low K^+ diets (<0.05% (w/w) K^+) had no additional K^+ added, and normal K^+ was obtained by adding KCl to make a 1% (w/w) K^+ diet. This resulted in the following diets: normal Na^+/normal K^+ (NN/NK), normal Na^+/low K^+ (NN/LK), high Na^+/normal K^+ (HN/NK), and high Na^+/low K^+ (HN/LK).

Electrolyte and renin measurements

Serum and urinary total Mg^{2+} concentrations were determined using a colorimetric xylidyl-II blue assay kit according to the manufacturer's protocol (Roche/Hitachi), on a Bio-Rad plate reader at 600 nm. Serum and urinary total Ca^{2+} were colorimetrically determined with a chromogenic/buffer dual-component kit (Sigma Aldrich), on a Bio-Rad plate reader at 570 nm. The obtained values were calibrated using a Precinorm standard solution (Precinorm U, Roche). Serum and urinary Na^+, K^+, and Cl^- determinations were performed at the university hospital central clinical lab on an automated system according to the manufacturer's protocol (Abbott Diagnostics, Hoofddorp, The Netherlands). Total urine volume was used to calculate 24 hours excretion. Active plasma renin concentration (APRC) was measured with a

radioimmunoassay that detects the amount of angiotensin I (ang I) produced per hour in the presence of excess angiotensinogen (nanograms of ang I produced per milliliter of plasma per hour) (9).

Immunoassays

Enzyme-linked immunosorbent assays (ELISA) was used to determine circulating levels of fibroblast growth factor (FGF)23 (C-terminal FGF23 ELISA) and PTH 1–84 in the plasma of the mice (both Immutopics International, San Clemente, CA, USA).

Immunohistochemistry

Immunohistochemistry was performed as previously described (25). In brief, co-staining of TRPV5 with NCC were performed on 5-μm sections of poly-L-lysine paraformaldehyde (PLP) fixed frozen mouse kidney samples. Sections were incubated for 16 hours at 4°C with guinea pig anti-TRPV5 primary antibody. TRPV5 staining was enhanced using TSA fluorescence System according to manufacturer protocol (Perkin Elmer, Groningen, The Netherlands). Subsequently, sections were incubated for 2 hours at room temperature with rabbit anti-NCC primary antibody. The NCC proteins were visualized with anti-rabbit Alexa Fluor® 594 conjugated secondary antibody. Fluorescence microscopy was performed using 10x and 40x objectives on a Leica DMI6000 confocal microscope, and images were processed using LAS AF software.

Quantitative real-time PCR

Total kidney RNA was isolated using TRIzol agent (Invitrogen, Breda, The Netherlands) according to the manufacturer's protocol, and subsequently treated with DNase (Promega, Fitchburg, MA, USA) to remove genomic DNA. Reverse transcription of the mRNA was performed by M-MLV reverse transcriptase (Invitrogen) for 1 hour at 37°C. Gene expression levels were determined by SYBR Green (Bio-Rad, Veenendaal, The Netherlands) real time PCR on a Bio-Rad (Hercules) analyzer and normalized for glyceraldehyde 3-phosphate dehydrogenase (*Gapdh*) expression levels. Relative expression was calculated according to the Livak method ($2^{-\Delta\Delta Ct}$, ΔCt (cycle threshold)=Ct gene of interest – Ct housekeeping gene) and presented as fold change of expression compared to control diet (NN/NK). Primer sequences are indicated in **Table 1**.

Table 1 | Primer sequences.

Gene	Forward primer 5'-3'	Reverse primer 5'-3'
Gapdh	TAACATCAATGAGGGTGAGG	GGTTCACACCCTACACAAAC
Trpm6	AAAGCCATGCGAGTTATCAGC	CTTCACAATGAAAACCTGCCC
Trpm7	GGTTCCTCCTGTGGTGCCIT	CCCCATGTCGTCTCTGTCGT
Trpv5	CTGGAGCTGTGGTTTCCTC	TCCACTTCAGGCTCACC
Trpv6	GGCCTCACAACCTCATTTAC	CTCAATGAGCAGTCTAACAATC
Cyp24a1	GGAGTCCATGAGGCTACCC	GGTAGCGTGTTACTACCCAGA
Cyp27b1	GTGITGAGATTGTACTCGCTGG	TGGGGAATTACATATGCITCTACAC
$CaBP_{28k}$	GACGGAAGTGTGTACCTGG	AITTCCGGTGATAGCTCC
Renin	GCACCGCTACCTTTGAA	GCTGTGAATCCCACAAGC
NaPi2a	TCAGGAAGAGGAGCAAAAGC	AAAGGAAAGCCAGCATCAGA
NaPi2c	GTGGTCAGCAGCTTTCTCAA	ACAGCACCACATTGTCCTTG
Cldn 19	GGTTCCTTTCTCTGCTGCAC	CGGGCAACTTAACAACAGG
Cldn 14	GTCCAGCTCCTAGGCTTCCT	CATCCACAGTCCCTTCAGGT
Cldn 16	CCATCATTGAATCGCTCTCC	GAGGAGCGTTCGACGTAAAC
Cldn 2	CCAGGGCAATCGTACCAACT	ACTCTTGGCTTTGGGCTGTT
Slc8a1	CTCCCTTGTGCTTGAGGAAC	CAGTGGCTGCTTGTCATCAT
Slc12a1	GGCTTGATCTTTGCTTTTGC	CCATCATTGAATCGCTCTCC
SLC9a3	TCACCTTCAAATGGCACCAC	TGGGACAGGTGAAAGACGATT

Protein isolation

Cortex and medulla sections were macroscopically isolated from kidney tissue and homogenized in ice cold lysis buffer. The kidney lysates were clarified by centrifugation at 4 °C for 15 minutes at 16,000 g and supernatants were snap frozen in aliquots and stored at -80 °C. Protein concentrations were determined using the Bradford method according to the manufacturer's protocol (Bio-Rad).

Immunoblotting

Lysates (50 µg) in SDS sample buffer were subjected to electrophoresis on Criterion TGX precast gels (Bio-Rad) and then transferred to PVDF membranes. The membranes were blocked in TBS-T containing 5% (w/v) nonfat dry milk (NFDM) for 30 minutes at room temperature. Subsequently, they were immunoblotted overnight at 4°C with primary antibody (in TBS-T containing 5% (w/v) NFDM). Next day, the blots were washed with TBS-T to remove unbound primary antibody and incubated with horseradish peroxidase (HRP) conjugated secondary antibodies for 1 hour at room temperature. After subsequent washes, the protein was visualized with chemiluminescent reagent (SuperSignal West femto/pico; Thermo Scientific, Waltham, MA, USA) and processed with the Bio-Rad ChemiDoc XRS. The NCC bands on the immunoblots were quantified with Image J software (NIH).

Statistical analysis

All data are shown as mean standard error of the mean (SEM). Statistical significance ($p<0.05$) was determined by analysis of variance and a Bonferroni post-hoc test. All data were analyzed using GraphPad Prism 7.0 (GraphPad Software Inc).

Results

Effect of dietary intervention on electrolyte handling

To investigate the role of dietary Na^+ and K^+ intake on renal electrolyte handling, the mice were fed 4 different diets (NN/NK (control), NN/LK, HN/NK, and HN/LK) and blood, and 24-hour urine were collected using metabolic cages. No differences in body weight or food intake were observed between the groups (Table 2). Importantly, water intake and urine production were significantly elevated in the high Na^+ groups (HN/NK and HN/LK) compared to the control group. Moreover, the HN/LK group has a slightly higher water intake and urine output compared to high Na^+ alone (HN/NK) ($p=0.13$). The effect of the diets was also evident from changes in electrolyte handling (Table 3). First, the HN/LK group had significantly elevated serum Na^+ levels compared to all other groups. Second, serum K^+ levels were significantly lower in the groups fed a low K^+ diet compared to the normal K^+ groups. Of note, high Na^+ intake did not affect serum K^+. Third, serum Cl^- levels decreased significantly in the NN/LK group, while the other groups showed no differences. Next, urinary excretion of Na^+, K^+, and Cl^- were determined in 24-hour urine. Urinary K^+ excretion corresponded to the serum K^+ levels and was for instance drastically reduced in the low K^+ groups. The urinary Na^+ and Cl^- excretion was significantly enhanced in groups fed a high Na^+ diet. To confirm the dietary effect on NCC phosphorylation as previously described (53), kidney cortex samples were subjected to immunoblotting demonstrating enhanced phosphorylation of NCC in both low K^+ groups (Fig. 1A).

Interestingly, the low K^+ diet resulted in a reduced renal expression of Na^+-K^+-Cl^- cotransporter (NKCC2), the family member of NCC that transports Na^+, K^+, and Cl^- in the thick ascending limb of Henle's loop (TAL) (Fig. 1B). Furthermore, we analyzed the expression of the proximal tubular Na^+/H^+ exchanger NHE3 by qPCR. The HN/LK group showed a significant downregulation of *Slc9a3*, the gene encoding NHE3 (Fig. 1C), compared to groups fed a normal K^+ (NN/NK and HN/NK).

After establishing that the dietary intervention resulted in electrolyte changes, serum levels and 24-hour urine excretion of Ca^{2+} and Mg^{2+} were analyzed. There were no differences in serum Mg^{2+} levels or urinary Mg^{2+} excretion between the groups (Fig. 2, A and B). Interestingly, Ca^{2+} excretion was elevated upon high Na^+ intake and an additional rise was demonstrated in the HN/LK group compared to HN/NK (Fig. 2C). Serum Ca^{2+} levels

were also significantly decreased in the HN/LK group, while no changes were observed for the mice fed a HN/NK diet (Fig. 2D). In addition, phosphate (Pi) levels in urine and serum were examined. Urinary Pi excretion was significantly higher in mice fed a high Na^+ diet, independent of dietary K^+. Serum Pi was not different between the groups (Fig. 2, E and F).

Table 2. Metabolic parameters.

	NN/NK	NN/LK	HN/NK	HN/LK
Body weight (g)	24.0 +/- 0.3	23.7 +/- 0.3	23.4 +/- 0.3	23.1 +/- 0.3
Food intake (g)	3.4 +/- 0.2	3.8 +/- 0.5	3.0 +/- 0.2	3.4 +/- 0.2
Water intake (ml)	3.2 +/- 0.6	3.9 +/- 0.5	6.6 +/- 0.6[a]	9.4 +/- 1.4[a,b]
Urine volume (ml)	1.4 +/-0.1	1.7 +/- 0.3	4.4 +/- 0.4[a,b]	5.9 +/- 0.7[a,b]

Mice were fed the indicated diets for 4 days and were kept in individual metabolic cages for the last 24 hours. Values are depicted as mean +/- SEM (n=10). Significant differences are indicated as: [a] = $p<0.05$ compared to NN/NK, [b] = $p<0.05$ compared to NN/LK, and [c] = $p<0.05$ compared to HN/NK.

Table 3. Electrolyte levels in serum and urine.

	NN/NK	NN/LK	HN/NK	HN/LK
Serum electrolytes (mM)				
Na^+	157 +/- 1	157 +/- 1	159 +/- 1	163 +/- 1[a,b.c]
Cl^-	113 +/- 1	107 +/- 1a	112 +/- 1[b]	115 +/- 1[b]
K^+	5.2 +/- 0.1	4.3 +/- 0.2a	5.3 +/- 0.1[b]	3.9 +/- 0.1[a,c]
Urine electrolytes (μmol/24h)				
Na^+	230 +/- 19	131 +/- 10	1939 +/- 146[a,b]	1847 +/- 155[a,b]
Cl^-	530 +/- 44	155 +/- 14[a]	2444 +/- 195[a,b]	2023 +/- 155[a,b]
K^+	502 +/- 40	12.3 +/- 1.7[a]	549 +/- 32[b]	26.8 +/- 2.5[a,c]

Data were collected after housing the mice in metabolic cages for the last 24 hours. Urinary excretion (24h) and serum levels of Na^+, K^+, and Cl^- from mice kept on the indicated diets are shown as mean +/- SEM (n=10), and significance is indicated as: [a] = $p<0.05$ compared to NN/NK, [b] = $p<0.05$ compared to NN/LK, and [c] = $p<0.05$ compared to HN/NK.

Expression of renal electrolyte transporters

The expression of genes encoding for proteins involved in Mg^{2+} (re)absorption in kidney and intestine was analyzed in the different groups using RT-qPCR (Fig. 3). Renal transcript levels of *Trpm6*, encoding the apical Mg^{2+} channel TRPM6, were significantly higher in the high Na^+ groups, while no significant differences were observed for *Trpm6* expression levels in colon (Fig. 3, A and C). Of note, the renal expression of *Trpm7*, encoding the ubiquitous Mg^{2+} channel, was significantly lower in the HN/LK group (Fig. 3B).

Next, the expression of several calciotropic genes in kidney and intestine was examined. There was no difference between the groups in the expression levels of renal *Trpv5* or intestinal *Trpv6*, coding for luminal epithelial Ca^{2+} channels in the kidney and duodenum,

respectively (Fig. 4, A and B). Immunohistochemical analysis of mouse kidney sections also showed that there are no differences in TRPV5 protein abundance between the groups (Fig. 5, A and B). The sections were co-stained with NCC to confirm localization of TRPV5 in the DCT2, and demonstrate that NCC protein expression was not altered (Fig. 5, A and B). Interestingly, the expression levels of the genes coding for the basolateral Ca^{2+} transporter NCX1 (*Slc8a1*) and for Ca^{2+}-binding protein calbindin-D_{28k} (*CaBP$_{28k}$*) were significantly downregulated upon a low dietary K^+ intake (Fig. 4, C and D). This restored to control levels by addition of high Na^+, as the HN/LK group had significantly higher expression levels than NN/LK and did not significantly differ from NN/NK (Fig. 4, C and D). In addition, the high Na^+ diet (both HN/NK and HN/LK) was shown to increase $CaBP_{28k}$ protein levels in the kidney cortex (Fig. 4E).

The expression of several members of the paracellular pathway was also investigated. Claudin-16, -19 play an important role in transport of Ca^{2+} and Mg^{2+} in the TAL (26). While renal expression of *Cldn19* was not different, the *Cldn16* expression significantly decreased in mice fed a low K^+ diet (Fig. 3D). In addition, claudin-14 expression was examined as it is thought to be involved in claudin-16/19 function (22). There were no differences in *Cldn14* expression (Fig. 3E). Furthermore, expression of claudin-2, which participates in paracellular Ca^{2+} transport in the proximal tubule (33), is unaltered by the diet (Fig. 4F).

In order to assess the differences in urinary Pi excretion, expression of phosphate transporters was examined. The major part of filtered Pi is reabsorbed in the proximal tubule by the Na^+-dependent P_i cotransporters NaPi-2a and NaPi-2c (45). Genes encoding these transporters, *Napi2a* and *Napi2c,* respectively, were significantly downregulated in mice fed a HN/LK diet compared to control (NN/NK) (Fig. 6, A and B). Of note, *Napi2c* was also expressed significantly lower in the NN/LK group compared to NN/NK and HN/NK groups. Immunoblotting confirmed the mRNA expression data of *Napi2a* demonstrating a lower renal NaPi-2a protein expression in the HN/LK group compared to control (Fig. 6, C and D). In addition, NaPi-2c protein levels were significantly lower in the mice fed the high salt/low K^+ diet compared to other groups (Fig. 6, C and D).

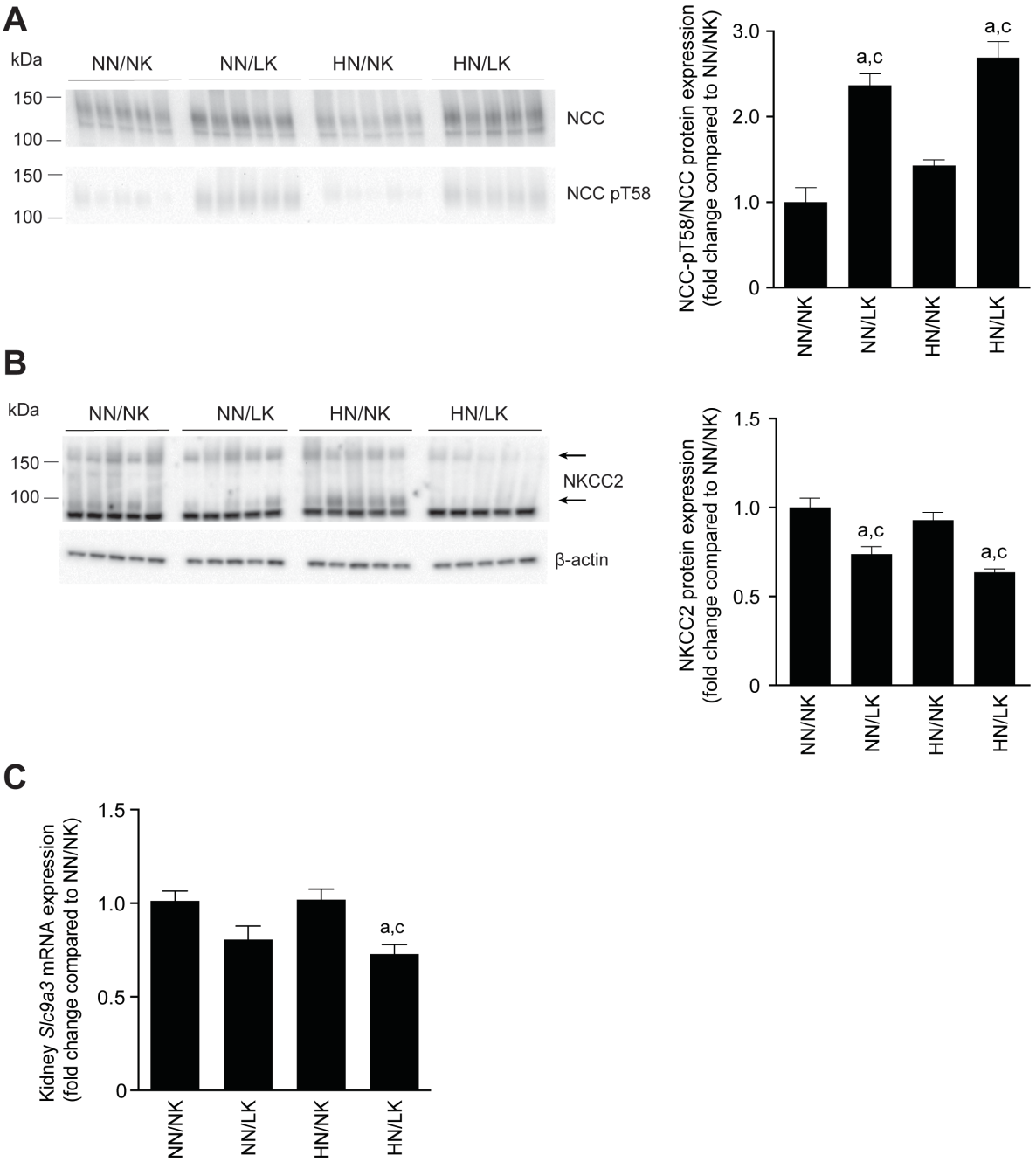

Figure 1 | Immunoblot analysis of NCC and pNCC (pT58) in kidney cortex from mice fed the indicated diet (left panel).

(**A**) Immunoblot analysis of NCC and pNCC (pT58) in kidney cortex from mice fed the indicated diet (left panel). Bar graph of the densitometry shows relative pNCC/NCC protein expression (right panel). (**B**) Immunoblot analysis of NKCC2 in kidney cortex from mice fed the indicated diet (left panel). Arrows indicate monomeric and dimeric form of NKCC2. Bar graph of the densitometry shows NKCC2 protein expression (right panel, corrected for β-actin). Data is shown as mean +/- SEM (n=5). Significance is indicated as: ^{a} = $p<0.05$ compared to NN/NK and ^{c} = $p<0.05$ compared to HN/NK.

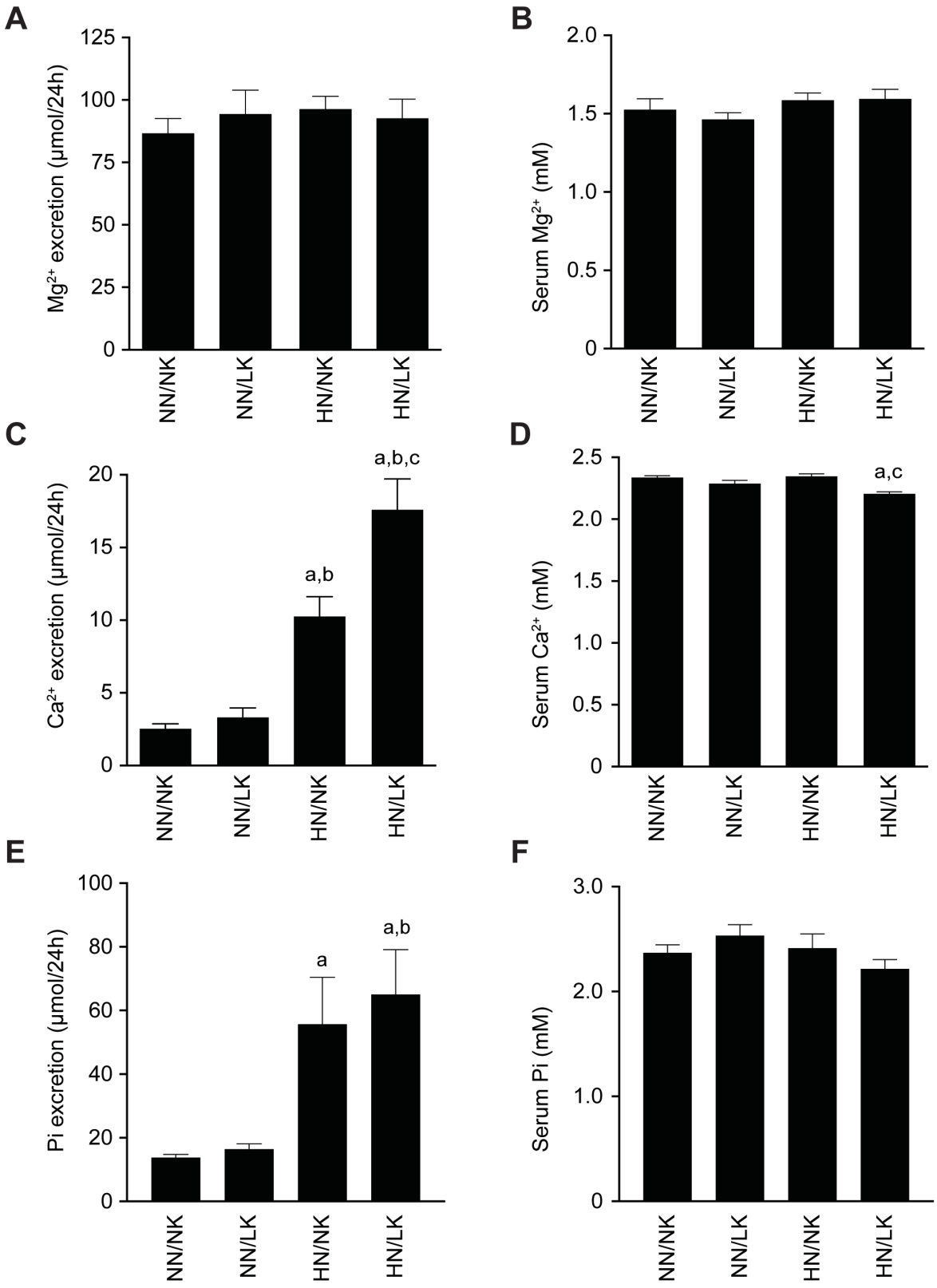

Figure 2 | Effect of dietary Na^+ and K^+ intake on urine and serum Mg^{2+}, Ca^{2+}, and Pi levels.

(**A** and **B**) Urine Mg^{2+} excretion (24h) and serum Mg^{2+} from mice kept on the indicated diets. (**C** and **D**) Urine Ca^{2+} excretion (24h) and serum Ca^{2+} from mice kept on the indicated diets. (**E** and **F**) Urine Pi excretion (24h) and serum Pi from mice kept on the indicated diets. Significant differences are indicated as: ^{a} = $p<0.05$ compared to NN/NK, ^{b} = $p<0.05$ compared to NN/LK, and ^{c} = $p<0.05$ compared to HN/NK.

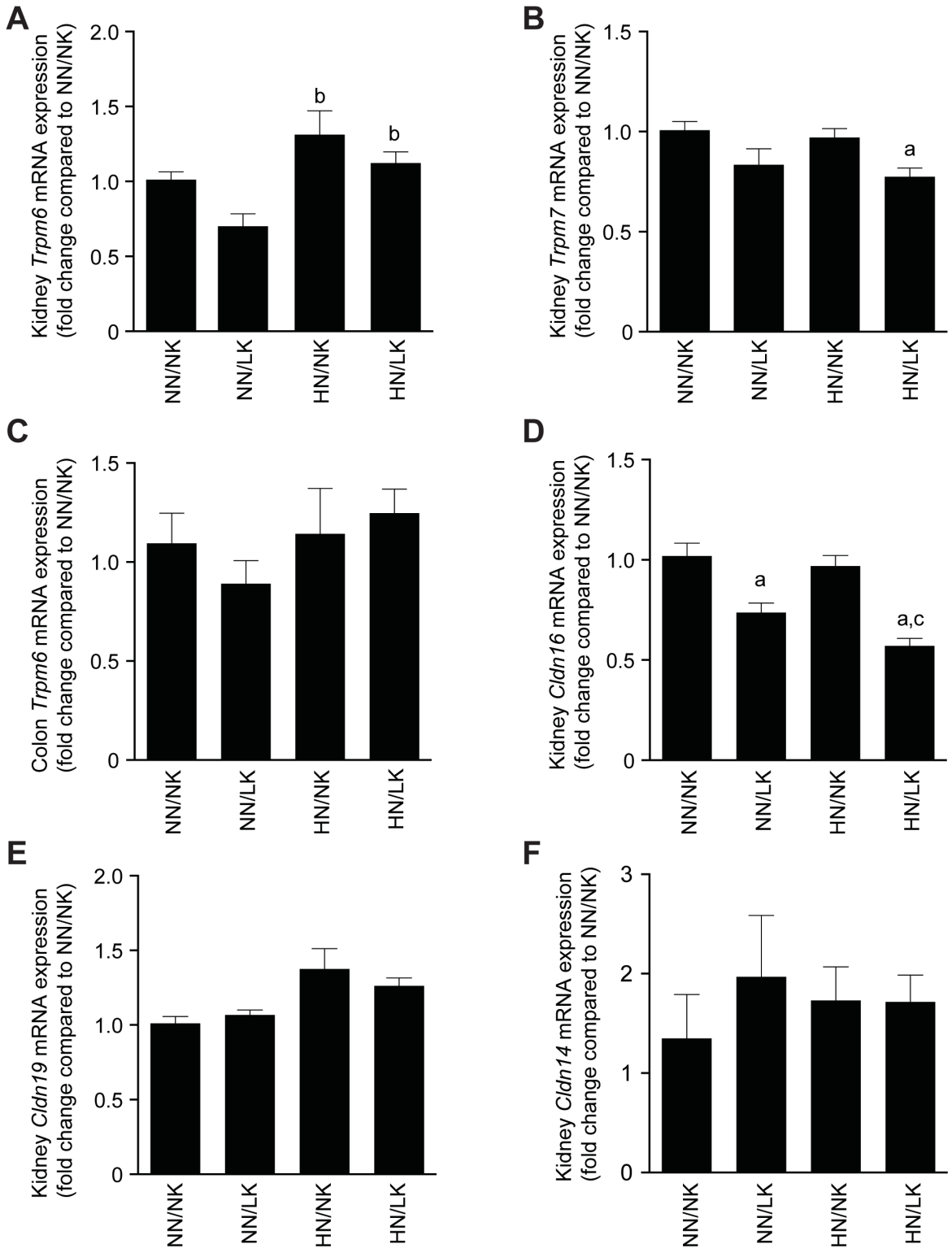

Figure 3 | The mRNA expression levels of the Mg^{2+} channels coding genes *Trpm6* and *Trpm7* in colon and kidney.

(**A-C**) Relative mRNA expression levels (corrected for GAPDH) are shown for *Trpm6* (**A**) and *Trpm7* (**B**) in the kidney, as well as for *Trpm6* in the distal colon (**C**). Data are shown as mean +/- SEM (n=10), [a] = $p<0.05$ compared to NN/NK, [b] = $p<0.05$ compared to NN/LK. **D-F**) Relative mRNA expression levels (corrected for GAPDH) are shown for *Cldn16* (**D**), *Cldn19* (**E**), and *Cldn14* (**F**) in the kidney.

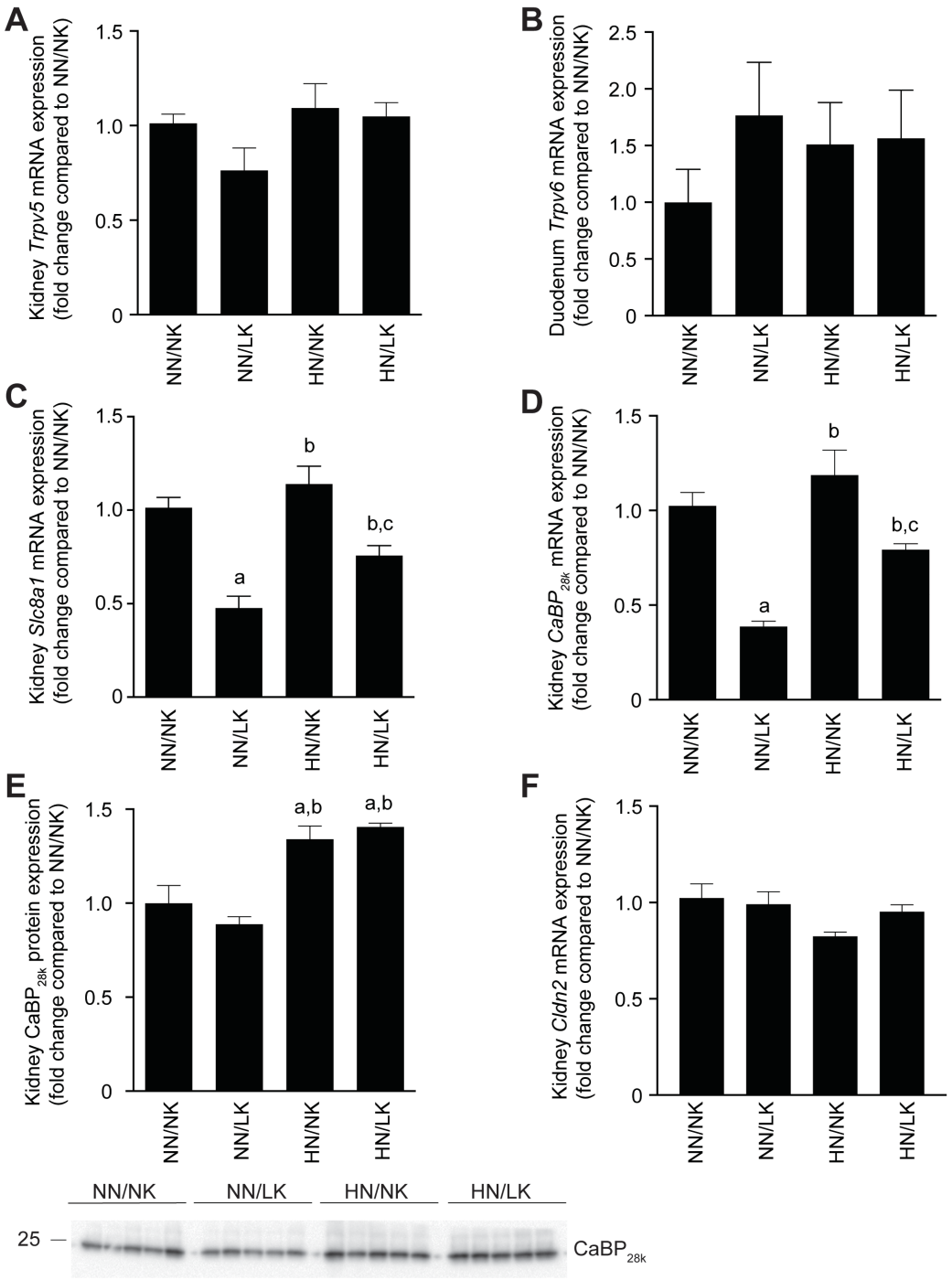

Figure 4 | The expression levels of calciotropic genes in kidney and duodenum.

(**A-D**) Relative mRNA expression levels (corrected for GAPDH) are shown for *Trpv5* (**A**), *Ncx1* (**C**), and *CaBP$_{28k}$* (**D**) in the kidney, as well as for *Trpv6* (**B**) in the proximal duodenum. Data are shown as mean +/- SEM (n=10). (**E**) Immunoblot analysis of $CaBP_{28k}$ in kidney cortex from mice fed the indicated diet (right panel). Bar graph of the densitometry shows relative $CaBP_{28k}$ protein expression (left panel) as mean +/- SEM (n=5). Significance is indicated as: [a] = $p<0.05$ compared to NN/NK, [b] = $p<0.05$ compared to NN/LK, and [c] = $p<0.05$ compared to HN/NK. (F) Relative mRNA expression levels (corrected for GAPDH) for *Cldn2* in the kidney.

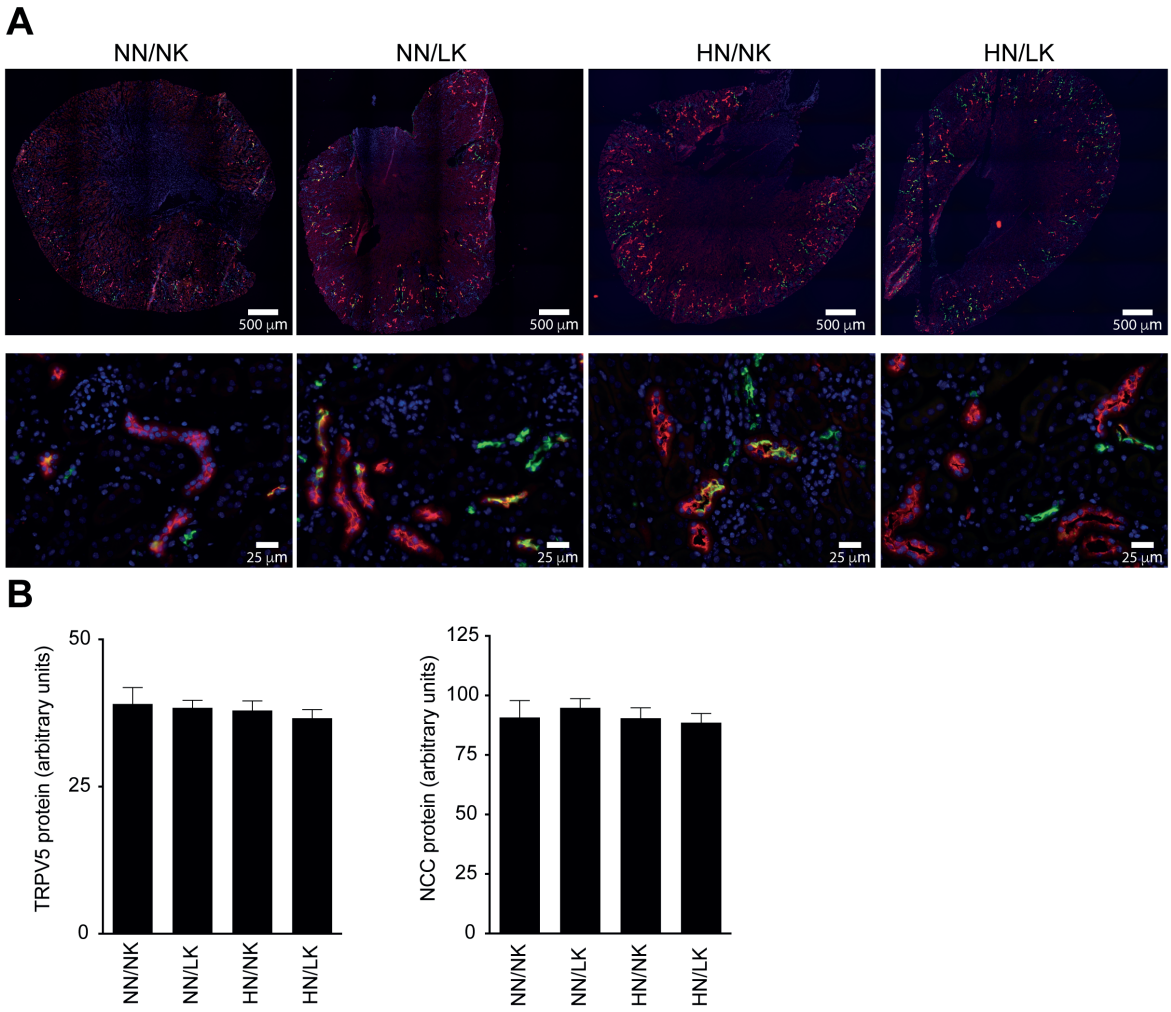

Figure 5 | Protein expression of TRPV5 in kidney.

(**A**) Representative microphotographs are shown for TRPV5 (green) and NCC (red) protein expression in mouse kidney tissue, with a 10x (upper) and 40x (lower) magnification. Groups are indicated above the images. (**B**) Protein expression of TRPV5 and NCC was quantified by fluorescence microscopy (Leica DMI6000B). Bar graph of the analysis shows arbitrary units for TRPV5 and NCC protein expression as mean +/- SEM (n=10).

Hormonal regulation upon dietary intervention

To assess the effect of the dietary regimes on hormonal regulation, the expression of *renin* in the kidney as well as APRC was examined. Both *renin* mRNA expression and APRC were significantly lower in the high Na^+ conditions (HN/NK and HN/LK), but there was no difference upon K^+ restriction in a high Na^+ diet (Fig. 7, A and B). Of note, K^+ restriction alone (NN/LK) led to higher APRC compared to all other groups (Fig. 7B).

Next, the expression of *Cyp27b1* and *Cyp24a1*, encoding for proteins that are responsible for the production and degradation of active vitamin D, respectively, was examined. While renal *Cyp24a1* expression levels did not differ between the groups, the

expression of *Cyp27b1* was lower in the groups fed either a low K^+ (NN/LK), high Na^+ (HN/NK) or a combined (HN/LK) diet compared to control (Fig. 7, C and D). Moreover, the expression was lowest in the HN/LK group, which was significant compared to HN/NK (Fig. 7C).

In order to understand whether hormones involved in the maintenance of the Ca^{2+} balance were altered, plasma PTH (PTH 1-84) and FGF23 (FGF23 C-term.) levels were analyzed. There were no differences in these hormone levels between the groups (Fig. 7, E and F).

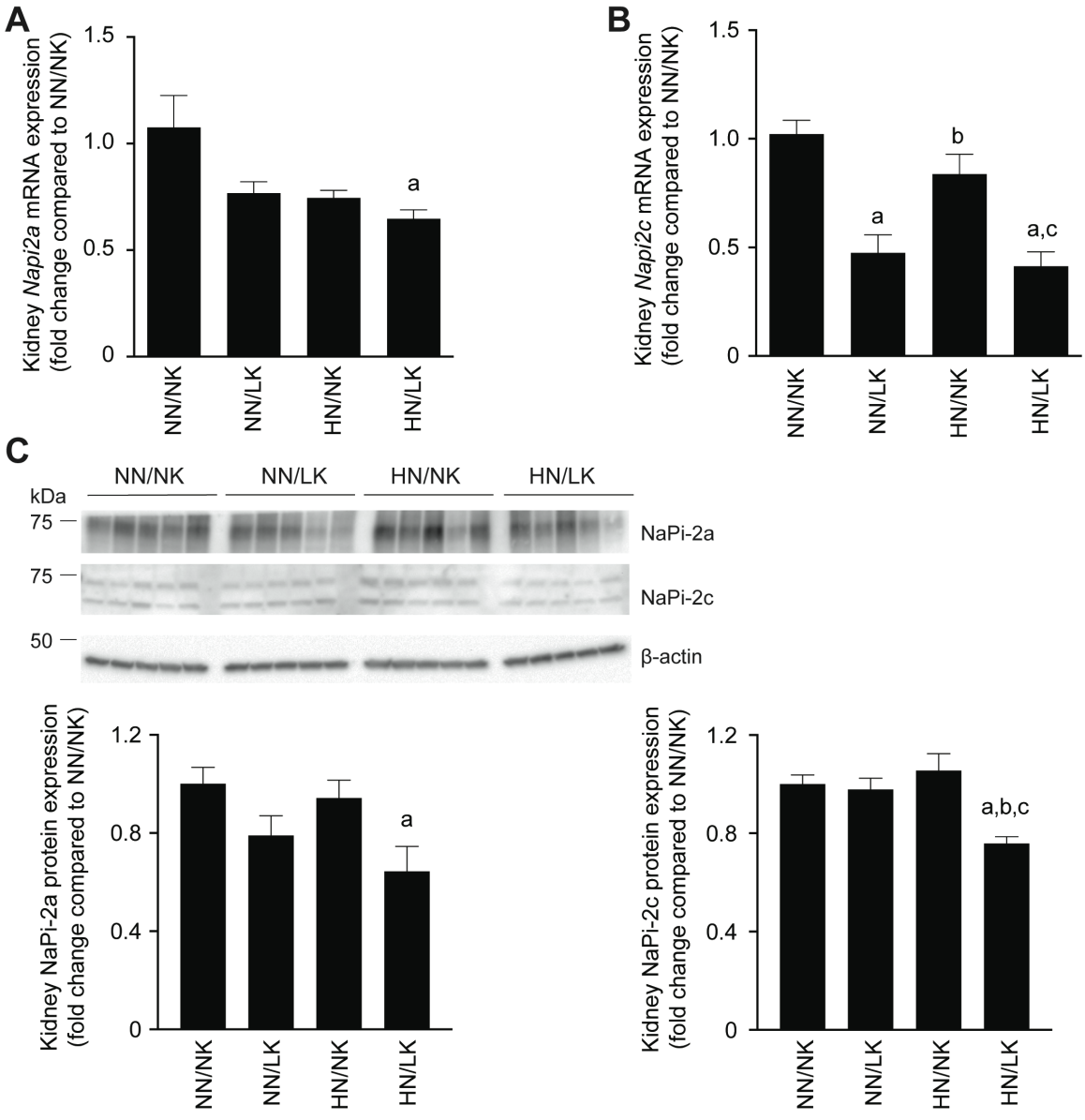

Figure 6 | Effect of dietary Na^+ and K^+ intake on renal Pi transporters.

(**A** and **B**) Relative mRNA expression levels (corrected for GAPDH) are shown for *Napi2a* (**A**) and *Napi2c* (**B**) in the kidney. Data are shown as mean +/- SEM (n=10). (**C**) Immunoblot of NaPi-2a and Napi-2c in kidney cortex from mice fed the indicated diet (right panel). (**D**) Bargraph of the densitometry shows relative NaPi-2a (left panel) and NaPi-2c (right panel) protein expression as mean +/- SEM (n=5). [a] = $p<0.05$ compared to NN/NK, [b] = $p<0.05$ compared to NN/LK.

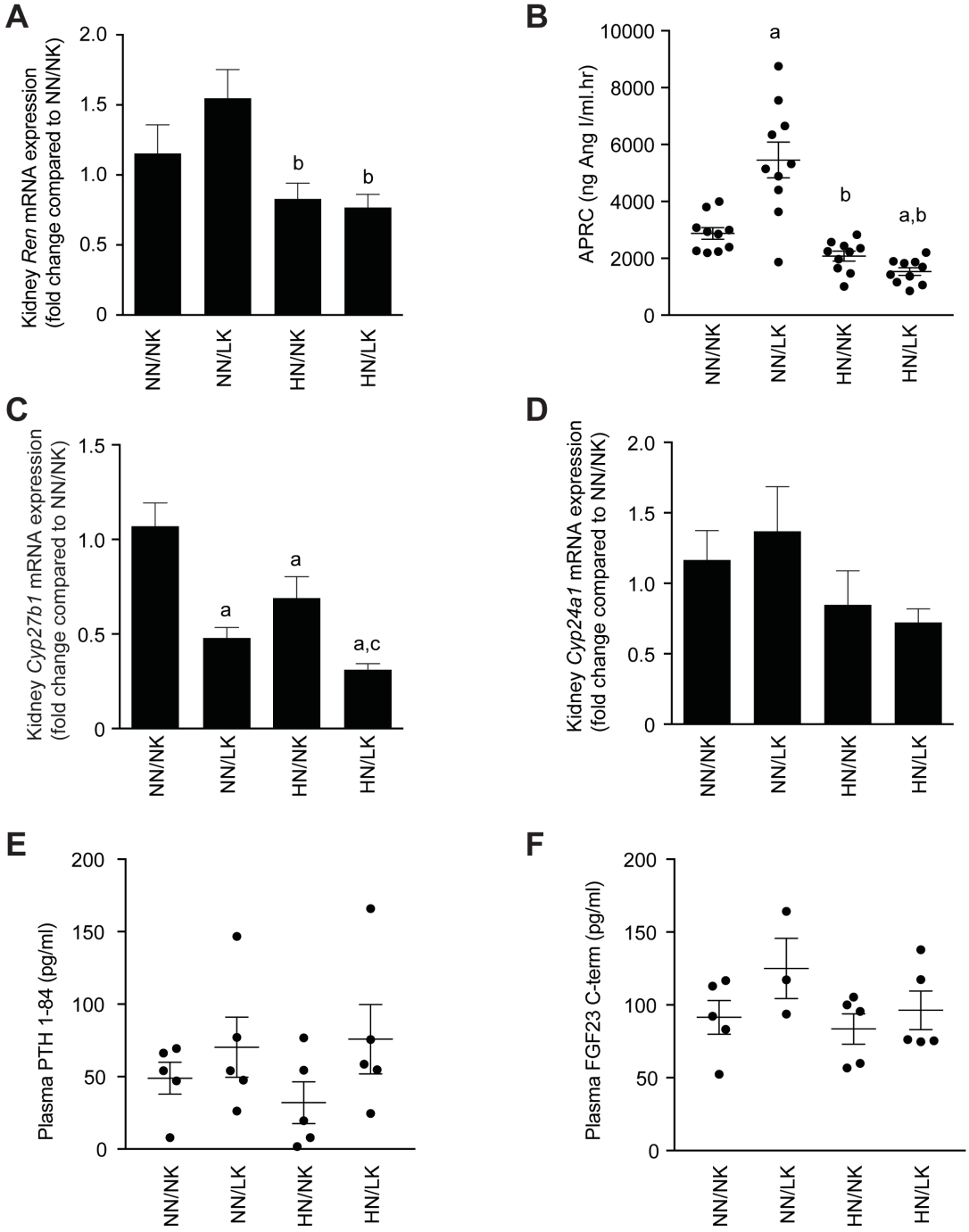

Figure 7 | Hormonal regulation upon changes in dietary Na^+ and K^+ intake.

Relative mRNA expression levels (corrected for GAPDH) are shown for *renin* (**A**), *Cyp27b1* (**C**), and *Cyp24a1* (**D**) in the kidney. Data are shown as mean +/- SEM (n=10). (**B**) Active plasma renin concentration (APRC) is measured as the amount of angiotensin I (Ang I) generated per volume per time in the presence of excess angiotensinogen. Data are shown as mean +/- SEM (n=10). Significance is indicated as: [a] = $p<0.05$ compared to NN/NK, [b] = $p<0.05$ compared to NN/LK, and [c] = $p<0.05$ compared to HN/NK. (**E-F**) Plasma PTH (**E**) and FGF23 (**F**) levels were measured in the different groups of mice. Data represents single values and depicts mean +/- SEM (n=3-5).

Discussion

The present study demonstrates that a diet containing high Na^+ with low K^+ can have significant effects on renal Ca^{2+} handling, while not affecting the Mg^{2+} balance. Serum and urine Mg^{2+} levels were not changed upon 4 days of diet. In contrast, the urinary Ca^{2+} excretion was significantly enhanced by high Na^+ intake, which was aggravated upon lowering dietary K^+ in combination with high Na^+. The latter also resulted in decreased serum Ca^{2+} levels. In addition, there was a significant increase in urinary Pi excretion upon high Na^+ intake. This study provides more insight into the effects of an altered Na^+ and K^+ intake on renal Ca^{2+}, Mg^{2+}, and Pi handling and offers further insight into the observed molecular changes in the kidney.

There is a growing body of evidence demonstrating that dietary K^+ intake associates inversely with blood pressure, often as strong as the positive correlation with dietary salt (1, 2, 17, 21, 31, 34). Importantly, it has recently been postulated that low blood K^+ levels are a key regulator of renal Na^+ reabsorption through stimulation of NCC-mediated Na^+ transport in the DCT (53). Our study demonstrated that low dietary K^+ intake enhances pNCC abundance in both NN/LK and HN/LK conditions, in line with a previous study by Terker *et al.* (53). In order to preserve extracellular fluid (ECF) volume, hence blood pressure, NCC is phosphorylated and activated via the renin-angiotensin-aldosterone system (RAAS) during dietary salt restriction (53). We showed an enhanced NCC phosphorylation despite low RAAS activation at HN/LK condition. Suppressed activation of RAAS was validated by decreased APRC in both HN/NK and HN/LK conditions. Together, this indicates that the effect of K^+ deficiency is more powerful than ECF volume by controlling Na^+ reabsorption in the DCT. High dietary K^+ was shown to suppress NCC phosphorylation during low Na^+ conditions likely to preserve kaliuresis (57).

Next to regulating Na^+ reabsorption, the DCT is also the main segment of active Mg^{2+} transport. The Mg^{2+} permeable channel TRPM6 is considered the gatekeeper of the Mg^{2+} balance as it determines the final urinary Mg^{2+} excretion (59). Importantly, our study showed that high Na^+ and/or K^+ deficiency does not affect Mg^{2+} transport in the DCT in a similar way as Na^+ transport, suggesting that the signaling pathway affecting NCC function is not linked to TRPM6-mediated transport. In contrast, a previous study demonstrated increased urinary Mg^{2+} excretion in rats fed a high Na^+ diet (29). This discrepancy could be due to the period of the diets (7 days versus 4 days), suggesting a time-dependent effect. A high Na^+ diet likely reduces paracellular Mg^{2+} transport in the proximal tubule and the TAL, resulting in an increased distal delivery of Mg^{2+} that is subsequently responsible for the observed upregulation of TRPM6. This could be the first defense mechanism to maintain blood Mg^{2+} levels constant.

While the various diets had no major effect on renal Mg^{2+} handling, there were prominent outcomes on urinary Ca^{2+} excretion and serum Ca^{2+} levels. Ca^{2+} homeostasis is maintained through the interplay between the intestines, bone, and kidney. Dietary Ca^{2+} is absorbed via the intestine into the blood, subsequently filtered by the glomerulus and reabsorbed along the nephron or stored in bone. The amount of filtered Ca^{2+} that is not reabsorbed along the nephrons will be excreted in the urine, demonstrating the important role of the kidney in the Ca^{2+} balance. An inappropriately high amount of urinary Ca^{2+} excretion, also known as hypercalciuria, contributes to the development of osteoporosis and kidney stone formation (4, 13). It has been established that a high salt diet induces hypercalciuria (12, 16), and that restricted salt intake is often used for prevention of kidney stones recurrence, particularly in cases of Ca^{2+}-containing stones (14, 30, 43, 47). Together, there is a clinical association between salt intake, hypertension, hypercalciuria and increased risk of kidney stones (10, 55). Interestingly, our study reveals a rapid renal response to dietary changes as inappropriate loss of urinary Ca^{2+} was observed in the HN/LK diet group after 4 days. Furthermore, urinary Pi excretion follows the same trend and is also significantly elevated in the HN/LK-fed mice. This is particularly interesting given the fact that ~10% of all kidney stones are calcium-phosphate stones (61). Our findings demonstrated that short-term dietary changes can already result in hypercalciuria and phosphaturia, which are important risk factors for stone formation. There is an increasing interest in dietary intervention for kidney stone prevention and a diet high in K^+ was recently associated with a lower risk of kidney stones (18). Future studies should aim at understanding the underlying molecular effects of low salt and high K^+ diet on progression of age-related bone loss and development of kidney stones.

The effect on urinary Ca^{2+} and Pi excretion suggests that the high Na^+/low K^+ diet initially affects proximal tubular reabsorption. It is widely assumed that the degree of hypercalciuria increases proportionately with the amount of Na^+ excreted in the urine and that dietary Na^+ restriction can decrease urinary Ca^{2+} excretion in both stone formers and healthy individuals (28, 37, 47, 52, 54). Earlier micropuncture studies have also demonstrated that Ca^{2+} reabsorption correlates with Na^+ reabsorption along the proximal tubule (39). Our study now demonstrated a reduced NHE3 expression, which indicates that Na^+ reabsorption in the proximal tubule could be reduced. Though, there was no increased urinary Na^+ excretion in the HN/LK group compared to high Na^+ diet alone, while urinary Ca^{2+} was significantly enhanced upon dietary K^+ depletion in combination with high Na^+ (HN/LK). This suggests an additional effect of low plasma K^+ levels on renal Ca^{2+} handling, next to the proposed Na^+-dependent Ca^{2+} reabsorption in the proximal tubule (51). We propose that the TAL-mediated reabsorption could be altered as a result of low K^+ diet. Both groups of mice, either NN/LK or HN/LK, have lower NKCC2 and claudin-16 expression.

Therefore, we propose that the high Na^+ diet alone mainly affects proximal tubular reabsorption via extracellular fluid expansion, resulting in increased urinary Ca^{2+} and Pi excretion. But the aggravated hypercalciuria in HN/LK animals might be due to a combined effect on the proximal tubule and TAL, which could not be completely compensated by the DCT. Furthermore, Terker *et al.* showed that NCC activation plays an essential role in the Ca^{2+} excretion under low K^+ condition. NCC knockout mice exhibited a diminished urinary Ca^{2+} excretion upon receiving a HN/LK diet (53). Our study demonstrated that $CaBP_{28k}$ protein levels were significantly enhanced in the high Na^+ groups, suggesting a compensatory mechanism for increased Ca^{2+} transport in the DCT. However, there was no change in expression of the apical Ca^{2+} channel TRPV5. Though, it should be noted that expression changes do not necessarily reflect alterations in protein function and transport capacity.

The body usually compensates for urinary Ca^{2+} loss by increased intestinal absorption of Ca^{2+}. Importantly, TRPV6 expression was not changed in duodenum, the main site for active (regulated) Ca^{2+} absorption. However, we demonstrated downregulation of renal *Cyp27b1*, encoding for 25-hydroxyvitamin D_3 1-alpha-hydroxylase (1α-hydroxylase), in the groups receiving either a low K^+ diet (NN/LK) or high Na^+ diet (HN/NK), or a combination diet (HN/LK). The 1α-hydroxylase is responsible for the generation of active vitamin D, which in turn acts towards increasing serum Ca^{2+} levels. Vitamin D can act towards increasing serum Ca^{2+} levels by stimulating intestinal Ca^{2+} absorption, renal Ca^{2+} reabsorption, and Ca^{2+} release from bone (19). Lower levels of this enzyme could partly explain the unchanged TRPV5 and TRPV6 mRNA expression despite extreme hypercalciuria. The *Cyp27b1* expression in the HN/LK group was even significantly lower than high Na^+ alone (HN/NK), in line with an aggravated hypercalciuria.

Interestingly, the trend of *Cyp27b1* expression coincided with that of *Napi2c* in the different dietary groups, as well as *Napi2a* downregulation in the HN/LK group. NaPi-2a and NaPi-2c protein levels were also significantly reduced in this group, which is in line with the phosphaturic response upon a HN/LK diet. Of note, it is proposed that the abundance of NaPi-2a protein reflects the capacity of the kidney to reabsorb Pi (5, 32). In contrast to our results, previous studies reported a significant decrease in NaPi-2c protein abundance upon longer (14 days) dietary K^+-deficiency in rats and mice, while the abundance of NaPi-2a increased (8, 62). This discrepancy could be due to the different dietary time frames (4 vs. 14 days) as we did not observe hyperphosphaturia or hypophosphatemia upon diet-induced hypokalemia by the low K^+ diet alone. The lack of changes in urinary or plasma Pi levels could also be explained by the significantly elevated APRC in the NN/LK group, which induces high angiontensin II levels that in turn stimulate proximal tubular reabsorption of Na^+ and other electrolytes.

In addition, it would be interesting to examine the effect of the diets on serum FGF23 and PTH levels. There is a clear interrelationship between hormonal control of Ca^{2+} and Pi handling, which involves the PTH-FGF23-vitamin D axis (6). While vitamin D is known to regulate intestinal Pi absorption, it has not been established whether vitamin D is directly involved in the regulation of renal Pi reabsorption. There are vitamin D-responsive elements in human genes encoding NaPi-2a and NaPi-2c, but data regarding its effect on expression have remained controversial so far (11, 20, 27). Vitamin D is known to act in concert with FGF23 and PTH to control renal Pi and Ca^{2+} reabsorption. For example, FGF23 can have instant effects on Pi homeostasis through reduction of renal NaPi-2a and *Cyp27b1* levels (46). Interestingly, it was recently shown in mice deficient in *Fgf23* that FGF23 can regulate renal Na^+ reabsorption via altering NCC expression and function (3). We have examined the effect of the diets on serum FGF23 and PTH levels, but did not find changes in response to the diets. Future studies should increase our understanding of the role of PTH-FGF23-vitamin D axis in high Na^+ and/or low K^+ diet-induced changes in electrolyte handling.

In conclusion, during short-term modification of Na^+ and K^+ intake, the kidney rapidly develops adaptation with corresponding changes in urinary electrolyte excretion. Our results suggest that instant dietary modifications have primary effects on proximal tubular reabsorption with a compensatory response in the DCT. As the majority of Ca^{2+} and Pi is reabsorbed in the proximal tubule, the distal part of the nephron is unable to recover for the excessive loss, while the mechanism is sufficient to maintain Mg^{2+} homeostasis.

Acknowledgements

The authors thank Anique ter Braake, Iza Peilouw, and Elco Eidhof for their assistance with the animal experiments.

Grants

This study was financially supported by the Netherlands Organization for Scientific Research (VENI 863.13.010 and VICI 016.130.668) and the Dutch Kidney Foundation (PHD12.14, CP16.01).

Disclosures

No conflicts of interest, financial or otherwise, are declared by the authors.

Author contribution

J.W., O.A.T., J.G.J.H., and R.J.M.B. conceived and designed the research; J.W., O.A.T., and C.B. performed the experiments; J.W. and O.A.T. analyzed the data and drafted the manuscript; A.H.J.D. performed the APRC analysis. E.J.H., J.G.J.H., and R.J.M.B. edited, revised and approved the manuscript. Funding acquisition is done by J.W., J.G.J.H., and R.J.M.B.

References

1. Aburto NJ, Hanson S, Gutierrez H, Hooper L, Elliott P, Cappuccio FP. Effect of increased potassium intake on cardiovascular risk factors and disease: systematic review and meta-analyses. *BMJ* 346: f1378–f1378, 2013.
2. Adrogué HJ, Madias NE. Sodium and potassium in the pathogenesis of hypertension. *N Engl J Med* 356: 1966–1978, 2007.
3. Andrukhova O, Slavic S, Smorodchenko A, Zeitz U, Shalhoub V, Lanske B, Pohl EE, Erben RG. FGF23 regulates renal sodium handling and blood pressure. *EMBO Mol Med* 6: 744–759, 2014.
4. Asplin JR, Donahue S, Kinder J, Coe FL. Urine calcium excretion predicts bone loss in idiopathic hypercalciuria. *Kidney Int* 70: 1463–1467, 2006.
5. Beck L, Karaplis AC, Amizuka N, Hewson AS, Ozawa H, Tenenhouse HS. Targeted inactivation of Npt2 in mice leads to severe renal phosphate wasting, hypercalciuria, and skeletal abnormalities. *Proc Natl Acad Sci USA* 95: 5372–5377, 1998.
6. Blau JE, Collins MT. The PTH-Vitamin D-FGF23 axis. *Rev Endocr Metab Disord* 16: 165–174, 2015.
7. Boyden LM, Choi M, Choate KA, Nelson-Williams CJ, Farhi A, Toka HR, Tikhonova IR, Bjornson R, Mane SM, Colussi G, Lebel M, Gordon RD, Semmekrot BA, Poujol A, Välimäki MJ, De Ferrari ME, Sanjad SA, Gutkin M, Karet FE, Tucci JR, Stockigt JR, Keppler-Noreuil KM, Porter CC, Anand SK, Whiteford ML, Davis ID, Dewar SB, Bettinelli A, Fadrowski JJ, Belsha CW, Hunley TE, Nelson RD, Trachtman H, Cole TRP, Pinsk M, Bockenhauer D, Shenoy M, Vaidyanathan P, Foreman JW, Rasoulpour M, Thameem F, Al-Shahrouri HZ, Radhakrishnan J, Gharavi AG, Goilav B, Lifton RP. Mutations in kelch-like 3 and cullin 3 cause hypertension and electrolyte abnormalities. *Nature* 482: 98–102, 2012.
8. Breusegem SY, Takahashi H, Giral-Arnal H, Wang X, Jiang T, Verlander JW, Wilson P, Miyazaki-Anzai S, Sutherland E, Caldas Y, Blaine JT, Segawa H, Miyamoto K-I, Barry NP, Levi M. Differential regulation of the renal sodium-phosphate cotransporters NaPi-IIa, NaPi-IIc, and PiT-2 in dietary potassium deficiency. *Am J Physiol Renal Physiol* 297: F350–61, 2009.
9. Campbell DJ, Nussberger J, Stowasser M, Danser AHJ, Morganti A, Frandsen E, Ménard J. Activity assays and immunoassays for plasma Renin and prorenin: information provided and precautions necessary for accurate measurement. *Clin Chem* 55: 867–877, 2009.
10. Cappuccio FP, Kalaitzidis R, Duneclift S, Eastwood JB. Unravelling the links between calcium excretion, salt intake, hypertension, kidney stones and bone metabolism. *J Nephrol* 13: 169–177, 2000.
11. Capuano P, Radanovic T, Wagner CA, Bacic D, Kato S, Uchiyama Y, St-Arnoud R, Murer H, Biber J. Intestinal and renal adaptation to a low-Pi diet of type II NaPi cotransporters in vitamin D receptor- and 1alphaOHase-deficient mice. *Am J Physiol, Cell Physiol* 288: C429–34, 2005.
12. Cirillo M, Ciacci C, Laurénzi M, Mellone M, Mazzacca G, De Santo NG. Salt intake, urinary sodium, and hypercalciuria. *Miner Electrolyte Metab* 23: 265–268, 1997.
13. Coe FL, Worcester EM, Evan AP. Idiopathic hypercalciuria and formation of calcium renal stones. *Nature Reviews Nephrology* 12: 519–533, 2016.
14. Colussi G, Surian M, De Ferrari ME, Pontoriero G, Rombolà G, Brando B, Malberti F, Cosci P, Aroldi A, Castelnovo C. Relationship between sodium intake, proximal tubular function and calcium excretion in normal subjects and in idiopathic hypercalciuria. *Proc Eur Dial Transplant Assoc* 20: 455–459, 1983.
15. Custer M, Lötscher M, Biber J, Murer H, Kaissling B. Expression of Na-P(i) cotransport in rat kidney: localization by RT-PCR and immunohistochemistry. *Am J Physiol* 266: F767–74, 1994.
16. Damasio PCG, Amaro CRPR, Cunha NB, Pichutte AC, Goldberg J, Padovani CR, Amaro JL. The role of salt abuse on risk for hypercalciuria. *Nutr J* 10: 3, 2011.
17. Ekmekcioglu C, Elmadfa I, Meyer AL, Moeslinger T. The role of dietary potassium in hypertension and diabetes. *J Physiol Biochem* 72: 93–106, 2016.
18. Ferraro PM, Mandel EI, Curhan GC, Gambaro G, Taylor EN. Dietary Protein and Potassium, Diet-Dependent Net Acid Load, and Risk of Incident Kidney Stones. *Clin J Am Soc Nephrol* 11: 1834–1844, 2016.
19. Fleet JC. The role of vitamin D in the endocrinology controlling calcium homeostasis. *Mol. Cell.*

Endocrinol. (April 9, 2017). doi: 10.1016/j.mce.2017.04.008.

20. Friedlaender MM, Wald H, Dranitzki-Elhalel M, Zajicek HK, Levi M, Popovtzer MM. Vitamin D reduces renal NaPi-2 in PTH-infused rats: complexity of vitamin D action on renal P(i) handling. *Am J Physiol Renal Physiol* 281: F428–33, 2001.
21. Geleijnse JM, Kok FJ, Grobbee DE. Blood pressure response to changes in sodium and potassium intake: a metaregression analysis of randomised trials. *J Hum Hypertens* 17: 471–480, 2003.
22. Gong Y, Renigunta V, Himmerkus N, Zhang J, Renigunta A, Bleich M, Hou J. Claudin-14 regulates renal Ca^{++} transport in response to CaSR signalling via a novel microRNA pathway. *EMBO J* 31: 1999–2012, 2012.
23. Hadchouel J, Ellison DH, Gamba G. Regulation of Renal Electrolyte Transport by WNK and SPAK-OSR1 Kinases. *Annu Rev Physiol* 78: 367–389, 2016.
24. Havas S, Roccella EJ, Lenfant C. Reducing the public health burden from elevated blood pressure levels in the United States by lowering intake of dietary sodium. *Am J Public Health* 94: 19–22, 2004.
25. Hoenderop JG, Hartog A, Stuiver M, Doucet A, Willems PH, Bindels RJ. Localization of the epithelial Ca(2+) channel in rabbit kidney and intestine. *J Am Soc Nephrol* 11: 1171–1178, 2000.
26. Hou J, Goodenough DA. Claudin-16 and claudin-19 function in the thick ascending limb. *Curr Opin Nephrol Hypertens* 19: 483–488, 2010.
27. Kido S, Kaneko I, Tatsumi S, Segawa H, Miyamoto K-I. Vitamin D and type II sodium-dependent phosphate cotransporters. *Contrib Nephrol* 180: 86–97, 2013.
28. KLEEMAN CR, BOHANNAN J, BERNSTEIN D, LING S, MAXWELL MH. EFFECT OF VARIATIONS IN SODIUM INTAKE ON CALCIUM EXCRETION IN NORMAL HUMANS. *Proc Soc Exp Biol Med* 115: 29–32, 1964.
29. Lee C-T, Lien Y-HH, Lai L-W, Ng H-Y, Chiou TT-Y, Chen H-C. Variations of dietary salt and fluid modulate calcium and magnesium transport in the renal distal tubule. *Nephron Physiol* 122: 19–27, 2012.
30. Martini LA, Cuppari L, Colugnati FA, Sigulem DM, Szejnfeld VL, Schor N, Heilberg IP. High sodium chloride intake is associated with low bone density in calcium stone-forming patients. *Clin Nephrol* 54: 85–93, 2000.
31. Mente A, O'Donnell MJ, Rangarajan S, McQueen MJ, Poirier P, Wielgosz A, Morrison H, Li W, Wang X, Di C, Mony P, Devanath A, Rosengren A, Oguz A, Zatonska K, Yusufali AH, Lopez-Jaramillo P, Avezum A, Ismail N, Lanas F, Puoane T, Diaz R, Kelishadi R, Iqbal R, Yusuf R, Chifamba J, Khatib R, Teo K, Yusuf S, PURE Investigators. Association of urinary sodium and potassium excretion with blood pressure. *N Engl J Med* 371: 601–611, 2014.
32. Murer H, Hernando N, Forster I, Biber J. Proximal tubular phosphate reabsorption: molecular mechanisms. *Physiol Rev* 80: 1373–1409, 2000.
33. Muto S, Hata M, Taniguchi J, Tsuruoka S, Moriwaki K, Saitou M, Furuse K, Sasaki H, Fujimura A, Imai M, Kusano E, Tsukita S, Furuse M. Claudin-2-deficient mice are defective in the leaky and cation-selective paracellular permeability properties of renal proximal tubules. *Proc Natl Acad Sci USA* 107: 8011–8016, 2010.
34. O'Donnell M, Mente A, Rangarajan S, McQueen MJ, Wang X, Liu L, Yan H, Lee SF, Mony P, Devanath A, Rosengren A, Lopez-Jaramillo P, Diaz R, Avezum A, Lanas F, Yusoff K, Iqbal R, Ilow R, Mohammadifard N, Gulec S, Yusufali AH, Kruger L, Yusuf R, Chifamba J, Kabali C, Dagenais G, Lear SA, Teo K, Yusuf S, PURE Investigators. Urinary sodium and potassium excretion, mortality, and cardiovascular events. *N Engl J Med* 371: 612–623, 2014.
35. Pacheco-Alvarez D, Cristóbal PS, Meade P, Moreno E, Vázquez N, Muñoz E, Díaz A, Juárez ME, Giménez I, Gamba G. The Na+:Cl- cotransporter is activated and phosphorylated at the amino-terminal domain upon intracellular chloride depletion. *J Biol Chem* 281: 28755–28763, 2006.
36. Pedersen NB, Hofmeister MV, Rosenbaek LL, Nielsen J, Fenton RA. Vasopressin induces phosphorylation of the thiazide-sensitive sodium chloride cotransporter in the distal convoluted tubule. *Kidney Int* 78: 160–169, 2010.
37. Phillips MJ, Cooke JN. Relation between urinary calcium and sodium in patients with idiopathic hypercalciuria. *Lancet* 1: 1354–1357, 1967.
38. Piala AT, Moon TM, Akella R, He H, Cobb MH, Goldsmith EJ. Chloride sensing by WNK1

involves inhibition of autophosphorylation. *Sci Signal* 7: ra41–ra41, 2014.

39. Poujeol P, Chabardes D, Roinel N, de Rouffignac C, Philippe P, Malorey P. Influence of extracellular fluid volume expansion on magnesium, calcium and phosphate handling along the rat nephron. *Pflugers Arch* 365: 203–211, 1976.
40. Rengarajan S, Lee DH, Oh YT, Delpire E, Youn JH, McDonough AA. Increasing plasma [K+] by intravenous potassium infusion reduces NCC phosphorylation and drives kaliuresis and natriuresis. *Am J Physiol Renal Physiol* 306: F1059–68, 2014.
41. Resnick LM, Bardicef O, Altura BT, Alderman MH, Altura BM. Serum ionized magnesium: relation to blood pressure and racial factors. *Am J Hypertens* 10: 1420–1424, 1997.
42. Rinner MD, Spliet-van Laar L, Kromhout D. Serum sodium, potassium, calcium and magnesium and blood pressure in a Dutch population. *J Hypertens* 7: 977–981, 1989.
43. Robertson WG. Dietary recommendations and treatment of patients with recurrent idiopathic calcium stone disease. *Urolithiasis* 44: 9–26, 2016.
44. Sacks FM, Svetkey LP, Vollmer WM, Appel LJ, Bray GA, Harsha D, Obarzanek E, Conlin PR, Miller ER, Simons-Morton DG, Karanja N, Lin PH, DASH-Sodium Collaborative Research Group. Effects on blood pressure of reduced dietary sodium and the Dietary Approaches to Stop Hypertension (DASH) diet. DASH-Sodium Collaborative Research Group. *N Engl J Med* 344: 3–10, 2001.
45. Segawa H, Onitsuka A, Furutani J, Kaneko I, Aranami F, Matsumoto N, Tomoe Y, Kuwahata M, Ito M, Matsumoto M, Li M, Amizuka N, Miyamoto K-I. Npt2a and Npt2c in mice play distinct and synergistic roles in inorganic phosphate metabolism and skeletal development. *Am J Physiol Renal Physiol* 297: F671–8, 2009.
46. Shimada T, Hasegawa H, Yamazaki Y, Muto T, Hino R, Takeuchi Y, Fujita T, Nakahara K, Fukumoto S, Yamashita T. FGF-23 is a potent regulator of vitamin D metabolism and phosphate homeostasis. *J Bone Miner Res* 19: 429–435, 2004.
47. Silver J, Rubinger D, Friedlaender MM, Popovtzer MM. Sodium-dependent idiopathic hypercalciuria in renal-stone formers. *Lancet* 2: 484–486, 1983.
48. Simon DB, Nelson-Williams C, Bia MJ, Ellison D, Karet FE, Molina AM, Vaara I, Iwata F, Cushner HM, Koolen M, Gainza FJ, Gitleman HJ, Lifton RP. Gitelman“s variant of Bartter”s syndrome, inherited hypokalaemic alkalosis, is caused by mutations in the thiazide-sensitive Na-Cl cotransporter. *Nat Genet* 12: 24–30, 1996.
49. Sorensen MV, Grossmann S, Roesinger M, Gresko N, Todkar AP, Barmettler G, Ziegler U, Odermatt A, Loffing-Cueni D, Loffing J. Rapid dephosphorylation of the renal sodium chloride cotransporter in response to oral potassium intake in mice. *Kidney Int* 83: 811–824, 2013.
50. Subramanya AR, Ellison DH. Distal convoluted tubule. *Clin J Am Soc Nephrol* 9: 2147–2163, 2014.
51. Sutton RA, Dirks JH. The renal excretion of calcium: a review of micropuncture data. *Can J Physiol Pharmacol* 53: 979–988, 1975.
52. Sutton RA, Walker VR. Responses to hydrochlorothiazide and acetazolamide in patients with calcium stones. Evidence suggesting a defect in renal tubular function. *N Engl J Med* 302: 709–713, 1980.
53. Terker AS, Zhang C, McCormick JA, Lazelle RA, Zhang C, Meermeier NP, Siler DA, Park HJ, Fu Y, Cohen DM, Weinstein AM, Wang W-H, Yang C-L, Ellison DH. Potassium modulates electrolyte balance and blood pressure through effects on distal cell voltage and chloride. *Cell Metab* 21: 39–50, 2015.
54. Ticinesi A, Nouvenne A, Maalouf NM, Borghi L, Meschi T. Salt and nephrolithiasis. *Nephrol Dial Transplant* 31: 39–45, 2016.
55. Timio F, Kerry SM, Anson KM, Eastwood JB, Cappuccio FP. Calcium urolithiasis, blood pressure and salt intake. *Blood Press* 12: 122–127, 2003.
56. Vallon V, Schroth J, Lang F, Kuhl D, Uchida S. Expression and phosphorylation of the Na+-Cl- cotransporter NCC in vivo is regulated by dietary salt, potassium, and SGK1. *Am J Physiol Renal Physiol* 297: F704–12, 2009.
57. van der Lubbe N, Moes AD, Rosenbaek LL, Schoep S, Meima ME, Danser AHJ, Fenton RA, Zietse R, Hoorn EJ. K+-induced natriuresis is preserved during Na+ depletion and accompanied by inhibition of the Na+-Cl- cotransporter. *Am J Physiol Renal Physiol* 305: F1177–88, 2013.
58. Vitari AC, Deak M, Morrice NA, Alessi DR. The WNK1 and WNK4 protein kinases that are

mutated in Gordon's hypertension syndrome phosphorylate and activate SPAK and OSR1 protein kinases. *Biochem J* 391: 17–24, 2005.

59. Voets T, Nilius B, Hoefs S, van der Kemp AWCM, Droogmans G, Bindels RJM, Hoenderop JGJ. TRPM6 forms the Mg2+ influx channel involved in intestinal and renal Mg2+ absorption. *J Biol Chem* 279: 19–25, 2004.
60. Wilson FH, Disse-Nicodème S, Choate KA, Ishikawa K, Nelson-Williams C, Desitter I, Gunel M, Milford DV, Lipkin GW, Achard JM, Feely MP, Dussol B, Berland Y, Unwin RJ, Mayan H, Simon DB, Farfel Z, Jeunemaitre X, Lifton RP. Human hypertension caused by mutations in WNK kinases. *Science* 293: 1107–1112, 2001.
61. Worcester EM, Coe FL. Nephrolithiasis. *Prim Care* 35: 369–91– vii, 2008.
62. Zajicek HK, Wang H, Puttaparthi K, Halaihel N, Markovich D, Shayman J, Béliveau R, Wilson P, Rogers T, Levi M. Glycosphingolipids modulate renal phosphate transport in potassium deficiency. *Kidney Int* 60: 694–704, 2001.

7

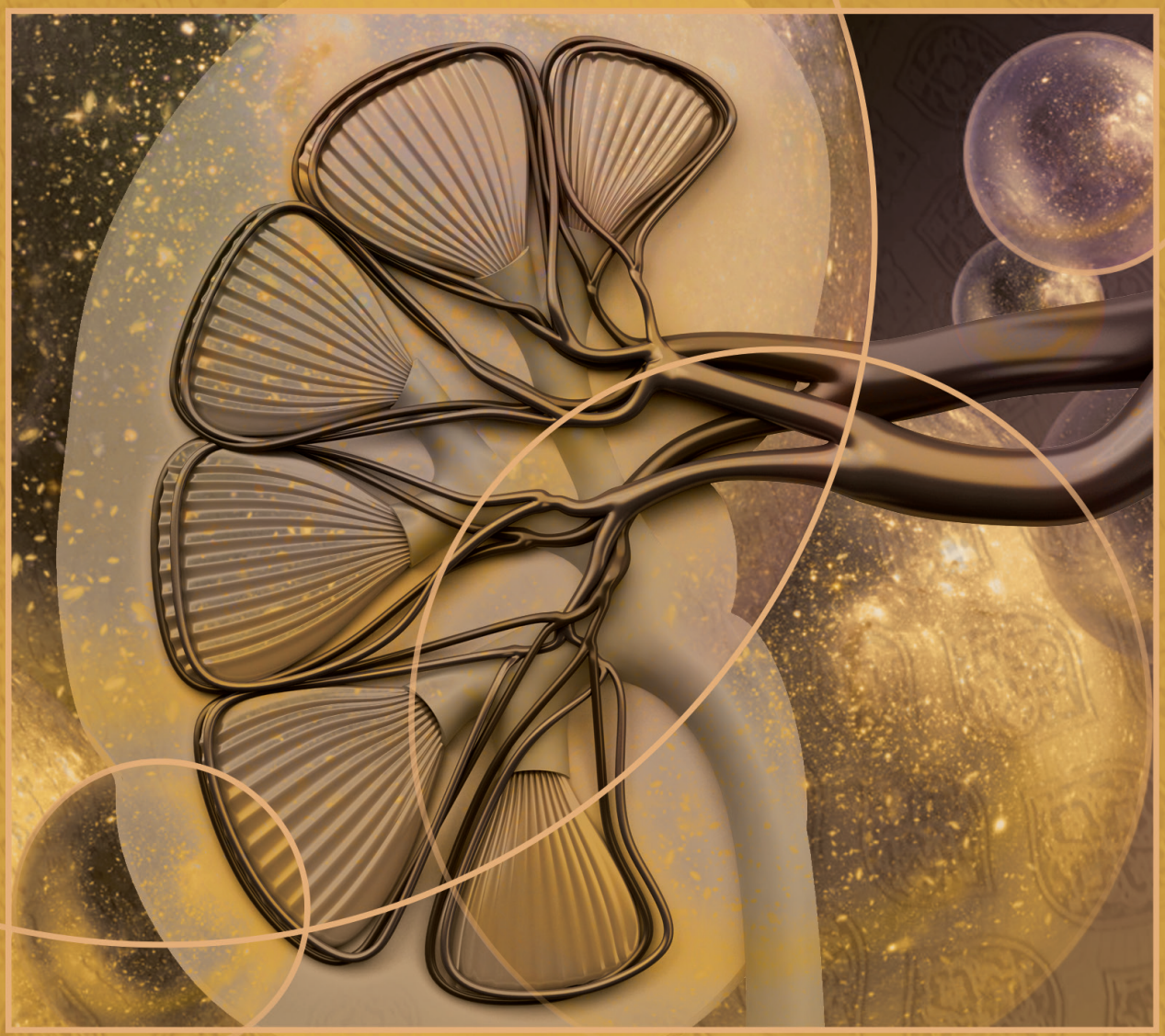

General discussion and summary

Electrolyte handling in the distal convoluted tubule

In the kidney, the distal part of the nephron that comprises the distal convoluted tubule (DCT), connecting tubule (CNT) and collecting duct (CD) plays a central role in maintaining the blood pressure by controlling the sodium (Na^+) reabsorption and potassium (K^+) secretion (Fig. 1) (5, 14, 16, 62). In the distal part of the nephron, Na^+ reabsorption primarily occurs through thiazide-sensitive NaCl co-transporter (NCC) (27) and residual Na^+ is reabsorbed by amiloride-sensitive epithelial Na^+ channel (ENaC) (62). The Na^+ reabsorption through ENaC is coupled to K^+ secretion via the renal outer medullary K^+ channel (ROMK) (59). NCC is expressed exclusively in the DCT with a robust expression in the early part of the DCT (DCT1) that decreases into the later part of the DCT (DCT2) (27, 49, 50, 67). The ENaC abundance increases gradually along the DCT2 and is highly expressed in the CNT and CD (6, 49, 92).

Na^+ reabsorption, through NCC, in the DCT1 determines the amount of Na^+ delivery to the downstream segments where the secretion of K^+ occurs (4). Therefore, NCC indirectly plays an important role in the regulation of K^+ secretion. This interplay between renal Na^+ and K^+ secretion is tightly regulated by the renin-angiotensin-aldosterone system (RAAS). Physiologically, the RAAS operates in the kidney to increase renal Na^+ retention in a hypovolemic condition (93). In short, renin is released from the kidney, which then cleaves angiotensinogen to produce angiotensin I that in turn is converted to angiotensin II (84). Subsequently, angiotensin II stimulates the secretion of aldosterone from the adrenal gland. During hypovolemia angiotensin II and aldosterone stimulate Na^+ reabsorption through activation of NCC and ENaC (23, 52, 88, 106). Additionally, aldosterone is also released upon an increase in plasma K^+ (hyperkalemia), favoring ROMK-mediated K^+ secretion from DCT2 onwards (107). This release occurs independent of the volemic state. Interestingly, NCC is not activated during hyperkalemia, even in hypovolemic state when Na^+ retention is desired (4, 84). Conversely, NCC is activated under hypokalemic conditions despite hypervolemia and decreased RAAS activation. NCC activation will reduce downstream tubular Na^+ delivery, thereby diminishing ENaC-mediated Na^+ transport and subsequently reduce K^+ secretion via ROMK. This mechanism controls the K^+ balance at the expense of Na^+ retention and increased blood pressure. Taken together, aldosterone can have a different mode of action in the distal part of the nephron upon concurrent changes in plasma K^+ and blood volume. This divergent function of aldosterone is referred to as the aldosterone paradox (4). Since angiotensin II is the hallmark of volume depletion and is not affected by plasma K^+ concentration, it is suggested to play an important role in mediating the distinctive response during hypovolemia and hyperkalemia.

The above-described key role of NCC in the regulation of Na^+ and K^+ is highlighted by

the molecular mechanisms underlying pseudohypoaldosteronism type 2 (familial hyperkalemic hypertension, FHHt), Gitelman syndrome and thiazide-type diuretics treatment. Patients with FHHt suffer from hypertension and hyperkalemia that results from gain-of-function of NCC (45, 85, 110, 113). This activation of NCC is a consequence of mutations in with no lysine (WNK) kinases, mainly WNK1 and WNK4, Kelch-like 3 (KLHL3), or Cullin 3 (*CUL3)* (7). Mutations in either of these genes results in phosphorylation of WNK kinases that leads to phosphorylation and thereby activation of two related proteins, SPAK (STE20/SPS1-related proline/alanine-rich kinase) and OSR1 (oxidative stress responsive protein type 1) (68, 85). Subsequently, SPAK and OSR1 kinases phosphorylate key residues in the amino (N)-terminal region of NCC, resulting in enhanced Na^+ reabsorption by increased transport activity of NCC (68). This leads to decreased Na^+ delivery to the downstream segments, thereby resulting in subsequent diminished K^+ secretion, which can explain the hyperkalemia in FHHt. The hypertension as well as the hyperkalemia disorders in FHHt patients can be corrected by a low dose of thiazide-type diuretics (42, 58, 77). Moreover, several guidelines recommend thiazide-type diuretics as first-line treatment for the management of hypertension, including in patients with FHHt (42, 77). Thiazide-type diuretics act by blocking NCC, thus increasing Na^+ delivery to the downstream segments of distal part of the nephron (27). Hence, more Na^+ is reabsorbed through ENaC which coincides with an increased K^+ secretion via ROMK, resulting in hypokalemia (Fig. 1) (59). Similarly, patients with Gitelman syndrome suffer from hypokalemia that can be explained by the loss-of-function mutations in the *NCC* gene (20, 34, 95) Recently, it has been shown that plasma K^+ levels, independent of hormonal effects, directly modulates the WNK-SPAK/OSR1-NCC cascade (102). The current molecular mechanism suggests that lower plasma K^+ levels hyperpolarize the DCT cell membrane, thereby driving chloride (Cl^-) efflux (101). Subsequently, a lower intracellular Cl^- concentration results in auto-phosphorylation of WNKs (102) that subsequently leads to activation of the SPAK/OSR1-NCC phosphorylation cascade (63, 73). There is accumulating evidence that a typical diet, containing high Na^+ and low K^+, activates NCC (36, 102) despite high Na^+ levels. Hence, the body attempts to maintain the K^+ balance at the expense of an increase in blood pressure, which could partly be responsible for the hypertension pandemic that is currently the most critical and expensive public health problem worldwide (84). Therefore, not only Na^+ restriction, but also K^+ supplementation, could be useful in the treatment to control the blood pressure.

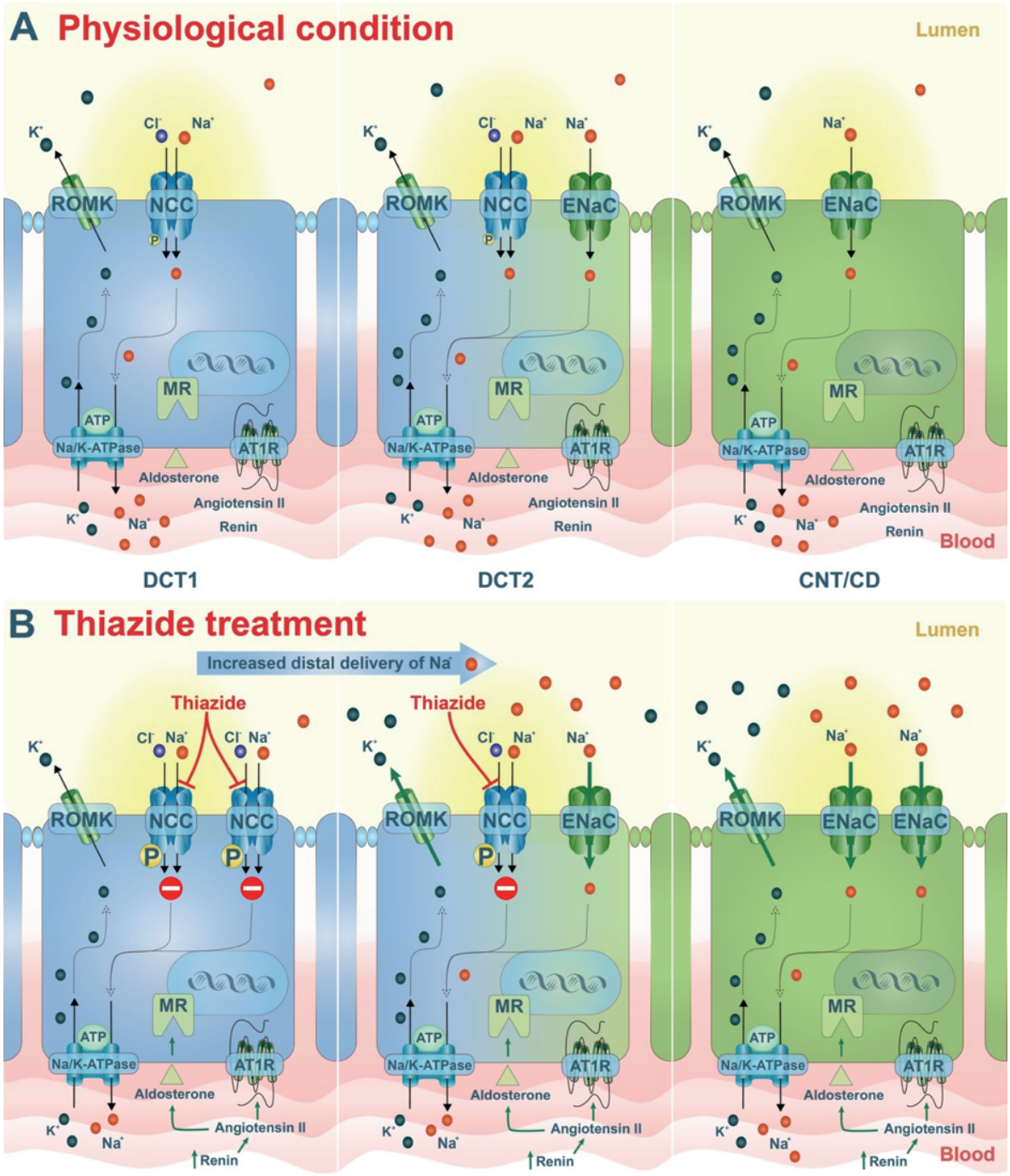

Figure 1 | Thiazide-induced Na^+ delivery and K^+ secretion in the distal part of the nephron.

(**A** and **B**) NCC is apically localized in epithelial cells lining the early part of the DCT (DCT1, blue), but its expression gradually decreases along the later part of the DCT (DCT2, blue-green), where it co-localizes with the epithelial Na^+ channel (ENaC) and renal outer medullary K^+ channel (ROMK). The ENaC expression increases gradually along the DCT2 and is robust in the connecting tubule (CNT, green) and collecting duct (CD, green). (**B**) Due to the inhibitory effect of thiazides on NCC activity, Na^+ delivery towards the DCT2, CNT and CD will increase. These segments will, therefore, reabsorb more Na^+ via ENaC. As a consequence, more K^+ is secreted by ROMK, ultimately resulting in decreased plasma K^+ levels. Thiazide-mediated NCC inhibition and subsequent decrease in plasma K^+ concentrations raise plasma renin and angiotensin II levels. Angiotensin II stimulates the secretion of aldosterone from the adrenal gland. Mineralocorticoid receptor (MR) is activated by the aldosterone. In addition, thiazide treatment increases both the abundance and activity of NCC and ENaC.

NCC in health and disease

The alternative splice variant of NCC (NCC_{SV})

Since the molecular cloning of human NCC in 1996, it has been shown that there are three isoforms of NCC present in the human kidney (53, 57, 96). While many studies over the past decades have emphasized the importance of NCC in electrolyte homeostasis and blood pressure control, these reports have focused on the shortest NCC isoform (NCC_3). The NCC isoform 1 and 2, collectively referred to as NCC splice variant (NCC_{SV}), remained unexplored. The NCC_{SV} is present in humans and higher primates, but it is not present in rodents (mouse and rat) as a result of the exon splicing. Generation of new antibodies specifically recognizing NCC_{SV} allowed us to demonstrate the presence of these isoforms at the apical membrane of the DCT, as well as in urinary extracellular vesicles (uEVs) (**Chapter 2**). The presence of NCC_{SV} in the uEVs was also confirmed by mass spectrometry. On average total NCC mRNA in the human kidney comprises ~45% of NCC_{SV} and ~55% of NCC_3. However, the ratio of NCC_{SV} to NCC_3 mRNA expression in human kidneys varied between 20-60%. These large differences in NCC_{SV} to NCC_3 ratio suggest that a splicing donor site at exon 20 (20a and 20b respectively) (56) is highly regulated. It has been shown that ~95% of human genes are alternatively spliced, including the *NCC* gene (69). The production of alternatively spliced mRNAs is diversely regulated by a variety of external stimuli. Mechanisms of alternative splicing are highly variable and not well understood (51). The differences in alternative spliced mRNAs can consequently impact abundance and/or function of a protein (51, 74), and are suggested to contribute to the development of various diseases, such as cancer and diabetes (2, 97, 100). In addition, altered splicing of genes is indicated to influence drug response (38).

In order to assess the role of NCC_{SV}, we have analyzed the NCC_{SV} and NCC_3 abundance in uEVs in several physiological (water loading; **Chapter 2**) and pathophysiological (essential hypertensive and calcineurin inhibitor-treated patients; **Chapters 3** and **5**) conditions. Our findings showed a robust decrease in expression of NCC_3, as well as NCC_{SV} protein, in uEVs in response to water loading (**Chapter 2**). Water loading will result in transient extracellular volume expansion and decrease in serum osmolality, which are known to deactivate RAAS and reduce arginine vasopressin (AVP, antidiuretic hormone) release (12, 71, 80, 86, 88-90, 105, 106). However, in response to hypovolemia, RAAS levels are increased to induce renal Na^+ reabsorption (83). AVP is mainly known for its water-retaining action on the CD by increasing the water channel aquaporin 2 (AQP2) abundance, phosphorylation, and membrane targeting (30). Vice versa, water loading is known to downregulate AQP2 to stimulate water excretion, hence decreasing the extra cellular volume (ECF) (98). Indeed, we showed that AQP2 abundance

in uEVs and urine osmolality was decreased after water loading. A growing body of evidence suggests an important role of AVP in activation of NCC_3 that may contribute to the Na^+ conservation in the DCT (64, 71). The decreased NCC_{SV} abundance in water-loaded subjects is likely a result of decline in RAAS levels and AVP release. Thus, our results demonstrate that NCC_{SV}, like NCC_3, is highly regulated under physiological condition.

The data presented in **Chapter 3** demonstrates that the NCC_{SV} also plays a role in pathophysiological conditions. Abundance of NCC_{SV} and NCC_3 in uEVs of essential hypertensive patients was increased upon chronic thiazide treatment, but not by valsartan. Valsartan is also a well-known anti-hypertensive drug that reduces blood pressure by antagonizing angiotensin II type I receptors (37). Our current data highlights that the blood pressure decrease correlates with NCC_{SV} abundance in uEVs and plasma K^+ levels of essential hypertensive patients treated with thiazides. As described above, the decline in plasma K^+ levels upon thiazide treatment might be explained by the increased distal delivery of Na^+ that results in increased K^+ secretion. Combination of the observations that NCC_{SV} is significantly expressed in the kidney, responsive to physiological stimuli such as water loading and involved in pathophysiological processes, denotes the key role of NCC_{SV} in renal salt handling.

Functional role of NCC_{SV}

Chapters 2 and **4** show that NCC_{SV} exhibits thiazide-sensitive Na^+ transport activity in both *Xenopus* oocytes and mammalian cells, similar to NCC_3. Recently, a novel phosphorylation site in NCC_{SV} at serine 811 (S811), solely present in NCC_{SV}, was identified (35). The lack of S811 in rodents and rabbit hampered the progress and interest towards further investigations (35). Our studies described in **Chapters 2** and **4** now reveal that NCC_{SV} S811 plays a key role in NCC_{SV} but also NCC_3 function (Fig. 2). First, a phosphorylation-deficient S811 mutant (NCC_{SV} S811A) showed decreased transport activity. *X. laevis* oocytes expressing NCC_{SV} S811A exhibited reduced $^{22}Na^+$-uptake compared to oocytes expressing wild-type NCC_{SV} (**Chapter 2**). This was confirmed in mammalian cells by fluorescence microscopy using the halide-sensitive YFP/mKate system as a measure for NCC activity (**Chapter 4**). Second, we demonstrated that co-expression of NCC_{SV} S811A and NCC_3 results in a dominant negative effect on NCC_3 function, while it does not affect the NCC abundance at the plasma membrane (**Chapter 4**). Together, these chapters indicate that S811 not only regulates NCC_{SV} activity, but also affects the function of NCC_3.

We postulate that S811 exerts its effect via altered phosphorylation of threonine residues 60 (T60) and 55 (T55) in NCC_{SV} and NCC_3. These N-terminal residues are key phosphorylation sites and essential for NCC activity (22, 68, 99, 116) and plasma membrane abundance (43, 114). This is highlighted by a loss-of-function mutation at T60 in *NCC* that is

linked to Gitelman syndrome (48, 114). Moreover, it has been shown that defective T60 phosphorylation corrects the phenotype of FHHt in mice (114). In NCC_3, T60 is postulated as dominant phosphorylation site as the non-phosphorylated form of T60 (T60A) inhibited phosphorylation of adjacent residues T46 and T55 (78). Additionally, it was shown that the T60A mutant strongly inhibits NCC_3 activity, while this was less prominent for the phosphorylation-deficient threonine 46 (T46A) and 55 (T55A) mutants (78). Several other studies have shown that T60 is an important site for NCC activity (68, 78, 114). Our findings demonstrate that S811, solely present in NCC_{SV}, has a dominant-negative regulatory role on Na^+ transport activity in both NCC_{SV} and NCC_3, as the S811A prevented the T60 and T55 phosphorylation in NCC_{SV} and NCC_3.

While it is known that T60 and T55 are phosphorylated via activation of WNK-SPAK signaling pathway (1, 68), the kinase involved in S811 phosphorylation remains to be elucidated. WNK4 inhibited NCC_{SV} and NCC_3 function independent of S811 (**Chapter 2**). Prediction software suggested that the amino acid sequence around S811 shows high similarity to a protein kinase A (PKA) consensus site. Therefore, potential hormones regulating the PKA pathway might be involved in regulating NCC_{SV}-mediated Na^+ reabsorption in DCT. There is a growing body of evidence demonstrating that NCC_3 abundance and phosphorylation is affected by protein kinase C (PKC) or PKA downstream of angiotensin II or AVP signaling, respectively (9, 64, 71, 90). After water loading, the decreased NCC_{SV} abundance in uEVs and urine osmolality indicates, at least in part, that PKA signaling pathway might be involved in NCC_{SV} regulation (**Chapter 2**). The effect of AVP is also demonstrated in the thick ascending limb of Henle's loop that expresses the type 2 vasopressin receptor (V_2R). Here, AVP stimulation leads to activation of cyclic AMP (cAMP) and PKA signaling that ultimately affects NKCC2 phosphorylation (109). Interestingly, V_2R has also been detected in DCT, and micropuncture studies have shown that AVP increases Na^+ absorption in DCT (9, 24, 25). The presented data in this thesis suggests that RAAS- as well as AVP-dependent signaling pathways might be involved in regulation of NCC_{SV}.

Regulation of NCC abundance at the plasma membrane

Another way to regulate Na^+ reabsorption in the kidney is to modulate NCC abundance at the plasma membrane. In **Chapter 4**, cell surface biotinylation of NCC-transfected cells revealed that a change in S811 phosphorylation of NCC_{SV} does not affect the abundance of NCC_{SV} at the plasma membrane, where NCC is functionally active. Moreover, there is no change in plasma membrane abundance of any of the NCC isoforms or mutants. These findings indicate that translocation of NCC to the plasma membrane or stability of NCC is not affected by S811; rather, intrinsic T60 and T55 phosphorylation of NCC is increased.

However, our study is in agreement with previous studies demonstrating that NCC_3 surface abundance is not affected by the phosphorylation status of T60 in *X. laevis* oocytes (**Chapter 4**) (68). Similarly, the triple mutation of T55, T60 and S73 to alanine did not significantly change the NCC_3 abundance at the plasma membrane (43). The relation between the T60 phosphorylation and membrane stability of NCC_3 has been postulated (114). Although, several studies demonstrated a decreased abundance of NCC_3 T60A in both the biotinylated fractions and input fraction, the ratio of biotinylated fractions to input was not reduced, suggesting unaltered abundance at the plasma membrane (43, 114).

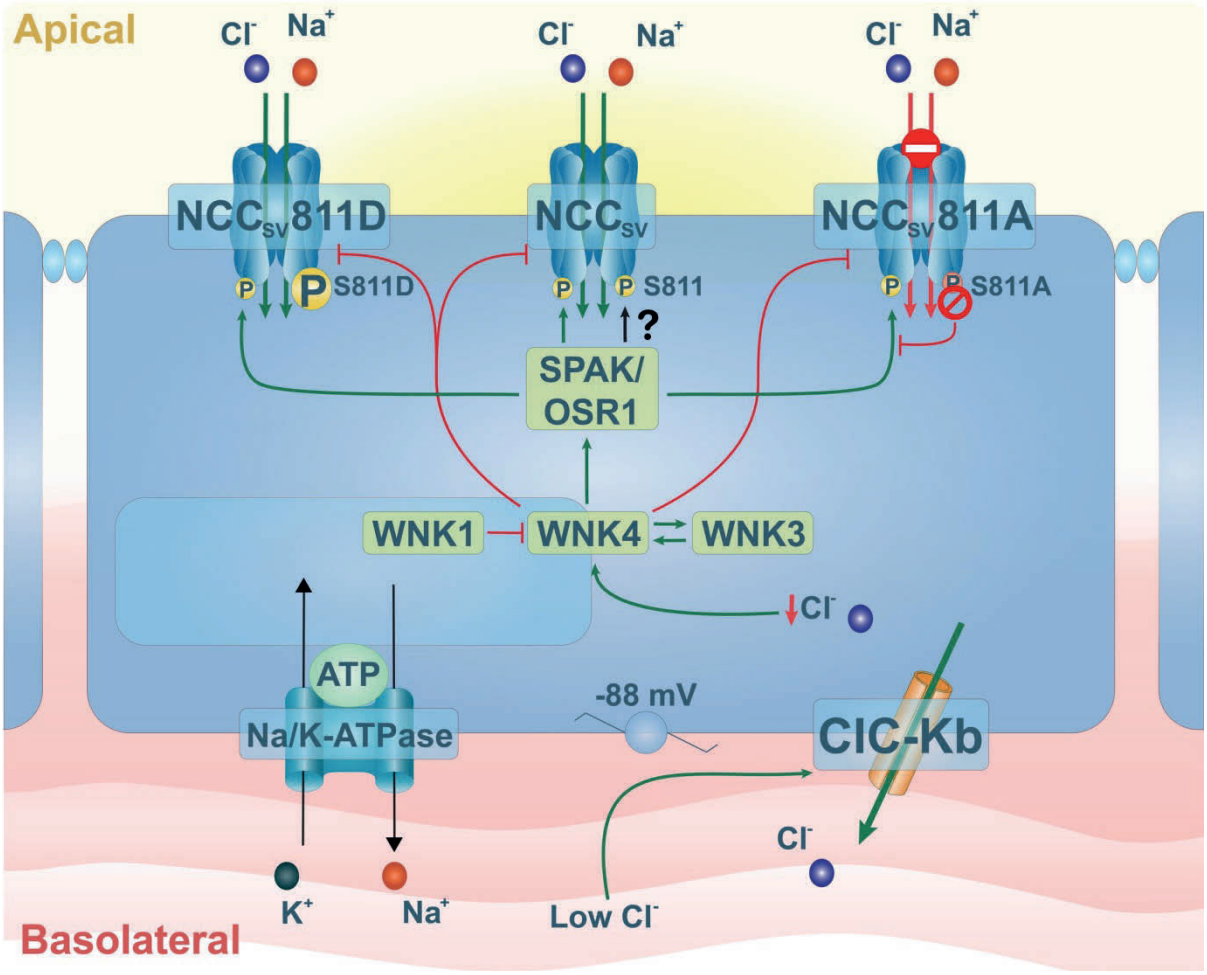

Figure 2 | Functional role of the novel phosphorylation site serine 811 (S811).

The amino (N)-terminal domain of NCC contains several key phosphorylation sites (T55/T66) that are essential for NCC activity and plasma membrane abundance. S811 acts as a dominant regulatory site for phosphorylation of T60 and T55 in NCC_{SV} and NCC_3. The various interactions of the NCC_{SV} regulatory pathway are shown as *green arrows* (stimulatory) or *red lines* (inhibitory). Phosphorylation is indicated with the symbol *P*. WNK4 (with no lysine kinase 4) is capable of activating SPAK (STE20/SPS1-related, proline alanine-rich kinase) and OSR1 (oxidative stress responsive protein type 1). Notably, the phosphorylation-deficient (S811A) mutant exhibits a decreased transport activity in NCC_{SV}. WNK4 inhibits the function of NCC_{SV} and both NCC_{SV} mutants independent of S811. The Cl^- channel CLC-Kb is responsible for efflux of Cl^-. In low Cl^- condition the intracellular Cl^- concentration decreases, which subsequently stimulates WNK-SPAK/OSR1 signaling.

NCC_{SV} and NCC_3 form hetero and homodimers

Chapter 4 describes the molecular mechanism by which NCC_{SV} S811 exerts a dominant-negative effect on NCC_3. Our data shows that both the constitutively phosphorylated and non-phosphorylated NCC_{SV} S811 mutants can form heterodimers with NCC_3, indicating that the effect of S811 on phosphorylation of NCC_3 can occur though interaction between the two isoforms. The phosphorylation status of S811 did not affect the dimerization of NCC_{SV} and NCC_3. Homodimerization of NCC_3 proteins has been proposed in previous studies (21), and it was also found that most NCC_3 proteins are present at the plasma membrane in a dimerized form (21, 33). However, previous studies observed the homodimerization of NCC_3 by using immunoblot analysis showing immunoreactive bands of ~130 kDa (monomer) and ~260 kDa (dimer) (21, 33, 79, 103). Importantly, this work shows for the first time that NCC_{SV} and NCC_3 form heterodimers in living cells and that NCC_{SV} competes with NCC_3 to form a heterodimer. Our data suggest that the dimerization of NCC might already occur in the intracellular compartment before the proteins reach the plasma membrane. Furthermore, the intracellularly retained NCC_{SV} mutants were also shown to dimerize with NCC_3, suggesting that the phosphorylation status of S811 does not affect the interaction between NCC_{SV} and NCC_3 from an early stage. From its dimeric nature, NCC resembles NaKCl cotransporter (NKCC2) (33, 61), suggesting that other members of the family of electroneutral cation-chloride cotransporters form similar oligomeric structures. Dimerization of transmembrane proteins is a common mechanism that precedes functional regulation of a protein. Previously, it was demonstrated that in the tyrosine kinase pathway, Erb2/Erb3 cross-phosphorylate each other after dimerization (55, 91). The heterodimerization of NCC_{SV} with NCC_3, provides an indication that NCC_{SV} S811 phosphorylation regulates the N-terminal T60 and T55 of NCC_3 via close interaction.

uEVs as a source of urinary biomarkers

Urine provides a source for the discovery of urinary biomarkers useful for detection of kidney diseases and for monitoring of treatment. uEVs, which also include exosomes, are nanosized vesicles (30–120 nm) that form when multivesicular bodies within the cell merge with the cell membrane and release internal vesicles into the extracellular space or pro-urine (76). These microvesicles are an appealing source for urinary biomarker, as they are normally secreted into the urine from all nephron segments, and its cargo reflects the physiological and pathophysiological state of the cell from which they were released (Fig. 3A) (41, 104). In the field of urinary biomarker discovery uEVs have sparked a great surge of interest in recent years (60, 115). In this thesis, we designed a detailed protocol for isolation and standardization of uEVs in order to assess the NCC regulation in humans. Our

observations, in **Chapters 2, 3 and 5**, demonstrate that uEVs provide a unique and novel non-invasive tool to study the regulation of NCC in the human kidney. This assessment of NCC in uEVs represents an alternative method to guide anti-hypertensive therapy in patients with high blood pressure.

Structural characterization of NCC in uEVs

To determine whether NCC abundance in uEVs reflects NCC present in the epithelial cells of the DCT, several biochemical analyses were performed (**Chapter 3**). NCC is present in oligomeric structures in both uEVs and human kidney membrane fractions. This was demonstrated by immunoblots showing NCC proteins as complex bands of ~260 and ~130 kDa, representing the dimeric and monomeric forms, respectively. Interestingly, uEVs or proteins isolated from urine or tissue, respectively, did not allow dissociation of the dimeric NCC complex in a monomeric form. This has been attempted by incubating the uEVs at temperatures up to 100 °C or exposing them to the reducing agents dithiothreitol (DTT) and β-mercaptoethanol (β-met). The NCC complexes of ~260 and ~130 kDa detected in the human uEVs are comparable to NCC expression in human kidney membrane fractions, indicative of NCC derived from epithelium lines the DCT. Furthermore, *N*-glycosidase F was used to assess glycosylation since it has previously been demonstrated that NCC is *N*-glycosylated in rat kidney. The *N*-glycosylation is essential for the cell surface expression, thiazide sensitivity and activity of NCC (39). Our study in **Chapter 3** indicated that NCC in uEVs is glycosylated similarly to kidney membrane fractions. In addition, both the dimeric and monomeric NCC forms in uEVs and human kidney membrane fractions were insensitive to endoglycosidase H (Endo H) digestion, indicating that NCC in uEVs is present as a matured protein with complex glycosylation. Proteins that are sensitive to Endo H digestion are suggested to be retained in the endoplasmic reticulum and pre-Golgi complex without further processing (20, 32, 81). For example, it was shown that a part of the NCC monomeric band of *Xenopus* oocytes was sensitive to Endo H digestion (20, 39), suggesting the presence of unprocessed NCC protein. Together, this suggests that the NCC protein in uEVs represents a mature plasma membrane protein. Therefore, NCC in uEVs can be used as representative of NCC in human kidney membrane fractions.

NCC abundance in uEVs predicts the anti-hypertensive response to thiazides

In the studies presented in **Chapters 3 and 5**, uEVs were used as a tool to study NCC regulation in essential hypertensive patients and kidney transplant recipients treated with calcineurin inhibitors (CNIs), including cyclosporine A and tacrolimus. In addition, both the essential hypertensive and CNI-induced hypertensive patients were treated with thiazide diuretic to assess their NCC abundance in uEVs and blood pressure response to thiazides.

In addition to uEV-NCC analysis, clinical parameters and blood pressure were assessed in the patients. Our study demonstrated that chronic treatment with CNIs increases both total NCC (tNCC) and phosphorylated NCC (pNCC) abundance in uEVs of kidney transplant recipients. In **Chapter 5**, tNCC and pNCC refers to all three NCC isoforms in uEVs of kidney transplant recipients. This observation indicates that the CNI-induced increase in NCC abundance and phosphorylation (activity) might be involved in the pathogenesis of hypertension in kidney transplant recipients. Furthermore, we propose that analysis of NCC abundance in uEVs might predict the blood pressure response to thiazide diuretics. Thiazide treatment decreased the blood pressure in several essential and CNI-induced hypertensive patients, referred to as the "responders" (Fig. 3B). The uEV analysis in these kidney transplant recipients demonstrated that pre-treatment abundances of tNCC and pNCC in uEVs correlate with the blood pressure response to thiazide diuretics (**Chapter 5**). The observed increase in tNCC and pNCC abundance after thiazide treatment is consistent with data obtained in animal models (65, 66). Of note, when separating the group of patients into thiazide responders (a decrease of ≥ 5 mmHg in blood pressure) and non-responders (a decrease of < 5 mmHg in blood pressure), it becomes clear that NCC abundance was mainly increased in responders. This is in line with several previous studies demonstrating that prolonged thiazide treatment enhances NCC abundance in rodent kidney (65, 66). Moreover, chronic thiazide infusion in mice upregulated the binding density of [^{3}H] metolazone, an indirect measure of NCC activity, thereby also confirming the increased NCC abundance after thiazides (11). The augmented abundance of NCC in the DCT, which is reflected by an increased abundance of NCC in uEVs, might be the result of compensatory mechanisms. These compensatory mechanisms are potentially mediated by the RAAS or/and K^+ balance, which counteract reduced NCC function by the thiazide treatment (93). This compensatory response could, therefore, partly contribute to diuretic resistance (28). Similarly, chronic administration of the diuretics furosemide and amiloride, which block NKCC2 and ENaC, respectively, was shown to enhance the abundance of these proteins in rodent kidney (44, 65).

Interestingly, a decrease in pNCC and pNCC/tNCC ratio upon thiazide treatment was observed in the non-responders (**Chapter 5**). This might be explained by the fact that the blood pressure response to thiazides is accompanied by altered plasma K^+ levels or/and RAAS activation resulting in different NCC excretion patterns in uEVs. Recently, it has been demonstrated that aldosterone treatment increased the tNCC and pNCC abundance in uEVs of hypertensive patients, possibly driven by changes in plasma K^+ levels (111). Our studies show that alterations in blood pressure correlate with NCC abundance and plasma K^+ levels of hypertensive patients treated with thiazides. Moreover, the serum K^+ concentrations were lower in responders compared to non-responders (**Chapters 3** and **5**). These reduced

plasma K^+ levels observed in responders may explain the increase in NCC abundance in uEVs of hypertensive patients following thiazide treatment. A recent study revealed that a modest decrease in plasma K^+ levels, within the narrow physiological range of 3.5–5.0 mmol/L, can already increase NCC abundance and activity (101). Furthermore, it has been demonstrated that K^+ depletion, as well as renal K^+ loss, stimulate NCC phosphorylation (40, 108). In contrast to thiazide diuretics, valsartan did not enhance the abundance of NCC in uEVs derived from essential hypertensive patients, nor did it change plasma K^+ levels in these patients **(Chapter 3**). The lack of NCC response and unaltered serum K^+ levels in valsartan-treated patients indicate that NCC activation is partly dependent on plasma K^+-mediated stimulation (10). The upstream regulatory pathways of NCC stimulation (such as RAAS) are still intact during thiazide treatment and may stimulate NCC abundance and phosphorylation, while its function is still blocked by thiazides. The renin levels were elevated in thiazide-treated patients. In addition, it has been shown that high dietary Na^+ ingestion contributes to non-responsiveness to the thiazide treatment (diuretic resistance) (75). Patients with resistant hypertension who consumed a low Na^+ diet showed significantly increased plasma renin levels (75)

Collectively, these observations indicate that the CNI-induced increases in NCC abundance and phosphorylation are involved in the pathogenesis of hypertension in kidney transplant recipients. Furthermore, the blood pressure response correlates with NCC abundance in uEVs and plasma K^+ levels of hypertensive patients treated with thiazides. Ultimately, our results show that NCC abundance in uEVs could be used as a biomarker to predict the blood pressure response to thiazide diuretics.

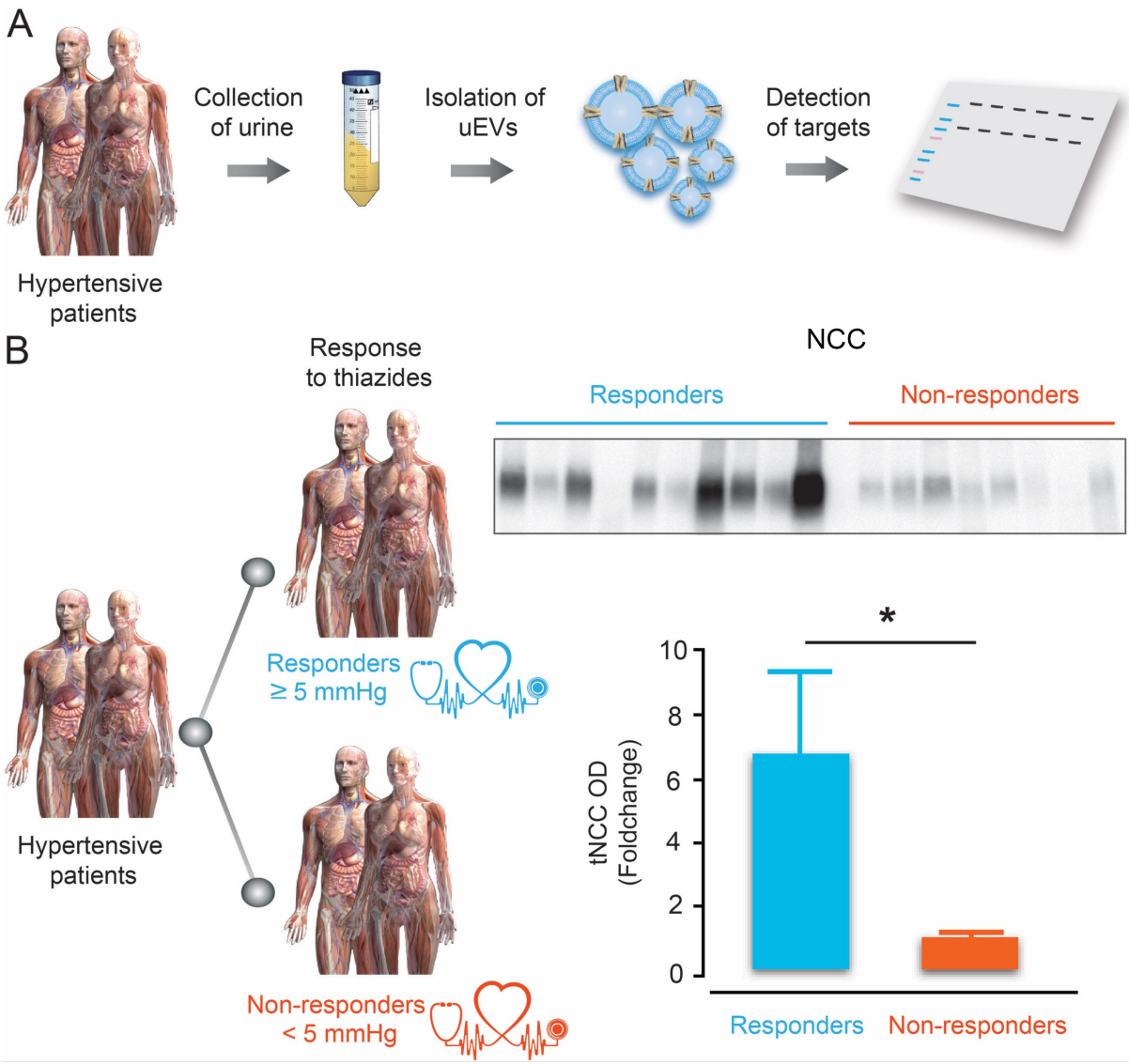

Figure 3 | NCC abundance in uEVs predicts the anti-hypertensive response to thiazides.

(**A**) Schematic diagram from collection of urine to the detection of specific proteins in urinary extracellular vesicles (uEVs). (**B**) Pre-treatment NCC abundance in uEVs isolated from hypertensive patients who did or did not respond to thiazides. The immunoblot and densitometry of tNCC in uEVs of hypertensive patients before the treatment with thiazide diuretics. Responders (n = 10) refer to patients who had a significant anti-hypertensive response (≥ 5 mmHg reduction in blood pressure) to treatment with thiazide diuretics. Non-responders (n = 8) did not have an anti-hypertensive response to thiazides (a decrease of < 5 mmHg in blood pressure). uEVs were isolated before the treatment with thiazides. tNCC abundance were significantly higher in responders compared to non-responders.

Effects of a high Na^+-low K^+ diet on renal electrolyte handling

Chapter 6 shows that a diet that is high in Na^+ and low in K^+ is not only involved in NCC regulation and pathogenesis of hypertension, but it is also associated with electrolyte disturbances. Our findings show that this diet has significant effects on renal calcium (Ca^{2+}) handling, while not affecting the magnesium (Mg^{2+}) balance. The high Na^+-low K^+ diet

enhances NCC abundance and activity, which subsequently increases the blood pressure (26, 101, 102). Similarly, patients with FHHt suffer from hypertension that results from gain-of-function of NCC (45, 85, 110, 113). In addition, patients with FHHt are characterized by decreased renal Na^+ and K^+ excretion and increased renal Ca^{2+} excretion, while their Mg^{2+} balance is not affected (70). In contrast, patients with Gitelman syndrome resulting from loss-of-function of NCC, have augmented renal Na^+, K^+, and Mg^{2+} wasting and reduced renal Ca^{2+} excretion (17, 29, 34, 47). Moreover, hypertensive patients treated with high-dose of thiazide diuretics may develop hypokalaemia, hypomagnesaemia and hypocalciuria (8, 19, 72), resembling the electrolyte disturbances observed in patients with Gitelman syndrome. The molecular mechanism explaining the renal Mg^{2+} handling in patients with FHHt and Gitelman syndrome is still not known. These data suggest that renal Mg^{2+} handling is mainly affected when NCC abundance or/and activity is decreased, while higher NCC activity due to a high Na^+-low K^+ diet or in FHHt patients does not result in Mg^{2+} imbalance. In addition to the cause of NCC related diseases, the duration of high Na^+-low K^+ diet is also known to show this discrepancy in Mg^{2+} handling. Serum and urine Mg^{2+} levels were not changed upon 4 days of diet in mice. In contrast, a previous study demonstrated increased urinary Mg^{2+} excretion in rats fed a high Na^+ diet (46). This discrepancy could be due to the period of the diets (7 days versus 4 days), suggesting a time-dependent effect.

Interestingly, the presented work described in **Chapter 6** reveals a prompt enhancement in renal Ca^{2+} and phosphate (Pi) excretion in response to high Na^+-low K^+ diet. Alterations in the gene and protein expression of players involved in Ca^{2+} and Pi transport indicates that high Na^+ intake inhibits proximal tubular reabsorption. We propose that the distal part of the nephron is unable to recover for the loss of Ca^{2+} and Pi by the proximal tubule, while the mechanism is sufficient to maintain Mg^{2+} homeostasis. Excessive renal excretion of Ca^{2+} and Pi are important risk factors for stone formation, as ~10% of all kidney stones are calcium-phosphate stones (112). Vice versa, several reports have shown that low Na^+ and high K^+ intake lowers the risk and progression of kidney stones (15, 31, 54, 82, 94). Previously, it has been postulated that a low K^+ diet-mediated renal Ca^{2+} loss is NCC dependent (102). The Ca^{2+} excretion was increased when mice were fed high Na^+ and low K^+ diet, while this effect on renal Ca^{2+} loss was absent in NCC knock out mice (102). Interestingly, in NCC knock out mice, the excessive Ca^{2+} excretion caused by only high Na^+ diet was not diminished, but only the effects of dietary K^+ on Ca^{2+} excretion were reversed in mice lacking NCC (102). This suggests that thiazide-treated or Gitelman syndrome patients might benefit from K^+ supplementation to diminish their NCC linked hypocalciuria. The current findings add to a growing body of literature showing that high Na^+ and low K^+ diet induces hypercalciuria (13, 18, 102). However, the exact mechanism underlying the altered renal Ca^{2+} handling needs further investigation.

Impact of this thesis and future perspective

This thesis highlights that NCC_{SV} is significantly expressed in the kidney where it operates as a fully functional thiazide-sensitive NaCl-transporting protein. NCC_{SV} is not a redundant protein since it plays an important role in (patho)physiological processes. Additionally, the phosphorylation site S811 in NCC_{SV} acts as a dominant-negative regulatory site for phosphorylation of T55 and T60. These findings reveal a new regulatory mechanism of NCC function that might be critical in renal salt handling and could, therefore, play an important role in the pathogenesis of essential hypertension. Hence, it is relevant to study the regulation of NCC_{SV} *in vivo* in several pathophysiological conditions. The generation of NCC_{SV} knock-in mice models that express solely NCC_{SV} and/or co-express both NCC_{SV} and NCC_3 in DCT are crucial to increase our understanding. Furthermore, unraveling the molecular signaling pathway and kinases that are involved in the phosphorylation of S811 might give more insight into the regulation of NCC_{SV}. Although, WNKs play an important role in the maintenance of the Na^+ balance, their abundant expression in different segments of the kidney makes it less effective to exploit them as therapeutic targets. However, utilizing the downstream kinases that are specifically involved in NCC regulation might be crucial to develop novel therapeutic strategies to combat the dysregulation of blood pressure. In addition, uEV analysis may have clinical utility as a non-invasive biomarker for a variety of physiological and pathological conditions. Notably, our data demonstrates that uEVs can be used as a non-invasive tool to guide anti-hypertensive therapy in patients with hypertension and may help to individualize anti-hypertensive treatment. An unresolved question in the uEV-field is whether the abundance of protein per uEV varies, or whether the number of uEVs is regulated. However, normalizing spot urines by creatinine for uEV analysis is currently an accepted approach (87, 104, 111, 117). Currently, the abundance of the uEV marker CD9 is often used to analyze whether normalization by urinary creatinine results in a similar number of uEVs for immunoblotting (3, 76, 87). Despite these methods (3, 76, 87), techniques that allow uEV counting will be necessary to address this point more conclusively. Furthermore, the development of high-throughput assay for uEV analysis will be necessary for further clinical applications.

References

1. Alessi DR, Zhang J, Khanna A, Hochdörfer T, Shang Y, Kahle KT. The WNK-SPAK/OSR1 pathway: master regulator of cation-chloride cotransporters. *Science signaling* 7: re3–re3, 2014.
2. Allagnat F, Christulia F, Ortis F, Pirot P, Lortz S, Lenzen S, Eizirik DL, Cardozo AK. Sustained production of spliced X-box binding protein 1 (XBP1) induces pancreatic beta cell dysfunction and apoptosis. *Diabetologia* 53: 1120–1130, 2010.
3. Alvarez ML, Khosroheidari M, Ravi RK, DiStefano JK. Comparison of protein, microRNA, and mRNA yields using different methods of urinary exosome isolation for the discovery of kidney disease biomarkers. *Kidney International* 82: 1024–1032, 2012.
4. Arroyo JP, Ronzaud C, Lagnaz D, Staub O, Gamba G. Aldosterone paradox: differential regulation of ion transport in distal nephron. *Physiology (Bethesda)* 26: 115–123, 2011.
5. Bianchi G, Fox U, Di Francesco GF, Bardi U, Radice M. The hypertensive role of the kidney in spontaneously hypertensive rats. *Clin Sci Mol Med Suppl* 45 Suppl 1: 135s–9, 1973.
6. Biner HL, Arpin-Bott M-P, Loffing J, Wang X, Knepper M, Hebert SC, Kaissling B. Human cortical distal nephron: distribution of electrolyte and water transport pathways. *J Am Soc Nephrol* 13: 836–847, 2002.
7. Boyden LM, Choi M, Choate KA, Nelson-Williams CJ, Farhi A, Toka HR, Tikhonova IR, Bjornson R, Mane SM, Colussi G, Lebel M, Gordon RD, Semmekrot BA, Poujol A, Välimäki MJ, De Ferrari ME, Sanjad SA, Gutkin M, Karet FE, Tucci JR, Stockigt JR, Keppler-Noreuil KM, Porter CC, Anand SK, Whiteford ML, Davis ID, Dewar SB, Bettinelli A, Fadrowski JJ, Belsha CW, Hunley TE, Nelson RD, Trachtman H, Cole TRP, Pinsk M, Bockenhauer D, Shenoy M, Vaidyanathan P, Foreman JW, Rasoulpour M, Thameem F, Al-Shahrouri HZ, Radhakrishnan J, Gharavi AG, Goilav B, Lifton RP. Mutations in kelch-like 3 and cullin 3 cause hypertension and electrolyte abnormalities. *Nature* 482: 98–102, 2012.
8. Brickman AS, Massry SG, Coburn JW. Changes in serum and urinary calcium during treatment with hydrochlorothiazide: studies on mechanisms. *J Clin Invest* 51: 945–954, 1972.
9. Castañeda-Bueno M, Arroyo JP, Zhang J, Puthumana J, Yarborough O III, Shibata S, Rojas-Vega L, Gamba G, Rinehart J, Lifton RP. Phosphorylation by PKC and PKA regulate the kinase activity and downstream signaling of WNK4. *Proc Natl Acad Sci* 114: E879–E886,2017.
10. Castañeda-Bueno M, Gamba G. Mechanisms of sodium-chloride cotransporter modulation by angiotensin II. *Curr Opin Nephrol Hypertens* 21: 516–522, 2012.
11. Chen ZF, Vaughn DA, Beaumont K, Fanestil DD. Effects of diuretic treatment and of dietary sodium on renal binding of 3H-metolazone. *J Am Soc Nephrol* 1: 91–98, 1990.
12. Chiga M, Rai T, Yang S-S, Ohta A, Takizawa T, Sasaki S, Uchida S. Dietary salt regulates the phosphorylation of OSR1/SPAK kinases and the sodium chloride cotransporter through aldosterone. *Kidney Int* 74: 1403–1409, 2008.
13. Cirillo M, Ciacci C, Laurénzi M, Mellone M, Mazzacca G, De Santo NG. Salt intake, urinary sodium, and hypercalciuria. *Miner Electrolyte Metab* 23: 265–268, 1997.
14. Coffman TM, Crowley SD. Kidney in hypertension: guyton redux. *Hypertension* 51: 811–816, 2008.
15. Colussi G, Surian M, De Ferrari ME, Pontoriero G, Rombolà G, Brando B, Malberti F, Cosci P, Aroldi A, Castelnovo C. Relationship between sodium intake, proximal tubular function and calcium excretion in normal subjects and in idiopathic hypercalciuria. *Proc Eur Dial Transplant Assoc* 20: 455–459, 1983.
16. Dahl LK, Heine M. Primary role of renal homografts in setting chronic blood pressure levels in rats. *Circ Res* 36: 692–696, 1975.
17. Dai LJ, Ritchie G, Kerstan D, Kang HS, Cole DE, Quamme GA. Magnesium transport in the renal distal convoluted tubule. *Physiological Reviews* 81: 51–84, 2001.
18. Damasio PCG, Amaro CRPR, Cunha NB, Pichutte AC, Goldberg J, Padovani CR, Amaro JL. The role of salt abuse on risk for hypercalciuria. *Nutr J* 10: 3, 2011.
19. Davies DL, Fraser R. Do diuretics cause magnesium deficiency? *Br J Clin Pharmacol* 36: 1–10, 1993.
20. de Jong JC, Van Der Vliet WA, van den Heuvel LPWJ, Willems PHGM, Knoers NVAM, Bindels RJM. Functional expression of mutations in the human NaCl cotransporter: evidence

for impaired routing mechanisms in Gitelman's syndrome. *J Am Soc Nephrol* 13: 1442–1448, 2002.

21. de Jong JC, Willems PHGM, Mooren FJM, van den Heuvel LPWJ, Knoers NVAM, Bindels RJM. The structural unit of the thiazide-sensitive NaCl cotransporter is a homodimer. *J Biol Chem* 278: 24302–24307, 2003.
22. Dimke H, San-Cristobal P, de Graaf M, Lenders JW, Deinum J, Hoenderop JGJ, Bindels RJM. γ-Adducin stimulates the thiazide-sensitive NaCl cotransporter. *J Am Soc Nephrol* 22: 508–517, 2011.
23. Eaton DC, Malik B, Saxena NC, Al-Khalili OK, Yue G. Mechanisms of aldosterone's action on epithelial Na + transport. *J Membr Biol* 184: 313–319, 2001.
24. Elalouf JM, Chabane Sari D, Roinel N, de Rouffignac C. NaCl and Ca delivery at the bend of rat deep nephrons decreases during antidiuresis. *Am J Physiol* 252: F1055–64, 1987.
25. Elalouf JM, Roinel N, de Rouffignac C. Effects of antidiuretic hormone on electrolyte reabsorption and secretion in distal tubules of rat kidney. *Pflugers Arch* 401: 167–173, 1984.
26. Ellison DH, Terker AS. Why Your Mother Was Right: How Potassium Intake Reduces Blood Pressure. *Trans Am Clin Climatol Assoc* 126: 46–55, 2015.
27. Ellison DH, Velazquez H, Wright FS. Thiazide-sensitive sodium chloride cotransport in early distal tubule. *Am J Physiol* 253: F546–54, 1987.
28. Ellison DH. Diuretic resistance: physiology and therapeutics. *Semi Nephrol*19: 581–597, 1999.
29. Ellison DH. Divalent cation transport by the distal nephron: insights from Bartter“s and Gitelman”s syndromes. *Am J Physiol Renal Physiol* 279: F616–F625, 2000.
30. Fenton RA, Moeller HB. Recent discoveries in vasopressin-regulated aquaporin-2 trafficking. *Prog Brain Res* 170: 571–579, 2008.
31. Ferraro PM, Mandel EI, Curhan GC, Gambaro G, Taylor EN. Dietary Protein and Potassium, Diet-Dependent Net Acid Load, and Risk of Incident Kidney Stones. *Clin J Am Soc Nephrol* 11: 1834–1844, 2016.
32. Freeze HH, Kranz C. Endoglycosidase and glycoamidase release of N-linked glycans. *Curr Protoc Protein Sci* Chapter 12: Unit12.4–12.4.25, 2010.
33. Frindt G, Palmer LG. Surface expression of sodium channels and transporters in rat kidney: effects of dietary sodium. *Am J Physiol Renal Physiol* 297: F1249–55, 2009.
34. Gitelman HJ, Graham JB, Welt LG. A new familial disorder characterized by hypokalemia and hypomagnesemia. *Trans Assoc Am Physicians* 79: 221–235, 1966.
35. Gonzales PA, Pisitkun T, Hoffert JD, Tchapyjnikov D, Star RA, Kleta R, Wang NS, Knepper MA. Large-scale proteomics and phosphoproteomics of urinary exosomes. *J Am Soc Nephrol* 20: 363–379, 2009.
36. Hadchouel J, Ellison DH, Gamba G. Regulation of Renal Electrolyte Transport by WNK and SPAK-OSR1 Kinases. *Annu Rev Physiol* 78: 367–389, 2016.
37. Hegner G, Faust G, Freytag F, Meilenbrock S, Sullivan J, Bodin F. Valsartan, a new angiotensin II antagonist for the treatment of essential hypertension: efficacy and safety compared to hydrochlorothiazide. *Eur J Clin Pharmacol* 52: 173–177, 1997.
38. Heinzen EL, Yoon W, Tate SK, Sen A, Wood NW, Sisodiya SM, Goldstein DB. Nova2 interacts with a cis-acting polymorphism to influence the proportions of drug-responsive splice variants of SCN1A. *Am J Hum Genet* 80: 876–883, 2007.
39. Hoover RS, Poch E, Monroy A, Vazquez N, Nishio T, Gamba G, Hebert SC. N-Glycosylation at two sites critically alters thiazide binding and activity of the rat thiazide-sensitive $Na(^{+}):Cl(^{-})$ cotransporter. *J Am Soc Nephrol* 14: 271–282, 2003.
40. Ishizawa K, Xu N, Loffing J, Lifton RP, Fujita T, Uchida S, Shibata S. Potassium depletion stimulates Na-Cl cotransporter via phosphorylation and inactivation of the ubiquitin ligase Kelch-like 3. *Biochem Biophys Res Commun* 480: 745–751, 2016.
41. Isobe K, Mori T, Asano T, Kawaguchi H, Nonoyama S, Kumagai N, Kamada F, Morimoto T, Hayashi M, Sohara E, Rai T, Sasaki S, Uchida S. Development of enzyme-linked immunosorbent assays for urinary thiazide-sensitive Na-Cl cotransporter measurement. *Am J Physiol Renal Physiol* 305: F1374–81, 2013.
42. James PA, Oparil S, Carter BL, Cushman WC, Dennison-Himmelfarb C, Handler J, Lackland DT, LeFevre ML, MacKenzie TD, Ogedegbe O, Smith SC, Svetkey LP, Taler SJ, Townsend RR, Wright JT, Narva AS, Ortiz E. 2014 evidence-based guideline for the management of high

blood pressure in adults: report from the panel members appointed to the Eighth Joint National Committee (JNC 8). *JAMA* 311 American Medical Association: 507–520, 2014.

43. Khan MZH, Sohara E, Ohta A, Chiga M, Inoue Y, Isobe K, Wakabayashi M, Oi K, Rai T, Sasaki S, Uchida S. Phosphorylation of Na-Cl cotransporter by OSR1 and SPAK kinases regulates its ubiquitination. *Biochem Biophys Res Commun* 425: 456–461, 2012.
44. Kim GH. Long-Term Adaptation of Renal Ion Transporters to Chronic Diuretic Treatment. *Am J Nephrol* 24: 595–605, 2005.
45. Lalioti MD, Zhang J, Volkman HM, Kahle KT, Hoffmann KE, Toka HR, Nelson-Williams C, Ellison DH, Flavell R, Booth CJ, Lu Y, Geller DS, Lifton RP. Wnk4 controls blood pressure and potassium homeostasis via regulation of mass and activity of the distal convoluted tubule. *Nat Genet* 38: 1124–1132, 2006.
46. Lee C-T, Lien Y-HH, Lai L-W, Ng H-Y, Chiou TT-Y, Chen H-C. Variations of dietary salt and fluid modulate calcium and magnesium transport in the renal distal tubule. *Nephron Physiol* 122: 19–27, 2012.
47. Lemmink HH, van den Heuvel LPWJ, van Dijk HA, Merkx GFM, Smilde TJ, Taschner PEM, Monnens LAH, Hebert SC, Knoers NVAM. Linkage of Gitelman syndrome to the thiazide-sensitive sodium-chloride cotransporter gene with identification of mutations in Dutch families. *Pediatr Nephrol* 10: 403–407, 1996.
48. Lin S-H, Shiang J-C, Huang C-C, Yang S-S, Hsu Y-J, Cheng C-J. Phenotype and genotype analysis in Chinese patients with Gitelman's syndrome. *J Clin Endocrinol Metab* 90: 2500–2507, 2005.
49. Loffing J, Kaissling B. Sodium and calcium transport pathways along the mammalian distal nephron: from rabbit to human. *Am J Physiol Renal Physiol* 284: F628–43, 2003.
50. Loffing J, Loffing-Cueni D, Valderrabano V, Kläusli L, Hebert SC, Rossier BC, Hoenderop JG, Bindels RJ, Kaissling B. Distribution of transcellular calcium and sodium transport pathways along mouse distal nephron. *Am J Physiol Renal Physiol* 281: F1021–7, 2001.
51. Lu Z-X, Jiang P, Xing Y. Genetic variation of pre-mRNA alternative splicing in human populations. *Wiley Interdiscip Rev RNA* 3: 581–592, 2012.
52. Mamenko M, Zaika O, Ilatovskaya DV, Staruschenko A, Pochynyuk O. Angiotensin II increases activity of the epithelial Na+ channel (ENaC) in distal nephron additively to aldosterone. *J Biol Chem* 287: 660–671, 2012.
53. Markadieu N, San-Cristobal P, Nair AV, Verkaart S, Lenssen E, Tudpor K, van Zeeland F, Loffing J, Bindels RJM, Hoenderop JGJ. A primary culture of distal convoluted tubules expressing functional thiazide-sensitive NaCl transport. *Am J Physiol Renal Physiol* 303: F886–92, 2012.
54. Martini LA, Cuppari L, Colugnati FA, Sigulem DM, Szejnfeld VL, Schor N, Heilberg IP. High sodium chloride intake is associated with low bone density in calcium stone-forming patients. *Clin Nephrol* 54: 85–93, 2000.
55. Maruyama IN. Mechanisms of activation of receptor tyrosine kinases: monomers or dimers. *Cells* 3: 304–330, 2014.
56. Mastroianni N, Bettinelli A, Bianchetti M, Colussi G, De Fusco M, Sereni F, Ballabio A, Casari G. Novel molecular variants of the Na-Cl cotransporter gene are responsible for Gitelman syndrome. *Am J Hum Genet* 59: 1019–1026, 1996.
57. Mastroianni N, Fusco MD, Zollo M, Arrigo G, Zuffardi O, Bettinelli A, Ballabio A, Casari G. Molecular Cloning, Expression Pattern, and Chromosomal Localization of the Human Na–Cl Thiazide-Sensitive Cotransporter (SLC12A3). *Genomics* 35: 486–493, 1996.
58. Mayan H, Vered I, Mouallem M, Tzadok-Witkon M, Pauzner R, Farfel Z. Pseudohypoaldosteronism type II: marked sensitivity to thiazides, hypercalciuria, normomagnesemia, and low bone mineral density. *J Clin Endo Metab* 87: 3248–3254,2002.
59. McDonough AA, Youn JH. Potassium Homeostasis: The Knowns, the Unknowns, and the Health Benefits. *Physiology (Bethesda)* 32: 100–111, 2017.
60. Melo SA, Luecke LB, Kahlert C, Fernandez AF, Gammon ST, Kaye J, LeBleu VS, Mittendorf EA, Weitz J, Rahbari N, Reissfelder C, Pilarsky C, Fraga MF, Piwnica-Worms D, Kalluri R. Glypican-1 identifies cancer exosomes and detects early pancreatic cancer. *Nature* 523: 177–182, 2015.
61. Moore-Hoon ML, Turner RJ. The structural unit of the secretory Na+-K+-2Cl- cotransporter (NKCC1) is a homodimer. *Biochemistry* 39: 3718–3724, 2000.

62. Mullins LJ, Bailey MA, Mullins JJ. Hypertension, kidney, and transgenics: a fresh perspective. *Physiological Reviews* 86: 709–746, 2006.
63. Murthy M, Kurz T, O'Shaughnessy KM. WNK signalling pathways in blood pressure regulation. *Cell Mol Life Sci* 74: 1261–1280, 2016.
64. Mutig K, Saritas T, Uchida S, Kahl T, Borowski T, Paliege A, Bohlick A, Bleich M, Shan Q, Bachmann S. Short-term stimulation of the thiazide-sensitive Na+-Cl- cotransporter by vasopressin involves phosphorylation and membrane translocation. *Am J Physiol Renal Physiol* 298: F502–9, 2010.
65. Na KY, Oh YK, Han JS, Joo KW, Lee JS, Earm J-H, Knepper MA, Kim G-H. Upregulation of Na+ transporter abundances in response to chronic thiazide or loop diuretic treatment in rats. *Am J Physiol Renal Physiol* 284: F133–F143, 2003.
66. Nijenhuis T, Vallon V, van der Kemp AWCM, Loffing J, Hoenderop JGJ, Bindels RJM. Enhanced passive Ca2+ reabsorption and reduced Mg2+ channel abundance explains thiazide-induced hypocalciuria and hypomagnesemia. *Journal of Clinical Investigation* 115: 1651–1658, 2005.
67. Obermuller N, Bernstein P, Velazquez H, Reilly R, Moser D, Ellison DH, Bachmann S. Expression of the thiazide-sensitive Na-Cl cotransporter in rat and human kidney. *Am J Physiol Renal Physiol* 269: F900–F910, 1995.
68. Pacheco-Alvarez D, Cristobal PS, Meade P, Moreno E, Vazquez N, Munoz E, Diaz A, Juarez ME, Gimenez I, Gamba G. The Na+:Cl- cotransporter is activated and phosphorylated at the amino-terminal domain upon intracellular chloride depletion. *J Biol Chem* 281: 28755–28763, 2006.
69. Pan Q, Shai O, Lee LJ, Frey BJ, Blencowe BJ. Deep surveying of alternative splicing complexity in the human transcriptome by high-throughput sequencing. *Nat Genet* 40: 1413–1415, 2008.
70. Pathare G, Hoenderop JGJ, Bindels RJM, San-Cristobal P. A molecular update on pseudohypoaldosteronism type II. *Am J Physiol Renal Physiol* 305: F1513–F1520, 2013.
71. Pedersen NB, Hofmeister MV, Rosenbaek LL, Nielsen J, Fenton RA. Vasopressin induces phosphorylation of the thiazide-sensitive sodium chloride cotransporter in the distal convoluted tubule. *Kidney Int* 78: 160–169, 2010.
72. Perez-Stable E, Caralis PV. Thiazide-induced disturbances in carbohydrate, lipid, and potassium metabolism. *Am Heart J* 106: 245–251, 1983.
73. Piala AT, Moon TM, Akella R, He H, Cobb MH, Goldsmith EJ. Chloride sensing by WNK1 kinase involves inhibition of autophosphorylation. *Science signaling* 7: ra41–ra41, 2014.
74. Pickrell JK, Marioni JC, Pai AA, Degner JF, Engelhardt BE, Nkadori E, Veyrieras J-B, Stephens M, Gilad Y, Pritchard JK. Understanding mechanisms underlying human gene expression variation with RNA sequencing. *Nature* 464: 768–772, 2010.
75. Pimenta E, Gaddam KK, Oparil S, Guyton AC, Husain S, Dell'Italia LJ, Calhoun DA. Effects of dietary sodium reduction on blood pressure in subjects with resistant hypertension: results from a randomized trial. *Hypertension* 54: 475–481, 2009.
76. Pisitkun T, Shen RF, Knepper MA. Identification and proteomic profiling of exosomes in human urine. *Proc Natl Acad Sci* 101: 13368–13373, 2004.
77. Psaty BN, Lumley T, Furberg CD, Schellenbaum G, Pahor M, Alderman MH, Weiss NS. Health outcomes associated with various antihypertensive therapies used as first-line agents - A network meta-analysis. *JAMA* 289: 2534–2544, 2003.
78. Richardson C, Richardson C, Rafiqi FH, Rafiqi FH, Karlsson HKR, Karlsson HKR, Moleleki N, Moleleki N, Vandewalle A, Vandewalle A, Campbell DG, Campbell DG, Morrice NA, Morrice NA, Alessi DR, Alessi DR. Activation of the thiazide-sensitive Na+-Cl- cotransporter by the WNK-regulated kinases SPAK and OSR1. *J Cell Sci* 121: 675–684, 2008.
79. Rieg T, Tang T, Uchida S, Hammond HK, Fenton RA, Vallon V. Adenylyl Cyclase 6 Enhances NKCC2 Expressionand Mediates Vasopressin-Induced Phosphorylation of NKCC2 and NCC. *The American Journal of Pathology* 182: 96–106, 2013.
80. Rieg T, Tang T, Uchida S, Hammond HK, Fenton RA, Vallon V. Adenylyl Cyclase 6 Enhances NKCC2 Expressionand Mediates Vasopressin-Induced Phosphorylation of NKCC2 and NCC. *The American Journal of Pathology* 182: 96–106, 2021.
81. Robbins PW, Trimble RB, Wirth DF, Hering C, Maley F, Maley GF, Das R, Gibson BW, Royal N, Biemann K. Primary structure of the Streptomyces enzyme endo-beta-N-

acetylglucosaminidase H. *J Biol Chem* 259: 7577–7583, 1984.

82. Robertson WG. Dietary recommendations and treatment of patients with recurrent idiopathic calcium stone disease. *Urolithiasis* 44: 9–26, 2016.
83. Rossier BC, Baker ME, Studer RA. Epithelial sodium transport and its control by aldosterone: the story of our internal environment revisited. American Physiological Society, 2015.
84. Rossier BC, Bochud M, Devuyst O. The Hypertension Pandemic: An Evolutionary Perspective. *Physiology (Bethesda)* 32: 112–125, 2017.
85. Rozansky DJ, Cornwall T, Subramanya AR, Rogers S, Yang Y-F, David LL, Zhu X, Yang C-L, Ellison DH. Aldosterone mediates activation of the thiazide-sensitive Na-Cl cotransporter through an SGK1 and WNK4 signaling pathway. *J Clin Invest* 119: 2601–2612, 2009.
86. Rozansky DJ, Cornwall T, Subramanya AR, Rogers S, Yang Y-F, David LL, Zhu X, Yang C-L, Ellison DH. Aldosterone mediates activation of the thiazide-sensitive Na-Cl cotransporter through an SGK1 and WNK4 signaling pathway. *J Clin Invest* 119: 2601–2612, 2009.
87. Salih M, Zietse R, Hoorn EJ. Urinary extracellular vesicles and the kidney: biomarkers and beyond. *Am J Physiol Renal Physiol* 306: F1251–9, 2014.
88. San-Cristobal P, Pacheco-Alvarez D, Richardson C, Ring AM, Vazquez N, Rafiqi FH, Chari D, Kahle KT, Leng Q, Bobadilla NA, Hebert SC, Alessi DR, Lifton RP, Gamba G. Angiotensin II signaling increases activity of the renal Na-Cl cotransporter through a WNK4-SPAK-dependent pathway. *Proc Natl Acad Sci* 106: 4384–4389, 2009.
89. Sandberg MB, Riquier ADM, Pihakaski-Maunsbach K, McDonough AA, Maunsbach AB. ANG II provokes acute trafficking of distal tubule Na+-Cl cotransporter to apical membrane. *Am J Physiol Renal Physiol* 293: F662–F669, 2007.
90. Saritas T, Borschewski A, McCormick JA, Paliege A, Dathe C, Uchida S, Terker A, Himmerkus N, Bleich M, Demaretz S, Laghmani K, Delpire E, Ellison DH, Bachmann S, Mutig K. SPAK differentially mediates vasopressin effects on sodium cotransporters. *Journal of the American Society of Nephrology* 24: 407–418, 2013.
91. Schlessinger J. Common and distinct elements in cellular signaling via EGF and FGF receptors. *Science* 306: 1506–1507, 2004.
92. Schmitt R, Ellison DH, Farman N, Rossier BC, Reilly RF, Reeves WB, Oberbäumer I, Tapp R, Bachmann S. Developmental expression of sodium entry pathways in rat nephron. *Am J Physiol* 276: F367–81, 1999.
93. Sevá Pessôa B, van der Lubbe N, Verdonk K, Roks AJM, Hoorn EJ, Danser AHJ. Key developments in renin-angiotensin-aldosterone system inhibition. *Nat Rev Nephrol* 9: 26–36, 2013.
94. Silver J, Rubinger D, Friedlaender MM, Popovtzer MM. Sodium-dependent idiopathic hypercalciuria in renal-stone formers. *Lancet* 2: 484–486, 1983.
95. Simon DB, Nelson-Williams C, Johnson Bia M, Ellison D, Karet FE, Morey Molina A, Vaara I, Iwata F, Cushner HM, Koolen M, Gainza FJ, Gitelman HJ, Lifton RP. Gitelman“s variant of Barter”s syndrome, inherited hypokalaemic alkalosis, is caused by mutations in the thiazide-sensitive Na–Cl cotransporter. *Nat Genet* 12: 24–30, 1996.
96. Simon DB, Nelson-Williams C, Johnson Bia M, Ellison D, Karet FE, Morey Molina A, Vaara I, Iwata F, Cushner HM, Koolen M, Gainza FJ, Gitelman HJ, Lifton RP. Gitelman“s variant of Bartter”s syndrome, inherited hypokalaemic alkalosis, is caused by mutations in the thiazide-sensitive Na-Cl cotransporter. *Nat Genet* 12: 24–30, 1996.
97. Skotheim RI, Nees M. Alternative splicing in cancer: noise, functional, or systematic? *Int J Biochem Cell Biol* 39: 1432–1449, 2007.
98. Soodvilai S, Jia Z, Wang M-H, Dong Z, Yang T. mPGES-1 deletion impairs diuretic response to acute water loading. *Am J Physiol Renal Physiol* 296: F1129–35, 2009.
99. Subramanya AR, Liu J, Ellison DH, Wade JB, Welling PA. WNK4 diverts the thiazide-sensitive NaCl cotransporter to the lysosome and stimulates AP-3 interaction. *J Biol Chem* 284: 18471–18480, 2009.
100. Sveen A, Kilpinen S, Ruusulehto A, Lothe RA, Skotheim RI. Aberrant RNA splicing in cancer; expression changes and driver mutations of splicing factor genes. *Oncogene* 35: 2413–2427, 2016.
101. Terker AS, Zhang C, Erspamer KJ, Gamba G, Yang C-L, Ellison DH. Unique chloride-sensing properties of WNK4 permit the distal nephron to modulate potassium homeostasis. *Kidney International* 89: 127–134, 2015.

102. Terker AS, Zhang C, McCormick JA, Lazelle RA, Zhang C, Meermeier NP, Siler DA, Park HJ, Fu Y, Cohen DM, Weinstein AM, Wang W-H, Yang C-L, Ellison DH. Potassium modulates electrolyte balance and blood pressure through effects on distal cell voltage and chloride. *Cell Metab* 21: 39–50, 2015.
103. Valdez-Flores MA, Vargas-Poussou R, Verkaart S, Tutakhel OAZ, Valdez-Ortiz A, Blanchard A, Treard C, Hoenderop JGJ, Bindels RJM, Jeleń S. Functionomics of NCC mutations in Gitelman syndrome using a novel mammalian cell-based activity assay. *Am J Physiol Renal Physiol* 311: F1159–F1167, 2016.
104. van der Lubbe N, Jansen PM, Salih M, Fenton RA, van den Meiracker AH, Danser AHJ, Zietse R, Hoorn EJ. The phosphorylated sodium chloride cotransporter in urinary exosomes is superior to prostasin as a marker for aldosteronism. *Hypertension* 60: 741–748, 2012.
105. van der Lubbe N, Lim CH, Fenton RA, Meima ME, Jan Danser AH, Zietse R, Hoorn EJ. Angiotensin II induces phosphorylation of the thiazide-sensitive sodium chloride cotransporter independent of aldosterone. *Kidney Int* 79: 66–76, 2011.
106. van der Lubbe N, Lim CH, Meima ME, van Veghel R, Rosenbaek LL, Mutig K, Danser AHJ, Fenton RA, Zietse R, Hoorn EJ. Aldosterone does not require angiotensin II to activate NCC through a WNK4–SPAK–dependent pathway. *Pflugers Arch - Eur J Physiol* 463: 853–863, 2012.
107. van der Lubbe N, Moes AD, Rosenbaek LL, Schoep S, Meima ME, Danser AHJ, Fenton RA, Zietse R, Hoorn EJ. K+-induced natriuresis is preserved during Na+ depletion and accompanied by inhibition of the Na+-Cl− cotransporter. *Am J Physiol Renal Physiol* 305: F1177–F1188, 2013.
108. Veiras LC, Han J, Ralph DL, McDonough AA. Potassium Supplementation Prevents Sodium Chloride Cotransporter Stimulation During Angiotensin II Hypertension. *Hypertension* 68: 904–912, 2016.
109. Welker P, Böhlick A, Mutig K, Salanova M, Kahl T, Schlüter H, Blottner D, Ponce-Coria J, Gamba G, Bachmann S. Renal Na+-K+-Cl- cotransporter activity and vasopressin-induced trafficking are lipid raft-dependent. *Am J Physiol Renal Physiol* 295: F789–802, 2008.
110. Wilson FH, Disse-Nicodème S, Choate KA, Ishikawa K, Nelson-Williams C, Desitter I, Gunel M, Milford DV, Lipkin GW, Achard J-M, Feely MP, Dussol B, Berland Y, Unwin RJ, Mayan H, Simon DB, Farfel Z, Jeunemaitre X, Lifton RP. Human hypertension caused by mutations in WNK kinases. *Science* 293: 1107–1112, 2001.
111. Wolley MJ, Wu A, Xu S, Gordon RD, Fenton RA, Stowasser M. In Primary Aldosteronism, Mineralocorticoids Influence Exosomal Sodium-Chloride Cotransporter Abundance. *Journal of the American Society of Nephrology* (July 5, 2016). doi: 10.1681/ASN.2015111221.
112. Worcester EM, Coe FL. Nephrolithiasis. *Prim Care* 35: 369–91– vii, 2008.
113. Yang C-L, Zhu X, Ellison DH. The thiazide-sensitive Na-Cl cotransporter is regulated by a WNK kinase signaling complex. *J Clin Invest* 117: 3403–3411, 2007.
114. Yang S-S, Fang Y-W, Tseng M-H, Chu P-Y, Yu I-S, Wu H-C, Lin S-W, Chau T, Uchida S, Sasaki S, Lin Y-F, Sytwu H-K, Lin S-H. Phosphorylation Regulates NCC Stability and Transporter Activity In Vivo. *J Am Soc Nephrol* 24: 1587–1597, 2013.
115. Yáñez-Mó M, Siljander PR-M, Andreu Z, Zavec AB, Borràs FE, Buzás EI, Buzas K, Casal E, Cappello F, Carvalho J, Colás E, Cordeiro-da Silva A, Fais S, Falcon-Perez JM, Ghobrial IM, Giebel B, Gimona M, Graner M, Gursel I, Gursel M, Heegaard NHH, Hendrix A, Kierulf P, Kokubun K, Kosanovic M, Kralj-Iglic V, Krämer-Albers E-M, Laitinen S, Lässer C, Lener T, Ligeti E, Linē A, Lipps G, Llorente A, Lötvall J, Manček-Keber M, Marcilla A, Mittelbrunn M, Nazarenko I, Nolte-'t Hoen ENM, Nyman TA, O'Driscoll L, Olivan M, Oliveira C, Pállinger É, Del Portillo HA, Reventós J, Rigau M, Rohde E, Sammar M, Sánchez-Madrid F, Santarém N, Schallmoser K, Ostenfeld MS, Stoorvogel W, Stukelj R, Van der Grein SG, Vasconcelos MH, Wauben MHM, De Wever O. Biological properties of extracellular vesicles and their physiological functions. *J Extracell Vesicles* 4: 27066, 2015.
116. Zhou B, Zhuang J, Gu D, Wang H, Cebotaru L, Guggino WB, Cai H. WNK4 enhances the degradation of NCC through a sortilin-mediated lysosomal pathway. *J Am Soc Nephrol* 21: 82–92, 2010.
117. Zhou H, Yuen PST, Pisitkun T, Gonzales PA, Yasuda H, Dear JW, Gross P, Knepper MA, Star RA. Collection, storage, preservation, and normalization of human urinary exosomes for biomarker discovery. *Kidney International* 69: 1471–1476, 2006.

8

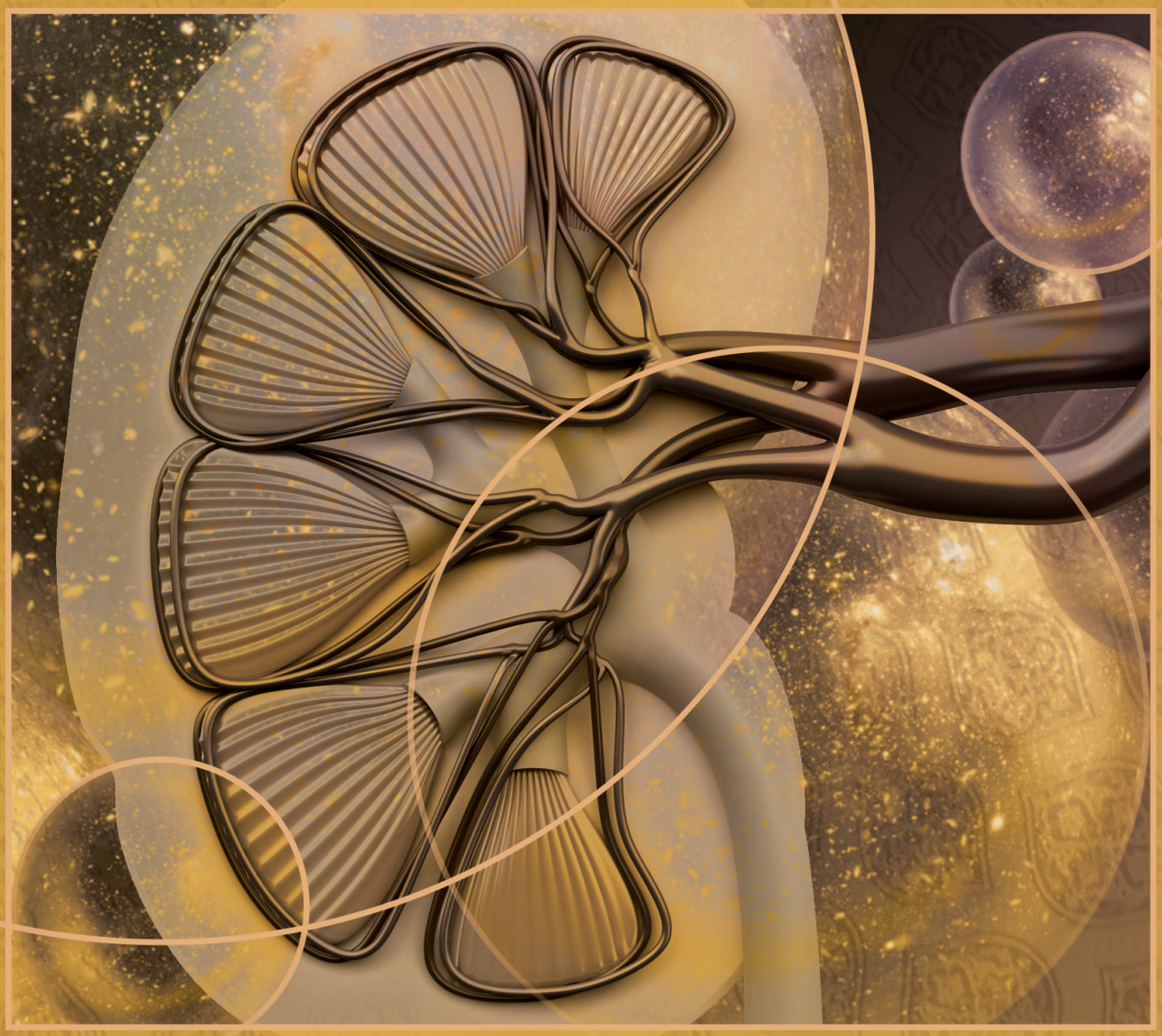

Nederlandse samenvatting

Inleiding

Hoge bloeddruk (hypertensie) is een risicofactor voor hart- en vaatziekten, en chronisch nierfalen en verhoogt hiermee het risico op sterven. Met een prevalentie van 1,4 miljard mensen, ofwel 1 op de 3 volwassenen wereldwijd, is hypertensie één van de meest ernstige volksgezondheidsproblemen. Opmerkelijk genoeg is de helft van de patiënten met hypertensie niet op de hoogte van hun conditie, en daarom wordt hypertensie vaak aangeduid als 'de stille moordenaar'. Bovendien is de oorzaak in ~90% van de patiënten met hypertensie niet bekend en het wordt dan ook wel ‘essentiële hypertensie’ genoemd.

Bloeddruk wordt gehandhaafd door een samenspel tussen bepaalde delen van de hersenen (de hersenstam), de nieren en het hart. De nieren regelen voor een belangrijk deel het vocht- en het zoutgehalte in ons lichaam, en dragen daarmee bij aan de hoogte van de bloeddruk. De nier is opgebouwd uit ongeveer 1 miljoen nefronen, de functionele eenheden van de nier. Ze filteren het bloed en zorgen voor de uitscheiding van afvalstoffen en ‘overtollig’ zout en vocht via de urine. Elk nefron bestaat uit een glomerulus (een kluwen hele kleine bloedvaatjes), het kapsel van Bowman (een kapsel dat om de glomerulus heen ligt) en een nierbuis (tubulus). Na filtratie van het bloed in de glomerulus ontstaat er voorurine die door de nierbuis stroomt. Er vindt dan een uitwisselingsproces van opname en afgifte van water en zouten plaats tussen de voorurine en het bloed, dat in kleine bloedvaatjes rondom de nierbuis stroomt. Het laatste gedeelte van nierbuis speelt een sleutelrol in de regulatie van bloeddruk door het beïnvloeden van natrium (Na^+) en kalium (K^+) uitwisseling. Dit deel bestaat uit het distaal convoluut (DCT), de verbindingsbuis (CNT) en de verzamelbuis. De opname, ofwel resorptie, van Na^+ in dit deel van de nierbuis staat onder controle van specifieke transporteiwitten, de NaCl cotransporter (NCC) en het epitheliale Na^+ kanaal (ENaC). NCC komt specifiek voor in de DCT, met name in het vroege deel van de DCT (DCT1) en lokalisatie neemt geleidelijk af langs het latere deel van de DCT (DCT2). De lokalisatie van ENaC neemt geleidelijk toe van DCT2 naar CNT en verzamelbuis. Opname van Na^+ door NCC in DCT1 bepaalt de hoeveel Na^+ die doorstroomt naar DCT2, CNT en verzamelbuis en daarmee heeft NCC een indirecte rol op Na^+ opname via ENaC. De opname van Na^+ via ENaC is gekoppeld aan de afgifte (excretie) van K^+ via het transporteiwit ROMK. Er zijn verschillende hormonen die dit netwerk van opname en afgifte van Na^+ en K^+ regelen. Het hormonale renine-angiotensine-aldosteron-systeem (RAAS) is een belangrijke component hierin en speelt een essentiële rol in de regulatie van de bloeddruk.

Het belang van NCC in regulatie van Na^+ en K^+ wordt gekenmerkt door de onderliggende moleculaire mechanismen van pseudohypoaldosteronisme type 2 (familiale hyperkaliëmische hypertensie; FHHt), Gitelman syndroom en thiazidediuretica. FHHt is een erfelijke ziekte die wordt veroorzaakt door mutaties in het WNK4, WNK1, CUL3 of KLHL3 gen. Deze genen zijn

op hun beurt uiteindelijk weer verantwoordelijk voor de activiteit van de NCC. Patiënten met FHHt lijden aan hypertensie en hyperkaliëmie ten gevolge van een verhoogde activiteit van de NCC. Beide symptomen van patiënten met FFHt, hypertensie en hyperkaliëmie, kunnen worden gecorrigeerd door een lage dosis thiazidediuretica. Thiazidediuretica remmen NCC in de DCT. Dit zorgt voor de verhoogde Na^+ afgifte, wat vervolgens leidt tot verlaging van de bloeddruk. Verschillende richtlijnen adviseren thiazidediuretica als de eerstelijnsbehandeling van hypertensie. Vanwege het remmende effect van thiaziden op NCC-activiteit zal er meer Na^+ bij de DCT2, CNT en verzamelbuis terecht komen. Deze segmenten zullen vervolgens meer Na^+ via ENaC opnemen. Als gevolg hiervan wordt er meer K^+ via ROMK uitgescheiden, wat uiteindelijk resulteert in een te lage K^+ concentratie in het bloed. Gitelman syndroom is een erfelijke aandoening, veroorzaakt door mutaties in het *NCC* gen. Ook hebben patiënten met Gitelman syndroom een te lage K^+ concentratie in het bloed, veroorzaakt door het verlies van NCC functie. Recentelijk is aangetoond dat de K^+ concentratie in het bloed, onafhankelijk van hormonale effecten, de NCC functie kan moduleren. Het Westers dieet, dat veel Na^+ en weinig K^+ bevat, kan de bloed K^+ concentratie verlagen, wat vervolgens leidt tot verhoging van de NCC activiteit, zelfs als er sprake is van hypertensie. Het lichaam probeert de K^+ balans te handhaven ten koste van een hoge bloeddruk. Dit kan een belangrijke oorzaak zijn van de hypertensiepandemie. Daarom kan niet alleen het beperken van de dagelijkse Na^+ inname, maar ook het verhogen van K^+ inname, nuttig zijn voor de behandeling en preventie van hypertensie.

Het bestuderen van nieuwe NCC-isovormen

Alternatieve splicing variant van NCC (NCC_{SV})

Sinds de ontdekking van NCC in de mens in 1996, is het aangetoond dat er drie vormen van NCC in de menselijke nier aanwezig zijn, die ook wel de NCC isovormen genoemd. Hoewel veel studies in de afgelopen decennia het belang van NCC voor de zoutbalans en bloeddruk hebben benadrukt, hebben deze studies zich geconcentreerd op de kortste NCC isovorm (NCC_3). De NCC isovormen 1 en 2, gezamenlijk aangeduid als NCC splicing variant (NCC_{SV}), zijn tot nu toe niet bestudeerd. NCC_{SV} komt uitsluitend tot expressie in mensen en hogere primaten. Met het genereren van een nieuw antilichaam dat specifiek NCC_{SV} herkent, hebben we aangetoond dat NCC_{SV} (net als NCC_3) gelokaliseerd is op het apicale membraan van cellen in de DCT (**hoofdstuk 2**). De aanwezigheid van NCC_{SV} werd ook bevestigd in exosomen. Dit zijn kleine blaasjes, ook aangeduid als extracellulaire vesikels, die door lichaamscellen worden afgescheiden in bloed en urine. Hierdoor kunnen exosomen geïsoleerd worden uit de urine. Exosomen bevatten de bouwstenen van de oorspronkelijke cellen, waaronder eiwitten en RNA en ze kunnen gebruikt worden voor de analyse van NCC

eiwitten en zijn representatief voor de cellen in de DCT. Uit de resultaten bleek dat het totale mRNA van NCC in de menselijke nier gemiddeld voor ~45% uit NCC_{SV} RNA en voor ~55% uit NCC_3 RNA bestaat. Echter, als we deze verhouding in mRNA expressie tussen NCC_{SV} en NCC_3 in menselijke nieren per individu bekijken, dan zien we dat het varieert tussen 20-60%. Deze grote verschillen in de ratio NCC_{SV}:NCC_3 suggereren dat splicing van het NCC gen gereguleerd wordt. Er is daarnaast aangetoond dat ~95% van de menselijke genen gespliced wordt, inclusief het NCC gen.

Om de rol van NCC_{SV} in verschillende fysiologische en pathofysiologische condities te onderzoeken is er eerst een methode ontwikkeld voor het bestuderen van NCC in de exosomen verkregen vanuit menselijke urine. In **hoofdstuk 2** is de fysiologische rol van NCC_{SV} bestudeerd door analyse van NCC expressie in exosomen bij proefpersonen die overmatig veel water (0,5 L in 30 min) hadden ingenomen. Onze bevindingen toonden een sterke afname aan in eiwittenexpressie van NCC_{SV} en NCC_3 in de urinaire exosomen, als gevolg van overmatige waterinname (**hoofdstuk 2**). Forse waterinname resulteerde in een stijging van het bloedvolume en een afname in serum osmolaliteit, wat leidt tot RAAS inactivatie en afgifte van vasopressine (antidiuretisch hormoon) door de hersenen. De verminderde eiwitexpressie van NCC_{SV} in de proefpersonen is daarom waarschijnlijk een gevolg van RAAS inactivatie en verhoogde afgifte van vasopressine. Zo toonden onze resultaten aan dat NCC_{SV}, net als NCC_3, sterk gereguleerd wordt onder fysiologische condities.

De **hoofdstukken 3** en **5** richten zich op de pathofysiologische rol van NCC_{SV} in patiënten met essentiële hypertensie en patiënten die behandeld worden met calcineurineremmers. In **hoofdstuk 3** wordt aangetoond dat NCC_{SV} een rol speelt in de pathogenese van essentiële hypertensie. Expressie van NCC_{SV} en NCC_3 in urinaire exosomen van essentieel hypertensieve patiënten was verhoogd na het gebruik van thiazidediuretica, maar niet na de behandeling met valsartan. Valsartan behoort tot de angiotensine-II-blokkers en is bekend als bloeddrukverlagend middel. Onze resultaten toonden aan dat de bloeddrukverlaging na gebruik van thiazidediuretica correleert met de expressie van NCC_{SV} in urinaire exosomen en met de K^+ concentratie in het bloed van essentieel hypertensieve patiënten. Daling in K^+ concentratie in het bloed van de patiënten behandeld met thiazidediuretica kan leiden tot een verhoging van de Na^+ concentratie in het distale deel van het nefron, wat vervolgens resulteert in verhoogde K^+ afgifte. De combinatie van de waarnemingen in dit proefschrift, zoals een significante eiwitexpressie van NCC_{SV} in de nier en betrokkenheid van NCC_{SV} bij fysiologische en pathofysiologische processen, duidt op een sleutelrol voor NCC_{SV} in het reguleren van de water- en zouthuishouding.

Functionele rol van NCC_{SV}

In **hoofdstuk 2** en **4** was de thiazidegevoelige transportactiviteit van NCC_{SV} in zowel oocyten als menselijke embryonale niercellen onderzocht. Recentelijk is er een nieuw residu geïdentificeerd (serine 811, S811), uitsluitend aanwezig in NCC_{SV}, dat gemodificeerd kan worden via fosforylatie. De afwezigheid van NCC_{SV} in muizen, ratten en konijnen heeft de voortgang en belangstelling voor verdere onderzoeken belemmerd. De studies in dit proefschrift onthullen dat NCC_{SV}-S811 niet alleen een sleutelrol speelt in NCC_{SV}, maar ook in NCC_3 functie. Fosforylering-deficiënte S811-mutant (NCC_{SV}-S811A) toonde een verminderde transportactiviteit in oocyten en menselijke embryonale niercellen. **Hoofdstuk 4** laat ook zien dat co-expressie van NCC_{SV} S811A en NCC_3 resulteert in een remmend effect van NCC_{SV} S811A op NCC_3 functie. Samengevat beschrijft dit hoofdstuk dat S811 niet alleen de activiteit van NCC_{SV} reguleert, maar ook de functie van NCC_3 beïnvloedt. Daarnaast hebben wij voor het eerste aangetoond dat NCC_{SV} en NCC_3 interacties aangaan en zogenaamde heterodimeren vormen in menselijke embryonale niercellen. Dimerisatie van membraan-eiwitten is een gemeenschappelijk mechanisme dat voorafgaat aan de functionele regulatie van een eiwit. Onze bevinding van heterodimerisatie van NCC_{SV} en NCC_3 suggereert dat NCC_{SV}-S811 op deze wijze de activiteit van NCC_{SV} en NCC_3 kan beïnvloeden. Daarnaast zien we dat de dimerisatie van NCC al intracellulair kan optreden, nog voordat de eiwitten de plasmamembraan bereiken.

Urinaire exosomen als bron van biomarkers

Exosomen worden continu uitgescheiden in de urine en daarom vormen ze een makkelijk toegankelijke bron van biomarkers voor nierziekten. Bovendien is het verzamelen van urinaire exosomen voor de patiënt minimaal belastend. In dit proefschrift hebben we een gedetailleerde methode ontwikkeld om NCC eiwitten in urinaire exosomen te kunnen analyseren. **Hoofdstukken 2**, **3** en **5** laten zien dat urinaire exosomen als een unieke en non-invasieve methode kunnen worden gebruikt om de NCC regulatie in de menselijke nier te bestuderen. Daarnaast biedt het analyseren van NCC in urinaire exosomen een alternatieve methode om patiënten met hypertensie te begeleiden bij anti-hypertensieve therapie. Urinaire exosomen kunnen daarom bijdragen aan een effectieve en persoonlijke behandeling van hypertensie.

NCC in urinaire exosomen voorspelt de respons van de patiënt op thiazidediuretica

Hoofdstukken 3 en **5** richten zich op het analyseren van NCC in urinaire exosomen van essentieel hypertensieve patiënten en patiënten die een niertransplantatie ondergaan hebben

en behandeld zijn met calcineurineremmers. In beide hypertensieve patiëntengroepen was de expressie van NCC in de urinaire exosomen en de bloeddrukrespons op thiazidediuretica geanalyseerd. Onze studie heeft aangetoond dat chronische behandeling met calcineurineremmers zowel de expressie van totaal NCC (tNCC) als de gefosforyleerde (actieve) vorm van NCC (pNCC) verhoogt in urinaire exosomen van patiënten die een niertransplantatie hebben ondergaan. Deze bevindingen geven aan dat de toename in de expressie van NCC die geïnduceerd is door calcineurineremmers mogelijk betrokken is bij de pathogenese van hypertensie in deze patiëntengroep. We weten dat er interindividuele variatie in de gevoeligheid voor thiaziden bestaat. Opmerkelijk genoeg onze resultaten laten zien dat het analyseren van NCC expressie in urinaire exosomen alvorens de behandeling met thiaziden de bloeddrukrespons op thiazidediuretica kan voorspellen. Dit betekent dat voor de behandeling met thiazidediuretica, de exosoom-analyse kan helpen bij het vast stellen van individuele gevoeligheid voor de behandeling met thiaziden en zo onnodige thiazidediuretica gebruik voorkomen kunnen worden. Het is ook interessant om te onderzoeken of urinaire exosomen alvorens de behandeling met andere diuretica dan thiaziden de bloeddrukrespons kan voorspellen. Dit proefschrift toont eveneens aan dat veranderingen in de bloeddruk correleren met de NCC eiwitexpressie en de K^+ concentratie in het bloed van hypertensieve patiënten die behandeld zijn met thiazidediuretica. Daarnaast is gebleken dat een hoge Na^+ inname bijdraagt aan een ongevoeligheid voor de behandeling met thiaziden.

Effecten van een Westers dieet op renale elektrolythomeostase

Het is bekend dat een Westers dieet de NCC activiteit stimuleert, wat leidt tot verhoogde bloeddruk. **Hoofdstuk 6** laat zien dat een Westers dieet niet alleen bij de NCC regulatie en pathogenese van hypertensie betrokken is, maar ook met andere stoornissen in de zoutbalans wordt geassocieerd. Uit onze bevindingen blijkt dat het Westerse dieet aanzienlijke effecten heeft op de renale calcium (Ca^{2+}) en fosfaat (Pi) regulatie, zonder dat het de balans van magnesium (Mg^{2+}) beïnvloed wordt. We laten zien dat het Westerse dieet resulteert in een verhoogde renale afgifte van Ca^{2+} en Pi in de urine. De hypothese is dat de opname van Ca^{2+} en Pi in het eerste deel van het nefron, de proximale tubulus, lager is als gevolg van hoge Na^+ opname in dit deel van het nefron. Waarschijnlijk kan het distale deel van het nefron het ontstane renale verlies in Ca^{2+} en Pi niet herstellen, terwijl er wel voldoende capaciteit is om Mg^{2+} balans te handhaven. Overmatige uitscheiding van Ca^{2+} en Pi door de nieren is een belangrijke risicofactor voor het ontwikkelen van nierstenen. Verschillende studies hebben aangetoond dat lage Na^+ en een hoge K^+ inname het risico en de progressie van nierstenen kan verminderen. Gezamenlijk dragen deze bevindingen bij aan een groeiend aantal studies

die aantonen dat een dieet bestaande uit weinig Na^+ en veel K^+ een voordelige invloed kan hebben op onze gezondheid.

Impact van dit proefschrift en toekomstperspectief

Dit proefschrift benadrukt dat NCC_{SV} in aanzienlijkemate in de nier aanwezig is en dat het fungeert als een volledig functioneel NaCl-transporterend eiwit. NCC_{SV} is duidelijk geen overbodig eiwit, aangezien hier aangetoond is dat het een belangrijke rol speelt in (patho)fysiologische processen in de mens. Bovendien functioneert S811 in NCC_{SV} als een dominant-negatieve regulator van de NCC activiteit. Deze bevindingen onthullen een nieuw mechanisme voor de regulatie van NCC functie, dat belangrijk kan zijn bij de zouthuishouding en daarom een belangrijke rol zou kunnen spelen in de pathogenese van essentiële hypertensie. Het is relevant om de regulatie van NCC_{SV} in verschillende pathofysiologische omstandigheden te bestuderen met behulp van muismodellen. Het inbrengen van NCC_{SV} gen in muismodellen die uitsluitend NCC_{SV} en/of NCC_{SV} en NCC_3 in de nier tot expressie brengen is cruciaal om onze kennis verder te kunnen vergroten. Bovendien kan het ontrafelen van kinase eiwitten die betrokken zijn bij de fosforylering van S811 meer inzicht geven in de regulatie van NCC_{SV}. Het is bekend dat WNK kinases NCC op residuen anders dan S811 kunnen fosforyleren. Hoewel WNK kinases een mogelijk therapeutische alternatief bieden, de expressie van deze kinases in verschillende segmenten van de nier maakt het minder effectief om ze te gebruiken als therapeutische doelen. Het vinden van een kinase dat specifiek de fosforylatiestatus van S811 en dus NCC activiteit in de DCT zou kunnen beïnvloeden, lijkt essentieel om nieuwe therapeutische strategieën te ontwikkelen zodat de bloeddruk beter gecontroleerd kan worden. Hoewel thiazidediuretica vaak de eerste keuze zijn voor het verlagen van de bloeddruk, verhogen zij vaak het urinezuurgehalte van het bloed met uiteenlopende negatieve gevolgen.

In dit proefschrift hebben we ook aangetoond dat urinaire exosomen als non-invasief hulpmiddel gebruikt kunnen worden om anti-hypertensieve therapie bij patiënten met een hoge bloeddruk te begeleiden. Exosoom-analyse kan helpen bij het personaliseren van anti-hypertensieve behandeling. Urine is niet alleen een belangrijke bron van biomarkers voor de prognose van anti-hypertensieve therapieën, maar mogelijk ook voor de diagnose van verschillende nierziekten. Het ontstaan en de voortschrijding van nierziekten kan hiermee worden beperkt. In de toekomst kan het wellicht voor sommige ziekten een nierbiopt overbodig maken. Recentelijk zijn er methoden ontwikkeld om urinaire exosomen makkelijker en sneller te kunnen onderzoeken. Echter, voor de verdere klinische toepassingen zijn de ontwikkeling van high-throughput assays voor exosoom-analyse noodzakelijk. Exosomen zijn dus veelbelovend, maar hun klinische toepassing zal in de toekomst verder ontwikkeld moeten worden.

9

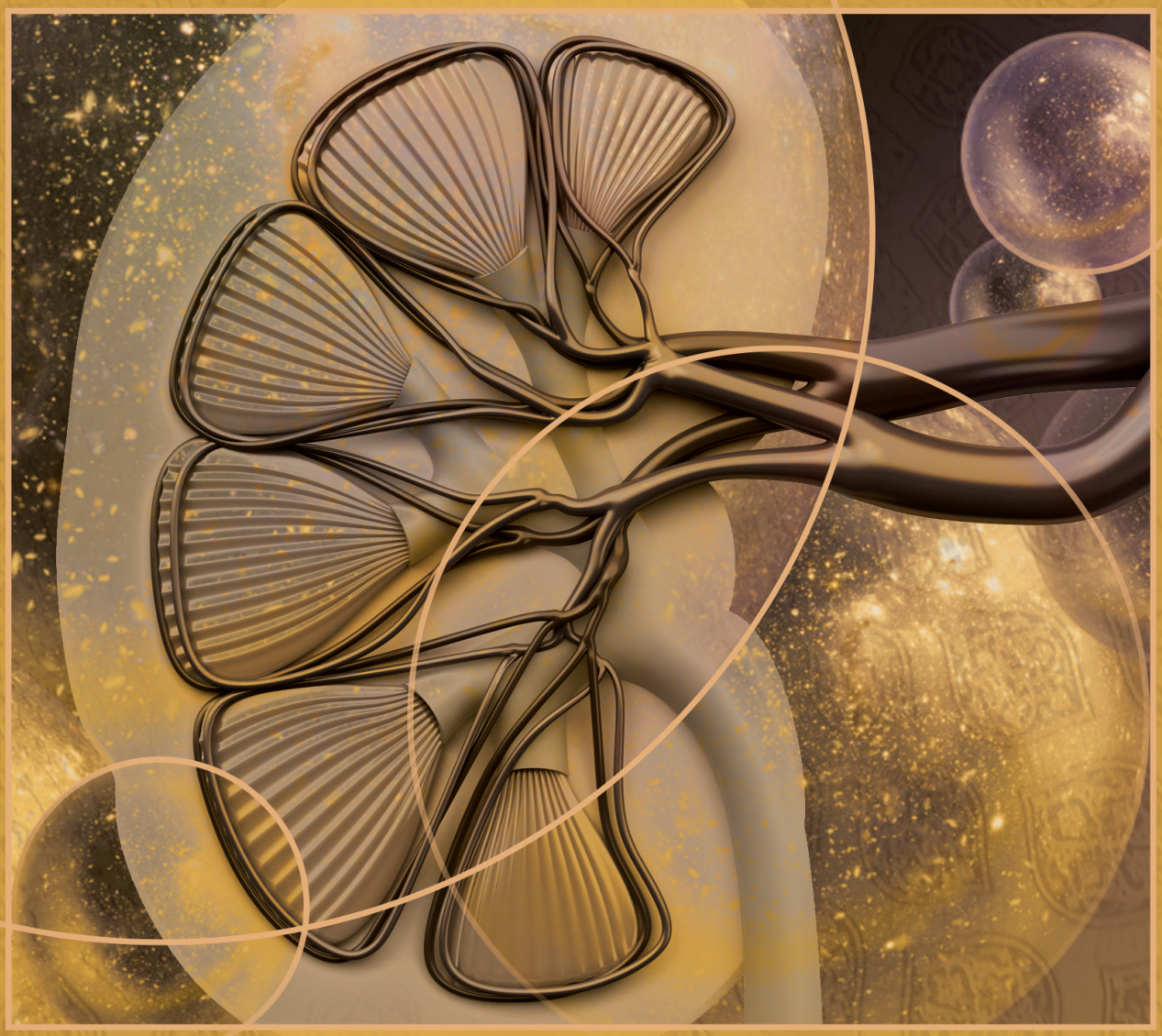

List of abbreviations

List of publications

Curriculum vitae

Research data management

RIMLS Portfolio

List of abbreviations

AQP2	Aquaporin-2
ATP	Adenosine triphosphate
AVP	Arginine vasopressin
C-terminal	Carboxy-terminal
Ca^{2+}	Calcium
cAMP	Cyclic AMP
CD	Collecting duct
cDNA	Complementary DNA
CKD	Chronic kidney disease
Cl^-	Chloride
CLC-Kb	Cl^- channel
CNIs	Calcineurin inhibitors
CNT	Connecting tubule
CsA	Cyclosporine A
CUL3	Cullin 3
DCT	Distal convoluted tubule
DCT1	Early part of the DCT
DCT2	Later part of the DCT
DASH	Dietary Approaches to Stop Hypertension
DMEM	Dulbecco's modified eagle's medium
DNA	Deoxyribonucleic acid
DTT	Dithiothreitol
ECF	Extracellular fluid
EDTA	Ethylene diamine tetraacetic acid
eGFP	Enhanced green fluorescent protein
eGFR	Estimated glomerular filtration rate
EGTA	Ethylene glycol tetraacetic acid
ENaC	Amiloride-sensitive epithelial Na^+ channel
Endo H	Endoglycosidase H
ESRD	End stage renal disease
FHHt	Familial Hyperkalemic Hypertension
FLIM	Fluorescence lifetime imaging microscopy
FRET	Förster resonance energy transfer
GFP	Green fluorescent protein
GFR	Glomerular filtration rate

HCT	Hydrochlorothiazide
HCTZ	Hydrochlorothiazide
HEK293	Human embryonic kidney
IB	Immunoblotting
IHC	Immunohistochemistry
K^+	Potassium
KDa	Kilo dalton
KLHL3	Kelch-like 3
KS-WNK1	Kidney-specific WNK1
mDCT	Mouse distal convoluted tubule
Mg^{2+}	Magnesium
MQ	Milli-Q water
MR	Mineralocorticoid receptor
mRNA	Messenger ribonucleic acid
MS	Mass spectrometry
MS/MS	Tandem MS
N-terminal	Amino-terminal
Na/K-ATPase	Na^+/K^+ pump
Na^+	Sodium
NaCl	Salt
NAMIS	Nijmegen Anti-hypertensive Management Improvement Study
NaPi	Sodiumphosphate symporters
NCC	Thiazide-sensitive NaCl cotransporter
NCC_{1-3}	Isoforms 1, 2 and 3 of the thiazide-sensitive NaCl cotransporter
$NCC_{1/2}$	Isoforms 1 and 2 of the thiazide-sensitive NaCl cotransporter
NCC_3	Isoform 3 of the thiazide-sensitive NaCl cotransporter
NCC_3	NaCl cotransporter isoform 3
NCC_{SV}	NaCl cotransporter isoform 1 and 2
NCC_{SV}	NCC splice variant
NHE3	Na^+/H^+ exchanger type 3
NKCC2	Furosemide-sensitive NaKCl cotransporter
NT-proBNP	N-terminal of the prohormone brain natriuretic peptide
OSR1	Oxidative stress responsive protein type 1
PCR	Polymerase chain reaction
PHAII	Pseudohypoaldosteronism type II
Pi	Phosphate
PKA	Protein kinase A

PKC	Protein kinase C
pNCC	Phosphorylated thiazide-sensitive NaCl cotransporter
$pNCC_{1-3}$	Phosphorylated total thiazide-sensitive NaCl cotransporter
PNGase F	*N*-glycosidase F
PROBE	Prospective open-label and blinded end-point
PT	Proximal tubule
PVDF	Polyvinylidene difluoride
RAAS	Renin-angiotensin-aldosterone system
RNA	Ribonucleic acid
ROMK	Renal outer medullary K^+ channel
RT	Reverse transcriptase
RT-PCR	Real time PCR
S811	Serine 811
SDS-PAGE	Sodium dodecyl sulfate polyacrylamide gel electrophoresis
SEM	Standard error of the mean
SGK1	Serum and glucocorticoid-inducible kinase 1
SPAK	STE20/SPS1-related proline alanine-rich kinase
T55	Threonine 55
T60	Threonine 60
Tac	Tacrolimus
TAL	Thick ascending limb of Henle's loop
tNCC	Total thiazide-sensitive NaCl cotransporter
uEVs	Urinary extracellular vesicles
V_2R	Type 2 vasopressin receptor
Val	Valsartan
WNK	With no lysine
YFP	Yellow fluorescent protein
β-met	β-mercaptoethanol

List of publications

Tutakhel OAZ, Bianci F, Daniël A. Smits, Bindels RJM, Hoenderop JGJ, Van der Wijst J. Dominant functional role of the novel phosphorylation site S811 in the human renal NaCl cotransporter. *Submitted,* 2017.

Van der Wijst J*, **Tutakhel OAZ***, Bos C, Danser A.H.J., Hoorn E.J., Hoenderop JGJ, Bindels RJM. Effects of a high sodium-low potassium diet on renal calcium, magnesium, and phosphate handling. *Am J Physiol Renal Physiol,* in press.

Tutakhel OAZ*, Moes AD*, Valdez-Flores MA, Kortenoeven MLA, Van de Vrie M, Jeleń S, Fenton RA, Zietse R, Hoenderop JGJ, Hoorn EJ, Hilbrands L, Bindels RJM. NaCl cotransporter abundance in urinary vesicles is increased by calcineurin inhibitors and predicts thiazide sensitivity. *PLOS One* 12: e0176220, 2017.

Pathare G*, **Tutakhel OAZ***, Van der Wel MC, Shelton LM, Deinum J, Lenders JMW, Hoenderop JGJ, Bindels RJM. Hydrochlorothiazide treatment increases the abundance of the NaCl cotransporter in urinary extracellular vesicles of essential hypertensive patients. *Am J Physiol Renal Physiol* 312: F1063-F1072, 2017.

Valdez-Flores MA, Vargas-Poussou R, Verkaart S, **Tutakhel OAZ**, Valdez-Ortiz A, Blanchard A, Treard C, Hoenderop JGJ, Bindels RJM, Jeleń S. Functionomics of NCC mutations in Gitelman syndrome using a novel mammalian cell-based activity assay. *Am J Physiol Renal Physiol* 311: F1159-F1167, 2016.

Tutakhel OAZ*, Jeleń S*, Valdez-Flores M, Dimke H, Piersma SR, Jimenez CR, Deinum J, Lenders J W, Hoenderop JGJ, Bindels RJM. Alternative splice variant of the thiazide-sensitive NaCl cotransporter: a novel player in renal salt handling. *Am J Physiol Renal Physiol* 310: F204-F216, 2016.

*Authors contributed equally to this work.

Curriculum vitae

Omar A.Z. Tutakhel was born in Kabul, Afghanistan, on 20 February 1988. After graduating from high school in 2006 at Merlet College in Grave, The Netherlands, he studied Life Sciences for four years at the HAN University in Nijmegen, The Netherlands. He obtained his Bachelor major in Microbiology and minor in Biochemistry. In 2010, he decided to pursue his interest in health sciences and enrolled in the Master of Biomedical Sciences (dual major Toxicology and Human Pathobiology) at Radboud University in Nijmegen, The Netherlands. For his first Master internship, he performed an internship at the departments of Pharmacology-Toxicology and Physiology under the supervision of Prof. dr. Roos Masereeuw and Prof. dr. Joost G.J. Hoenderop. During this internship, he investigated the regulation of sodium-dependent phosphate transporters in a conditionally immortalized human proximal tubule cell line. He performed his second Master internship in 2013 at the department of Biochemistry, Université de Montréal, Canada, where he studied the genome-wide expression profiling of the response to nicotinamide in *Candida albicans* using RNA sequencing. The same year, after obtaining his Master's degree, Omar joined the department of Physiology of the Radboud university medical center (Radboudumc) as a PhD candidate. Under the supervision of Prof. dr. René J.M. Bindels, Prof. dr. Joost G.J. Hoenderop, Dr. Jenny van der Wijst and Dr. Ewout J. Hoorn, he studied the novel molecular and functional implications of the NaCl cotransporter in hypertension. Additionally, his PhD research demonstrated that urinary exosomes can be used as a non-invasive tool to guide anti-hypertensive therapy in patients with hypertension. Subsequently, as postdoctoral researcher at the department of Physiology of the Radboudumc, Omar is dedicated to clinically utilize urinary exosomes as a non-invasive biomarker for a variety of (patho)physiological conditions. During his graduation research, Omar's work was selected for poster presentations at the American Society for Nephrology (ASN) in USA and EURenOmics Heidelberg Meeting in Germany. Additionally, he obtained a NVBMB Travel Award to attend the Experimental Biology (EB) Meeting in USA. Moreover, he was awarded with the 'Best Oral Presentation Award' at the 23rd edition of the PhD retreat of the Radboud Institute for Molecular Life Sciences (RIMLS). He successfully followed the PhD training programme of the RIMLS and supervised 16 students from Biomedical Sciences, Medicine, Medical Biology and Molecular Mechanisms of Disease Bachelor's and Master's studies.

Research data management

Appropriate research data management is important for safeguarding scientific integrity, open science, safekeeping of valuable datasets and the reuse of data. The data obtained during my PhD at the Radboud university medical center (Radboudumc) are archived according to the Findable, Accessible, Interoperable and Reusable (FAIR) principles (1). At the beginning of my PhD we introduced a digital lab book called Labguru, which is centrally stored and daily backed up on the local server of Radboudumc. The primary (raw) and secondary (processed) data that were generated, have been stored on Labguru and local server of the department of Physiology and viewed by the associated principal investigators (PIs). Both the local server of our department and Labguru are supported by the Information and Communications Technology (ICT) of Radboudumc. Primary and secondary data of all projects that were stored the local server were weekly backed-up on the university servers. The data archives on the Labguru and local server are accessible by the associated scientific staff members. However, once the data are locked, the staff members can only view (= download) data files of the archive from Labguru and the local server, but not edit or remove any archived file. In **Chapter 2**, **3**, and **5**, human studies were conducted according to the principles expressed in the Declaration of Helsinki. All participants gave written informed consent for the use of their data and samples. The study protocols, including the data management plan were approved by the associated Medical Ethics Committee of the Radboudumc and Erasmus Medical Center. Animal studies in **Chapter 5** and **6** were approved by the Central Animal Laboratory and the Animal Ethics Board of the associated Universities. Published data generated or analyzed in this thesis are included in published articles and its additional files are available from the associated corresponding authors on request. To ensure general accessibility of the data, all file names, all primary and secondary data, metadata, descriptive files and program code and scripts used to produce the final results such as figures, tables, statistical analyses were documented according to the protocol of the department of Physiology.

Reference

1. Wilkinson MD, Dumontier M, Aalbersberg IJ, Appleton G, Axton M, Baak A, Blomberg N, Boiten J-W, da Silva Santos LB, Bourne PE, Bouwman J, Brookes AJ, Clark T, Crosas M, Dillo I, Dumon O, Edmunds S, Evelo CT, Finkers R, Gonzalez-Beltran A, Gray AJG, Groth P, Goble C, Grethe JS, Heringa J, ESH ESC Task Force for the Management of Arterial Hypertension, Hooft R, Kuhn T, Kok R, Kok J, Lusher SJ, Martone ME, Mons A, Packer AL, Persson B, Rocca-Serra P, Roos M, van Schaik R, Sansone S-A, Schultes E, Sengstag T, Slater T, Strawn G, Swertz MA, Thompson M, van der Lei J, van Mulligen E, Velterop J, Waagmeester A, Wittenburg P, Wolstencroft K, Zhao J, Mons B. The FAIR Guiding Principles for scientific data management and stewardship. *Sci Data* 3: 160018, 2016.

RIMLS Portfolio

Name PhD student:	***Omar A.Z. Tutakhel***	**PhD period:**	***01-09-2013 – 31-08-2017***
Department:	***Physiology***	**Promotors:**	***Prof. dr. R.J.M. Bindels***
Research School:	***Radboud Institute for Molecular Life Sciences***		***Prof. dr. J.G.J. Hoenderop***
			Prof. dr. E.J. Hoorn, Erasmus MC
		Copromotor:	***Dr. J. van der Wijst***

TRAINING ACTIVITIES	Year(s)	ECTS
a) **Courses & Workshops**		
- RIMLS Graduate Course	2014	2
- Winterschool Nierstichting	2014	1
- Academic Writing	2015	2.8
- Scientific Integrity course	2015	1
b) **Seminars & lectures**		
- RIMLS Radboud Research Rounds / Lecture Series	2013-2016	2.1
- RIMLS Seminars	2014-2017	1.5
- RIMLS Spotlights / Kidney Theme Meetings	2015-2017	1
- RIMLS Technical Forums	2016	0.5
c) **(Inter)national Symposia & Congresses**		
- RIMLS Radboud New Frontiers	2013	1
- RIMLS PhD retreat *#	2014-2017	3
- NfN Najaarssymposium *	2014	0.75
- ERA-EDTA Congress	2014	1
- RIMLS Radboud New Frontiers #	2014	1.5
- Dutch Nephrology Days *	2015, 2017	2
- EURenOmics Meeting *	2015	0.75
- Radboud Science Day *	2015	0.75
- RIMLS Radboud New Frontiers	2015	0.25
- RIMLS Radboud Research Rounds *	2015	0.25
- RIMLS Kidney Theme Meeting *	2015	1
- Pre-ASN Kidney Week	2016	0.5
- ASN Kidney Week #	2016	1.5
- RIMLS Radboud New Frontiers #	2016	1.5
- Experimental Biology Meeting *#	2017	2
d) **Other**		
- RIMLS public lecture: Customized kidney *	2015	0.75
- Organization RIMLS Technical Forum	2016	1
TEACHING ACTIVITIES		
e) **Lecturing**		
- RIMLS Teaching Scientific Skills course for MMD students	2014-2017	1.8
- RIMLS Teaching Scientific Illustration course for MMD, BMW and Medicine	2014-2017	0.8
- Teaching Medical course: Practicum Water en Zouthuishouding Q3	2016, 2017	0.8
- Teaching Medical course: Vrije Keuzeruimte	2016, 2017	0.4
- Teaching Medical course: Learning community 'Nieren'	2016, 2017	0.4
- Teaching Medical course: Introduction to laboratory	2016, 2017	0.2
- Radboud Summer School: Ins and outs of the kidney - Learning about exosomes	2016, 2017	0.2
f) **Students**		
- Supervision Master student: Hamed Qaderdan	2014	2
- Supervision Honours programme: Lisa Huis in 't Veld	2014	1
- Supervision Bachelor student: Barof Sanan	2015	2
- Supervision Bachelor student: Tessa Wijninga	2016	1.5
- Supervision Honours programme: Henrieke van Elst	2016	1
- Supervision Bachelor student: Vera Poort	2016	1
- Supervision Master student: Daan Smits	2017	2
- Supervision Bachelor students: Wouter van Megen, Liyan Smeding & Danielle Wevers	2017	1.5
- Supervision Bachelor students: Floor Jacobs, Evi Kremers & Suzanne Comans	2017	1.5
- Supervision Bachelor students: Jeroen Pas, Bas Doelman & Jurgen Moonen	2017	1.5
TOTAL		**51.0**

Oral and poster presentation are indicated with a * and # after the name of the activity, respectively

10

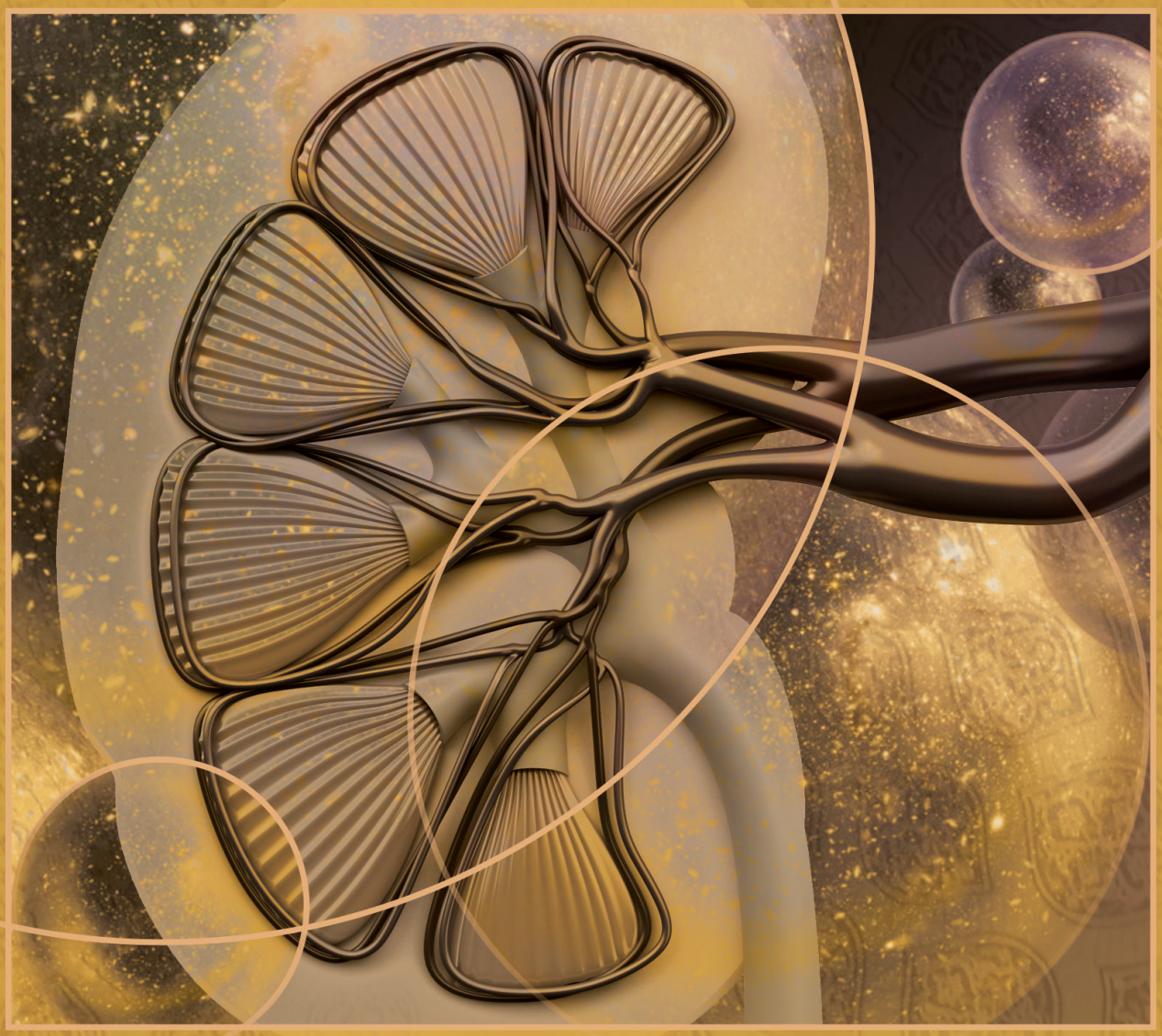

Dankwoord
Acknowledgements

Mijn wereldreis begon in Afghanistan in een zeer dynamische periode. Door mijn constant veranderende leefomgeving gedurende mijn vlucht periode waarbij ik door 17 landen gereisd heb in 10 jaar, heb ik veel geleerd. In deze reis van mijn leven wil ik alle mensen van harte bedanken die mij hebben gevormd, bijgestaan, mij lieten en leerden glimlachen in het leven ondanks de vele moeilijkheden waarmee we te maken hadden. Met dit proefschrift sluit ik een zeer leerzame en positieve deel van mij leven af. Ik hoop dat ik met dit proefschrift mijn steentje heb kunnen bijdragen aan de kennis van zouttransport in de nier en hiermee wil ik graag mijn promotoren, collega's, vrienden en families bedanken.

Ten eerste wil ik mijn promotoren prof. dr. René Bindels, prof. dr. Joost Hoenderop en prof. dr. Ewout Hoorn en copromotor dr. Jenny van der Wijst veel bedanken voor hun steun en vertrouwen. Ik dank mijn promotieteam ook voor alle kansen en mogelijkheden die ze mij de afgelopen jaren hebben gegeven. Ik heb genoten van mijn tijd op afdeling Fysiologie. **René**, ik bewonder jouw gedrevenheid, ambitie, energie en inspanning voor de afdeling Fysiologie en het RIMLS. Dankzij jouw kennis, organisatievaardigheden, efficiëntie en proactieve houding staat de afdeling Fysiologie hoog in het vaandel van in de (inter)nationale onderzoeksgemeenschap. Elke keer als ik ergens tegen aanliep, kon ik snel bij je terecht. Dankzij jouw begeleiding is dit proefschrift geworden wat het nu is. Ik heb ontzettend veel van je geleerd en ik hoop nog heel veel van je te mogen leren aankomende tijd bij de afdeling Fysiologie. **Joost**, jouw passie, inzet en enthousiasme voor onderzoek was zeer motiverend en leerzaam. Bedankt voor je meedenken en adviezen gedurende mijn onderzoek. Jou inzet in het succesvol afronden van mijn PhD speelt een belangrijke rol. Bedankt voor je ondersteuning en vertrouwen in de afgelopen jaren. **Ewout**, ik vind het een groot voorrecht om samen met jou te mogen werken. Het was zeer cruciaal voor mijn PhD om kennis, ideeën en expertise tussen beide afdeling uit te wisselen. Onze gezamenlijke inspanning hebben tot mooie publicaties geleid. Ik ben je daarvoor ontzettend dankbaar! We hopen deze samenwerking in de toekomst succesvol door te zetten. **Jenny**, je hebt mij ontzettend veel geholpen met het schrijven van dit proefschrift. Ik heb veel geleerd van jouw directe begeleiding en moleculaire kennis. Dankzij jou inzet en kennis zijn hoofdstukken 4 en 6 van dit proefschrift tot stand gekomen. Ik wens je heel veel succes in de toekomst! Ik dank jullie allen voor de steun door dik en dun. Ik heb ontzettend veel geleerd van jullie schrijf en presentatievaardigheden. Jullie zorgden ervoor dat we gefocust waren en dat er aan het einde van vier jaar een mooi boekje klaarligt.

prof. dr. **Luuk Hilbrands**, hartelijk dank voor het mogelijk maken van het hoofdstuk 5, zonder jouw kennis, hulp en de patiënten samples, was het ons niet gelukt om een mooi verhaal neer

te zetten. Bij deze wil ik ook **Mathijs van de Vrie** bedanken voor zijn inzet bij het verzamelen van de urinemonsters van de patiënten.

prof. dr. **Rob Zietse**, bedankt voor de stimulerende discussie en fijne samenwerking. Bedankt voor je inzet in het hoofdstuk 5 en gezellige praatjes tijdens onze traditionele diners. **Arthur Moes**, bedankt voor de prettige samenwerking. Ik heb veel van je geleerd tijdens onze gezamenlijke meetings. Jij was de brug tussen Nijmegen en Rotterdam. Ik wens jou veel geluk en plezierige toekomst. dr. **Mahdi Salih**, bedankt voor het delen van je kennis over extracellular vesicles. Ik bewonder jou schrijf- en presentatievaardigheden. **David Severs**, bedankt voor de interessant wetenschappelijke discussies en gezellig praatjes tijdens onze diners.

Leden van de manuscriptcommissie, prof. dr. **Frans Russel**, prof. dr. ir. **Ronald Roepman** en dr. **Jaap Joles**, bedankt voor het beoordelen van mijn proefschrift. Bij deze wil ik alvast de overige leden, prof. dr. **Jacques Lenders**, dr. **Fons van de Loo**, dr. **Rachel van Swelm** en dr. **Jaap Deinum** ook bedanken voor het beoordelen van mijn proefschrift. dr. **Jaap Deinum** en prof. dr. **Jacques Lenders**, bedankt voor jullie kennis, ideeën en inzet in de afgelopen jaren.

prof. dr. **Peter Deen**, bedankt voor je kritische vragen tijdens de FLM, maar ook de gezellige praatjes tijdens de pauzes of afdelingsuitjes.

prof. dr. **Robert Fenton**, dr. **Marleen Kortenoeven** and dr. **Henrik Dimke**, thank you for your valuable review. I greatly appreciated your constructive remarks and suggestions.

Dorien Swinkels, ik wil je enorm bedanken voor het mentorschap. Je hebt mij al die jaren gestimuleerd voor mijn promotie. Bedankt voor alle adviezen en kennis over het leven binnen en buiten het lab.

Ik wil graag alle collega's in chronologische volgorde van mijn PhD periode bedanken.

Sabina, it was my great pleasure to work with you in A team. I really enjoyed your company and directness towards me and Marco. After each sodium team meeting I was jumping in excitement to run all the projects at the same time that were discussed during the meeting, but you would always calm me down and advise me to stay focussed and realistic. I will never forget your jokes, dynamic communication with Marco and FIREBALL.

Marco, I really enjoyed working with you. I thank you for all the nice discussion and advice you gave me. Still, when I hear a timer ringing that no one turns off, I think of you! I really

admire your relaxed attitude and funny jokes. I wish you all the success in your scientific career.

Mijn grote vriend **Mohammad**, het is een grote eer voor mij dat wij als hechte vrienden, studie genoten en collega's oftewel als broers, totaal meer dan 15 jaar, door het leven zijn gegaan. Bedankt voor alle hulp en adviezen binnen en buiten het lab in de afgelopen jaren! Ik ben van overtuigd dat we deze hechte vriendschap tot eeuwigheid kunnen doorzetten. Ik wens jou, Claudia en binnenkort Maryam alvast heel veel geluk, gezondheid en vooral plezierige toekomst toe. Ik wens je heel veel succes met de nieuwe avontuur binnen Radboudumc! **Claudia**, thank you for all the great time inside and outside the lab. Thank you very much for your hospitality. I always enjoyed your Italian delicious cuisine and cakes. Wish you all the best! I hope Asiya, Maryam and Aisha will be best friends for forever!

Sami, you have many nicknames, but the one that stands out the most is the Cilia Man, especially with your hair style and PhD projects. I thank you for all the support and help during my PhD. Thank you for also being a part of my family ☺. And I am sure you will be successful in your new adventure and future career!

Sjoerd, bedankt voor alle wetenschappelijke discussies. Jouw nieuwsgierigheid, moleculaire kennis creativiteit en ROPER-assay heeft mijn NCC splice variant kleur gegeven. **Ellen**, bedankt voor alle gezellige momenten in het lab. Ik bewonder jouw doorzettingsvermogen tijdens je PhD.

Jeroen, ik wil je ook graag bedanken voor alle leuke wetenschappelijke discussies en gezellige momenten. Ik zal onze reizen samen naar San Diego, Heidelberg en Chicago niet vergeten. **Caro**, zonder jouw hulp en expertise binnen de CDL was ons niet gelukt om hoofdstuk 6 van mijn het proefschrift tot stand te brengen. Ik wil je daarvoor enorm bedanken! **Andreas**, het was zeer fijn om in de laatste jaren de unit met jou te delen. Ik waardeer jou fijne manier van advies geven, bedankt! **Steef**, bedankt voor alle suggesties en adviezen tijdens de FLM en elektrolyten meetings. **Chao**, thank you for helping me with the cell culture experiments for the chapter 4 of my thesis. **Hassan**, **Hacene**, thank you for the nice time inside and outside the Lab. **Anique**, bedankt voor het helpen bij het uitvoeren van dierexperiment voor het hoofdstuk 6. **Lisanne**, ik ben jou ook enorm dankbaar voor de gezellige sfeer op het lab. Ik heb diepe respect voor jou inzet en oprechte zorgzaamheid voor de mede collega's, harde werk en vrolijkheid.

Paco, **Pacito**, thank you for your friendship and completing my acute water loading experiments! **Femke L**, bedankt voor je hulp met de celkweek voor de NCC splice variant

verhalen. **Eric**, ik wil je ook erg bedanken voor alle buffers, die tot iedere Na^+, Cl^- en K^+ molecule nauwkeurig waren gemaakt.

Irene, heel erg bedankt voor alle bestellingen en voor alles wat een functionerend lab nodig heeft. **Theun**, ik vond het altijd erg fijn en gezellig met jou over veel zaken van gedachte te wisselen. **Ganesh**, I want to thank you for your contribution to the exosome work. **Luke**, thank you for helping me to write chapter 3 and 5 of my thesis. **Frans**, bedankt voor het gebruiken van je geweldige FRET techniek in het hoofdstuk 4! Het was een mooie samenwerking wat tot een mooi verhaal heeft geleid. **Jojanneke**, ik wil je graag bedanken voor de mogelijkheden om mijn onderwijsvaardigheden te verbeteren. Het was zeer leuk en leerzaam om daarbij betrokken te zijn. **Rachaël**, hartelijk bedankt voor alle reserveringen van de lokalen, het organiseren van interne en externe meetings en alle gezellige momenten.

Daarnaast wil ik alle collega's bedanken die ieder op hun wijze hebben bijgedragen aan een zeer leuke en leerzame tijd op het lab: **Wilco**, **Dennis**, **Liz**, **Erik**, **Kukiat**, **Mark**, **Marla**, **Joris**, **Fareeba**, **Anke**, **Seng**, **Femke**, **Eline**, **Michiel**, **Kim**, **Niki**, **Marjolein**, **Elja**, **Selma**, **Niky**, **Gijs**, **Venkatesh**, collega's van Integratieve Fysiologie en iedereen die ik hier nog vergeet!

Roos, bedankt voor de mogelijkheid en vertrouwen tijdens mijn masterstage. Meerdere competenties heb ik tijdens mijn stage ontwikkeld en verbeterd. Ik wens je veel succes in Utrecht! **Martijn**, the ciPTEC Man, tijdens mijn masterstage heb ik met veel plezier met de ciPTEC cellen gewerkt en heel veel van jou geleerd. Deze kennis is goed van pas gekomen tijdens mij PhD en bedankt daarvoor! Ik wens je veel succes met jouw gezinnetje en heel veel succes in de toekomst! **Jitske**, jouw vrolijkheid, goed humeur en behulpzaamheid waren vaak doorslaggevend voor een goede samenwerking. Bij deze wil ik je ook bedanken voor alle hulp en humane samples die ik in mijn hoofdstuk 2 heb gebruikt.

Ik heb tijdens mijn PhD met veel plezier veel studeten begeleid. Het was een eer om hun te mogen begeleiden. **Hamed**, ik ben je enorm dankbaar voor alle experimentele hulp voor het hoofdstuk 5. Het was zeer prettig met jou te mogen samenwerken. **Daan**, jouw hulp en inzit was onmisbaar voor het hoofdstuk 4 van mijn thesis. Heel erg bedankt! **Lisa**, **Vera** en **Wouter** bedankt voor jullie hulp en inzet.

Yasien, **Yasser**, **Yahya**, **Mustafa**, **Mutez**, **Pieter**, **Lieven**, **Zain**, **Nezar**, **Rafih**, **Parweez**, **Hemen**, **Anoush**, **Hassan**, **Faisal**, **Edo** en **Sarmen** bedankt voor jullie steun en begrip voor drukke tijden. Haji **Kabir**, ik ben je enorm dankbaar voor de gastvrijheid en lekkere eten bij Rotana. **Maiwand**, **Nooristani**, Haji **Said**, **Rohullah** en **Masuma** bedankt voor je hulp en steun.

Hashim and Jamalludin uncles thank you for your support and motivation throughout my long journey! I would like to thank all my uncles and aunts in Afghanistan, Germany, America and UK for their support and understanding. I hope to catch up and visit you!

Dear **parents-in-law**, I thank you for helping me with the Dari and Pashto summary of my thesis. Thank you for unconditional support, patience and stimulation in past and coming years. I really appreciate it!

Grandmother, thank you for your love and support during my early age. I will never forget your kindness.

Lieve broer **Abdullah**, ik ben je enorm dankbaar voor en na mijn vlucht voor het betere leven. Zonder jouw hulp en motivatie was ik nooit zover gekomen. Onze dynamische leven heeft ons niet de kans gegeven om onder één dak te leven, maar mijn liefde en broederschap is nooit minder van geworden. Lieve broer **Nektar**, het is soms moeilijk om te beseffen dat je niet meer bij ons bent, maar jouw herenneringen waren altijd een onuitputtelijke bron van inspiratie en motivatie voor mij.

Mijn lieve **moeder** en **vader**, aan jullie heb ik alles te danken. Het leven is niet makkelijk geweest voor jullie. Jullie hebben zeer dynamische leven gekend, vooral na het verlies van jullie zoon, mijn broer Nektar, op 23-jarige leeftijd. In goede en slechte tijden onze toekomst was voor jullie een vooropgesteld doel. Jullie hebben het huis en haard verlaten om ons een goed toekomst te bieden. Jullie hebben mij gevormd tot de persoon die ik nu geworden ben en daarom draag ik ook dit proefschrift aan jullie op.

Mijn lieve dochter **Asiya**, ik kan niet in woorden uitbrengen hoeveel geluk, voldoening, liefde en blijdschap je mij gegeven hebt. Ik hou ontzettend veel van je. Mijn lieve dochter **Aisha**, ik ben gezegend om jou ook in de jaar van mijn promotie te mogen gaan omhelzen. Ik hou nu al heel veel van je en laat staan als ik je zie.

Lieve **Raihana**, **Nargis**, je bent er altijd voor mij geweest. Je hebt jouw families, vrienden en huis achtergelaten voor mij. Bedankt dat je mijn wederhelft bent, je hebt mij gestimuleerd en gesteund door dik en dun. Zonder jouw steun was ik nooit zover gekomen. Ik ben super trots op jou en bedankt voor je liefde, zorgzaamheid en mooie gezelschap. Ik kan het niet vaak genoeg zeggen, ik hou van je!

Alhamdulillah (alle dank aan Allah), het is zover! Hora est!

استفاده اگزوزوم رهنمای تداوی دقیق فشار بالای خون را از طریق معاینه ادرار نشان میدهد.

اگزوزوم به طور مداوم از طریق ادرار دفع می شوند و به همین ترتیب آنها یک منبع تشخیص بیماری برای بیماری های کلیوی هستند. در این پایان نامه، ما یک روش دقیق برای تجزیه و تحلیل پروتئین های NCC در اگزوزم های ادراری ایجاد کرده ایم. در این پایان نامه، فصل ۱، ۳ و ۵ نشان می دهد که اگزوزوم های ادراری به عنوان یک روش منحصر به فرد و غیر تهاجمی برای مطالعه تنظیم NCC در کلیه انسان استفاده می شود. علاوه بر این، تجزیه و تحلیل NCC در اگزوزم های ادراری یک روش جایگزین برای نظارت بر بیماران مبتلا به فشار خون بالا، و درمان ضد فشار خون را فراهم می کند. اگزوزوم در ادرار می تواند به درمان موثر و شخصی فشار خون بالا کمک کند. NCC دراگزوزوم های ادراری فایده شخصی بیماران به دیورتیک های تیازید را پیش بینی میکند. تیازید دیورتیک یکی از دوا های است که برای فشار بالای خون استفاده میشود. تیازید دیورتیک اولین داوای است که برای فشار بلند داده میشود. تیازید دیورتیک دروازه های NCC را بند میسازد. به این طریق سودیم دفع کلیه میشود. و با دفع سودیم آب همچنان از بدن خارج میشود. به این طریق فشار خون را کاهش میدهد. ما می دانیم تنوع بین فردی در کاهش فشار خون به تیازید ها وجود دارد. شایان ذکر است، نتایج ما نشان میدهد که تجزیه و تحلیل بیان NCC در اگزوزوم های ادراری قبل از درمان تیازیدی می توانید پاسخ فشار خون را به دیورتیک های تیازیدی پیش بینی کند. همچنان جالب است که قبل از درمان با دیورتیک های دیگر، اگزوزم های ادراری بررسی شود تا بتوانند پاسخ فشار خون را پیش بینی کنند.

تأثیر این پایان نامه و دیدگاه آینده.

در این پایان نامه، ما نشان دادیم که اگزوزم های ادراری می تواند به عنوان ابزار غیر تهاجمی همراه با درمان ضد فشار خون در بیماران مبتلا به فشار خون بالا مورد استفاده قرار گیرد. تجزیه و تحلیل اگزوزم های ادراری می تواند کمک کند به شخصی درمان ضد فشار خون. ادرار نه تنها منبع مهم تشخیص بیماری برای پیش آگهی درمان های ضد فشار خون است، بلکه همچنین برای تشخیص بیماری های مختلف کلیوی است. این ممکن است شروع و پیشرفت بیماری های کلیوی را محدود کند. در آینده، ممکن است برخی از بیماری ها گرفتن پارچه از کلیه غیر ضروری باشد. به تازگی روش هایی برای بررسی اگزوزم های ادراری به کار گرفته شده است. با این حال، برای برنامه های کاربردی بالینی بیشتر، توسعه آزمایش های با کارایی بالا برای تجزیه و تحلیل اگزوزم ضروری است. بنابراین اگزوزوم امیدوار کننده است، اما استفاده اگزوزم با تشخیص بیماری کلیه درشفاخانه ها در آینده باید تحقیقات شود.

بنام خداوند یکتا و نهایت مهربان.

مقدمه.

فشار خون.

فشار خون بالا یک عامل خطر برای بیماری های قلبی عروقی و نارسایی مزمن کلیه است و در نتیجه خطر ابتلا به مرگ را افزایش می دهد. با شیوع ۱.۴ میلیارد نفر یا ۱ در ۳ بزرگسالان در سراسر جهان، فشار خون دارد، به این خاطر یکي از جدي ترين مشكلات سلامتي عمومي است. قابل توجه است که نیمی از بیماران مبتلا به فشار خون بالا از وضعیت خود آگاهی ندارند و بنابراین فشارخون اغلب به عنوان "قاتل خاموش" نامیده می شود. علاوه بر این علت تقریبا ٪۹۰ بیماران مبتلا به فشارخون ناشناخته است.

فشار خون توسط ترکیبی از بخش های خاص مغز، کلیه ها و قلب نگهداری می شود. کلیه ها عمدتا رطوبت و شوری را در بدن ما کنترل می کنند و درنتیجه باعث افزایش فشار خون می شوند. کلیه از حدود ۱ میلیون نفرون، واحد های عملکردی کلیه تشکیل شده است. آنها خون را صاف می کنند و بیش از حد نمک و رطوبت رااز طریق ادرار فراهم می کنند. پس از فیلتر کردن خون به گلومرول (درهم و برهم کردن رگ های کوچک خونی)، ادرار را از طریق لوله های کلیه جریان می دهد. فرآیند مبادله جذب و تحویل آب و نمک بین ادرار و خون وارد رگ های خونی در اطراف لوله کلیه اتفاق می افتد. قسمت نهایی لوله کلیه نقش مهمی در تنظیم فشار خون توسط تأثیر تبادل سودیم (Na^+) و پتاسیم (K^+) ایفا می کند. این قسمت شامل پیچش دیستال (DCT) و لوله اتصال (CNT) است. ضبط، و یا تحلیل، از سودیم در این بخش از لوله کلیه به طریق سودیم کلوراید کوترانسپوتر (NCC) و کانال های سودیم اپیتلیال سودیم (ENaC) تحت کنترل از طریق ادرار می شود. NCC خاص در DCT است و ENaC خاص در CNT است. در DCT میزان سودیم تعیین میزان سودیم در CNT می شود. بنابر این در نتیجه NCC نقش غیر مستقیم در جذب سودیم از طریق ENaC دارد. جذب سودیم از طریق ENaC به انتشار (دفع) پتاسیم از طریق ROMK می شود. هورمون های متعددی وجود دارد که این شبکه از شبکه های سودیم و پتاسیم را کنترول می کند. سیستم رنین-آنژیوتانسین-آلدوسترون هورمونی (RAAS) نقش مهمی در تنظیم فشار خون دارد. بنابراین کم خوردن نمک و زیاد خوردن پتاسیم شناخته شده است و خطر ابتلا به پرفشاری خون را کاهش دهد. باید یاداور شویم که پتاسیم به مقدار زیاد در ترکارها و میوجات تازه و خشک موجود میباشد از جمله مانند کیله، مالته، اب ناریال، سبزی پالک، بادنجان رومی، کشمش، بادام وغیره.

د اګزوزوم (Exosomes) موجودیت په ادرار کی د وینی لور فشار دقیق لارښود دي.

اګزوزوم په دوامدار شکل د ادرارو په واسطه دفع کیږی. نو ځکه د بډوډو د ناروغۍ لپاره سرچینې د تشخیص دي. په دی پای لیک کی، مونږ په د مثال کې د NCC پروټینونو د ادرارو اګزوزومو تحلیل او تجزیه د لپاره یو واضح میتود تیار کړی دی. جور کری ۲، ۳، ۵ فصلونه چه د ادرارو اګزوزوم ښه د یو لارښود او یو غیر یرغلیز په توګه د انسان په بډوډی کی استفاده ګیږی، سربیره پر دی NCC مطالعه د ادرارو په اګزوزوم یولارښود ده. NCC پروټینونو د ادرارو اګزوزومو تجزیه تحلیل د وینی لور فشارناروغان او د هغوی درملنی نظارت کوی. د ادرارو اګزوزوم د لور فشار موثره درملنه کی مرسته کوی. NCC د ادرارو په اګزوزوم کی د ناروغ ځواب د تیازید دیورتیک په مقابل کی وراندنیه کوی. تیازید دیورتیک هغه دوا ده چه د وینو د لور فشار د پاره استفاده کیږی. تیازید دیورتیک لومړنی دارو ده چه د لور فشار ناروغانو ته ورکول کیږی. تیازید دیورتیک د NCC دروازی بندوی. په همدی لاره کی Na^+ د بډوډو چخه دفع کیږی. د Na^+ د انتقال نه ورسته اوبو هم د بدن څخه راوځی، او په همدی دول د وینی فشار تیتوی. مونږ پوهیګو چه حساسیت د تیازید دیورتیک په مقابل کی په اشخاصوکی موجود دی. زمونږ نتایج ښی تحلیل او تجزیه د درملنی نه مخکی د NCC د ادرارو په اګزوزوم کی کولی شی چه تیازید دیورتیک تاسیر اټکل کوی. دا په دی معنی ده چه د اګزوزم تجزیه او تحلیل کولی شو چه غیری ضروری استفاده نه یی مخنیوی وکرو او هم جالبه ده چه مخکی له دی چه د نورو دیورتیک په واسطه درملنه وشی د ادرارو اګزوزوم معاینه شی، تر څو تیازیدو نه وکولای شی د لور فشار ځواب وراندوینه وکری.

د پای لیک اغیز او د راتلونکی پس منظر.

په دی پای لیک کی مونږ و ښودله چه ادرارو اګزوزم کولی شی چه د غیر بریدګر په شکل د لور فشار ضد ادویه سره یو ځای د وینی لورفشار ناروغانو کی استفاده کیږی. اګزوزوم تحلیل او تجزیه هغه کسانو سره چه د فشار ضد دوایی اخلی مرسته کوی. اګزوزم ادرار نه یوازی د تشخیص مهمه منبه ده چه د لورفشار ضد تداوی ښی. بلکه د مختلفو بډوډو او ناروغیو د تشخیص د پاره هم مهم دی. دا ممکن د بډوډو ناروغی د پیل او پرمختګ اټکل کری. او په راتلونکی د بیوپسی (د بډوډو توته) اخیستل هم ضرور نوی. د اوس مختلفی طریقو ځخه د ادرارو اګزوزم د برسی لپاره په کار اخیستل شوی ده. بیا هم په راتلونکی د روغتونون کی دا استفاده د اګزوزوم باید څرینه وشي.

د لوی او ببنونکی خدای په نامه.

د پایلیک لنډیز.

د وینې فشار.

د وینې لوړ فشار د زړه د عروقي ناروغیو د خطر او د بډوډي د ناروغیو یو لوی لامل دی، چې په پایله کې یې مرګ پیښیدلای شي. په ټوله نړۍ کې د وینې په فشار د ۱،۴ میلیاردو کسانو یا د لویانو ۱ په ۳ کسانو اخته کیدنه یوه عمومي روغتیایي ستونزه ده. دا د پام وړ ده چې د وینې په فشار نیمایي اخته کسان د ځان له وضعیته خبر ندي، نوځکه د وینې فشار د پټ وژونکي په نام هم یادیږي. برسیره پر دې، د ۹۰٪ ناروغانو لامل ناپیژانده دی.

د وینې فشار د خاص مغز، بډوډو او زړه په واسطه ساتل کیږي. بډوډي په وجود کې رطوبت او مالګه کنټرولوي، چې په پایله کې یې د وینې فشار لوړیږي. بډوډي د شا او خوا ۱ میلیون نفرون، د بډوډي د کړنې واحد څخه جوړ شویدي. هغوی وینه دفع کوي او اضافي مالګه او رطوبت د ادرارو له لارې دفع کوي. وروسته له هغې چې ګلومرول (د وینې د کوچنیو رګونو ګډوډولو) ته وینه فلتر کړي، ادرار د بډوډو ټیوبونو له لارې تیریږي. د مالګې او اوبو جذب او انتقال کول د ټیوبونو او وینې ترمینځ کیږي. د بډوډي د لولې وروستۍ برخه د وینې فشار په تنظیم کې د مالګه (Na^+) او د پوتاشیم (K^+) د تبادلې کې مهم رول لري. دغه د بډوډي د لولې وروستۍ برخه د دیستال پیچش (DCT) او د نښلولو لوله (CNT) څخه یا دیږي. بډوډي پدغه برخه کې سودیم کلورایډ کوترانسپوتر (NCC) د Na^+ جذبو لو او خارجکول کې مهم رول لري. هورمونونه په نامه د رنین آنژیوتانسین آلدوسترون سیستم (RAAS) د دغې یوه مهمه برخه ده او د وینې فشار په تنظیم که ډیر مهم رول لري. نو ځکه مالګې لک استفاده کول او پتاسیم دیر خورل د لور فشار خطر کموی. په دیره اندازه پتاسیم په ترکاریو، تازه او وچه میوه کی شته لکه په کیله، مالته، د ناریال اوبه، سبزی پالک، رومی بانجان، ممیز، بادام او داسی نور.

Dari Summary
پایان نامه (خلاصه)

Pashto Summary
د پایلیک لنډیز

11